

**Pyrrolizidine- and quinolizidine alkaloid biosynthesis in
nodule forming species from the genistoid clade (Fabaceae)**

Dissertation in fulfillment of Requirements of the Doctoral Degree

Doctor rerum naturalium

of the Faculty of Mathematics and Natural Science at
Christian-Albrechts-Universität zu Kiel

submitted by Nadine Jacky

Kiel, March 2023

1. Supervisor: Prof. Dr. Dietrich Ober

2. Supervisor: Prof. Dr. Jennifer Selinski

Submitted on: 30.03.2023

Date of oral examination (Disputation): 16.06.2023

Print permission approved: 28.06.2023

*"A story can be new and yet tell about olden times.
The past comes into existence with the story."*

Michael Ende



*Dried Flower
of
Laburnum x watereri 'Vossii'*

Abstract

Fabaceae, also frequently referred to as legumes, are a plant family whose representatives form a symbiosis with nitrogen-fixing bacteria and harbor them in specially formed root-nodules. For defense against herbivores, plants within the monophyletic group of Genistoids in particular produce toxic alkaloids, which belong to either the pyrrolizidine alkaloids (PAs) or quinolizidine alkaloids (QAs). In both biosynthetic pathways, the first specific enzymes (for PAs homospermidine synthase, HSS, and for QAs lysine decarboxylase, LDC) have been studied in several species in the past. Interestingly, both enzymes arose by gene duplication starting from an enzyme of primary metabolism. Data show that PA biosynthesis developed several times independently in various plant lineages during evolution. The site of biosynthesis appears to be often species specific, whereas for QA biosynthesis, leaves are described as site of synthesis.

For the fabaceous species *Crotalaria spectabilis* it was already shown that PA biosynthesis is dependent on the formation of root-nodules. From this point of view, two main questions arose, which were investigated within this work: 1. Which are further enzymes of PA biosynthesis 2. Which influence has nodulation on QA and PA biosynthesis?

To identify additional enzymes involved in PA biosynthesis, *C. spectabilis* was chosen as experimental plant. A subtractive approach was used to identify transcripts that occur only in PA-producing tissues. For this purpose, two tissues, from roots (without PA biosynthesis) and nodules (with PA biosynthesis), were selected and their transcriptome sequenced. In total, five copper amine-dependent oxidases (CuAOs) were identified, whereof two were identified to be involved in PA biosynthesis in further experiments by real-time PCR, by analyses of knockout mutants, and by tracer-feeding experiments. The results suggest, contrary to what has been postulated in the literature so far, that two CuAOs are involved in the oxidation of homospermidine to allow the formation of the bicycle (= basic scaffold of PAs, the necine base). Furthermore, antibodies against the HSS could be successfully used to identify the HSS expressing tissues within the nodules.

Although many species show different sites for the production of PAs, it was suspected that *Laburnum spec.* as a nodule-forming PA and QA producer, follows the scheme of *C. spectabilis*. Initially, this assumption was supported since *hss* transcript and localization of HSS protein were both detected almost exclusively in nodules (except for low intensity

of *hss* transcript in immature pods) by real-time PCR and immunolocalization. However, further analytical analyses showed that non-nodulated *Laburnum spec.* also produced PAs. Of note, an undescribed PA of unknown structure was detected in these experiments. As for *C. spectabilis*, five CuAOs have been successfully identified in SRA archives of a published *L. anagyroides* genome using the known sequences of *Crotalaria*. Sequence fragments have been completed using diverse PCR techniques. Consequently, PA biosynthesis in *L. x watereri 'Vossii'* does not seem to be exclusively linked to nodules and is quite different from that mechanism of *C. spectabilis*.

As *Crotalaria* and *Laburnum* are closely related with other QA-producing species three QA-producing species have been examined for a possible *hss* transcript in nodules to allow conclusions about the evolution of this PA-specific enzyme. *Cytisus scoparius* indeed showed plant *hss* transcript within the nodules, although the plant does not produce PAs. The influence of nodulation on PA biosynthesis allows speculation if this symbiosis between plant and rhizobia might have similar effects on QA biosynthesis in related species of the Genistoid clade. As models, *L. x watereri 'Vossii'* and two species of the genus *Lupinus* (*L. arboreus* and *L. polyphyllus*) were studied. First, rhizobia were isolated from field-grown plants, identified and used to induce nodule-formation under controlled conditions in *in vitro* cultures. After identification of the LDC- and ornithine decarboxylase (ODC)-encoding cDNAs, heterologous expression, and protein assays were performed to verify the identity of these enzymes. *ldc* and *odc* transcript levels have been analyzed in various tissues to test for a correlation between nodulation and QA biosynthesis. Here, the *ldc* transcripts were found to be more abundant in the "green", i.e., chloroplast-associated tissues, while they were not detectable in roots and nodules, while *odc* transcript was detectable in all analyzed tissues. In consequence, a dependency of QA biosynthesis on the formation of nodules in the analyzed fabaceous species can be ruled out, at least as far as the first catalytic step is concerned.

Zusammenfassung

Fabaceae, auch häufig als Leguminosen bezeichnet, ist eine Pflanzenfamilie, deren Vertreter mit Stickstoff-fixierenden Bakterien eine Symbiose eingehen und diese in extra gebildeten Wurzelknöllchen beherbergen. Zur Abwehr von Herbivoren stellen insbesondere Pflanzen innerhalb der monophyletischen Gruppe der Genistoide giftige Alkaloide her, welche entweder zu den Pyrrolizidinalkaloiden (PAs) oder Chinolizidinalkaloiden (QAs) gehören. In beiden Biosynthesewegen ist das Eingangsenzym (für PAs die Homospermidinsynthase, HSS, und für QAs die Lysindecaboxylase, LDC) mittlerweile in mehreren Arten untersucht worden. Interessanterweise sind beide Enzyme durch jeweils eine Genduplikation ausgehend von einem Primärstoffwechselenzym entstanden. Daten zeigen, dass die PA-Biosynthese im Laufe der Evolution in mehreren Pflanzenfamilien unabhängig voneinander entstanden ist und der Ort der Biosynthese artspezifisch zu sein scheint, während für die QA-Biosynthese die Blätter als Syntheseort beschrieben werden.

Für die Fabaceae *Crotalaria spectabilis* wurde bereits eine Abhängigkeit der PA-Biosynthese von der Ausbildung von Wurzelknöllchen gezeigt. Von diesem Standpunkt aus entstanden zwei Hauptfragestellungen, welche innerhalb dieser Arbeit untersucht wurden: 1. Welche weiteren Enzyme sind an der PA-Biosynthese in diesem Gewebe beteiligt? und 2. Welchen Einfluss hat die Nodulation auf die QA-Biosynthese und auf die PA-Biosynthese einer weiteren PA-produzierenden Art der Fabaceae?

Zur Identifikation von weiteren Enzymen der PA-Biosynthese wurde *C. spectabilis* gewählt. Durch einen subtraktiven Ansatz sollten Transkripte identifiziert werden, welche nur in PA-produzierenden Geweben vorkommen. Dazu wurden zwei Gewebe (Wurzeln ohne PA-Biosynthese und Knöllchen mit PA-Biosynthese) ausgewählt und deren Transkriptom sequenziert. Durch Vergleich der Transkriptome konnten insgesamt fünf kupferabhängige Aminoxidasen (CuAOs) identifiziert werden, von denen zwei in den folgenden Experimenten durch Realtime-PCR, Analyse von Knock-out-Mutanten und Tracerfütterungsversuche als Enzyme identifiziert werden konnten, die an der PA-Biosynthese beteiligt sind. Die Ergebnisse sprechen dafür, anders als bislang in der Literatur postuliert, dass zwei CuAOs benötigt werden, um vom Homospermidin zu einem stickstoffhaltigen Bicyclus, dem Grundgerüst der PAs, der Necinbase, durch Oxidation zu

gelangen. Des Weiteren konnten Antikörper gegen die HSS erfolgreich eingesetzt werden, um innerhalb der Knöllchen das HSS-exprimierende Gewebe zu identifizieren.

Obwohl bereits viele untersuchte PA-produzierende Arten unterschiedlichste PA-Biosyntheseorte aufweisen, wurde vermutet, dass *Laburnum spec.* als knöllchenbildender PA- und QA-Produzent, ähnlich wie *C. spectabilis*, an die Nodulation für die PA-Biosynthese gebunden sein könnte. Zunächst wurde diese Vermutung untermauert, da *hss*-Transkript mittels Realtime-PCR und HSS-Protein durch Immunolokalisation fast ausschließlich in den Knöllchen (mit Ausnahme von geringen *hss*-Transkriptmengen in den unreifen Hülsen) detektiert wurden. Jedoch zeigten weitere analytische Analysen, dass auch nicht knöllchenbildende *L. x watereri 'Vossii'* PAs produzierten. Dabei wurde ein bisher unbeschriebenes PA mit unbekannter Struktur entdeckt. Die Ergebnisse lassen vermuten, dass die PA-Biosynthese in *L. x watereri 'Vossii'* nicht ausschließlich an die Knöllchen gebunden ist und unterscheidet sich somit durchaus von der von *C. spectabilis*. Des Weiteren konnten für *L. x watereri 'Vossii'* auch fünf CuAOs identifiziert werden, deren Bedeutung für die Alkaloidbiosynthese noch nicht geklärt werden konnte. Das hohe Transkriptvorkommen von *hss* in den Knöllchen von *L. x watereri 'Vossii'* und *C. spectabilis* deuten auf einen Mechanismus hin, der durch Knöllchenbildung kontrolliert wird. Deshalb wurden drei weitere QA-produzierende Arten, welche auf Basis genomischer DNA-Daten das Vorkommen einer *hss*-artigen Sequenz zeigten, auf mögliches *hss*-Transkript in den Knöllchen untersucht. Tatsächlich wies eine der drei Pflanzen, *Cytisus scoparius*, pflanzliches *hss*-Transkript in den Knöllchen auf und das ohne PAs zu produzieren.

Der Einfluss der Nodulation auf die PA-Biosynthese lässt Spekulationen zu, ob diese Symbiose ähnliche Auswirkungen auch auf die QA-Biosynthese haben könnte. Hierzu wurden *L. x watereri 'Vossii'* und zwei Vertreter aus der Gattung *Lupinus* (*L. arboreus* und *L. polyphyllus*) untersucht. Zunächst wurden Rhizobien aus im Freiland wachsenden Vertretern dieser Arten isoliert, identifiziert und zur Anzucht von knöllchenbildenden als auch knöllchenlosen *in vitro*-Kulturen unter standardisierten Bedingungen genutzt. GC-MS Untersuchungen führten zu keinem eindeutigen Ergebnis hinsichtlich einer knöllchenabhängigen QA-Produktion. Nach Identifizierung der LDC- und Ornithindecaboxylase (ODC)-codierenden cDNA, deren heterologer Expression und Proteinassays zur Bestätigung der Enzymidentität beitrugen, wurden Transkriptanalysen in unterschiedlichen Geweben durchgeführt. Hierbei zeigten sich verstärkt die *ldc*-Transkripte

in den „grünen“, also Chloroplasten-enthaltenden Geweben, während diese in Wurzeln und Knöllchen nicht detektierbar waren. *odc*-Transkripte waren hingegen in allen analysierten Geweben nachweisbar. Eine Abhängigkeit der QA-Biosynthese von der Ausbildung von Knöllchen ist somit zumindest, was den ersten katalytischen Schritt betrifft auszuschließen.

CONTENTS

CONTENTS	I
1. INTRODUCTION.....	1
1.1 The Fabaceae and the origin of plant toxins	1
1.2 Nodules – Site of symbiosis with nitrogen-fixing rhizobia	2
1.3 Alkaloids in Genistoids and their toxicity	4
1.3.1 Lupins.....	5
1.3.2 Laburnum.....	6
1.3.3 Crotalaria	6
1.4 The biosynthesis of Quinolizidine alkaloids.....	7
1.5 The biosynthesis of Pyrrolizidine alkaloids.....	10
2. AIMS OF THIS WORK	12
3. CHAPTER A.....	15
Tissue Homospermidine conversion to the pyrrolizidine backbone is catalyzed by two distinct copper-containing amine oxidases in <i>Crotalaria spectabilis</i> (Fabaceae)	15
3.1 ABSTRACT	16
3.2 INTRODUCTION.....	17
3.3 RESULTS	19
3.3.1 Two CuAO-encoding genes show co-expression with HSS and are regarded as candidates for an HSO	19
3.3.2 Transformation of <i>C. spectabilis</i> allowed editing of selected genes	21
3.3.3 Inactivation of the genes encoding CsCuAO1 or CsCuAO5 results in mutants that are unable to produce PAs	25
3.3.4 CsCuAO1 and CsCuAO5 are involved in necine base formation but accept different substrates	27
3.3.5 The formation of the pyrrolizidine backbone requires both active CsCuAO1 and CsCuAO5	32
3.4 DISCUSSION	34
3.4.1 Two independent CuAOs are involved in PA backbone formation in <i>C. spectabilis</i>	35
3.4.2 CsCuAO1 and CsCuAO5 belong to the same clade as other PA-specific CuAOs.....	35
3.4.3 Nodulated <i>Crotalaria</i> plants harbor two well-separated Hspd pools	38
3.4.4 Several organs and tissues might be involved in PA biosynthesis in <i>C. spectabilis</i>	39

3.5	MATERIAL AND METHODS.....	42
3.5.1	Plant material	42
3.5.2	Confirmation of cDNA sequences and identification of genomic sequences of the genes encoding CsCuAO1 and CsCuAO5	42
3.5.3	Transcript quantification by RT-qPCR.....	43
3.5.4	Constructs for editing the genes encoding CsCuAO1, CsCuAO5, and CsHSS by CRISPR/Cas9.....	43
3.5.5	Stable transformation of <i>C. spectabilis</i> plants.....	44
3.5.6	Genomic DNA screen for mutations in the <i>cscuao</i> and <i>cshss</i> genes.....	45
3.5.7	Pyrrolizidine alkaloid extraction and purification and GC-MS analysis.....	46
3.5.8	Extraction and Quantification of Polyamines.....	46
3.5.9	Feeding experiments to nodules of <i>C. spectabilis</i> knockout plants	47
3.5.10	Phylogenetic analysis.....	47
3.6	SUPPLEMENTAL DATA	48
4.	CHAPTER B.....	57
	Nodulation has no impact on the regulation of lysine decarboxylase, the first specific enzyme of quinolizidine alkaloid biosynthesis, in golden chain and yellow bush lupin .	57
4.1	Abstract.....	58
4.2	INTRODUCTION.....	59
4.3	RESULTS	63
4.3.1	Specific rhizobia induce nodulation in <i>L. x watereri</i> 'Vossii', <i>L. arboreus</i> , and <i>L. polyphyllus</i>	63
4.3.2	Identification of candidate QA biosynthetic genes and housekeeping genes in <i>L. x watereri</i> 'Vossii' and <i>L. arboreus</i>	66
4.3.3	ODC and LDC of <i>L. x watereri</i> 'Vossii' and <i>L. arboreus</i> show both bi-functionality <i>in vitro</i>	67
4.3.4	Phylogenetic classification based on sequence similarities supports their tested functions of the identified LDCs and ODCs.....	71
4.3.5	Non-infected and infected (nodulated) <i>in vitro</i> grown plants contain several QAs with different patterns	73
4.3.6	<i>Idc</i> transcripts are detectable in plants with and without nodules.....	77
4.4	DISCUSSION	83
4.4.1	Isolation of plant-specific rhizobial interaction partners	83
4.4.2	Influencing factors on QA biosynthesis	84
4.4.3	Substrate preferences and activity of LDCs and ODCs	86

4.4.4	Phylogenetic classification.....	87
4.5	EXPERIMENTAL	90
4.5.1	Plant Material	90
4.5.2	Isolation and identification of <i>N</i> -fixing bacteria from root nodules	90
4.5.3	Nucleic acid extraction and cDNA synthesis.....	91
4.5.4	Identification of <i>Idc</i> , <i>odc</i> and housekeeping genes	92
4.5.5	Cloning and heterologous expression of sequences encoding putative LDC and ODC	92
4.5.6	Activity assays of recombinant LDCs and ODCs	93
4.5.7	Data base retrieval and gene tree	94
4.5.8	Quantitative Real-Time PCR (RT-qPCR) and primer design	95
4.5.9	QA extraction and analytics by GC-MS.....	95
4.6	SUPPLEMENTAL DATA	97
5.	CHAPTER C	109
	Unexpected findings in terms of pyrrolizidine alkaloid biosynthesis in the ornamental plant <i>Laburnum x watereri</i> 'Vossii' and an additional deeper insight in the localization of the homospermidine synthase and their origin within the genistoid clade (Fabaceae)	109
5.1	ABSTRACT	110
5.2	INTRODUCTION.....	111
5.3	RESULTS	114
5.3.1	Identification of putative <i>hss</i> , <i>dhs</i> and housekeeping genes in <i>L. x watereri</i> 'Vossii' and selected non-PA producing Genisteae	114
5.3.2	Levels of <i>hss</i> transcript are restricted to nodules and pods in <i>L. x watereri</i> 'Vossii'	116
5.3.3	The first specific enzyme in PA biosynthesis – HSS – is expressed in the parenchyma of <i>C. spectabilis</i> and <i>L. x watereri</i> 'Vossii' root-nodules.....	119
5.3.4	Nodule free plants of <i>L. x watereri</i> 'Vossii' contain several PAs	122
5.3.5	Level of <i>hss</i> transcript was detectable in nodules of a non-PA producing plant	127
5.4	DISCUSSION	128
5.4.1	The origin of an HSS copy in the Genistoids.....	128
5.4.2	<i>L. x watereri</i> 'Vossii' has two sites for the synthesis of homospermidine via HSS	129
5.4.3	Nodules are not necessary for the production of PAs in <i>L. x watereri</i> 'Vossii'	130
5.4.4	Speculative structure of the found unknown necine base	132

5.5	MATERIAL AND METHODS.....	134
5.5.1	Plant material and culturing	134
5.5.2	Preparation and affinity purification of polyclonal antibodies	134
5.5.3	Immuno histochemical localization	134
5.5.4	Identification of putative <i>dhs</i> , <i>hss</i> and housekeeping genes in <i>L. x watereri</i> 'Vossii' and of further species of Genisteae	135
5.5.5	Quantitative realtime PCR (RT-qPCR)	136
5.5.6	PA analytics in <i>L. x watereri</i> 'Vossii'	137
5.6	SUPPLEMENTAL DATA	138
6.	MISCELLANEOUS CHAPTER D.....	143
	Study of CuAOs in the Fabaceae golden chain as potential involved enzymes in the biosynthesis of PAs	143
6.1	INITIAL POSITION AND GOAL SETTING	144
6.2	RESULTS	144
6.2.1	Sequence identification of five <i>cuaos</i> in <i>L. x watereri</i> 'Vossii'	144
6.2.2	Phylogenetic classification	145
6.2.3	Only one <i>cuaao</i> is co-transcribed with <i>hss</i> in nodules	147
6.3	SUMMARY/OUTLOCK	150
6.4	SUPPLEMENTAL DATA	151
7.	CONCLUSION AND OUTLOCK	157
8.	CONTRIBUTIONS	163
	LIST OF ABBREVIATIONS	165
	REFERENCES	171
	LEBENS LAUF	Fehler! Textmarke nicht definiert.
	ERKLÄRUNG	188

1. INTRODUCTION

1.1 The Fabaceae and the origin of plant toxins

Plants are sessile organisms and exposed to biotic and abiotic factors (Gull et al. 2019) within their environment. Many species produce as response specialized chemical compounds, also referred to as secondary metabolites (Grotewold 2005; Swain 1977). Until today, the identified number of secondary metabolites is estimated up to 200 000 and are classified into different groups, e.g. alkaloids, tannins, anthocyanins, essential oils, saponins, lectins, terpenes, phenols, glucosinolates and flavonoids (Erb and Kliebenstein 2020; Pichersky and Lewinsohn 2011; Wink 2015). Contrary to primary metabolites, which are highly conserved and indispensable for the plant growth, secondary metabolites are often species-specific and play an important role for the adaptation and survival of the plant population in a continuously changing environment (Hartmann 1996). In former times, these metabolites were considered to be waste products with no function. Today we know that they are intentionally produced. They can serve as defense against impairment by competitors, herbivores, or pathogens, as enticement of pollinators or symbiotic partners, and as protection against ultraviolet radiation or evaporation (Swain 1977; Wink 2015). When they have a defense function, secondary metabolites act as toxins by targeting mainly proteins, biomembranes or nucleic acids of the herbivores. One well-

known neurotoxin is coniine, a piperidine alkaloid from the common poison hemlock (*Conium maculatum*, Apiaceae). According to reports, it has been used to kill Sokrates during ancient times. However, some toxic compounds can serve as medicine, when dosed in lower concentration. As Paracelsus once said: "Alle Ding sind Gift und nichts ist ohne Gift. Allein die Dosis macht, dass ein Ding kein Gift ist." According to that it is not an underestimated application using valuable drugs in medical implementation for humans, e.g. the use of galantamine an alkaloid from snowdrops for Alzheimer treatment or paclitaxel an alkaloid from yew tree is an important chemotherapeutic for cancer therapy (Wink 2015). Moreover, the compounds that attract other organisms might be pigments or volatiles and also shaped co-evolution between plants and beneficial interaction partners such as insects and bacteria (Hartmann and Ober 2000; Martínez-Romero 2009). This impressive diversity of compounds let arise the following question: How is the emergence of this diversity of metabolites to explain? The mentioned abiotic and biotic factors impose selection pressure on plants, which should have an impact on the evolution of new enzymes by gene duplication. The duplicated gene is able to receive due to random mutations novel functions (Grotewold 2005; Pichersky and Lewinsohn 2011).

Fabaceae, also referred to as legumes, represent one of the largest families of flowering plants with about 730 genera and more than 19,000 species. They have agricultural, economic, and ecological importance, like as crops, as medicinal or for soil enrichment (Cardoso et al. 2012). The following stated species depict some examples: clover – *Trifolium spec.*, bean (*Phaseolus vulgaris*), soybeans (*Glycine max*), peanuts (*Arachis hypogaeae*), rooibos (*Aspalathus linearis*), or various species of *Crotalaria* and sweet lupins (Graham and Vance 2003; Herridge et al. 2008; Johnson et al. 2017; Morton 1983; Ross et al. 2009; Sy et al. 2001). Especially their unique feature to enter a mutualistic symbiosis with nitrogen fixing rhizobia provide a benefit through the availability of atmospheric nitrogen.

1.2 Nodules – Site of symbiosis with nitrogen-fixing rhizobia

Symbiosis is the opposite of parasitism where those organisms involved derive benefit from (Douglas 1998). In this particular case, representatives of the Fabaceae enter into symbiosis with nitrogen-fixing bacteria, so-called rhizobia, and host them in specific developed organs, the nodules (Bond 1948; Peter et al. 1996). Rhizobia are able to reduce the

abundant atmospheric nitrogen to ammonia by using the enzyme complex nitrogenase and supply it subsequently to the plant. On exchange, the plant provides the bacteroides with carbon compounds. Thus, the plant achieves a growth advantage towards competitors since nitrogen often limits plant growth (Brear et al. 2013; Ferguson et al. 2010).

Bacterial species of the family Rhizobiaceae belong to the subclass of α -Proteobacteria and encompass six genera based on phylogenetic studies of their 16S rRNA gene: *Rhizobium*, *Sinorhizobium*, *Mesorhizobium*, *Allorhizobium*, *Azorhizobium* and *Bradyrhizobium* (De Meyer et al. 2011; Laguerre et al. 2001). Interestingly, a high host specificity occurs between the rhizobia and the legume host and is determined by the diverse chemical modifications of the nodulation (Nod) factors by the rhizobia (Albrecht 1999; Downie and Walker 1999). Nevertheless, some legume-rhizobia interactions seem to be less specific since nodules of some plants contain more than one particular rhizobia species (De Meyer et al. 2011).

However, nodule morphogenesis can only be initiated by a molecular “conversation” between the host and the symbiont. This interaction is triggered by the exudation of secondary metabolites by the plant roots such as flavones and isoflavones, which act together with bacterial regulatory NodD proteins to activate the transcription of the rhizobial nodulation (*nod*) genes (Fisher and Long 1992; Sajnaga et al. 2001). General *nod* genes (*nodA*, *nodB*, *nodC*) are present in all rhizobia and control the synthesis of lipochitooligosaccharides (LCO) signal molecules known as Nod factors, which cause morphological changes on the plant root, e.g., root hair deformation and activation of root cortical cell divisions (Ferguson et al. 2010; Hirsch 1992; Sajnaga et al. 2001).

Subsequently, rhizobia use different paths to invade plant roots, which are controlled by the host plant. The entry can proceed via root hair bending with formation of an infection thread. Alternatively, rhizobia invade along an intercellular path lacking the infection threads (Ibáñez et al. 2016). The developed nodules are varying in shape and categorized in the two types: indeterminate and determinate. The formation of the type is again, defined by the host plant. Indeterminate nodules are induced by cell division in the inner cortex layers of the plant root and exhibit a lasting apical meristem. Thus, the nodule possesses the ability of an ongoing growth where new cells will be continually added to the distal nodule part, resulting in an elongated cylindrical shape. While the nodule ages the

rhizobia containing area can be divided in the senescence zone, where rhizobia die-off and the nitrogen fixing zone, where rhizobia are still active. In contrast, determinate nodules are characterized by a spherical shape and emerge by the dividing cells in the outer cortex of the plant root. The early cease of cell divisions leads to lack a persistent meristem and the initial nitrogen fixating tissue is entrapped at the center of the nodule and cannot be replaced. Thus, the nodule perishes when it expires (Corby 1988; Hirsch 1992; Sprent 2007). In particular for plant species of the Genistoid clade as well as the Crotalarieae an epidermal infection without infection thread is described and result at least in this species in indeterminate nodules (Sprent et al. 2017).

1.3 Alkaloids in Genistoids and their toxicity

The Genistoid clade of the Fabaceae is incorporated into the subfamily of Papilionoideae of the Fabaceae and encompasses the closely related tribes Crotalarieae, Genisteae, Podalyrieae, Thermopsidae, Sophoreae and Euchrestae. Species of this group are well known for featuring alkaloids as secondary metabolites (Figure 1), particularly quinolizidine alkaloids (QAs) and pyrrolizidine alkaloids (PAs). Due to the distribution of the alkaloids within the genera, a convergent origin is assumed. While QAs are present in most genera of this clade, PAs are only found in Thermopsidae, Genisteae and Crotalarieae (Feitoza and Lima 2021; Wink 2013).

QAs are neurotoxins and PAs are mutagenic and carcinogenic (Wink 2013) and both are able to interfere with different receptors and ion channels of herbivores, bacteria and even viruses, as defense mechanism. QAs bind to either nicotinic- or muscarinic receptors, while some are capable to interact with dopamine or GABA receptors (Wink 2000). Whereas, PAs bind to serotonin receptors (Schmeller et al. 1997), which are involved in many regulations such as appetite, mood, sleep or memory (Wink 2019).

However, they do not have to all herbivores a toxic effect, since a few insect species like aphids, moths or beetles adapted during evolution by developing mechanisms to either detoxify the absorbed alkaloids (QAs or PAs) or store them for reuse as shield against their own predators (Wink 2019).



Figure 1. Phylogeny of the Fabaceae with color-coded distribution of secondary metabolites. Characteristically for species of the Genistoid clade are quinolizidine alkaloids (QAs) and pyrrolizidine alkaloids (PAs) within the Crotilarieae PA taxa. Selected species of the asterisk's labelled taxa are of interest in the following study. Red: quinolizidine alkaloids, green: pyrrolizidine alkaloids, blue: erythrina alkaloids, yellow: physostigmine, black: β -carboline alkaloids (modified from Wink 2013).

1.3.1 Lupins

Lupins (*Lupinus* spp.) are a large genus and include about 500 species (Wink et al. 1995), which are distributed all over the world (Abraham et al. 2019). Relations within the Genistaceae indicates lupins as a separate monophyletic group (Lupininae), clearly defining from the Genistinae (Aïnouche et al. 2003). They produce beans with remarkably high levels of protein (40%) and fiber (30%) as well as low levels of fat and starch, whereby gaining attention to be considered as human health food (Frick et al. 2017). However, they were initially used mainly as fertilizer due to their toxic QAs and the symbiosis with *N*-fixing rhizobia, which they host in indeterminate root-nodules (Sprent 2007; Yang et al. 2017). A

closer look at QAs shows that the alkaloid profiles vary distinctly among the species (Wink et al. 1995).

1.3.2 Laburnum

Laburnum, popularly known as golden chain or bean tree due to its pods resembling miniature beans, is a popular ornamental plant in today's gardens (Schade and Jockusch 2018). This is in most cases the hybrid *Laburnum x watereri*, which was first found growing wild in southern Tirol in 1856. It is a hybrid and combines the characteristic features of large flowers from *L. anagyroides* and the fragrance plus flower color from *L. alpinum* (Greinwald et al. 1990). However, as beautiful as this plant may appear, it belongs to the poisonous plants because of its ingredients. Symptoms of poisoning begin with a burning sensation in the throat, followed by nausea to convulsions and hallucinations before death may occur from respiratory failure. These symptoms are caused by the produced secondary metabolites – QAs and PAs – which are present in all parts of the plant. The prominent alkaloids are the QAs cytisine and *N*-methyleytisine, and the PA laburnine (Neuner-Jehle et al. 1965; Schade and Jockusch 2018). Cytisine is known to be a partial agonist of nicotinic acetylcholine receptors and showed interestingly greater success than nicotine replacement therapy in a New Zealand smoking cessation study (Walker et al. 2014). In the past during the time of the 1st World War, *Laburnum* was smoked as a tobacco substitute. Later, in the 1960s, cytisine was used for smoking cessation, especially in the eastern bloc countries, because it was already known that it had no addictive effect (Jungmayr 2015). Recently, since December 2020, the first cytisine-based preparation for smoking cessation (Asmoken®) is available on the German pharmaceutical market. As the typical fruit shape has already suggested, *Laburnum* belongs to the Fabaceae family and is located within the Genistoid clade (Cardoso et al. 2013). Like most members of this family, *Laburnum* forms a symbiosis with nitrogen-fixing bacteria and harbors them in indeterminate root-nodules (Sprent et al. 2017).

1.3.3 Crotalaria

Crotalaria ("rattlepods") comprised bushes and herbs, which are distributed in tropical and subtropical regions of the world, like Africa, Australia and the U.S. Occasionally it comes to

intoxication of grazing livestock due to the toxic PAs (Fletcher et al. 2009; Johnson et al. 1985; Sy et al. 2001). Nevertheless, various *Crotalaria* species are often planted as crops for fodder or partly used as green manure, because of their symbiosis with nitrogen fixing rhizobia mostly from the genera *Bradyrhizobium* and *Methylobacterium*. For hosting their symbiont, plants forming specialized organs, referred to as indeterminate root-nodules (Sprent et al. 2017). They are incorporated in the Genistoid clade, tribe Crotalariaeae, and produce PAs as secondary metabolites (Wink 2013). In *C. spectabilis*, PA biosynthesis of the main alkaloid monocrotaline is nodule-dependent (Irmer et al. 2015). Monocrotaline exhibits carcinogenic activity and causes liver tumors in rats when administered orally ("Monocrotaline" 1976). Studies in recent years have shown, that the biosynthetic site of PAs seems to be localized in a wide variety of tissues, when considering different species through the plant kingdom (Moll et al. 2002; Anke et al. 2008; Niemüller et al. 2012).

1.4 The biosynthesis of Quinolizidine alkaloids

More than 200 different QAs occur naturally and are typically found in some phylogenetically related tribes of the leguminosae, in particular within lupins (Wink 1992; Ohmiya et al. 1995). Additionally, they have been found in some unrelated genera such as Chenopodiaceae, Berberidaceae, Ranunculaceae, Santalaceae, Scrophulariaceae and Solanaceae (Bunsupa et al. 2012a; Woldemichael and Wink 2002).

For decades, a lysine decarboxylase (LDC) has been postulated to be involved in QA biosynthesis (Hartmann et al. 1980). Later it was shown that LDC emerged from the duplication of a gene encoding enzyme of primary metabolism, an ornithine decarboxylase (ODC) (Bunsupa et al. 2012a). Some studies have already been shown that essential genes of primary metabolism provide an important pool of genes for duplicates that have been recruited for specific functions in secondary metabolism (Nakajima et al. 1993; Hashimoto et al. 1998; Ober and Kaltenegger 2009; Teuber et al. 2007; Kraker and Gershenzon 2011; Bunsupa et al. 2012a). Besides, Takatsuka et al. (2000) described already a lysine decarboxylase in the bacterium *Selenomonas ruminantium* that decarboxylate both ornithine and lysine.

ODCs are pyridoxal-5'-phosphate (PLP)-dependent amino acid decarboxylases that occur as homodimers and catalyze the first step in the polyamine biosynthesis by producing putrescine (Kern et al. 1999; Pegg 2006; Figure 2).

Already Sandmeier et al. (1994) speculated an PLP-depending enzyme to be involved in the formation of cadaverine. Bunsupa et al. (2012a) evidenced in *Lupinus angustifolius* not only that LDC catalyzes lysine to cadavarine as PLP-depending enzyme (Figure 2) but also being substantially involved in the first step of QA biosynthesis by means of site-directed mutagenesis and protein modelling. Within this study they tested recombinant enzymes that might have both LDC as well ODC (L/ODCs) activity and were able to show that these enzymes are able to catalyze the decarboxylation of L-lysine to cadaverine. Furthermore, L/ODC was fused to a green fluorescent protein and was then localized in chloroplasts by the use of *in vivo* experiments in *Arabidopsis thaliana* (Bunsupa et al. 2012a). Plastid genes have no introns due to their bacterial origin which fit to the findings in the L/ODC gene that showed no introns (Bunsupa et al. 2012a).

After the decarboxylation of lysine to cadaverine, the next step in QA biosynthesis is the oxidation of cadaverine (Saito and Murakoshi 1995; Bunsupa et al. 2012a) by a copper amino oxidase (Yang et al. 2017). The resulting 5-aminopentanal will spontaneously cyclizes to Δ^1 -piperidine, an intermediate in the biosynthesis of various lysine derived alkaloids (Bunsupa et al. 2012b).

All QAs feature as distinct structure a quinolizidine ring (Figure 2), which is mainly grouped into (1) bicyclic alkaloids such as lupinine and (2) into tetracyclic alkaloids like sparteine, lupanine, and hydroxylupanine as well as their derivates (Wink 1987; Bunsupa et al. 2012b). Derivates can be obtained by further modifications as acetylation, esterification, dehydrogenation, hydroxylation, glycosylation, and oxygenation resulting in the previous mentioned great structural diversity of QAs (Osorio and Till 2022). The QAs are transported via the phloem and the transport is related to the diurnal rhythm, like the synthesis of QAs as well (Wink and Hartmann 1982; Wink and Witte 1984; Wink 1985). QAs are bitter tasting compounds and are toxic to humans, farmer animals and insects, whereby the toxicity and deterrence effect can vary. Described as most toxic QAs to humans and animals are sparteine and lupanine (Osorio and Till 2022). To survive aphid attacks plants have the best chance with lupanine followed by, in descending order, sparteine, lupinine, 13- α -

hydroxylupanine and angustifoline which have a moderate impact (Philippi et al. 2015). Recent studies reported also QA toxicity on larvae of different species (Elma et al. 2021). A better knowledge about QA biosynthesis would provide the base for improved pest control and risk assessment with respect to the use of fabaceous plants as agricultural crops.

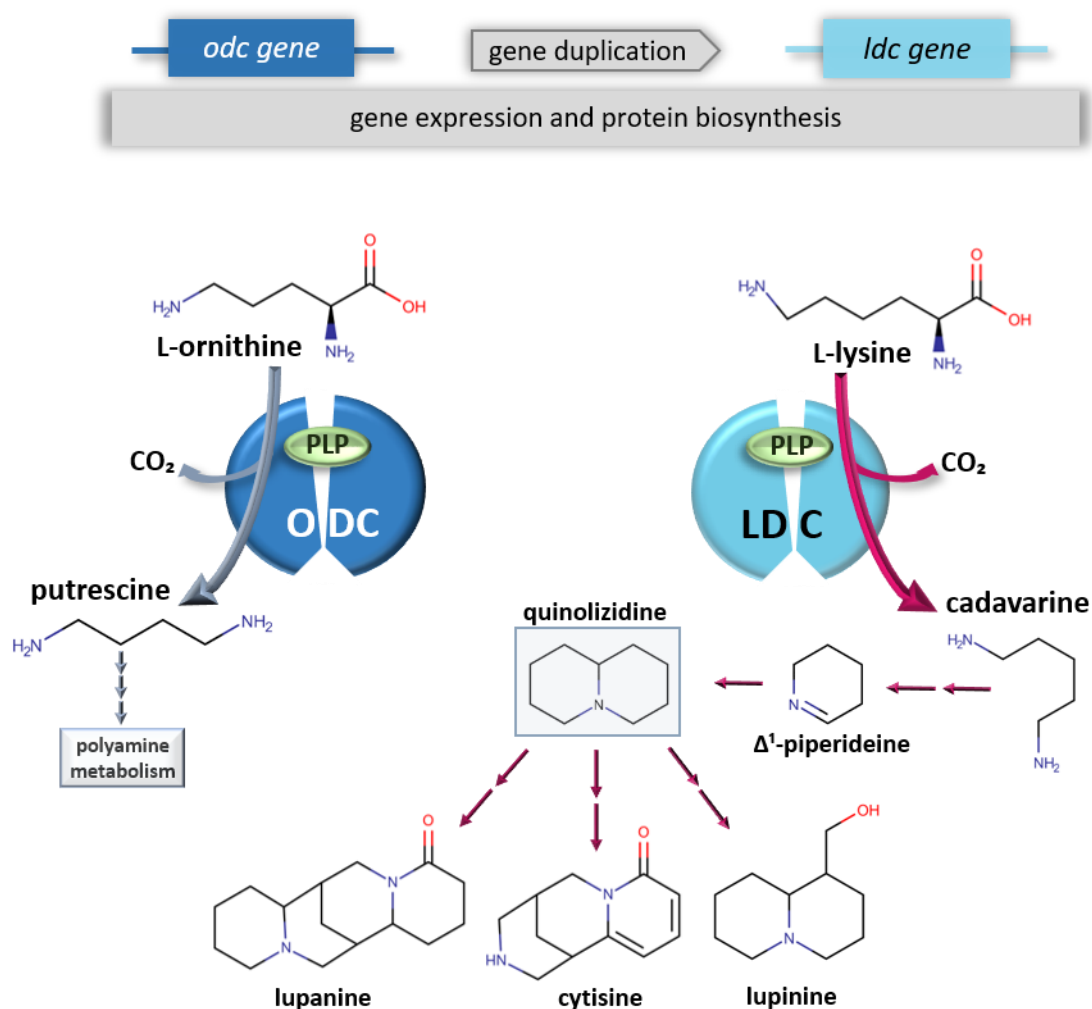


Figure 2. Origin of lysine decarboxylase (LDC) by duplication of the gene encoding ornithine decarboxylase (ODC). Both enzymes are pyridoxal 5'-phosphate (PLP)-dependent amino acid decarboxylases and occur as homodimers. While ODC catalyzes the first step in the polyamine biosynthesis by producing putrescine from ornithine, LDC is reported to catalyze the first step in the quinolizidine alkaloid pathway by converting lysine into cadavarine. Further steps are involved to constitute a complete QA.

1.5 The biosynthesis of Pyrrolizidine alkaloids

PAs are plant toxins and serve as general defense against herbivores. The research was intensified after the mid-20th century, when the first PAs were identified. From 27 isolated structures in the 1950s up to over 400 (Hartmann and Witte 1995). PAs are considered more precisely as ester alkaloids and are assembled of a characteristic nitrogen containing bicyclic backbone, the necine base, and of one or more necic acids (Hartmann and Toppel 1987). The numerous possibilities of esterifications lead to the large variety of structures (Hartmann and Witte 1995; Hartmann and Ober 2000). The typically form of PAs in plant tissues is their hydrophilic non-toxic *N*-oxide, which is transportable as well as storable within the the plant. The conversion of the non-toxic *N*-oxide into the lipophilic protoxic tertiary amines happens not until PAs are ingested by herbivores (Lindigkeit et al. 1997). While the hydrophilic non-toxic *N*-oxides are incapable to pass membranes, the lipophilic protoxic forms are able to penetrate membranes and are accepted as substrate by cytochrome P450 enzymes (Hartmann 1994; Hartmann 1999). These bioactivating enzymes are present in insects as well as in liver of vertebrates (Lindigkeit et al. 1997; Chang and Hartmann 1998). The pyrrolic intermediates resulting from this bioactivation react easily with nucleophiles like nucleic acids and proteins of the herbivor and cause cell-toxicity (Fu et al. 2004). While a lot of research was invested in the elucidation of their chemical structures und functions, less progress was achieved within the fields of potential involved enzymes within the biosynthesis of PAs. An exception here is the first specific enzyme in the PA pathway which is evidenced to be a homospermidine synthase (HSS, EC 2.5.1.45) that evolved at least six times (Irmer et al. 2015; Kaltenegger et al. 2013; Reimann et al. 2004) independently within the angiosperms by duplication of the gene encoding deoxyhypusine synthase (DHS, EC 2.5.1.46), an enzyme involved in primary metabolism (Ober and Hartmann 1999b). DHS core activity is catalyzing the posttranslational activation of the eukaryotic initiation factor 5A (eIF5A), which is involved in indispensable cell regulations (Park et al. 1997). DHS catalyzes the first step of the posttranslational activation by transferring the 4-aminobutyl moiety of spermidine to a specific lysine residue in the eIF5A precursor protein. The resulting protein-bound amino acid deoxyhypusine (Figure 3) is hydroxylated in the second step to hypusine resulting in the activation of the eIF5A protein (Park et al. 1993; Park et al. 1997). Furthermore, DHS shows a side-activity by

catalyzing the formation of homospermidine by transferring the 4-aminobutyl moiety of spermidine to putrescine (Ober and Hartmann 1999a; Ober et al. 2003). While this side-activity of DHS seems to have minor relevance in plants, HSS shows this activity as core-activity and lost completely the ability to bind the eIF5A precursor protein (Figure 3). The formed homospermidine is the precursor of the necine base of PAs (Ober and Kaltenegger 2009). For the second step of PA biosynthesis a homospermidine oxidase (HSO) was identified recently in the Heliotropiaceae *Heliotropium indicum* (Indian Heliotrope) that oxidizes both primary amino groups of homospermidine to form the bicyclic 1-formylpyrrolizidine a PA pathway intermediate (Zakaria et al. 2022).

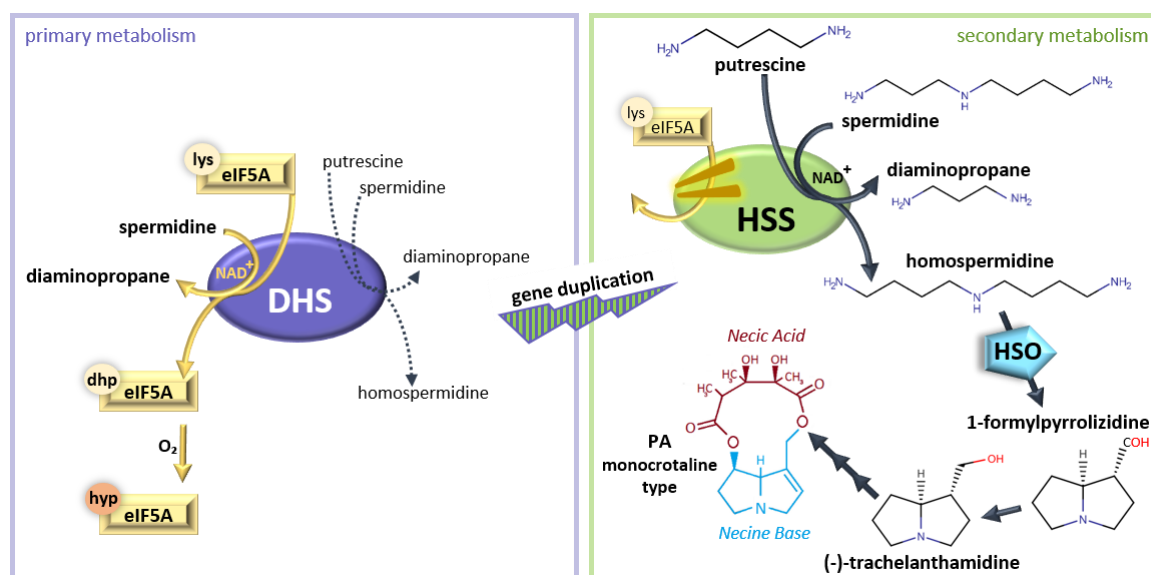


Figure 3. Illustration of the origin of homospermidine synthase (HSS) by duplication of the gene encoding deoxyhypusine synthase (DHS). The newly formed functional enzyme HSS catalyzes the first specific step in PA biosynthesis, while DHS catalyzes as core activity the first step of the posttranslational activation of the eukaryotic initiation factor (eIF5A). HSS lost the ability to bind the eIF5A precursor protein and instead produces homospermidine as precursor for the necine base moiety of PAs. The second step was recently identified by identifying a homospermidine oxidase (HSO) of *Heliotropium indicum*, a species belonging to the Heliotropiaceae. HSO catalyzes homospermidine to 1-formylpyrrolizidine a pathway intermediate that has been shown to be incorporated into trachelanthamidine. Further steps remain still unknown. dhp, deoxyhypusine residue; hyp, hypusine residue; lys, lysine residue.

2. AIMS OF THIS WORK

The Fabaceae are well known for their symbiosis with nitrogen fixing rhizobia and encompass many crops. Several genera contain secondary metabolites such as alkaloids as a defense strategy. Within the tribe Genisteae, two alkaloid types occur, the QAs and the PAs. For both biosynthetic pathways quite a broad knowledge exists about the first specific enzyme. However, little is known about further involved enzymes. Likewise of further interest is to study the impact of the biotic factor nodulation on the two above mentioned alkaloid biosynthesis in different species.

Accordingly, the main questions of this thesis are: Which are the next involved genes within the biosynthesis of PAs? Which cells within nodules contain HSS, the first specific enzyme of PA biosynthesis? Are there existing more species where *hss* transcript is only detectable in nodules? Which impact has nodulation on the biosynthesis of QAs?

Three main species have been chosen as model plants to study these questions: (1) *Crotalaria spectabilis*, a plant in which PA biosynthesis is nodule dependent. (2) The two lupins *L. arboreus* and *L. polyphyllus* which produce QAs, and (3) *Laburnum x watereri* 'Vossii', which contains both PAs and QAs.

In **CHAPTER A** the focus is directed to the identification of genes that are involved in further steps of synthesizing PAs of PA producer *Crotalaria*. Transcript analysis identified two potential *cuaos* out of 5 as “hot candidates” being involved in the PA biosynthesis. Subsequently, a method was established to generate transgenic *Crotalaria* plants using CRISPR/Cas9 to knockout the candidate genes. Genomic DNA screening revealed mutations within the candidate genes. Plants with mutations were considered as possible “knockouts” and were further cultivated, infected with rhizobia for nodule development and subsequently examined for the presence of PAs. Further analytical investigations revealed which enzyme of the two candidates catalyze the second- and which the third step.

CHAPTER B focuses mainly on the possible impact of nodulation on QA biosynthesis of lupins and golden chain. For this purpose, we first isolated species-specific rhizobia to establish *in vitro* cultures to allow cultivation under controlled conditions. Then, sequences of the first specific enzyme (*Idc*) were identified. *Idc* transcripts were analyzed via RT-qPCR in a wide variety of tissues from infected and non-infected plants. Also, the content (QAs) was analyzed by GC-MS. Results of present *Idc* transcripts and QAs were compared between infected and non-infected plants to find out if differences occur regarding nodulation. Furthermore, to verify the LDC function, the activity was determined by protein assays where we developed a new HPLC-based method.

CHAPTER C describes the studies on the influence of nodulation on PA biosynthesis in the ornamental plant *L. x watereri* ‘Vossii’. First, sequences of *hss*, *dhs*, and housekeeping genes *ubiquitin* and *ef1a* were identified and their transcripts quantified by RT-qPCR in different tissues of nodulated and nodule-free plants. In addition to the nodules, which showed a high transcript level of the first specific enzyme *hss*, the pods also showed a low *hss* transcript level. Furthermore, we located the HSS protein via immunolabeling with HSS specific antibodies in *C. spectabilis* and *L. x watereri* ‘Vossii’. Since two PA-producing Fabaceae already show nodule dependency, it is exciting to see whether non-PA producers also have a *hss*-like transcript expressed in the nodules. Therefore, we tested tissues of three selected non-PA producing species of the Genistoids. If non-PA producer also still contain *hss* transcript in nodules, it would indicate that the *hss* has come under nodule control during gene duplication.

The last **CHAPTER D** contains the identification of further involved genes within the PA biosynthesis of the species *L. x watereri* 'Vossii'. So far, five different *cuaos* were identified by using known sequences of *C. spectabilis* for blast searches against an unassembled *L. anagyroides* genome available online. The transcripts of the five *cuaos* were quantified in various tissues of infected and non-infected plant individuals for co-transcription with *hss* via RT-qPCR.

3. CHAPTER A

Homospermidine conversion to the pyrrolizidine backbone is catalyzed by two distinct copper-containing amine oxidases in *Crotalaria spectabilis* (Fabaceae)

Nadine Jacky ^a, Mahmoud M. Zakaria ^{a,b}, Britta Milewski ^a, Anna-Lena Sprick, and Dietrich Ober ^a

^a Botanical Institute and Botanic Gardens, Kiel University, Kiel, Germany

^b Department of Pharmacognosy, Faculty of Pharmacy, Zagazig University, 44519 Zagazig, Egypt

Detailed author contributions are listed at the end of the thesis.

3.1 ABSTRACT

CuAOs are known to regulate the intracellular levels of polyamines, metabolites that are known to be involved in a plethora of developmental processes and stress response reactions of the plant. Polyamines are also described as key intermediates in the biosynthesis of various alkaloids, where they are converted by CuAOs to aldehydes that easily cyclize to characteristic heterocyclic structures. Recently, using *Heliotropium indicum* (Heliotropiaceae, Boraginales) and *Symphytum officinale* (Boraginaceae, Boraginales) as models, CuAOs have been described to be involved in the biosynthesis of pyrrolizidine alkaloids (PAs), a class of toxic alkaloids that are part of the plant's chemical defense against herbivores. In contrast to other CuAOs, this CuAO, now named homospermidine oxidase (HSO), was shown to oxidize both primary amino groups of homospermidine and to control the formation of the bicyclic pyrrolizidine backbone. Studies on the first pathway-specific enzyme, homospermidine synthase (HSS), suggest that PA biosynthesis evolved independently in the various PA-producing lineages, also supporting an independent evolution in the Boraginales lineage and the PA-producing genus *Crotalaria* of the Fabaceae lineage. Using *Crotalaria spectabilis* as a model, we have recently shown that nodules, the structures formed as part of the symbiosis with rhizobial bacteria, are the site of PA biosynthesis. Here we show that we have been able to identify two CuAO-encoding sequences as candidates for HSO from nodules of *C. spectabilis*, CsCuAO1 and CsCuAO5. By a CRISPR/Cas9-mediated approach, the previously described gene-encoding HSS of *C. spectabilis* has been inactivated, resulting in mutant plants that are unable to produce PAs. Using the same strategy for the two candidate CuAO sequences, we provide *in planta* evidence for their involvement in PA biosynthesis, as the inactivation of both candidate genes resulted in PA-free mutants. Analyses of polyamine levels of these mutants and GC-MS analytics of putative intermediates in the CsHSS-knockout line after feeding of homospermidine suggest that the two CuAOs act sequentially with CsCuAO5 first oxidizing homospermidine to a monocyclic intermediate that is further converted by CsCuAO1 to 1-formylpyrrolizidine providing the characteristic bicyclic ring structure of PAs. Our data show that in contrast to the previously described HSO of *H. indicum* and *S. officinale*, the conversion of homospermidine to the pyrrolizidine backbone is realized in *Crotalaria* by two sequentially acting CuAOs subdividing the reaction in two subreactions providing further support for the interpretation of an independent evolution of PA biosynthesis in these lineages.

3.2 INTRODUCTION

Copper-containing amine oxidases (CuAOs) are a class of ubiquitously occurring enzymes that are described to be involved in central processes as cell differentiation and proliferation, cell signaling, or detoxification (Li et al. 1998; Lunelli et al. 2005; Medda et al. 2009). In plants, CuAOs are involved in developmental processes and adaptive responses to various environmental stresses (Bouchereau et al. 1999; Walters 2003). CuAOs regulate polyamine levels by catalyzing the oxidative deamination of a primary amino group of various mono-, di-, and polyamines, in plants, mainly putrescine (Put), spermidine (Spd), spermine (Spm), and cadaverine (Cad) (Liu et al., 2015; Tavladoraki et al., 2016). The corresponding amino aldehydes, hydrogen peroxide, and ammonia are the products, of which H_2O_2 was shown to act as signal molecule responsible for a plethora of secondary effects (Groß et al. 2017).

The amino aldehydes formed by CuAOs have been shown to be important early precursors in the biosynthesis of a variety of plant-derived alkaloids that cyclize and build up the cyclic backbone of tropane alkaloids and nicotine (Hashimoto et al. 1990; Heim et al. 2007; Katoh et al. 2007; Naconsie et al. 2014), quinolizidine alkaloids (Yang et al. 2017) or piperine alkaloids (Gerdes and Leistner 1979). The involvement of CuAOs was also postulated for the biosynthesis of pyrrolizidine alkaloids (PAs) (Böttcher et al. 1993; Frölich et al. 2007). PAs are a group of specialized metabolites that are produced by the plant as part of its chemical defense against herbivores (Ober and Hartmann 2000; Hartmann and Ober 2008). Studies on the first specific step in PA biosynthesis, *i.e.*, the formation of homospermidine (Hspd) by homospermidine synthase (HSS), suggested that PA biosynthesis evolved several times independently during angiosperm evolution (Reimann et al. 2004; Kaltenegger et al. 2013). Knowledge about further steps of PA biosynthesis is scarce. Recently, using *Heliotropium indicum* (Indian heliotrope, Heliotropiaceae, Boraginales) and *Symphytum officinale* (comfrey, Boraginaceae, Boraginales) as models, we have been able to identify homospermidine oxidase (HSO), a CuAO that catalyzes the oxidative deamination of both primary amino groups of Hspd and controls the formation of the bicyclic pyrrolizidine backbone (Zakaria et al. 2022).

The genus *Crotalaria* (rattlepods, Fabaceae) encompasses herbs and bushes with a tropical and subtropical distribution (Polhill and Raven 1981; Mosjidis and Wang 2011). *Crotalaria* is well known for the production of toxic PAs that are not only part of fascinating plant-

insect interactions (Eisner and Meinwald 1995), but also hold responsible for occasional intoxications of grazing livestock and humans (Fletcher et al. 2009; Anjos et al. 2010; Botha et al. 2012). Nevertheless, various *Crotalaria* species are often planted as crops for fodder or as green manure because of their symbiosis with nitrogen fixing rhizobia. Recently, it was shown that in *Crotalaria spectabilis*, the biosynthesis of monocrotaline, the only PA produced in this species, is dependent on nodulation after infection with a specific *Bradyrhizobium* strain (Irmer et al. 2015). Transcripts encoding HSS have been detectable only in nodules that have been interpreted as the site of PA biosynthesis from where PAs are transported to the shoot (Irmer et al. 2015). Phylogenetic data of HSS suggest an independent origin of this enzyme in the Fabaceae lineage, well separated from the PA-producing lineages of the Boraginales including *H. indicum* and *S. officinale*. Therefore, we analyzed Hspd oxidation in more detail in *C. spectabilis* as the step in PA biosynthesis that is quintessential for the formation of the characteristic bicyclic backbone. Using transcriptome data, we identified two CuAO candidates that showed exclusive expression in root nodules. After developing a protocol for stable transformation of *C. spectabilis* with *Agrobacterium tumefaciens*, we have been able to analyze the effects of inactivation of the two candidates on PA biosynthesis in genome-edited transgenic plants infected with *Bradyrhizobium*.

Here we show that, in *C. spectabilis*, two CuAOs are involved in the oxidation of Hspd by dividing this enzymatic step that was shown to be catalyzed by a single enzyme in species of the Boraginales order into two successive and distinct steps. Only if both enzymes were active, PAs have been detectable in *C. spectabilis*. This observation shows that Hspd oxidation is realized in different ways in the PA-producing lineages of the Boraginales and the Fabaceae and allows not only deeper insights into the evolution of PA biosynthesis, but also into hitherto undescribed properties of CuAOs in general.

3.3 RESULTS

3.3.1 Two CuAO-encoding genes show co-expression with HSS and are regarded as candidates for an HSO

To identify CuAOs that are involved in *C. spectabilis* in the oxidation of Hspd, five transcripts encoding CuAO-like proteins (CsCuAO1 to CsCuAO5) have been identified in transcriptome data of *C. spectabilis* roots and nodules (unpublished data). To test for a co-expression of these CuAO-coding genes with the gene encoding HSS, cDNA of leaves, stems, roots, and nodules of two, four-, and twelve-months old individuals of *C. spectabilis* were used for reverse transcription quantitative polymerase chain reaction (RT-qPCR) analyses using the gene encoding *ubiquitin* (UBQ) as reference. The gene encoding CsHSS is shown to be expressed exclusively in nodules, confirming previous observations that HSS expression is restricted to nodules (Irmer et al. 2015; Figure 1A). From the *cscuao* genes, only *cscuao4* shows balanced expression levels in all analyzed tissues (Figure 1E). The other *cscuao* genes have the highest transcript levels in nodules (Figure 1, B, C, D and F). However, nodule-specific expression, *i.e.*, expression only in nodules and not even in traces in any other analyzed tissue, was only observed for the genes encoding CsCuAO1 and CsCuAO5 (Figure 1, B and F). As the first steps of PA biosynthesis are most likely restricted to nodules and are not expressed in any other tissue as it is observed for the transcript of CsHSS, CsCuAO1 and CsCuAO5 have been regarded as most promising candidates to encode an HSO. Of note, a gradual decrease of transcript levels of these two *cua* genes and of *cshss* was observed as plants and nodules age. Referring the RT-qPCR data to the transcript level of the gene encoding actin (ACT) resulted in essentially the same conclusions (Supplemental Figure S1). The transcript sequences of the genes encoding CsCuAO1 and CsCuAO5 were validated by PCR amplification of cDNA isolated from nodules with proofreading DNA polymerases. The open reading frames were shown to be 2,022 and 2,073 bp long for CsCuAO1 and CsCuAO5, respectively, and are predicted by the SignalP-5.0 server (Almagro Armenteros et al. 2019b) and the TargetP-2.0 server (Almagro Armenteros et al. 2019a) to encode *N*-terminal signal peptides of 22 and 24 amino acids in length, respectively, directing the encoded proteins to the secretory pathway. CsCuAO3 is also predicted to encode an *N*-terminal signal peptide of 19 amino acids, while a signal peptide was not predicted for CsCuAO2 and CsCuAO4.

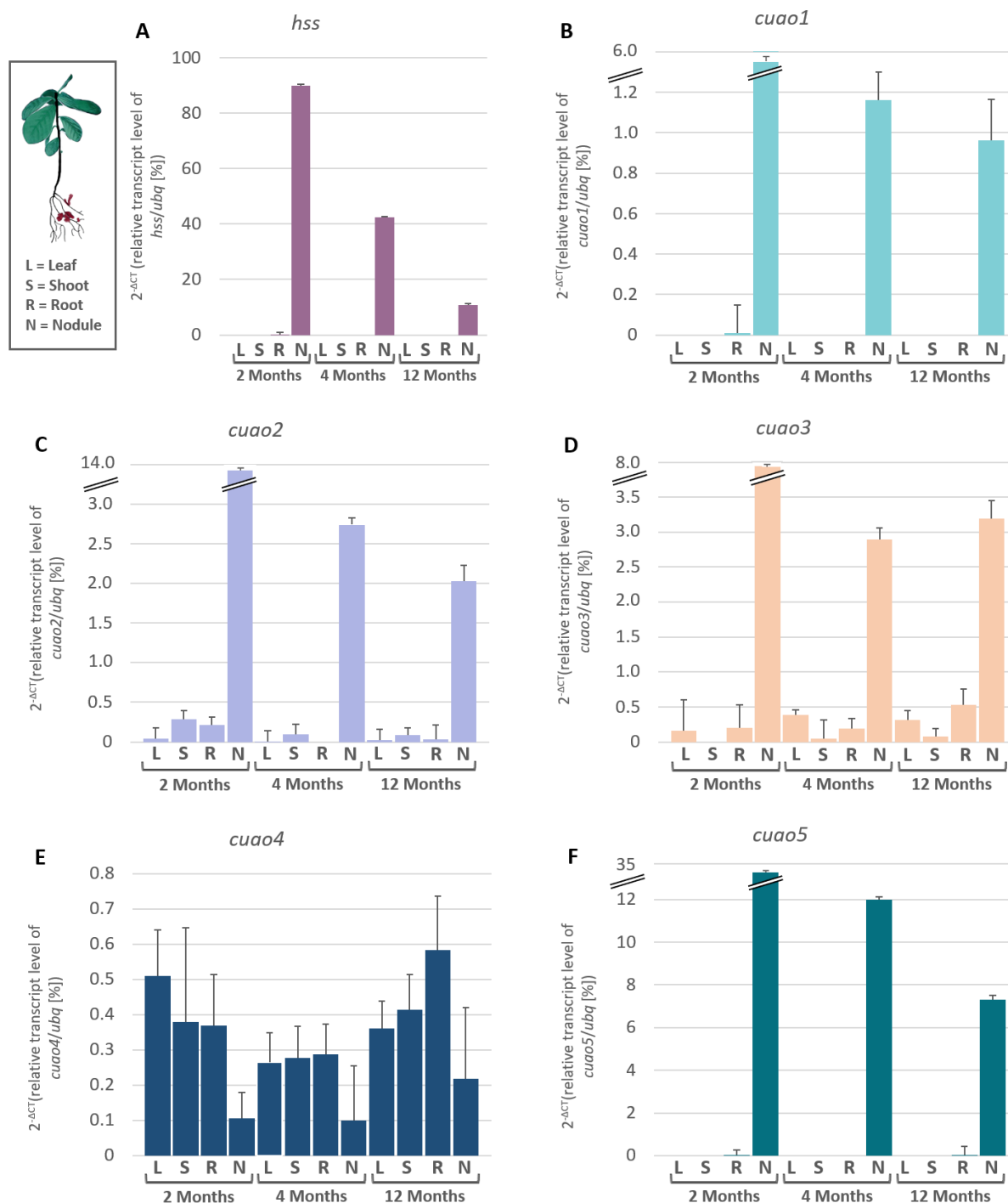


Figure 1. Relative expression profile of the genes encoding CuAOs in *C. spectabilis*. Various tissues of in vitro-grown *C. spectabilis* individuals that nodulated after infection with *Bradyrhizobium* were analyzed after 2, 4, and 12 months. The gene encoding ubiquitin (UBQ) served as reference for normalization of expression levels. L, leaf; S, stem; R, root; N, nodule.

3.3.2 Transformation of *C. spectabilis* allowed editing of selected genes

To study the relevance of *CsCuAO1* and *CsCuAO5* for PA biosynthesis, mutants were generated, in which one of these genes was inactivated using CRISPR/Cas9-mediated genome editing (Figure 2). To ensure that only protospacer motives have been selected that do not cover an exon-intron boundary, genomic sequences of the *cscuao1* and *cscuao5* genes have been amplified and sequenced, resulting in identification of a partial genomic sequence encompassing two partial exon sequences separated by an intron of *cscuao1* and the full sequence of the *cscuao5* gene (Figure 2, A and B). For the transformation of plants, binary vectors have been used carrying CRISPR/Cas9 cassettes harboring the gene encoding Cas9 protein and two sgRNAs targeting two different protospacer motives within two neighboring exons of the target gene to increase the chance for larger deletions (sites A and B and sites C and D for *cuao1* and *cuao5*, respectively). Genome editing of the *hss* gene has been included in this study as a positive control as it is well-characterized gene involved in PA biosynthesis. The corresponding CRISPR/Cas9 construct targeted only one protospacer motif in exon 1 of the *hss* gene (Figure 2C). Using these binary vector constructs, we generated transgenic plants of *C. spectabilis* by transformation with *A. tumefaciens* as described in Supplemental Figure S2. To test the individual transgenic plants for genome editing effects, the targeted gene regions have been amplified from genomic DNA of leaves. Transgenic plants resulting from transformation with the empty binary vector still containing the *ccdB* suicide gene served as control lines.

Table 1 lists the sequences of these genes in the area of the protospacer motives as they resulted from genotyping of the mutants compared to the two control lines (CL1 and CL2), which showed the wild-type sequence in all target sites.

Using the construct encoding two sgRNAs targeting the sites A and B in the *cscuao1* gene, five transgenic plants were obtained (plants CuAO1-1 to CuAO1-5). Except for plant CuAO1-3, all plants showed modifications of the genomic sequence within the target site B, while target site A was unaffected. For three out of the four lines with genome editing effects, the analyzed sequence revealed different mutations within the two alleles. Such a mutation type was classified as ‘biallelic’ mutation type according to our classification in Zakaria et al. (2021). Lines that showed identical mutations within the two alleles were

classified as ‘homozygous’ mutation type accordingly. In three plants, the modifications at site B were small insertions or deletions of 1 and 5 nucleotides in length. Plant CuAO1-4 had a large insertion of 133 nucleotides at this site in one of the alleles.

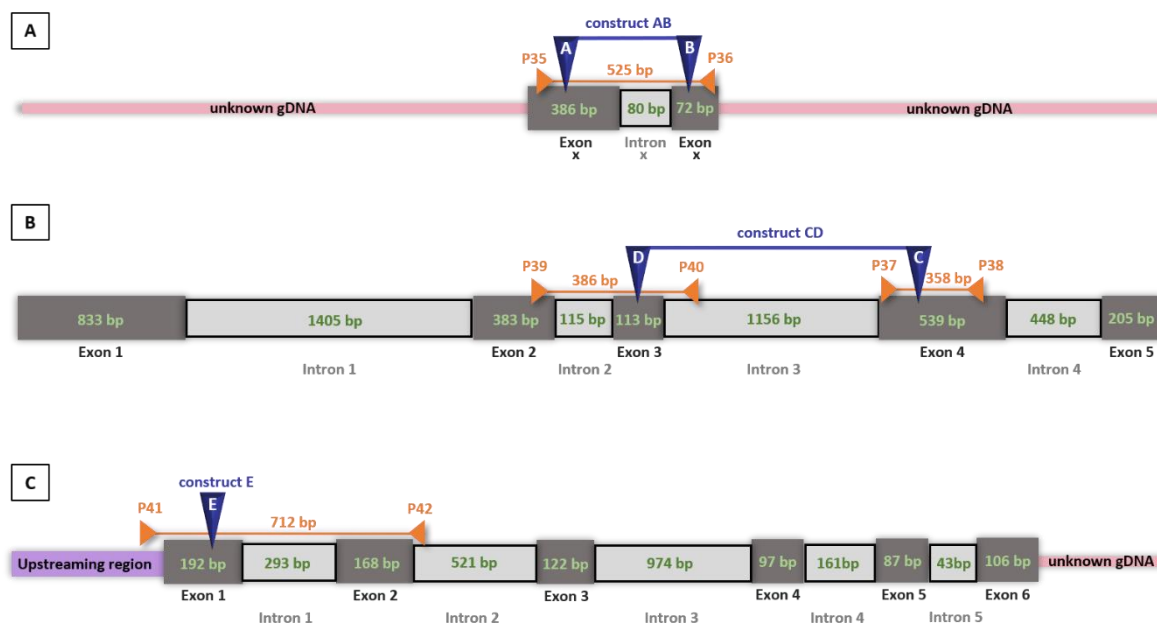





Figure 2. DNA sequences of the genes encoding *CsCuAO1*, *CsCuAO5*, and *CsHSS* of *C. spectabilis* used to select protospacer motives for genome editing. **A** Partial genomic sequence of the *cscuaa1* gene spanning parts of two exons that are separated by an intron. For *cscuaa1*, one construct comprised two sgRNAs (sites A and B). **B** Complete genomic sequence covering the complete ORF of the *cscuaa5* gene being composed of five exons separated by four introns. For *cscuaa5*, the construct comprised two sgRNAs (sites C and D) as well. **C** Partial genomic sequence of the *cshss* gene, starting with parts of upstreaming region to exon 6. For *cshss*, the construct comprised only one sgRNA (site E). Blue longitudinal arrows show gene regions targeted by the three different CRISPR/Cas9 constructs. Orange arrows display primer positions and their expected product size (without mutations) for the later screening of transgenic plants to determine possible mutations. ORF, open reading frame; PAM, protospacer adjacent motif; sgRNA, single guide RNA.

Transformation with the construct encoding the two sgRNAs targeting the sites C and D in *cscuaa5* resulted in eight transgenic plants that showed sequence modifications at both target sites, except for plant CuAO5-3 that possessed the wild-type sequence in both target sites. In the seven edited lines, the biallelic type was the predominant type showing small insertions or deletions ranging between 1 and 15 nucleotides in length, except for plant CuAO5-4 that showed a large deletion of 41 nucleotides in one of the two edited alleles. Of note, nucleotide substitutions were observed together with nucleotide deletions in one

allele at the target site C of plant CuAO5-1 and the target site D of plant CuAO5-8. Of note, in none of the analyzed mutants, we have detected a deletion of a larger stretch of genomic DNA resulting from Cas9-induced double-strand breaks at both targeted positions simultaneously.

Using the construct E targeting exon 1 of *cshss*, only two transformed plants could be regenerated. One plant, *i.e.*, HSS-1, showed two different insertions of one nucleotide at the target site in the two alleles. The other transformed plant, *i.e.*, HSS-2, showed an identical deletion of 9 nucleotides in the two alleles ('homozygous' mutation type).

Table. 1. Sequence analyses of CRISPR/Cas9-induced mutations within the genes encoding CsCuAO1, CsCuAO5, and CsHSS in transgenic plant lines of *C. spectabilis*. For genome editing of the genes encoding CsCuAO1 and CsCuAO5, constructs have been used that targeted two different protospacer motives in two neighboring exons to increase the possibility to obtain larger mutations. For *cshss*, a construct was used that targeted only one protospacer motif in exon 1. Sequences obtained from the control lines (CL1, CL2) are identical to the sequence of the wild-type plant (WT). The red arrowhead indicates the Cas9 cleavage site. Red hyphens indicate deletions, red nucleotides represent insertions or substitutions, Ⓢ labels a large insertion of 133 nucleotides. Predicted and established effects on the respective gene: KO, knockout, NE, no effect. Established effects are given for transgenic nodulated plants of which three technical/biological replicates have been examined for the presence of PAs.

Gene of Interest	Transgenic Plant	First Construct Sequence of Protospacer Motif including PAM	Size of Del./Ins./Sub. (-/+/->)	Allelic Differences of Mutations	Second Construct Sequence of Protospacer Motif including PAM	Size of Del./Ins./Sub. (-/+/->)	Allelic Differences of Mutations	Expected Effect	PA Screen	Established Effect
	CL1	GAATGTTATACGTTACCTACTTTGATTGGTGAATATGGGT	0	WT	Site A Protospacer 20 nt GTAAGAATGATAACAA C AGCTGG C AACTACGACT * active center PAM	0	WT	NE	+	NE
	<i>cuao1-1</i>	GAATGTTATACGTTACCTACTTTGATTGGTGAATATGGGT	0	WT	GGTAAGAATGATAA - - - - AGCTGG CAACTACGACT	-4	Homozygous	KO	-	KO
	<i>cuao1-2</i>	GAATGTTATACGTTACCTACTTTGATTGGTGAATATGGGT	0	WT	GGTAAGAATGATAACAA C AGCTGG CAACTACGACT	+1	Biallelic	KO	-	KO
	<i>cuao1-3</i>	GAATGTTATACGTTACCTACTTTGATTGGTGAATATGGGT	0	WT	GGTAAGAATGATAACAA C AGCTGG CAACTACGACT	0	WT	NE	+	NE
	<i>cuao1-4</i>	GAATGTTATACGTTACCTACTTTGATTGGTGAATATGGGT	0	WT	GGTAAGAATGATAACAA C AGCTGG CAACTACGACT	+133	Biallelic	KO	-	KO
	<i>cuao1-5</i>	GAATGTTATACGTTACCTACTTTGATTGGTGAATATGGGT	0	WT	GGTAAGAATGAT - - - - C AGCTGG CAACTACGACT	-5	Biallelic	KO	-	KO
					GGTAAGAATGATAA - - - - GCTGG CAACTACGACT	-5				
	CL1	GGATTGGAGTTTACCGATCATTACATTTACATTTACGATCTTGACCTTGACATTGAT	0	WT	Site D Protospacer 20 nt ATCCGATC TATAGTACATCTGTGGGCAACTATGAC * active center PAM	0	WT	NE	+	NE
	<i>cuao5-1</i>	GGTGA - - - - - TCCAACTTCAGACG TGAAGGTCA CCGAT	-15/Sub.	Biallelic	ATCCGATC T - - - - - CACTGTGGGCAACTATGAC	-5	Monoallelic	KO	-	KO
	<i>cuao5-2</i>	GGATTGGAGTTTACCATG - TCACCTTTACATTTACCATCTTGACCTTGACA TTGAT	-1		ATCCGATC T - - - - - GTGGGCAACTATGAC	-9	Homozygous	KO	-	KO
	<i>cuao5-3</i>	GGATTGGAGTTTACCATGATCATTATACATTTACCATCTTGACCTTGACA TTGAT	0	WT	ATCCGATC TATAGTACATCTGTGGGCAACTATGAC	0	WT	NE	+	NE
	<i>cuao5-4</i>	GGATTGGAGT - - - - - CACTTTACATTTACCATCTTGACCTTGACA TTGAT	-10	Biallelic	ATCCGATC T - - - - - CACTGTGGGCAACTATGA	-5	Monoallelic	KO	-	KO
	<i>cuao5-5</i>	GGATTGGAGT - - - - - CACTTTACATTTACCATCTTGACCTTGACA TTGAT	-41/+1		ATCCGATC - - - - - ACTGTGGGCAACTATGAC	-7				
	<i>cuao5-6</i>	GGATTGGAGTTTACCATG - - - - - TTACATTTACCATCTTGACCTTGACA TTGAT	-9	Biallelic	ATCCGATC T - - - - - CACTGTGGGCAACTATGAC	-5	Biallelic	KO	-	KO
	<i>cuao5-7</i>	GGATTGGAGTTTACCATG - TCACCTTTACATTTACCATCTTGACCTTGACA TTGAT	-6	Biallelic	ATCCGATC T - - - - - CACTGTGGGCAACTATGAC	-5	Biallelic	KO	-	KO
	<i>cuao5-8</i>	GGATTGGAGTTTACCATG - - - - - TTACATTTACCATCTTGACCTTGACA TTGAT	-2	Biallelic	ATCCGATC T - - - - - CACTGTGGGCAACTATGAC	+1	Biallelic	KO	-	KO
		GGATTGGAGTTTACCATG - TCACCTTTACATTTACCATCTTGACCTTGACA TTGAT	-5	Biallelic	ATCCGATC - - - - - ACTGTGGGCAACTATGAC	-5	Biallelic	KO	-	KO
	CL2	ATTGAAGGTTATGACTTCAACCGGGCAT	0	WT	Site E Protospacer 20 nt ATTGAAGGTTATGACTTCAACCGGGCAT PAM	Sub/-6		KO	-	KO
	<i>hss-1</i>	ATTGAAGGTTATGACTTCAACCGGGCAT	+1	Biallelic						
	<i>hss-2</i>	ATTGAAGGTTA - - - - - CCGCGGCAT	-9	Homozygous						
								NE, KO, KO	-	KO

3.3.3 Inactivation of the genes encoding CsCuAO1 or CsCuAO5 results in mutants that are unable to produce PAs

To test the transgenic *C. spectabilis* plants for an effect of the modified genomic sequence within the *cscuao1*, *cscuao5*, and *cshss* genes on their ability to produce PAs, the *in vitro*-cultivated plants were inoculated with a specific *Bradyrhizobium* strain to induce the formation of nodules. It was shown recently that, in *Crotalaria*, PA biosynthesis is nodule-specific, suggesting that central steps of PA biosynthesis are expressed in this specific organ (Irmer et al. 2015). Nodule primordia have been detectable usually 10 to 14 days after infection. Nodulated plants were cultivated for about ten to twelve months before PA levels have been quantified separately in nodules and leaves by using a GC-MS based method (Zakaria et al. 2021).

Both plants serving as control lines (CL1 and CL2) have shown distinct accumulation of the PA monocrotaline, an observation identical to that obtained for a wild-type plant in this study. No monocrotaline was detectable in the positive control, *i.e.*, the plants with edited *hss* gene, providing *in planta* evidence for the involvement of HSS in PA biosynthesis also in *Crotalaria*. Of note, this was also the case for line HSS-2 that was characterized to possess a homozygous 9 nt-deletion. Even though no frame shift is induced, the deletion of three amino acids is obviously fatal for HSS activity. Also, none of the CsCuAO1 or CsCuAO5 knockout lines was able to produce PAs, suggesting that both enzymes are involved in the biosynthesis of the PA monocrotaline (Figure 3, Table 1).

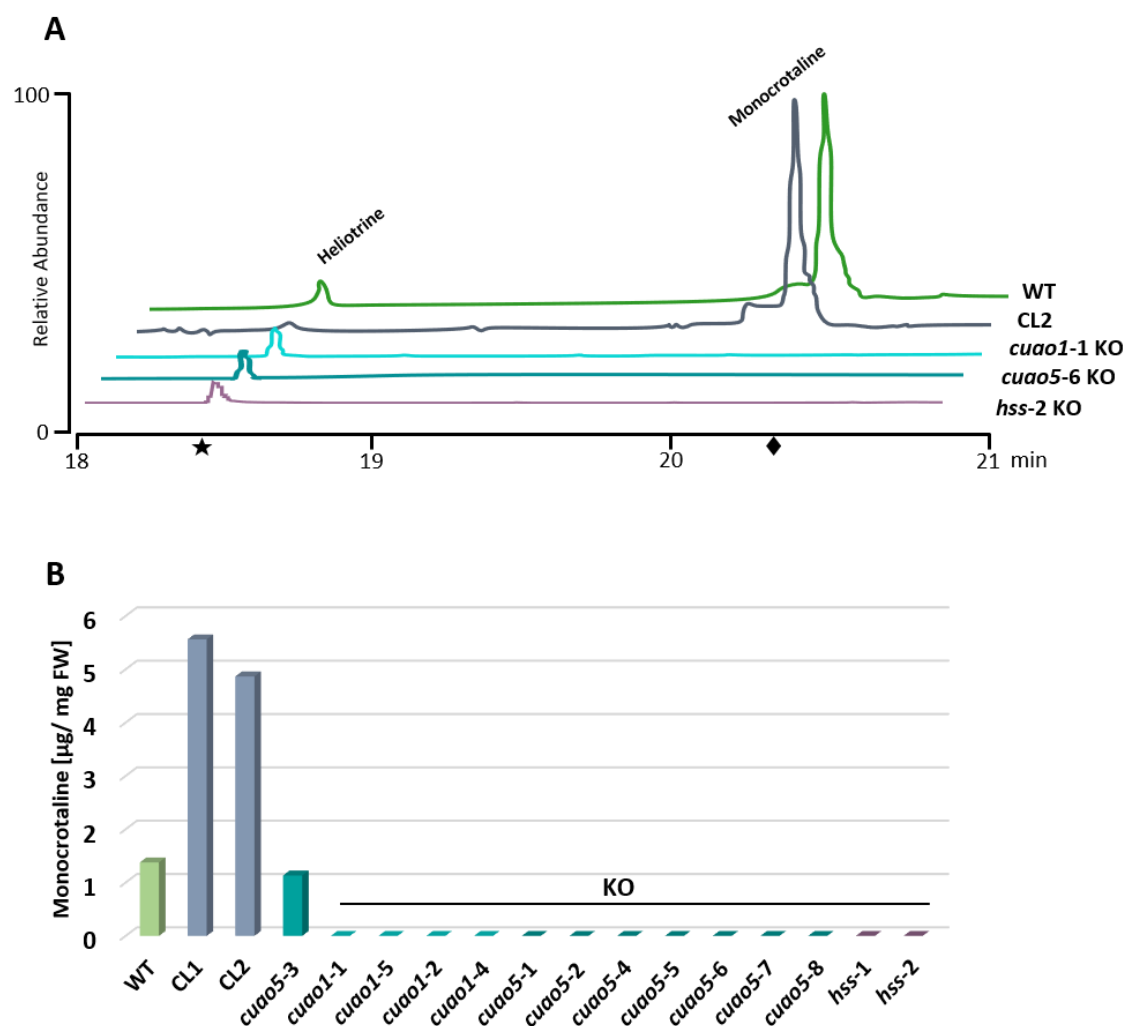


Figure 3. PA analyses of transgenic nodulated plants of *C. spectabilis*. **A** Gas chromatography total ion chromatograms (GC-TICs) in the area between 18 and 21 min of selected wild-type, control, and knockout lines. The PA heliotrine served as internal standard (retention time (RT) = 18.46) and the PA monocrotaline (RT = 20.14) is the only PA detectable in *C. spectabilis*. WT, wild-type plant grown under identical conditions, CL, control line plant CL-2, *cscuao1*-KO, plant *cscuao1*-P1, *cscuao5*-KO, plant *cuao5*-P6, *cshss*-KO, plant *hss-2* (numbering refers to Table 1). **B** PA levels are given as the amount of monocrotaline detected in fresh leaves of the wild-type and the transgenic plants resulting from genome editing.

3.3.4 CsCuAO1 and CsCuAO5 are involved in necine base formation but accept different substrates

The observation that two CuAOs, namely CsCuAO1 and CsCuAO5, are obviously essential for PA biosynthesis in *C. spectabilis*, was an unexpected result, as in *H. indicum* and *S. officinale* one enzyme, *i.e.*, the HSO, proved to be sufficient. To provide further evidence and to substantiate the involvement of CsCuAO1 and CsCuAO5 in the formation of the PA monocrotaline, Hspd was quantified by HPLC-based polyamine analyses in nodules taken from the knockout lines of *cscuao1* (one line *cuao1-1* with three technical replicates) and *cscuao5* (three lines *cuao5-2*, *-4*, and *-6* with one technical replicate each) in comparison with a control line (CL2, three technical replicates) (Figure 4).

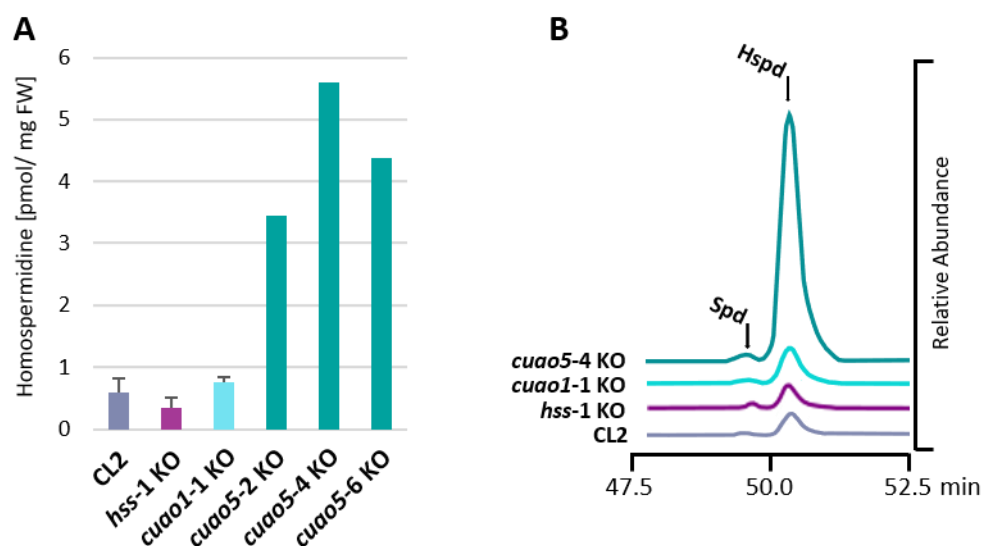


Figure 4. Polyamine levels of Hspd in nodules of transgenic *C. spectabilis* plants. **A** Hspd levels were quantified in genome-edited plants with inactivated CsHSS (*HSS-1* KO), CsCuAO1 (*CuAO1-1* KO), CsCuAO5 (*CuAO5-2* KO, *CuAO5-4* KO, and *CuAO5-6* KO), and in a control line resulting from transformation with the empty vector (CL2) by calculating the concentration in relation to the internal standard diaminoheptane and the amount of fresh weight (FW). For the control line (CL2) and for the knockout plants of *hss* (*HSS-1* KO) and *cuao1* (*CuAO1-1* KO), three technical replicates of the same line have been analyzed. For knockout lines of *cuao5*, three biological replicates have been available represented by one technical replicate each. **B** HPLC chromatograms of selected knockout lines showing the peak separation of Spd and Hspd.

Only in nodules of the *cscuao5*-knockout lines, a significant accumulation of Hspd was detectable up to levels by approx. 15-fold (4.47 ± 1.09 pmol/mg FW) compared to Hspd levels of the control line CL2 (0.33 ± 0.25 pmol/mg FW) (unpaired t-test, $p = 0.003$). Hspd

levels in nodules of the *cscuao1* knockout line did not show any significant differences compared to those of the control lines (0.55 ± 0.10 pmol/mg FW, unpaired t-test, $p = 0.223$). These data suggest that Hspd is most likely the substrate for CsCuAO5. This interpretation was supported by the fact that none of the previously described intermediates of Hspd oxidation like monocyclic pyrrolinium ions (Zakaria et al. 2022) has been detectable in the *cscuao5*-knockout lines and not after increasing the endogenous Hspd level in the nodules of the knockout plant by feeding with Hspd either (Figure 5A).

In contrast to the nodules of the *cscuao5* knockout lines, the nodules of the *cscuao1* knockout lines did not accumulate Hspd as Hspd levels were very similar to that in control lines (Figure 4). This observation suggests that Hspd is converted even in lines with an inactivated *cscuao1*. As the *cscuao1* and *cscuao5* knockout lines both do not produce PAs, we hypothesized that CsCuAO5 and CsCuAO1 might catalyze two successive steps of Hspd oxidation. To test this hypothesis, we searched for possible intermediates of Hspd oxidation as they have been described earlier in a study characterizing *HiHSO* (Zakaria et al. 2022). GC-MS analyses revealed that these knockout mutants accumulated two compounds that have been undetectable in control lines or the *cscuao5* knockout lines (Figure 5A). According to the detected masses and fragmentation patterns, they were identified as 1-(carboxybutyl)pyrrolidine and its methyl ester in a ratio of 1 to 9, respectively (Figure 5, B and C).

The identity of the carboxyl group of 1-(carboxybutyl)pyrrolidine was confirmed by GC-MS analyses after derivatization with *N*-methyl-*N*-(trimethylsilyl)trifluoroacetamide (MSTFA). The detected compound showed the expected mass m/z of 229 (Figure 5, D and E).

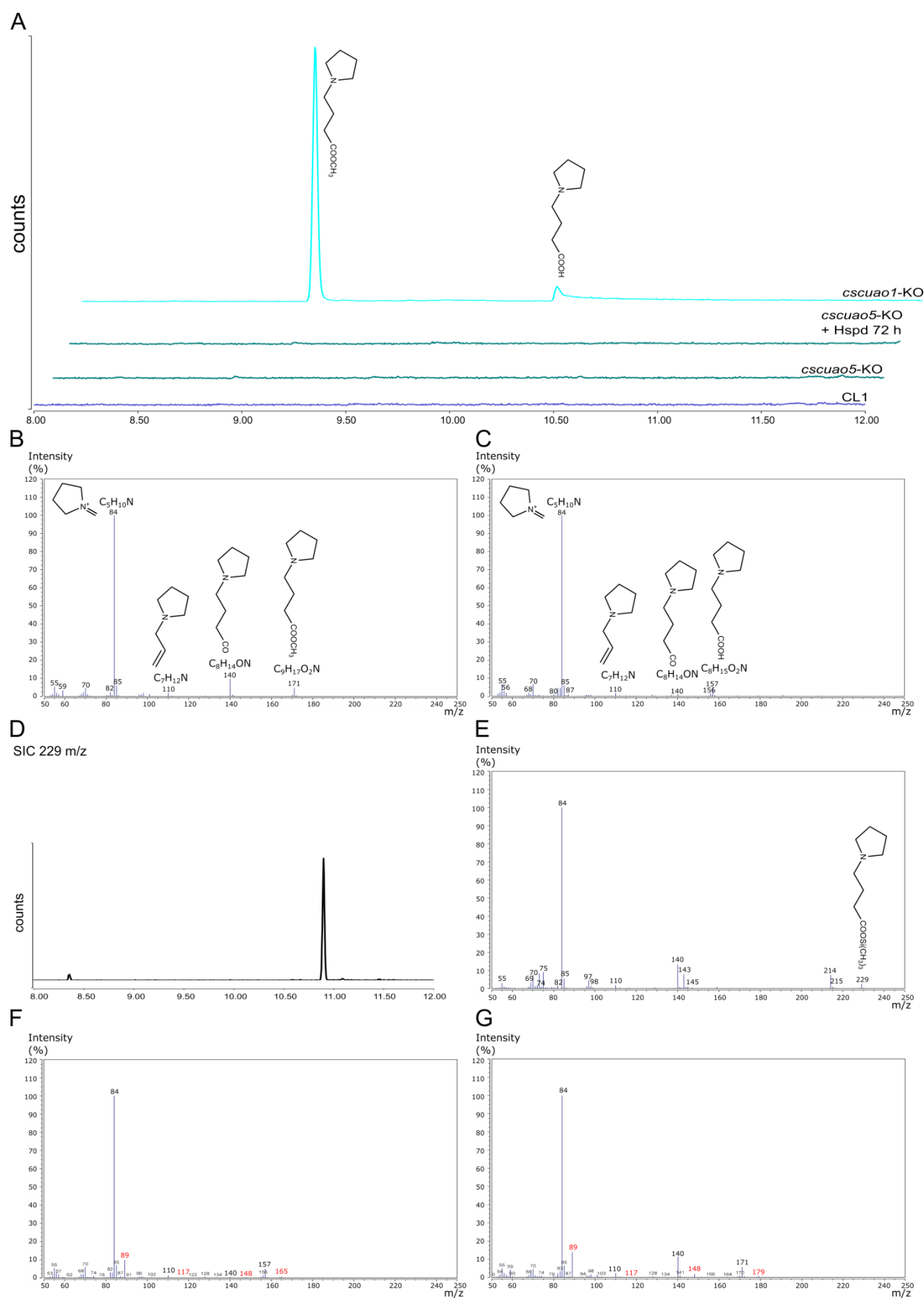


Figure 5. Characterization of the two compounds accumulating in nodules of *cscua1* knockout mutants. **A** GC-TICs showing two compounds that accumulate only in *cscua1* knockout lines but are undetectable in the control line (CL1) and the *cscua5* knockout (*cscua5-KO*) without and after feeding with Hspd. **B** and **C** GC-MS fragmentation pattern of the accumulating compounds,

1-(carboxybutyl)pyrrolidine with m/z of 157 (**B**) and its methyl ester with m/z of 171 (**C**). **D** Single ion chromatogram (SIC) of m/z of 229 representing the peak of trimethylsilylated 1-(carboxybutyl)pyrrolidine after derivatization with *N*-methyl-*N*-(trimethylsilyl)trifluoroacetamide (MSTFA). **E**, The detailed mass fragmentation pattern of the derivative shown in **D**, **F** and **G** GC-MS fragmentation patterns of 1-(carboxybutyl)pyrrolidine (**F**) and its methyl ester (**G**) after feeding [^{13}C]Hspd to detached nodules of the *cscuao1* knockout mutants for 72 h showing the corresponding isotopic shift of the specific masses (labeled in red).

To verify the biosynthesis of these two compounds from Hspd, [^{13}C]Hspd was fed to detached nodules of *cscuao1* knockout plants. After 72 h, GC-MS analyses showed the same two peaks of the previously identified compounds with the expected isotopic shift in the MS spectra (Figure 5, F and G). Therefore, the two compounds result from Hspd after oxidative deamination at both primary amino groups and a cyclization resulting in the pyrrolidine ring. However, the typical product of a CuAO-catalyzed oxidative deamination should be an aldehyde. Furthermore, characterization of the HSO of *H. indicum* has shown that carboxylic intermediates in the conversion of Hspd are, at least *in vitro*, most likely artifacts attributable to the co-evolving hydrogen peroxide that converts the aldehydes to their carboxylic counterparts (Zakaria et al. 2022). Also, in the case of the two compounds accumulating *in vivo*, *i.e.*, in the *cscuao1* knockout plants, oxidation of the aldehyde that results from oxidation of Hspd to the corresponding acid could also be caused by the co-evolving hydrogen peroxide. Most likely is this due to their accumulation in consequence of the nonfunctional CsCuAO1 that catalyzes the conversion of the aldehyde to the pyrrolizidine structure. In the study of Zakaria et al. (2022), we have recently been able to show that hydrogen peroxide is able to convert 1-formylpyrrolizidine resulting from the CuAO-catalyzed oxidation of Hspd in *H. indicum* to 1-carboxypyrrolizidine. The formation of the corresponding ester might be due to methylation by the plant as part of endogenous detoxification mechanisms or as an artifact resulting from methanolic sample preparation.

To test this hypothesis also for *Crotalaria*, we analyzed whether 1-(carboxybutyl)pyrrolidine and its methyl ester are intermediates of PA biosynthesis or derivatives of intermediates that result from oxidation by hydrogen peroxide and tested whether the two compounds can be incorporated into the bicyclic pyrrolizidine backbone of PAs and later into monocrotaline. Therefore, extracts of nodules taken from a *cscuao1* knockout plant (plant *cscuao1-1*) containing both compounds were fed to detached nodules of both *cscuao5*

knockout plant (plant *cuao5*-P6) and *cshss* knockout plant (plant *hss-2*) for five days as these plants should have the capacity to convert the intermediates resulting from oxidation of Hspd by CsCuAO5. Although both intermediates were taken up into the nodules, no further conversion to any other compound was detectable (Figure 6). This data clearly shows that both compounds are no precursors in the formation of the bicyclic pyrrolizidine and supports the interpretation that these compounds are modified intermediates accumulating after genome editing in *cscuao1* knockout.

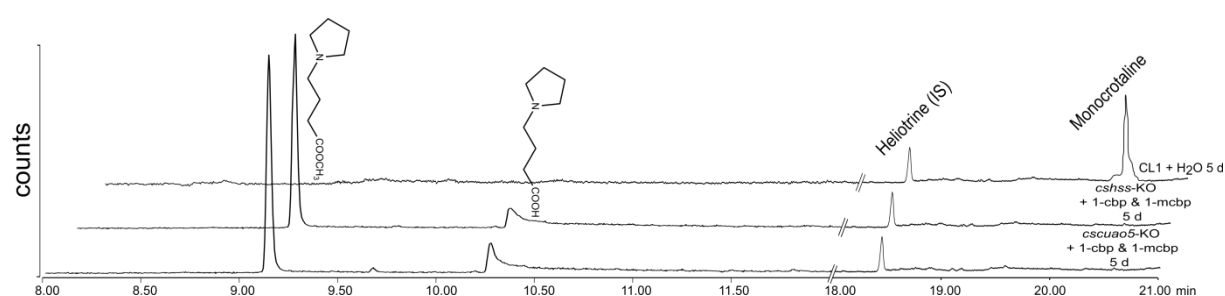


Figure 6. GC-TICs after incubating detached nodules of both *cscuao5* knockout plants and *cshss* knockout plants with extracts containing 1-(carboxybutyl)pyrrolidine (1-cbp) and its methyl ester (1-mcbp) for 5 days. Heliotrine was used as internal standard (IS).

Our data suggest that both CsCuAO1 and CsCuAO5 are involved in PA biosynthesis but catalyze two successive reactions between Hspd and the bicyclic pyrrolizidine backbone. While CsCuAO5 catalyzes the oxidation of Hspd at both primary amino groups resulting in a monocyclic intermediate, CsCuAO1 catalyzes the cyclization of the second ring to result in the formation of the pyrrolizidine backbone.

3.3.5 The formation of the pyrrolizidine backbone requires both active CsCuAO1 and CsCuAO5

To further evaluate the individual steps involved in Hspd oxidation in *C. spectabilis* and to study the intermediates involved, [^{12}C]Hspd was fed to detached nodules of the *cshss* knockout plant, in which CshSS is non-functional while both CsCuAO5 and CsCuAO1 are active. As these plants are unable to produce Hspd as the first specific intermediate of PA biosynthesis, they are also devoid of any pathway intermediates and PAs. Nodules were incubated with Hspd for 8, 24, 48, and 120 h and putative intermediates were analyzed by GC-MS using a method recently developed to capture the early intermediates formed after Hspd oxidation with low background signals such as the monocyclic *N*-(4-aminobutyl)pyrrolinium ion and 1-formylpyrrolizidine, but also 1-carboxypyrrolizidine and further methylated derivatives most likely representing artifacts due to the co-evolving hydrogen peroxide and to the methanolic extraction procedure (Zakaria et al. 2022).

Already after 8 h, the bicyclic pyrrolizidine derivatives trachelanthamidine, 1-formylpyrrolizidine and 1-carboxypyrrolizidine were detectable (Figure 7). After 24 and 48 h, 1-formylpyrrolizidine was the prominent intermediate, but 1-carboxypyrrolizidine and trachelanthamidine were also well detectable intermediates. After 120 h, 1-formylpyrrolizidine was not detectable anymore, while the peak of trachelanthamidine increased, indicating an efficient conversion of this intermediate into the necine base of PAs. However, the PA characteristic for *C. spectabilis*, i.e., monocrotaline, was not detectable after all three feeding intervals. 1-carboxypyrrolizidine, 1-methylcarboxypyrrolizidine, and 1-(4-methylcarboxybutyl)pyrrolidine were detected as minor compounds and hardly no change in their detected levels after feeding for 48 and 120 h (Figure 7). These derivatives of the previously characterized intermediates of PA biosynthesis resulting from oxidation and further methylation were not considered to be further intermediates of the biosynthesis of the pyrrolizidine backbone. Instead, they may have been formed as part of the plant's counter reaction to the feeding of large quantities of Hspd and as artifact from the methanolic sample preparation.

Of note, analyzing the liquid medium in which the nodules were incubated at the end of the experiment after 120 h revealed the presence of the deprotonated form of the monocyclic

N-(4-aminobutyl)pyrrolinium ion ($C_8H_{16}N_2$). The pyrrolinium ion was described earlier to result from cyclization after oxidation of Hspd at only one of the two primary amino groups in a study on amine oxidase from bovine serum (Houen et al. 2005). It was shown recently to be an intermediate in the formation of the pyrrolizidine backbone during oxidation of Hspd with HSO of *H. indicum* (Zakaria et al. 2022).

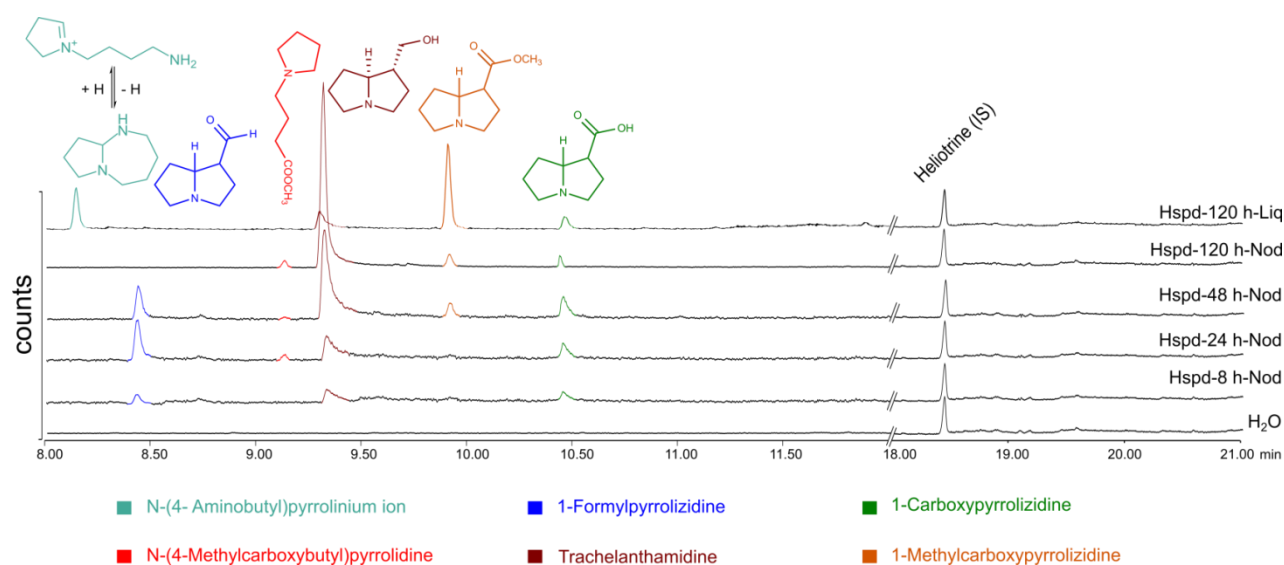


Figure 7. Feeding of $[^{12}C]$ Hspd to detached nodules of *cshss* knockout plants. GC-TICs of extracts of nodules after feeding for different time intervals and of the remaining liquid surrounding the nodules during the feeding at the end of the feeding experiment (after 120 h). Heliotrine served as internal standard (IS).

3.4 DISCUSSION

In the early steps of PA biosynthesis, Hspd is converted to the bicyclic necine base moiety, the characteristic building block of all PAs. This conversion requires two consecutive oxidative deamination reactions and two cyclization reactions. In the earlier literature (Robins 1982; Khan and Robins 1985; Kelly and Robins 1988; Robins 1989), it was discussed whether these two oxidations are catalyzed by two individual CuAOs (formerly called “diamine oxidases”) or by a single enzyme. Furthermore, following the knowledge about cyclizations in the biosynthesis of various groups of alkaloids (Aniszewski 2007), each cyclization reaction was proposed to proceed spontaneously through the reaction of the aldehyde group resulting from the CuAO reaction with the internal amino group via Mannich-type reaction mechanism. Recent studies on Hspd oxidation in *H. indicum* and *S. officinale* resulted in the identification of HSO, an enzyme that catalyzes, in a kind of “one-pot-reaction”, not only the oxidation of both primary amino groups of Hspd, but also the cyclization to the bicyclic pyrrolizidine (Zakaria et al. 2022; Zakaria unpublished). The formation of the bicyclic pyrrolizidine backbone requires two cyclizations, of which the second one, the scaffold-forming step that results in the closure of the second ring, is stereospecific (Zakaria et al. 2022; Zakaria unpublished). This observation gave support to previous speculations about a somehow enzyme-controlled cyclization reaction in the biosynthesis of the necine base moiety (Schramm et al. 2019; Lichman 2021).

In this study, in contrast to our findings in Zakaria et al. (2022) and Zakaria (unpublished), we show that there are further options for the challenging formation of the pyrrolizidine backbone of PAs in the plant kingdom. We show that in *C. spectabilis* the reaction of HSO is taken over by two independent CuAOs, *i.e.*, CsCuAO1 and CsCuAO5. Both enzymes are typical CuAOs as their amino acid sequences contain the characteristic functional amino acids of the catalytic site of CuAOs: three conserved histidine residues coordinating the copper ion in the active site and a strictly conserved tyrosine residue (Supplemental Figure S4) that is post-translationally modified into the cofactor topaquinone active in the redox reaction (Kumar et al. 1996).

3.4.1 Two independent CuAOs are involved in PA backbone formation in *C. spectabilis*

Following earlier ideas about two CuAOs involved in Hspd oxidation, it was assumed that these two enzymes should oxidize one of the primary amino groups of Hspd successively followed in each case by the (spontaneous) cyclization. However, here we show that the two enzymes split this task in a completely different manner.

The first CuAO (CsCuAO5) oxidizes Hspd already at both primary amino groups and results in only a monocyclic intermediate that accumulates in plants with an inactivated *cscuao1* gene. However, the precise nature of this monocyclic intermediate could not be confirmed in this study most likely due to the effects of co-produced hydrogen peroxide and due to compensating reactions of the plant by methylations of accumulating intermediates in the transgenic background. Further studies have to show whether this intermediate is the same as the postulated pathway intermediate in the HSO-catalyzed reaction in *H. indicum* and *S. officinale*, i.e., a monocyclic pyrrolinium ion or a monocyclic pyrrolidine as the corresponding reduced form, both with a free aldehyde group.

The second CuAO (CsCuAO1) is not accepting Hspd as a substrate and is not catalyzing any oxidative deamination, but obviously allows and controls the closure of the second ring associated with the formation of the pyrrolizidine scaffold. Again, this is not a characteristic property of CuAOs as they are described in the literature. Although this enzymatic cyclization could explain the observed stereospecificity, the mechanism behind this novel activity of a CuAO remains open. Future studies have to show whether the oxidative deamination and the cyclization reaction catalyzed by the two PA-specific CuAOs of *Crotalaria* are mechanistically related reactions or not.

3.4.2 CsCuAO1 and CsCuAO5 belong to the same clade as other PA-specific CuAOs

Several examples in the literature have shown that gene duplication followed by diversification of the gene copies is a common mechanism to develop functional innovations in plant secondary metabolism (Ober and Hartmann 1999b; Pichersky and Gang 2000; Conant and Wolfe 2008; Innan and Kondrashov 2010; Rensing 2014). These include also the evolutionary origin of HSS by duplication of the gene encoding DHS (Ober and

Hartmann 1999b; Reimann et al. 2004; Kaltenegger et al. 2013). Several models have been developed to explain how a gene copy might develop a new function without being lost due to pseudogenization (Conant and Wolfe 2008; Panchy et al. 2016). Phylogenetic analyses have the potential to show how a new function evolved, especially if other functionally characterized sequences are available. Figure 8 shows such a gene tree of CuAO-encoding cDNA sequences of selected angiosperm species. The CuAOs are separated in three clusters, of which cluster I and III are closer related to each other than cluster II. All CuAOs involved in Hspd oxidation, *i.e.*, the HSOs of *H. indicum* (HiHSO), *S. officinale* (SoCuAO1 and SoCuAO5), and also the two CuAOs identified in this study from *C. spectabilis*, *i.e.*, CsCuAO1 and CsCuAO5, are members of cluster I. Early in this clade, the CuAOs of different systematic lineages separate, resulting in subclades encompassing sequences from *Arabidopsis*, from species belonging to the Boraginales order, and from the Fabaceae family, respectively.

The two sequences described from *S. officinale* (Zakaria unpublished), SoCuAO1 and SoCuAO5, share a sequence identity of 81% on the amino acid level and 85% on the nucleic acid level and are directly sisters within the Boraginales subclade suggesting that their common ancestor might have optimized already for a PA-specific function. The duplication of this ancestor gene resulted in these two HSOs that retained the ancestral function but diverged with respect to gene expression, as the two gene products are expressed in different tissues, *i.e.*, in roots and in young leaves subtending an inflorescence, to increase plant fitness (Zakaria unpublished). Figure 8 shows also that these two sequences of *S. officinale* are related to that of the HiHSO, the CuAO of *H. indicum* that was shown to catalyze the same reaction as the SoCuAO1 and SoCuAO5. Whether the common ancestor of all these PA-specific CuAOs in the Boraginales order preceding the speciation events possessed already the HSO activity or whether this characteristic mechanism evolved later remains open, especially as this subclade encompasses also further still uncharacterized CuAOs, *i.e.*, HiCuAO3 and HiCuAO5.

The situation is completely different for CsCuAO1 and CsCuAO5 from *Crotalaria*, which were identified in this project. Based on the mechanistic data, one is tempting to speculate that, in *C. spectabilis*, the ancestral functions have been partitioned into two separate genes after gene duplication, a term known as sub-functionalization (Lynch and Force 2000). This means

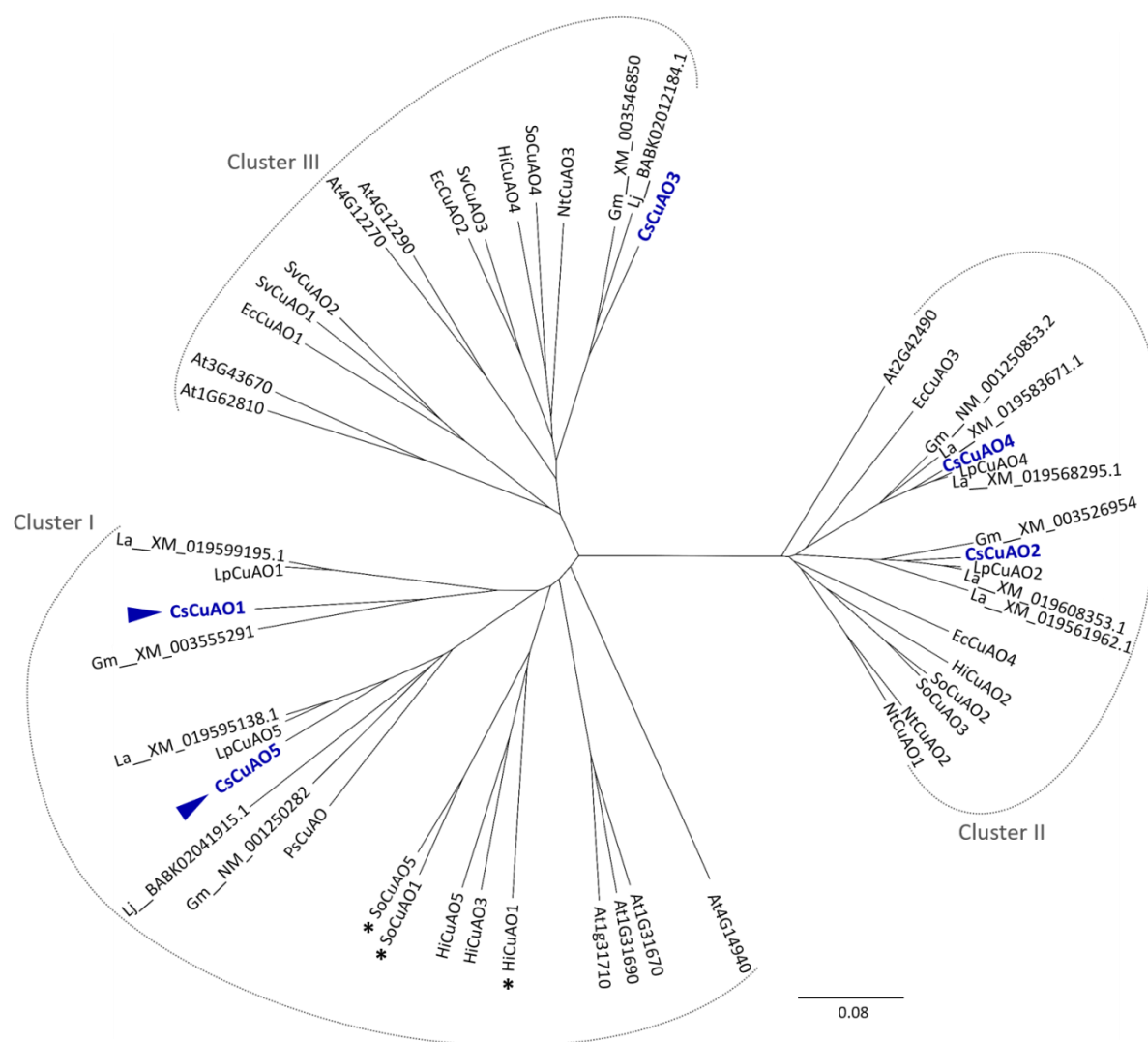


Figure 8. Neighbor-joining tree of CuAO encoding cDNA sequences of various species of the plant kingdom. The CuAOs of *C. spectabilis* identified in this study are labeled in blue. Blue arrows point to the two CuAOs involved in PA biosynthesis in *C. spectabilis*. Black asterisks label the CuAOs (= HSOs) of the two species *H. indicum* and *S. officinale* that have been characterized recently as being involved in PA biosynthesis.

that the ancestral gene was bifunctional and could catalyze in our case both reactions, the oxidative deamination and the cyclization. After gene duplication, the two copies diverged with respect to their function by specializing on only one of these two functions: CsCuAO1 retained the cyclization function while CsCuAO5 retained the two oxidative deaminations. However, even though these sequences are expressed at the same site (the nodules) and share the same subclade of Fabaceae sequences, they are no close sisters. This phylogenetic distance is reflected also in a lower identity on amino acid (56%) and nucleic acid level (64%).

Further research is needed to characterize the function and mechanism of further sequences of the cluster I of CuAOs to see whether the cluster is based not only on sequence similarity but also on common characteristic mechanistic properties. Such studies might also provide additional data to test whether both activities, *i.e.*, the oxidative deamination and cyclization, are originated from a common mechanism. Thus, a conformational shift caused by single mutations might have promoted the emergence of a completely new active site in both CsCuAOs facilitating transition-state binding with different substrates and intermediates.

3.4.3 Nodulated *Crotalaria* plants harbor two well-separated Hspd pools

Hspd has been reported to be frequently found in nodules of leguminous plants as well as in the symbiotic rhizobia that belong to the α -proteobacteria and contain Put and Hspd as major polyamines, while Spd is often missing (Smith 1977; Hamana and Matsuzaki 1992; Fujihara et al. 1994; Krossa et al. 2016). Hspd is synthesized in the bacteroides by a bacterial HSS (EC 2.5.1.44) that is different from the HSS of plants (EC 2.5.1.45) as it couples two molecules of Put in an NAD⁺-dependent reaction (Tholl et al. 1996; Ober et al. 1996). Although little is known about the physiological role of Hspd produced in the symbionts embedded in these nodules, it is reported that it contributes to stress tolerance like salinity in both free-living and symbiotic bacteria and to the protection of the bacteroides from environmental changes (López-Gómez et al. 2016) but might also be the functional analog of Spd (Hamana and Matsuzaki 1992). Furthermore, the involvement of Hspd in nodule organogenesis is discussed (Fujihara 2009).

In *C. spectabilis*, it was shown that nodulation induced by the infection with the soil-borne *Bradyrhizobium* strain triggers PA biosynthesis (Irmer et al. 2015). However, an intriguing question was which partner of the symbiosis provides Hspd for PA biosynthesis: the microsymbiont or the plant. The same study ruled out the involvement of the bacterial HSS in PA biosynthesis and established the HSS identified in *C. spectabilis* to be of plant origin based on both the conserved genomic DNA structure with introns and exons and on the ability of this enzyme to catalyze the formation of Hspd from Spd and Put, which are distinct features of plant-derived HSS (Irmer et al. 2015). However, it was not possible to exclude that Hspd of bacterial origin might be used at least in parts for PA biosynthesis in the

nodules, as the exchange of nutrients, metabolites, and even polyamines such as cadaverine between the host plant and the bacterial microsymbiont in legume nodules is well defined (Fujihara et al. 1994; White et al. 2007).

In our study, polyamine analyses of the CsHSS knockout lines showed that nodules still accumulate significant amounts of Hspd. This confirms that the bacterial HSS was not affected by the induced silencing of CsHSS and is still able to synthesize Hspd. However, these nodules were completely devoid of PAs, indicating no flux of bacterial Hspd to the PA synthesizing tissues of the nodules. Moreover, it confirms, that exclusively the plant and not the rhizobia are the provider of Hspd for PA biosynthesis. This was further confirmed by feeding of Hspd to isolated nodules of the CsHSS knockout plant by which PA synthesis could be restored. The externally fed Hspd seems to be able to enter the PA producing plant tissues, while Hspd synthesized within the symbiotic bacteria is restricted to the infected zone. This clear result shows that the bacterial and plant Hspd pools in *C. spectabilis* are completely separated from each other and serve distinct functions.

3.4.4 Several organs and tissues might be involved in PA biosynthesis in *C. spectabilis*

Many classes of plant specialized metabolites show a restricted occurrence in only specific organs, tissues, and cell types (Li et al. 2016), suggesting a tight regulation of the responsible biosynthetic pathways. For instance, plant defense metabolites are frequently produced in specialized tissues or cell types to avoid autotoxicity in the surrounding tissues without an impact on the effectiveness of these metabolites as defense against herbivores (Schillmiller et al. 2010; Tissier 2012). In several cases, the sites of biosynthesis and accumulation may differ. Examples are the alkaloids nicotine and hyoscyamine of tobacco and *Atropa belladonna*, which are synthesized in the roots and transported to the leaves to exert their defensive functions in the tissue with the highest probability of an attack by herbivores (Hashimoto and Yamada 1994; Katoh et al. 2005; Tan et al. 2020).

For PAs, the same was described in *Senecio vulgaris*, where PAs are synthesized in the roots and accumulate mainly in the reproductive tissues of the flower heads (Hartmann et al. 1989) providing best defense of the reproductive structures according to the optimal defense theory (Mckey 1979). Furthermore, it was confirmed by tracer feeding experiments

using various *Senecio* species that the PA backbone structure in *Senecio*, *i.e.*, senecionine *N*-oxide, is produced in the roots, but that shoots are capable of transforming senecionine *N*-oxide into the unique species-specific PA patterns (Hartmann and Dierich 1998).

In *Crotalaria*, although the majority of PAs are accumulated in the shoot, nodules have been considered to be the site of PA-biosynthesis as PA concentration was highest in the nodules and as the *hss* transcript was exclusively present in nodules (Irmer et al. 2015). This observation also applies to the two transcripts encoding CsCuAO1 and CsCuAO5 that have been shown to be involved in the biosynthesis of the necine base in *Crotalaria* in this study. This is consistent with the exclusive presence of both Hspd and necine base in nodules. However, the non-detection of the final PA, monocrotaline, after feeding detached nodules for up to 120 h raises questions about the regulation of the whole pathway of PA biosynthesis in *C. spectabilis*. This observation indicates that other tissues outside of the nodules may take part in at least one of the later steps of PA-biosynthesis, *i.e.*, the steps following the formation of the free necine base trachelanthamidine. These steps include 7C-hydroxylation, 1,2-desaturation, necic acid formation, and linkage of the necine base to the necic acids. Therefore, a transport of the necine base to tissues outside the nodules is required to allow such modifications by enzymes later in the pathway.

Not surprisingly, compartmentalization studies have revealed many unique aspects for various of plant metabolic pathways (Lunn 2007). This could be exemplified by the textbook example C4-photosynthetic pathway that it is compartmented between two different cell types - mesophyll and bundle sheath cells (Furbank and Lunn 1997) and differential tissue localization of early and late stages of indole alkaloid biosynthesis in *Catharanthus roseus* (St-Pierre et al. 1999).

An intracellular compartmentalization of parts of PA biosynthesis have been postulated since many years (Böttcher et al. 1993) and have further substantiated recently (Zakaria et al. 2022; Zakaria unpublished). Also, the data obtained for CuAOs of *Crotalaria* supports an intracellular compartmentalization, as the two CuAOs involved in PA biosynthesis are predicted to possess *N*-terminal signal peptides directing the proteins to the secretory pathway. Our findings in *Crotalaria* suggest that in addition to this intracellular

compartmentalization of necine base formation, the whole PA biosynthetic pathway seems to be compartmented between different types of tissues in *Crotalaria*, one of them being outside the nodules. Consequently, this requires the intercellular translocation of pathway intermediates to allow the production of the final PA monocrotaline. Future studies should investigate how the different parts of the PA pathway are coordinately regulated in *Crotalaria* and other PA-producing plants.

3.5 MATERIAL AND METHODS

3.5.1 Plant material

Crotalaria spectabilis were cultivated *in vitro* as described by Irmer et al. (2015) with modifications. Briefly, the pH of the media was adjusted to 6.5 and the infection with the specific *Bradyrhizobium* strain (Gamo et al. 1991) was conducted by pipetting the suspension containing *Bradyrhizobium* cells in water (up to 100 µL) directly alongside the roots.

3.5.2 Confirmation of cDNA sequences and identification of genomic sequences of the genes encoding CsCuAO1 and CsCuAO5

To identify CuAOs that are involved in PA biosynthesis of *C. spectabilis*, we performed Illumina® sequencing with roots and nodules (unpublished data). Five transcripts predicted to encode CuAO-like proteins (CsCuAO1 to CsCuAO5) have been identified. The transcripts encoding CsCuAO1 and CsCuAO5 have been verified by PCR amplification with the proofreading DNA polymerase, Phusion Hot Start II DNA polymerase (ThermoFisher Scientific, Waltham, MA, USA) according to manufacturer protocol using the primer pairs P1/P2 (CsCuAO1) and P3/P4 (CsCuAO5). Primer sequences are given in Supplemental Table S1. PCR products were purified via agarose gel electrophoresis (NucleoSpin®Gel and PCR Clean-up, MACHEREY-NAGEL, Düren, Germany), A-tailed, and cloned into the pGEM T-easy vector (Promega, Fitchburg, WI, USA). Sequence identity was confirmed by sequencing (Eurofins Genomics, Hamburg, Germany).

To design constructs for CRISPR/Cas9-mediated genome editing, genomic DNA of CsCuAO1 and CsCuAO5 was amplified to identify exon-intron boundaries. Genomic DNA of leaves taken from sterile culture was used as template. For amplification of the genomic sequence encoding CsCuAO5, the primers were identical to those used for amplification of the cDNA. Amplification of the complete genomic sequence encoding CsCuAO1 failed. Instead, a small part of the sequence (ca. 330 bp) could be identified by using the primer pair P5/P6. An additional part of sequence (ca. 200 bp) resulted from an inverse PCR approach using genomic DNA digested with *EcoRV* and self-ligated according to Triglia et al. (1988) as template for amplification with Accu Taq LA polymerase (ThermoFisher Scientific) according to manufacturer protocol with primer pair P7/P8.

3.5.3 Transcript quantification by RT-qPCR

To quantify transcript levels of the genes encoding the HSS and the CuAOs of *C. spectabilis*, cDNA was isolated from three individuals of different ages (cultivated under *in vitro* conditions as given above for 2, 4, and 12 months after germination), and all of which had well-developed nodules. Total RNA was tested with MOPS by agarose gel (3%) electrophoresis to exclude degradation (Supplemental Figure S3). PCR primers were designed using the Geneious Prime software package with the following settings: length 18 to 30 nucleotides, melting temperature 59°C to 61°C, GC content 30% to 60%, product size 90 to 155 bp. Primer sequences are given in Supplemental Table S1. To exclude unspecific binding of these primers to other sequences encoding CuAOs due to sequence similarities, primer quality was validated in a RT-qPCR run followed by analysis of the melting curves and sequencing the resulting PCR products (Supplemental Figure S5).

RT-qPCR was performed in a Rotor-Gene® Q System (Qiagen, Hilden, Germany). Amplification reactions were performed in a total volume of 20 µL with 10 µL GoTaq® qPCR Master Mix (Promega), 0.125 pmol of each primer, 4 µL RNase-free water and 5 µL template DNA (10 ng). Thermal cycling conditions followed the two-step protocol: one cycle 95°C for 2 min; 40 cycles with 95°C for 15 s and 60°C for 60 s. Melting curves were analyzed to confirm the specificity of the PCR products. Each sample was analyzed in triplicate including the no-template controls for each primer pair of the gene of interest and the reference genes. Transcript levels of the genes encoding ubiquitin (UBQ) and actin (ACT) were used as references for the calculation of the relative transcript level ($2^{-\Delta CT}$) of the *hss* and *cucaos* genes (Schmittgen and Livak 2008). RT-qPCRs were performed in triplicate (n=1).

3.5.4 Constructs for editing the genes encoding CsCuAO1, CsCuAO5, and CsHSS by CRISPR/Cas9

To identify protospacer sequences that could be used as target of sgRNA, the Geneious Prime software package was used to predict possible target sites within the candidate genes (CsCuAO1 and CsCuAO5) and within the CsHSS for comparative purposes. For each CuAO-coding sequence, two target sites were chosen to increase the chance to obtain a CRISPR/Cas9 effects or even a larger deletion of genomic sequence, while for editing of the gene encoding HSS, only one targeting sequence was selected. Constructs used for the

genome editing approach were designed according to a protocol described by Schiml et al. (2016) that we used in a version recently adapted for genome editing in *S. officinale* (Zakaria et al. 2021). Shortly, complementary oligonucleotides covering the selected protospacer motives have been hybridized to result in sticky ends that allowed cloning into the entry vector pEn-Chimera (Schiml et al. 2016) for protospacers targeting sites A and C of *cscuao1* and *cscuao5*, respectively, and site E of *cshss* and transfer of the sgRNA cassettes to the destination vector pDe-Cas9-HYG (Zakaria et al. 2021) that harbors the expression cassette for Cas9 and for hygromycin resistance as plant selectable marker. Protospacers targeting sites B and D of *cscuao1* and *cscuao5* respectively, were cloned into the pEn-C1.1 (Schiml et al. 2016). Using *MluI* digestion, the destination vector constructs received the second sgRNA expression cassettes from the pEn-C1.1 construct resulting in constructs targeting sites A and B of the gene encoding CsCuAO1 and sites C and D of the gene encoding CsCuAO5. Sequences of the oligonucleotides are given in Supplemental Table S1.

3.5.5 Stable transformation of *C. spectabilis* plants

For genome editing of *C. spectabilis* using the CRISPR/Cas9 constructs targeting the genes encoding CsCuAO1, CsCuAO5, and CsHSS, a protocol for stable transformation with *Agrobacterium tumefaciens* EHA105 (Hood et al. 1993) was developed. Transformation with the empty destination vector pDe-Cas9-HYG served as control. *A. tumefaciens* EHA105 strains harboring one of the CRISPR/Cas9 constructs were cultivated in a preculture of 7 mL YEB medium (5 g/L beef extract, 1 g/L yeast extract, 5 g/L peptone, 5 g/L sucrose, 0.5 g/L $\text{MgSO}_4 \times 7 \text{ H}_2\text{O}$) supplemented with 50 $\mu\text{g}/\text{mL}$ spectinomycin and 15 $\mu\text{g}/\text{mL}$ rifampicin at 28°C (230 rpm, 48 h). 300 μL of preculture were used to inoculate 50 mL YEB medium supplemented with 50 $\mu\text{g}/\text{mL}$ spectinomycin and 15 $\mu\text{g}/\text{mL}$ rifampicin and incubated overnight (28°C, 230 rpm). At an OD_{600} of ca. 0.5, acetosyringone (150 μM) was added as a specific inductor for the expression of *vir*-genes (Lacroix and Citovsky 2019) and incubated for additional 2 h. Afterwards, 20 mL of each culture were centrifuged (10°C, 5,000 \times g, 15 min) and the pellet was resuspended in 50 mL MS20 medium (medium according to Murashige and Skoog (1962), but with only 20% of the original amount of NH_4NO_3) supplemented with 150 μM acetosyringone.

Leaves of *in vitro* grown *C. spectabilis* were cut to pieces and provided with additional cuttings on the leaf surface before they were incubated in a rotary shaker for 1 h at room

temperature in the agrobacterial suspension prepared in MS20 medium. Afterwards, the leaf section was dabbed dry with sterile filter paper and were transferred to solid MS20 supplemented with plant hormones (2 mg/mL 2,4-dichlorophenoxyacetic acid and 0.25 mg/mL thidiazuron) to induce callus growth. After incubation for 72 h in the dark at 26°C, leaf cuttings were washed in 200 mL sterilized water and then in 200 mL sterilized water supplemented with 500 µg/mL of a mixture of ticarcillin and clavulanic acid to remove remaining *A. tumefaciens* EHA105 cells. After dabbing dry with sterile filter paper, cuttings were transferred to fresh MS20 plates containing 500 µg/mL of a mixture of ticarcillin and clavulanic acid and 50 µg/mL hygromycin for selection of plant cells that successfully incorporated the transfer DNA of the CRISPR/Cas9 constructs and the empty vector control into their genomes. To allow the development of callus, plates were incubated for approx. 12 days in the dark at 24°C and were transferred into a climate chamber (Johnson Control, Mannheim, Germany) equipped with ceramic metal halide lamps (CMT360LS WBH EYE Iwasaki Electric Co., Japan) at 25°C, 65% humidity, and a 16/8-h light/dark cycle (206 µmol m⁻¹ sec⁻¹) as soon as the first calli developed. After separation of the individual calli from the leaf sections, they were transferred to fresh MS20 plates containing 500 µg/mL of a mixture of ticarcillin and clavulanic acid and 1 µg/mL thidiazuron to induce shoot development. When shoots reached a length of approx. 2 to 3 mm, they were transferred to transparent jars (Weck, Weck GmbH, Wehr-Öflingen, Germany) with 100 mL solid MS20 hormone-free medium. Elongated shoots with a length of more than 5 mm were separated from callus and the cut end was dipped into 1 mg/mL naphthaleneacetic acid to induce root formation, and then transferred to solid MS20 medium supplemented with 250 µg/mL of a mixture of ticarcillin and clavulanic acid. As soon as roots developed, plants were transferred to hormone-free NOD medium (5 mM nitrogen, pH 6.5; Irmer et al. 2015) before they were inoculated with *Bradyrhizobium*.

3.5.6 Genomic DNA screen for mutations in the *cscuao* and *cshss* genes

Genomic DNA of leaves developed from transgenic plants of *C. spectabilis* was extracted and used for PCR amplifications using the Phire Plant Direct PCR Kit (ThermoFisher Scientific) according to the manufacturer's instructions with an annealing temperature for the primers of 60°C. The primers have been designed to allow the amplification of those genomic regions of the *cscuao* and *cshss* genes that contain the sites targeted by genome editing.

Primer pair P35/P36 amplified a fragment of 525 bp (length refers to the non-edited sequence) covering target sites A and B within the *cscuao1* gene. Primer pairs P37/P38 and P39/P40 allowed amplification of fragments of 358 bp and 386 bp covering target site C and D, respectively. Primer pair P41/P42 amplified a fragment of 712 bp covering the target site E within the *cshss* gene. PCR fragments were sequenced directly or after cloning into the pGEM-T Easy vector (Eurofins Genomics).

3.5.7 Pyrrolizidine alkaloid extraction and purification and GC-MS analysis

Samples (fresh leaves (100-200 mg) or nodules (20-50 mg) were harvested from plants developed from *in vitro* culture and pulverized in liquid nitrogen with mortar and pestle, and extracted in 1.5 mL 0.05 M H₂SO₄ containing 20 µg of the PA heliotrine as an internal standard for 1.5 h at room temperature with end-over-end agitation (ca. 30 rpm). After centrifugation (14,000 x g, 10 min), 1 mL supernatant was taken, mixed with ca. 100 mg zinc dust, and incubated for 1.5 h at room temperature with end-over-end agitation (30 rpm) for reduction of PA *N*-oxides. After centrifugation (14,000 x g, 5 min), the supernatant was purified by solid phase extraction (Strata-SCX® cartridges, Phenomenex, Torrance, CA, USA) as described previously (Kruse et al. 2017). Leaves of control lines (containing empty vector) served as controls. GC-MS measurements were carried out as described in (Stegemann et al. 2018).

3.5.8 Extraction and Quantification of Polyamines

Fresh nodules (ca. 20 mg) from selected transgenic knockout plants grown *in vitro* on NOD medium containing 5 mM nitrogen were ground in 2-mL reaction tubes (Sarstedt, Nümbrecht, Germany) using the Mixer Mill MM 400 (Retsch, Haan, Germany) for 2 min by means of metal balls in liquid nitrogen. The resulting powder was extracted in 1 mL perchloric acid (5%, v/v) containing 1,7-diaminoheptane [3 nmol/1 mg FW] as internal standard for 1 h at 4°C with end-over-end agitation (ca. 30 rpm). After centrifugation (14,000 x g, 10 min), 500 µL of the supernatant were neutralized to pH 8 with 10 M NaOH. Sample derivatization, chromatographic separation, and quantification of polyamines were carried out according to Kaltenegger et al. (2021).

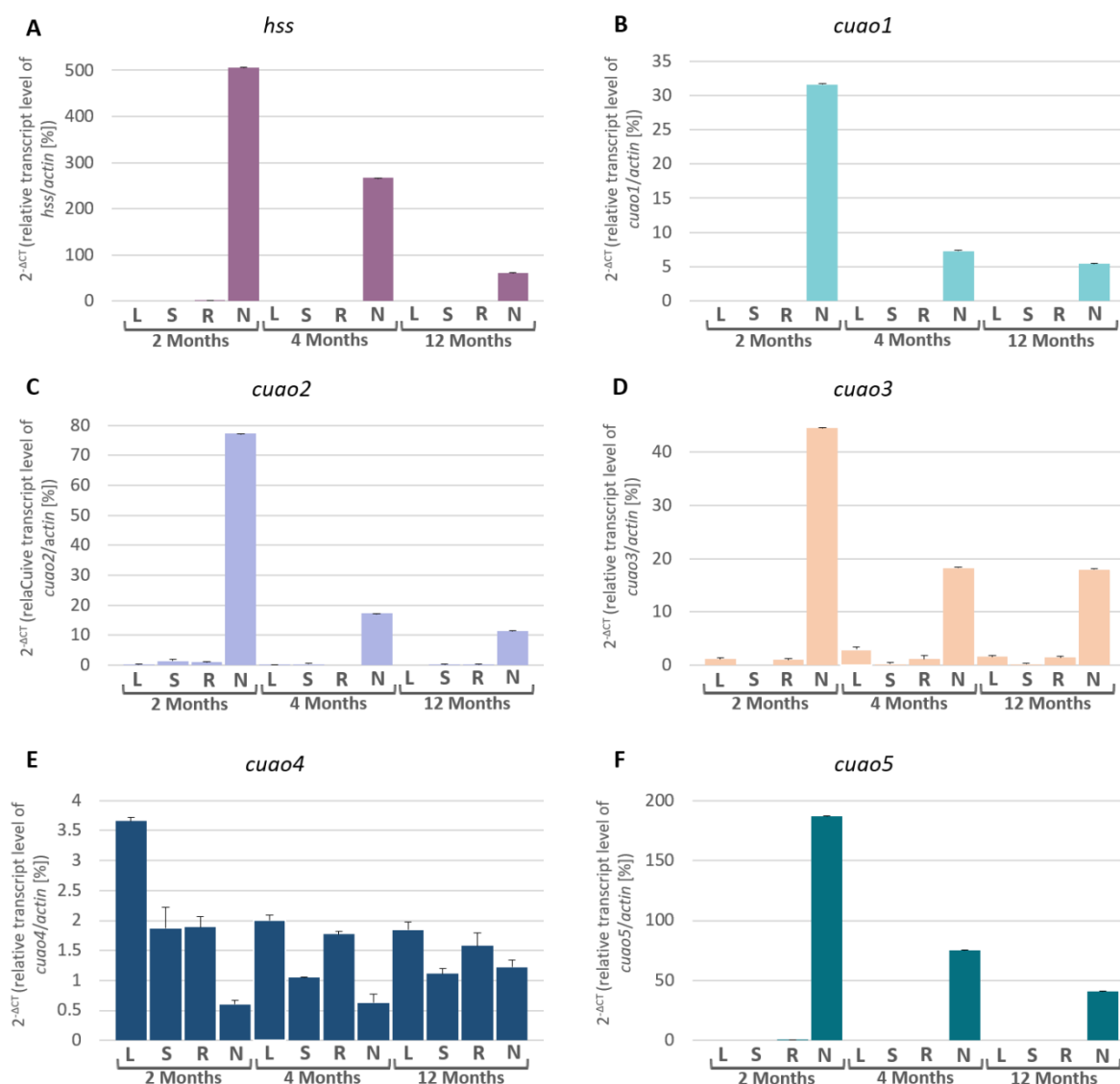
3.5.9 Feeding experiments to nodules of *C. spectabilis* knockout plants

[¹²C]- and [¹³C]-Hspd were prepared enzymatically from [¹²C]- and [¹³C]- Put, respectively, by using bacterial HSS and purified by ion exchange chromatography as described in Zakaria et al. (2022). Two detached nodules of selected knockout lines were incubated with 1 mM Hspd in 1 mL liquid NOD medium (5 mM nitrogen, supplemented with 500 µg/ml of a mixture of ticarcillin and clavulanic acid) in 2-ml reaction tubes for up to 120 h. Reaction tubes were fixed horizontally on an orbital shaker (100 rpm) and incubated in the climate chamber (settings identical to that used for *in vitro* cultivation of *C. spectabilis*, see above). At the end of the experiment, the nodules were harvested, washed with water, dabbed dry with tissue paper, and processed for analyses of PAs and intermediates as described above.

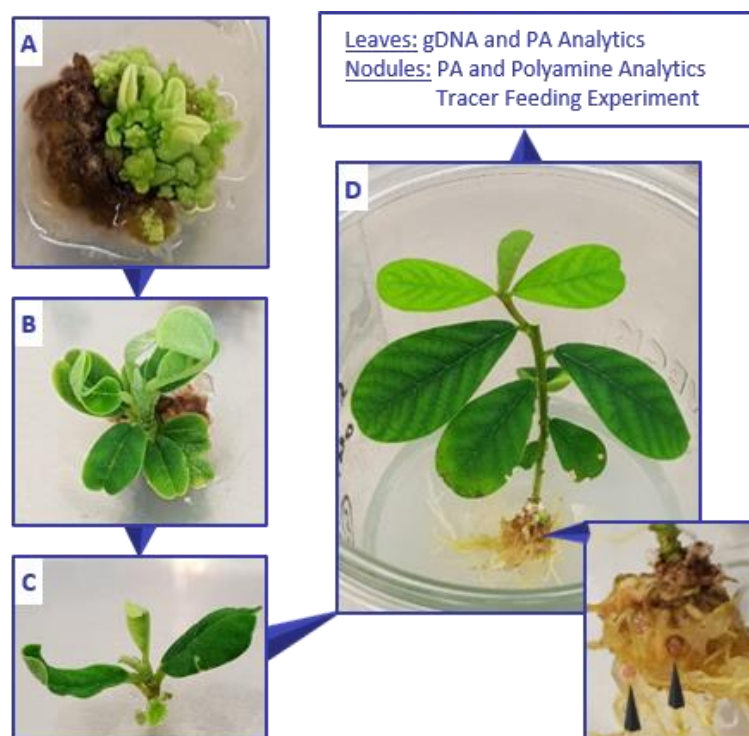
3.5.10 Phylogenetic analysis

Transcript sequences of 52 CuAO-like proteins were taken from the databases and used for phylogenetic analysis (Supplemental Table S2). The sequence alignment and the phylogenetic tree were obtained by using the Geneious software package (Geneious Prime®, Biomatters, Ltd., Auckland, New Zealand). Pairwise alignment options for building a distance matrix: alignment type: global alignment with free end gaps; cost matrix: 65% similarity (5.0/-4.0). Tree builder options: genetic distance model: Tamura-Nei; tree build method: Neighbor-Joining; no outgroup.

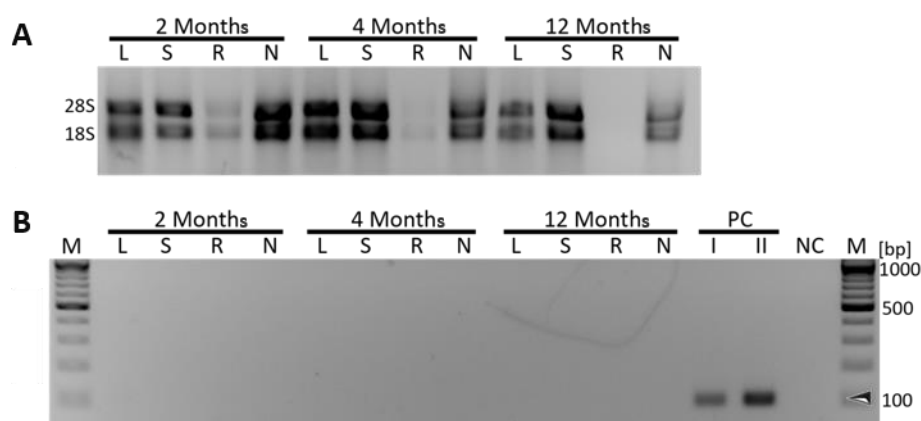
3.6 SUPPLEMENTAL DATA



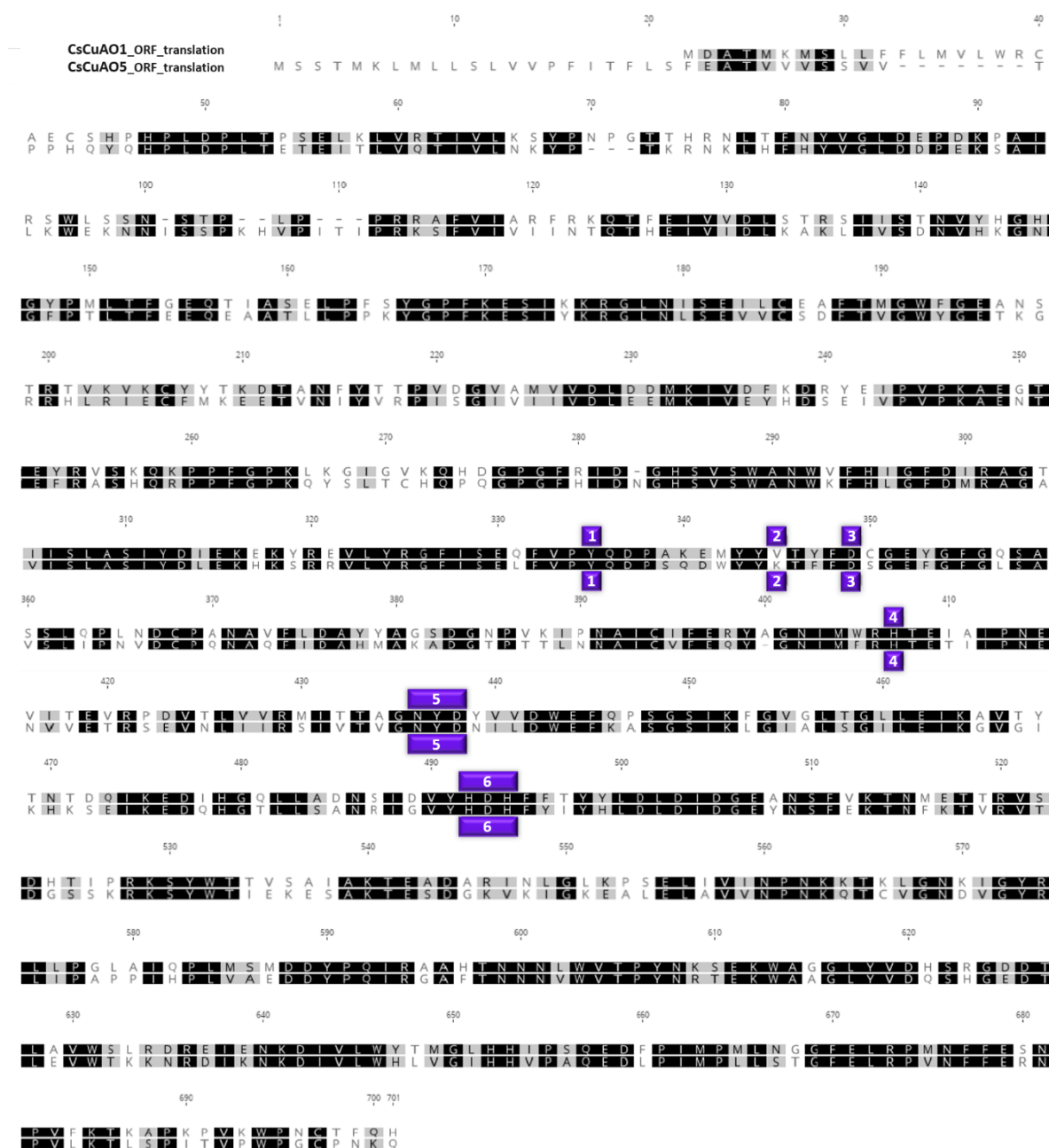
Supplemental Figure S1. Relative expression profile of the genes encoding HSS and CuAOs in *C. spectabilis*. Various tissues of *in vitro*-grown *C. spectabilis* individuals that nodulated after infection with *Bradyrhizobium* were analyzed after 2, 4, and 12 months. The gene encoding actin (ACT) served as reference for normalization of expression levels. L, leaf; S, stem; R, root; N, nodule.



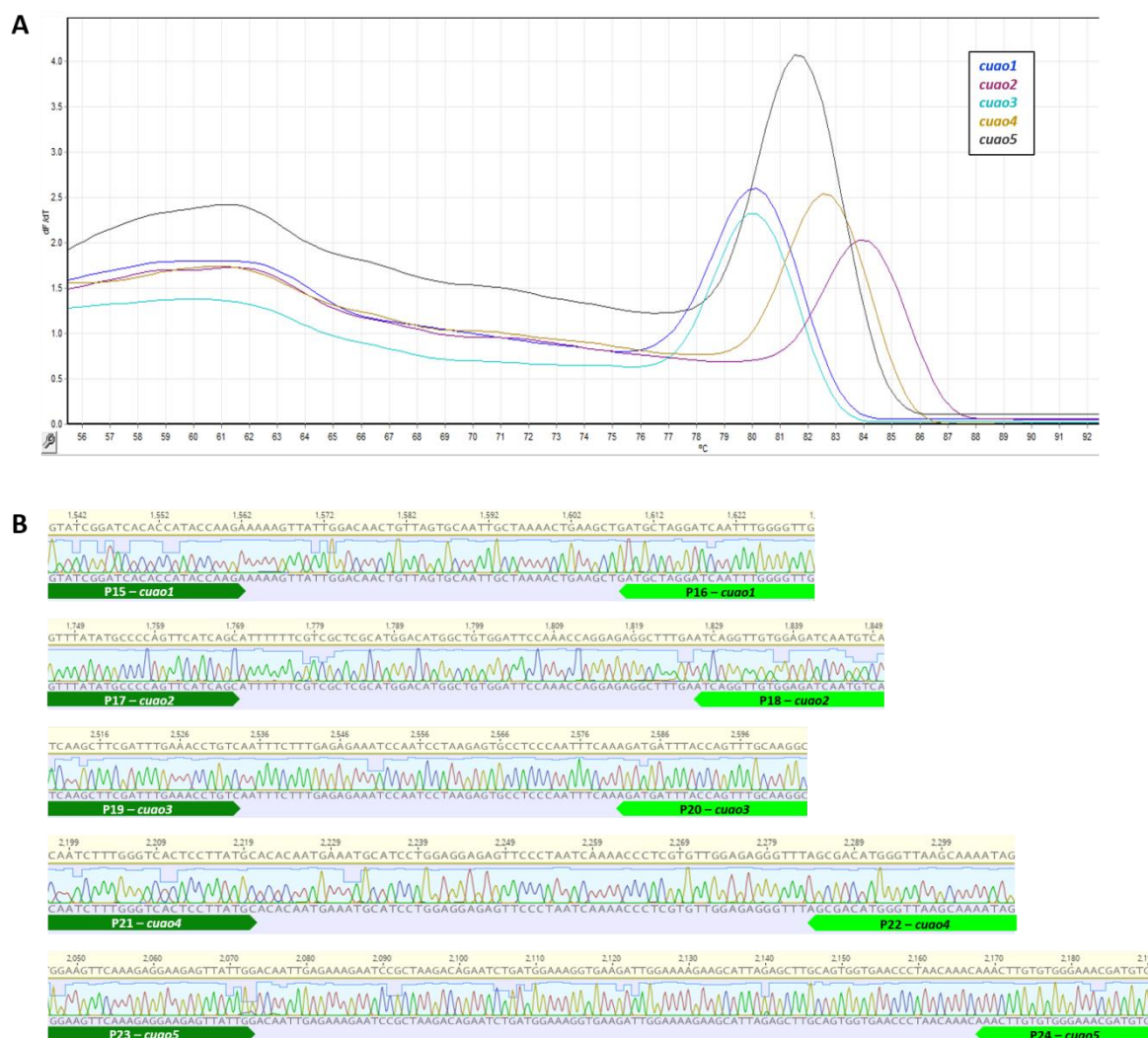
Supplemental Figure S2. Transformation stages to get nodulated plants of *C. spectabilis*. **A** Callus development after treatment with the hormones 2,4-Dichlorophenoxyacetic acid and thidiazuron. **B** Shoot development induced by thidiazuron. **C** Shoots were cut out of the callus and put on new media supplemented by naphthaleneacetic acid for root developing. **D** Fully developed plant forming nodules after infection with *Bradyrhizobium* strain.



Supplemental Figure S3. Quality tests of total RNA and cDNA of *C. spectabilis* used for reverse transcription and qPCR. **A** Total RNA was tested by agarose gel electrophoresis to exclude degradation. **B** cDNA was tested by PCR for contamination with gDNA. The PCR is based on amplification of the reference gene encoding ACT with primer pair (P11/P12) in samples that were prepared from total RNA without reverse transcription (-rt control). RNA was isolated from leaves (L), shoots (S), roots (R), and nodules (N). Contamination of RNA with gDNA would result in PCR products of an expected size of 100 bp as it is the case for the positive controls containing cDNA of a leaf (PC I, the amplified sequence stretch does not contain introns) and gDNA (PC II) (arrowhead). PCR was done with GoTaq DNA polymerase (Promega) at an annealing temperature of 60°C. M, DNA ladder (GeneRuler 100 bp Plus DNA Ladder, Thermo Scientific); PC, positive control; NC, no-template control. Please note that RNA concentration of 12-months-old root was too low for both reverse transcription and performing a RNA gel, therefore, the latter was not carried out.



Supplemental Figure S4. Sequence comparison on amino acid level of the ORFs of CsCuAO1 and CsCuAO5. Purple boxes display amino acids that are involved in the formation of the active site of the protein. 1 = conserved tyrosine; 2 = conserved valine (CsCuAO1) and lysine (CsCuAO5); 3 = conserved aspartic acid of the active center (CsCuAO1 and CsCuAO5); 4 = conserved histidine of the active center; 5 = active center consisting of asparagine, tyrosine and proline; 6 = conserved histidine, aspartic acid, and histidine.



Supplemental Figure S5. Specificity tests of the primers for qPCR analysis in *C. spectabilis*. **A** Melting curves of CuAO1 to 5 products resulting from the first RT-qPCR run were recorded and show that only one PCR product was synthesized. **B** Verification of the specificity of primer binding by sequencing of the PCR products amplified with primer pairs P15/P16, P17/P18, P19/P20, P21/P22, and P23/P24 for the transcripts of *cscuao1* to *cscuao5*, respectively.

Supplemental Table S1. Primer sequences.

No.	Sequence (5'-3')	Purpose	Lab name
P1	AGTAACCCCCAAAGTATAAACC	for, full-length cDNA CsCuAO1, binds in 5'UTR	NJ-CsDAO1-f1
P2	TGGGGTGAAATCTCATGTTCCC	rev, full-length cDNA CsCuAO1, binds in 3'UTR	NJ-CsDAO1-r1
P3	GCTTGAGCTAGGTAGCCATGAG	for, full-length cDNA and genomic DNA encoding CsCuAO5	NJ-CsDAO5-f6
P4	TTCTCATTAGAAATAGTTGCTGACATTGCA	rev, full-length cDNA and genomic DNA encoding CsCuAO5	NJ-CsDAO5-r4
P5	GCTAAAGAAATGTATTACGTTACCTACTTTGAT	for, first partial genomic sequence of the gene encoding CsCuAO1	AS_CS_DAO1A_forw
P6	ACATAGTCGTAGTTGCCAGCTG	rev, first partial genomic sequence of the gene encoding CsCuAO1	AS_CS_DAO1B_rev
P7	GGCGTCACACAGAAATCGCAATA	for, inverse PCR for amplification of partial genomic sequence encoding CsCuAO1	ASCSDAO1_Inv_for
P8	CCAGCATAGTATGCATCTAGGAAGAC	rev, inverse PCR for amplification of partial genomic sequence encoding CsCuAO1	ASCSDAO1_Inv_rev
P9	GTGGGGAGTGTGAACTGTGAT	for, transcript encoding UBQ, RT-qPCR, product size: 91 bp	NP25_UQ-Cs_for
P10	GTCGACTCGAGAATTC(T) ₁₇	rev, transcript encoding UBQ, RT-qPCR, product size: 91 bp	D4 Oligo(dt)
P11	TGGAAGCCACTGGAATTCATGA	for, transcript encoding ACT, RT-qPCR, product size: 100 bp	NP26_Act-Cs-for
P12	CCACCACTGAGCACGATATTTTC	rev, transcript encoding ACT, RT-qPCR, product size: 100 bp	NP27_Act-Cs-for
P13	AGATTCTCAAAGAGTAAGCTCGAATC	for, transcript encoding HSS, RT-qPCR, product size: 150 bp	NP13_Cs_A-for
P14	TAGTCTGAAGAAACAAAGAACAAGAAC	rev, transcript encoding HSS, RT-qPCR, product size: 150 bp	NP13_Cs_A-rev
P15	GTATCGGATCACACCATACCAAGA	for, transcript encoding CuCAO1, RT-qPCR, product size: 93 bp	NJ_CsDAO1_RT_for1
P16	CAACCCCAAATTGATCCTAGCATC	rev, transcript encoding CuCAO1, RT-qPCR, product size: 93 bp	NJ_CsDAO1_RT_rev1
P17	GTTTATATGCCCCAGTTCATCAGC	for, transcript encoding CuCAO2, RT-qPCR, product size: 105 bp	NJ_CsDAO2_RT_for1
P18	TGACATTGATCTCCACAACCTGAT	rev, transcript encoding CuCAO2, RT-qPCR, product size: 105 bp	NJ_CsDAO2_RT_rev1

P19	TCAAGCTTCGATTTGAAACCTGTC	for, transcript encoding CuCAO3, RT-qPCR, product size: 95 bp	NJ_CsDAO3_RT_for1
P20	GCCTTGCAAACGGTAAATCATCT	rev, transcript encoding CuCAO3, RT-qPCR, product size: 95 bp	NJ_CsDAO3_RT_rev1
P21	CAATCTTTGGGTCACCTTATGC	for, transcript encoding CuCAO4, RT-qPCR, product size: 111 bp	NJ_CsDAO4_RT_for1
P22	CTATTTTGCTTAACCCATGTCGCT	rev, transcript encoding CuCAO4, RT-qPCR, product size: 111 bp	NJ_CsDAO4_RT_rev1
P23	GGAAGTTCAAAGAGGAAGAGTTATTGG	for, transcript encoding CuCAO5, RT-qPCR, product size: 144 bp	NJ_CsDAO5_RT_for2
P24	CACATCGTTTCCACACAAGTTT	rev, transcript encoding CuCAO5, RT-qPCR, product size: 144 bp	NJ_CsDAO5_RT_rev2
P25	<u>ATTG</u> TACGTTACCTACTTTGATTG	protospacer sequence targeting site A within the gene encoding CsCuAO1	NJ_CsDAO1-crispA_for
P26	<u>AAAC</u> CAATCAAAGTAGGTAACGTA	protospacer sequence targeting site A within the gene encoding CsCuAO1	NJ_CsDAO1-crispA_rev
P27	<u>ATTG</u> GTAAGAATGATAACAACAGC	protospacer sequence targeting site B within the gene encoding CsCuAO1	NJ_CsDAO1-crispB_for
P28	<u>AAAC</u> GCTGTTGTTATCATTCTTAC	protospacer sequence targeting site B within the gene encoding CsCuAO1	NJ_CsDAO1-crispB_rev
P29	<u>ATTG</u> GGTAAATGTAAAAGTGATCA	protospacer sequence targeting site C within the gene encoding CsCuAO5	NJ_CsDAO5-crispC_for
P30	<u>AAAC</u> TGATCACTTTTACATTTACC	protospacer sequence targeting site C within the gene encoding CsCuAO5	NJ_CsDAO5-crispC_rev
P31	<u>ATTG</u> TGCCCACAGTGACTATAGAT	protospacer sequence targeting site D within the gene encoding CsCuAO5	NJ_CsDAO5-crispD_for
P32	<u>AAAC</u> ATCTATAGTCACTGTGGGCA	protospacer sequence targeting site D within the gene encoding CsCuAO5	NJ_CsDAO5-crispD_rev
P33	<u>ATTG</u> GAAGGTTATGACTTCAACCG	protospacer sequence targeting site E in exon 1 within the gene encoding CsHSS	Hier kenne ich den Labornamen nicht -> von BrM
P34	<u>AAAC</u> CGGTTGAAGTCATAACCTTC	protospacer sequence targeting site E in exon 1 within the gene encoding CsHSS	Hier kenne ich den Labornamen nicht -> von BrM

P35	GAGCTGGTACAATAATTTCTTAGCTTC	for, amplification of genomic sequence of <i>cscuo1</i> covering target sites A and B, product size: 525 bp	AS_CsDAO1_screen_for1
P36	CCACTAGGTTGAAATCCCAATCTAC	rev, amplification of genomic sequence of <i>cscuo1</i> covering target sites A and B, product size: 525 bp	AS_CsDAO1_screen_rev1
P37	AGCACTGTCGGGTATACTTGAAAT	for, amplification of genomic sequence of <i>cscuo5</i> covering target site C, product size: 358 bp	ASCSDAO5C_screen_for
P38	ACGGTACCCACATCGTTTC	rev, amplification of genomic sequence of <i>cscuo5</i> covering target site C, product size: 358 bp	ASCSDAO5C_screen_rev
P39	CACACAGAGACCATCATCCCT	for, amplification of genomic sequence of <i>cscuo5</i> covering target site D, product size: 386 bp	ASCSDAO5D_sreen_for
P40	ACATAAAGTACTAATATTTGAGTTCAAATTTA ACC	rev, amplification of genomic sequence of <i>cscuo5</i> covering target site D, product size: 386 bp	ASCSDAO5D_screen_rev
P41	ATCAGTGAAATCATTTTATTAACTTTAAAGAGT AAAC	for, amplification of genomic sequence of <i>cshss</i> covering target site E within exon 1, bind in upstreaming region, product size: 712 bp	ASCsHSS_Ex1_screen_for
P42	TCACCAAGCGATGTTGAGCA	rev, amplification of genomic sequence of <i>cshss</i> covering target site E within exon 1, bind at Exon2/Intron2 interface, product size: 712 bp	ASCsHSS_Ex2_screen_rev

Supplemental Table S2. Sequence origins for the phylogenetic analysis. *Sequences were taken from GenBank. ■Not the complete ORF.

Organism	Gene	ORF length [bp]	Accession number / Reference*
<i>Arabidopsis thaliana</i>	At1G31670	2226	At1G31670 /*
	At1G31690	2034	At1G31690 /*
	At1g31710	2046	At1g31710 /*
	At1G62810	2139	At1G62810/*
	At2G42490	2331	At2G42490/*
	At3G43670	2064	At3G43670/*
	At4G12270	1383	At4G12270/*
	At4G12290	2226	At4G12290/*
	At4G14940	1953	At4G14940/*
<i>Crotalaria spectabilis</i>	CsCuAO1	2022	This study
	CsCuAO2	2262	
	CsCuAO3	2214	
	CsCuAO4	2103	
	CsCuAO5	2073	
<i>Eupatorium cannabinum</i>	EcCuAO1	2148	Ober, unpublished
	EcCuAO2	2184	
	EcCuAO3	2313	
	EcCuAO4	2316	
<i>Glycine max</i>	Gm__NM_001250282	2025	NM_001250282/*
	Gm__NM_001250853.2	2301	NM_001250853.2/*
	Gm__XM_003526954	2325	XM_003526954/*
	Gm__XM_003546850	2199	XM_003546850/*
	Gm__XM_003555291	2049	XM_003555291/*
<i>Heliotropium indicum</i>	HiCuAO1	1986	MT597432/Zakaria et al. 2022
	HiCuAO2	2304	MT627598/Zakaria et al. 2022
	HiCuAO3	1980	MT627599/Zakaria et al. 2022
	HiCuAO4	2250	MT627600/Zakaria et al. 2022
	HiCuAO5	1983	MT627601/Zakaria et al. 2022
<i>Lotus japonicus</i>	Lj__BABK02012184.1	1322■	Lotus Base*
	Lj__BABK02041915.1	702■	
<i>Lupinus angustifolius</i>	La__XM_019561962.1	2122	XM_019561962.1/*
	La__XM_019568295.1	2036■	XM_019568295.1/*
	La__XM_019583671.1	2036■	XM_019583671.1/*
	La__XM_019595138.1	2015■	XM_019595138.1/*
	La__XM_019599195.1	1648	XM_019599195.1/*
	La__XM_019608353.1	2262	XM_019608353.1/*

<i>Lupinus polyphyllus</i>	LpCuAO1	1977 [■]	Jacky and Ober, unpublished
	LpCuAO2	2009 [■]	
	LpCuAO4	2066 [■]	
	LpCuAO5	2012 [■]	
<i>Nicotiana tabacum</i>	NtCuAO1	2373	DQ873385.1/*
	NtCuAO2	2301	AB289457.1/*
	NtCuAO3	2172	KJ730259.1/*
<i>Pisum sativum</i>	PsCuAO	2025	L39931.1/*
<i>Senecio vernalis</i>	SvCuAO1	2157 [■]	Ober unpublished
	SvCuAO2	2121 [■]	
	SvCuAO3	2175 [■]	
<i>Symphytum officinale</i>	SoCuAO1	2025	Zakaria, Kruse, and Ober, unpublished
	SoCuAO2	2253	
	SoCuAO3	2181	
	SoCuAO4	2169	
	SoCuAO5	2004	

4. CHAPTER B

Nodulation has no impact on the regulation of lysine decarboxylase, the first specific enzyme of quinolizidine alkaloid biosynthesis, in golden chain and yellow bush lupin

Nadine Jacky ^a, Elisabeth Kaltenegger ^a, and Dietrich Ober ^a

^a Botanical Institute and Botanic Gardens, Kiel University, Kiel, Germany

Detailed author contributions are listed at the end of the thesis.

4.1 Abstract

Fabaceae produce secondary metabolites like quinolizidine alkaloids (QAs) as chemical defense against herbivores and interact with *N*-fixing rhizobia to build up a symbiosis hosting these bacterial symbionts in special organs, the nodules. Interestingly it has been recorded that pyrrolizidine alkaloid (PA) biosynthesis depends on nodulation in *Crotalaria spectabilis* since the transcript of the specific enzyme is exclusively transcribed in nodules. To test the direct relation between nodulation and QA biosynthesis we investigated the first specific enzyme of this pathway, a lysine decarboxylase (LDC), in the following three mentioned QA producing species. In this study, we identified the sequences encoding lysine decarboxylase (*ldc*) and ornithine decarboxylase (*odc*) of *Laburnum x watereri* 'Vossii' (golden chain), *Lupinus arboreus* (yellow bush lupin) and *Lupinus polyphyllus* (large-leaved lupin), respectively. To characterize the protein functions of the identified LDCs and ODCs of *L. x watereri* 'Vossii' and *L. arboreus*, we developed a new HPLC-based method. Here, the two ODCs showed in a competition assay a clear preference for the substrate L-ornithine, whereas the two LDCs accepted both L-lysine and L-ornithine but with a strong preference for L-lysine. Moreover, we isolated successfully species-specific rhizobia strains: *Rhizobium* spec. for *L. x watereri* 'Vossii', a different *Rhizobium* spec. for *L. arboreus* and *Mesorhizobium huakuii* for *L. polyphyllus*, to trigger under controlled terms nodulation of *in vitro* grown plants. Analytics of *in vitro* grown infected (nodule possessing) and non-infected (nodule lacking) grown plants of the recent three mentioned species showed no differences within the QA content. Further investigations of several plant tissues of *L. arboreus* and *L. x watereri* 'Vossii' for *ldc* and *odc* transcript level by realtime – quantitative PCR supports the observation that nodulation has no impact on QA biosynthesis. *ldc* transcript was present in all green tissues of infield grown *L. arboreus*, while it was undetectable in roots and nodules. The same was the case for individuals cultivated under *in vitro* conditions, irrespective whether the plants formed nodules in response to rhizobial infection or not. In *L. x watereri* 'Vossii' *ldc* transcript was distinctly lower but clearly detectable in certain sampled tissue of infield grown and *in vitro* grown plants. Non-infected *in vitro* grown plants of *L. arboreus* and *L. x watereri* 'Vossii', had lower transcript level of *ldc* than infield grown ones, nevertheless contained transcript of *ldc* like infected ones.

4.2 INTRODUCTION

Members of the Fabaceae are important in ecology, economics and agriculture due to their symbiosis with nitrogen-fixing bacteria and their great diversity of secondary metabolites (Cardoso et al. 2012; Sy et al. 2001; Wink 2013). They accommodate their symbiotic partners, soil-borne rhizobia, in organs specially formed at the roots, i.e., indetermined or determined nodules (Figure 1A). Due to the possibility of the symbiotic bacteria to fix atmospheric nitrogen, fabaceous plants are grown as green manure to enriched fields with nitrogen without the use of artificial fertilizer (Bond 1948; Hirsch 1992). Various rhizobia occur in the soil but only specific species and even strains will be successful in the establishment of the symbiosis, a process controlled by the plant (De Meyer et al. 2011; Ibáñez et al. 2016).

Moreover, it has been shown that nodulation influences the pyrrolizidine alkaloid (PA) biosynthesis in the Fabaceae genus *Crotalaria*, since nodule free plants lack this group of alkaloids (Irmer et al. 2015).

Species of the Genisteae tribe within the Fabaceae produce mainly quinolizidine alkaloids (QAs) as secondary metabolites, which have a predominantly toxic and growth-inhibiting effect on competitors such as bacteria, plants or predators (Wink 2019). QAs feature a characteristic basic structure (Figure 1C), consisting of a nitrogen-containing bicyclic ring system, the quinolizidine skeleton (Bunsupa et al. 2016; Wink 2013). Lupins as well as golden chain trees are members of the Genisteae and are well known for producing QAs. A deeper insight in their genealogical relationship indicates lupins as a separate monophyletic group (Lupinae) definite from the Genistinae (Aïnouche et al. 2003).

It is assumed that a number of environmental factors influence the QA content (Figure 1B). Currently there are no studies on the influence of biotic factors, while there are a few on abiotic factors, i.e., higher ambient temperatures as well as light regulate QA biosynthesis (Jansen et al. 2015; Wink and Hartmann 1981). Accordingly, QA biosynthesis shows a diurnal rhythm in which the concentration is lower at night and higher during the day (Wink and Witte 1984). Furthermore, QA biosynthesis is dependent on soil parameters. A lower pH value of the soil (between pH 5.3 and 5.8) as well as a lack of potassium lead to increased levels of QAs, while higher soil pH values (between pH 6.7 and 7.1) or phosphorus deficiency significantly reduced the QA content (Jansen et al. 2012; Gremigni et al. 2003).

Mechanical leaf wounding increased the QA amount and could simulate an herbivorous attack, why this effect is interpreted to be a defense against nibbling predators (Frick et al. 2017). There are also studies for enhancement of nicotine biosynthesis in *Nicotiana* after leaf wounding (Baldwin et al. 1994)

The biosynthesis of QAs is not well understood. In the first specific step of QA biosynthesis (Figure 1C), L-lysine is decarboxylated to cadaverine by the key enzyme lysine decarboxylase (LDC, EC 4.1.1.18) (Bunsupa et al. 2012a). Further reactions involved in the biosynthesis of QAs are the oxidation of cadaverine followed by cyclizations and further steps to result finally in the characteristic quinolizidine backbone structure that is further diversified by reactions like esterification, dehydrogenation or oxygenation, leading to more than 170 naturally occurring structures known so far (Bunsupa et al. 2016; Frick et al. 2017). LDC derived from a duplication of a gene encoding an enzyme of primary metabolism, i.e., ornithine decarboxylase (ODC, EC 4.1.1.17). Both enzymes are classified within the enzyme class “lyases” (Webb 1992) and form homodimers as well as use pyridoxal-5'-phosphate (PLP) as cofactor (Kern et al. 1999; Bunsupa et al. 2012a). ODC converts the amino acid L-ornithine by decarboxylation to the diamine putrescine (Figure 1C) and thus catalyzes a central step in the biosynthesis of polyamines that are essential for a living cell (Kern et al. 1999).

Polyamines are small polycations derived from amino acids and are involved in a wide range of biological processes in eukaryotes and bacteria like cell growth and proliferation including processes like the translation of mRNA (Fuell et al. 2010). In plants they have a major role in response to abiotic and biotic stressors (Handa et al. 2018), whereas especially in rhizobia, polyamines are important for motility and the production of exopolysaccharides (Becerra-Rivera and Dunn 2019).

In this study, species-specific rhizobia were isolated to generate infected and non-infected *in vitro* grown plants under controlled conditions to investigate the impact of nodulation on QA biosynthesis. We studied three species of the Genisteae tribe, two lupins (*L. arboreus* and *L. polyphyllus*) as well as the cultivated variety of golden chain (*Laburnum x watereri* ‘Vossii’). These species are nodule forming plants and are described

to contain QAs and, in the case of golden chain, additionally PAs. Genes homologous to *ldc* and *odc* were successfully amplified. Following this, the correlating proteins were heterologously expressed in *E. coli* and characterized with respect to their substrate preference between L-ornithine and L-lysine. Using reverse transcription quantitative polymerase chain reaction (RT-qPCR), transcript levels of the genes encoding LDC and ODC were estimated and correlated with QA levels that have been determined by GC-MS in different organs of nodulated and non-nodulated plants.

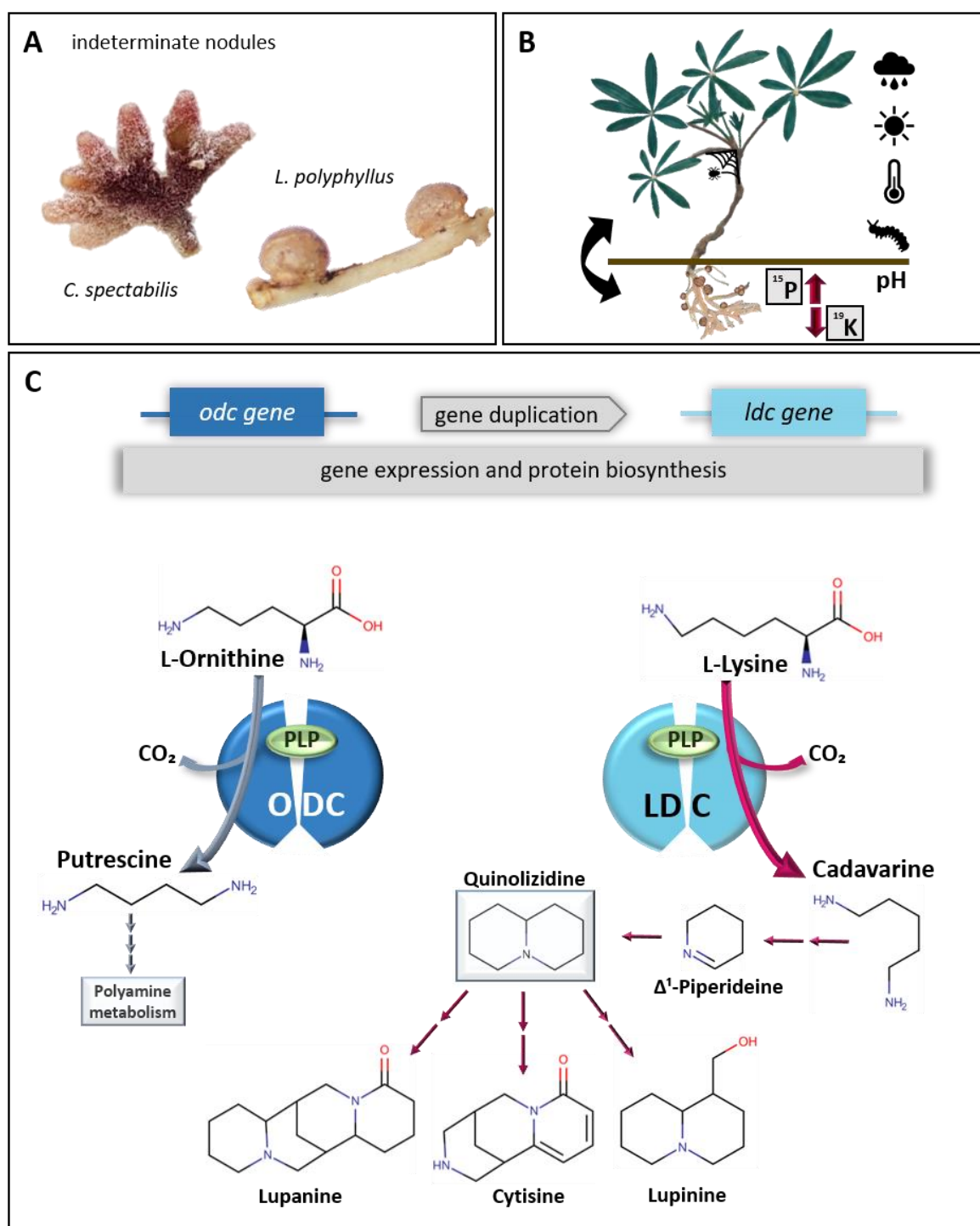


Figure 1. A Illustration of indeterminate branched (from *Crotalaria spectabilis*) and indeterminate non-branched (from *Lupinus polyphyllus*) nodules. B Environmental factors described to influence the quinolizidine alkaloid (QA) content within QA-producing plants. C Origin of the gene encoding lysine decarboxylase (LDC) by duplication of the gene encoding ornithine decarboxylase (ODC) and their relevance for QA biosynthesis and polyamine metabolism, respectively. Both enzymes are homodimers and pyridoxal-5'-phosphate (PLP) dependent amino acid decarboxylases. While ODC catalyzes a central step in polyamine metabolism by producing putrescine from L-ornithine, LDC is reported to catalyze the first step in the QA pathway by converting L-lysine into cadaverine, the precursor for the quinolizidine backbone of QAs. Tailoring reactions result in the diversification of the quinolizidine backbone.

4.3 RESULTS

4.3.1 Specific rhizobia induce nodulation in *L. x watereri* 'Vossii', *L. arboreus*, and *L. polyphyllus*

To investigate whether nodulation has an impact on QA biosynthesis and to be able to infect the three QA-producing species *L. x watereri* 'Vossii' (*Lawa*), *L. arboreus* (*Luar*), and *L. polyphyllus* (*Lupo*) under controlled conditions *in vitro* with rhizobia to induce nodulation (Figure 2), species-specific rhizobial strains were isolated from plants taken from the field. In total 13 bacterial isolates (BI) were successfully isolated from root nodules (Table 1). These bacterial isolates were identified by sequencing an amplified approx. 1500 bp long region of the 16S rRNA gene and comparing of approximately 660 – 850 bp with NCBI GenBank entries. BLAST analyses showed that 10 out of 13 isolated bacteria belong to the nitrogen fixing rhizobia group. From *Lawa* root nodules 7 isolates were sequenced. Bacterial isolate BI-1 was identified as *Burkholderia* sp. (Table 1), which is not reported to fixate nitrogen and thus was excluded from further studies. BI-3 and BI-6 proved to be identical, as well as BI-2, BI-5 and BI-7. BI-4 showed less sequence identity to the other five bacterial isolates, but all 6 were considered to be members of the *Rhizobium* genus (Table 1, Figure 3A). In a bait experiment, a mixture of these 6 rhizobial isolates was used to inoculate *Lawa* seedlings *in vitro* to trap and identify those strains that establish successfully the nodule symbiosis under these cultivation conditions. Therefore, from nodules that developed within two months, bacteria have been isolated and sequenced. Two isolates (*in vitro* BI-K1, BI-K2) were verified by sequencing, and both showed 100 % sequence identity with the isolates BI-3/BI-6 that have been considered before via BLAST search on NCBI to be *Rhizobium* sp. strain CI135 (Acc. No MG798781.1; Figure 3A). Both strains BI-K1 and BI-K2 were cultivated for further *in vitro* infections. From *Luar* merely two strains were isolated of root nodules, one showing highest similarity to nitrogen fixing rhizobia (BI-8, *Mesorhizobium* sp.) and the other with another bacterial species (BI-9, *Erwinia rhapontici*), the latter was not used for further studies. BI-8 was used to inoculate *in vitro* seedlings. Surprisingly, a different rhizobium strain was isolated (BI-K3) from *Luar* (BLAST search identified BI-K3 as *Rhizobium* sp. strain BF-E17; Acc. No KY292475.1; Figure 3B). It is possible that the initial bacterial isolate (BI-8) was not homogeneous and a rhizobial strain that was not discovered in that isolate before entered the symbiosis

efficiently. The re-isolate (BI-K3) was subsequently taken in culture and was successfully used for the succeeding experiments. For *Lupo* four isolates were isolated from root nodules. Except for BI-10, a *Tumebacillus* soil strain, belonged the other three isolates (BI-11, BI-12, BI-13) to the nitrogen fixing rhizobia. One *Mesorhizobium* strain (BI-11, *Mesorhizobium huakuii*) and two *Phyllobacterium* sp. (BI-12 and BI-13). BI-8 and BI-11 were used for a bait experiment *in vitro* to inoculate seedlings. The bacterial isolate (BI-K4) from the induced nodules of *Lupo* showed a 100% match (Figure 3C) compared to the BI-11 that have been identified via BLAST on NCBI to be *Mesorhizobium huakuii* strain Ach-305 (Acc. No MH628053.1). Through the isolated species-specific strains, cultivation of nodulated *in vitro* grown *Lawa*, *Luar* and *Lupo* were possible for the upcoming experiments. However, even after optimization the seed treatments for germination, germination and nodulation rates for *Lupo* remained extremely low. Thus, this species was excluded from further analyses (except for later following QA analytics).

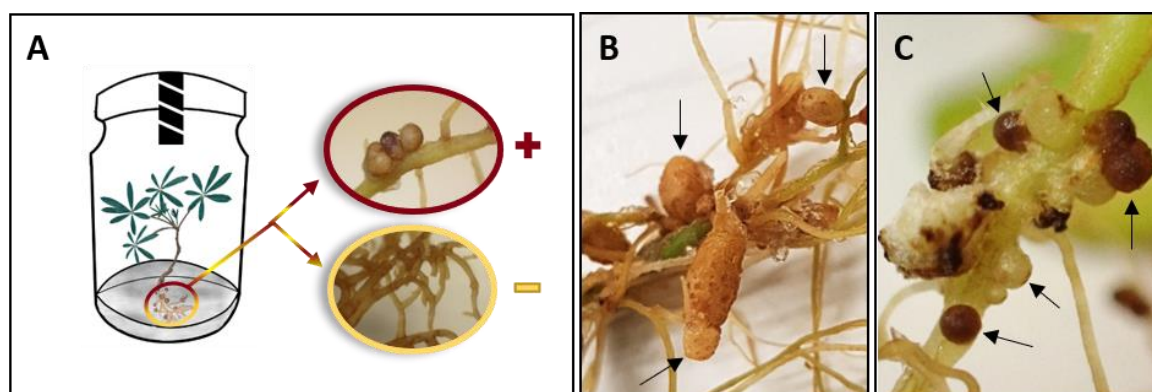


Figure 2. Developed nodules of different *in vitro* grown Fabaceae after infection with their species-specific rhizobia. **A** Schematic illustration of a *L. arboreus* plant grown *in vitro* to control nodulation. The detail images show roots with determinate nodules after infection with rhizobia (+) and roots without nodulation (-). **B and C** Roots with nodules after infection of *in vitro* grown *L. x watereri* 'Vossii' (indeterminate nodules) and *L. polyphyllus* (indeterminate nodules), respectively.



Figure 3. Sequence comparison (~130bp) of bacteria isolates (BI) of nodules taken from field grown plants and used for *in vitro* infection of selected Fabaceae. Shown in this illustration is a comparison of an out-take of 130 bp from the 660 to 850 bp amplified sequences. Nodules that developed *in vitro* on infected seedlings were used to isolate and analyze the bacterial strain involved in the symbiosis. **A** Six strains (BI-2 to BI-7) of *Rhizobium* that have been isolated and subsequently used as a mixture to infect *in vitro* grown *L. x watereri* 'Vossii' (Lawa). Of the resulting nodules bacteria were isolated again and compared to those used for the infection. Two isolated strains (BI-K1 and BI-K2) agree on sequence level with the strains BI-3 and BI-6 (red arrows) that show highest degree of identity to the *Rhizobium* sp. strain C1135 (Acc. No MG798781.1). Colony BI-K1 was cultured for further use. **B** Only one rhizobia strain (BI-8) was successfully isolated of field grown *L. arboreus* (Luar) and used for infection. Re-isolation from *in vitro* developed nodules resulted in a strain (BI-K3) that was not identical with BI-8. The used culture of BI-8 was most likely not homogenous and another rhizobial strain was able to enter the symbiosis successfully. The re-isolated strain (BI-K3) was identified as *Rhizobium* sp. with the highest similarity to Strain BF-E17 (Acc. No KY292475.1) from the database. **C** The isolated strain (BI-11) of field grown *L. polyphyllus* (Lupo) turned out to be the same *Mesorhizobium huakuii* Strain Ach-305 (Acc. No MH628053.1) triggering the nodulation of *in vitro* grown plants (BI-K4). For each species, the re-isolated rhizobia were cultured and used specifically for the approaching experiments.

Host Plant	Place of isolation	No. of isolates	Bacterial isolates (BI) from root nodules	BLAST scores			Cultivated strain for <i>in vitro</i> infection
				Query Coverage	E value	Identity	
<i>Laburnum x watereri</i> 'Vossii'	Kiel	7	BI-1 <i>Burkholderia</i> sp.	100%	0.0	100%	<i>Rhizobium</i> sp. Strain C1135 (Acc. No MG798781.1)
			BI-3/6 <i>Rhizobium</i> sp.	100%	0.0	99/100%	
			BI-2/4/5/7 <i>R. leguminosarum</i>	100%	0.0	95/100%	
<i>Lupinus arboreus</i>	Botanical Garden, Germany	2	BI-8 <i>Mesorhizobium</i> sp.	100%	0.0	100%	<i>Rhizobium</i> sp. Strain BF-E17 (Acc. No KY292475.1)
			BI-9 <i>Erwinia rhapontici</i>	99%	0.0	99.4%	
<i>Lupinus polyphyllus</i>		4	BI-10 <i>Tumebacillus</i> soil strain	98%	0.0	97%	<i>Mesorhizobium huakuii</i> Strain Ach-305 (Acc. No MH628053.1)
			BI-11 <i>Mesorhizobium huakuii</i>	98%	0.0	98%	
			BI-12/13 <i>Phyllobacterium</i> sp.	93%/97%	0.0	98%/96%	

Table 1. Bacterial isolates (BI) obtained from nodules of plants grown in the field and of plants used for a bait experiment to identify the most adequate strain for *in vitro* nodulation. Segments of 16S rRNA gene sequences (660 to 850 bp) of these strains have been compared with the data of the NCBI GenBank. The strains of the database with the highest degree of identity are listed as well as the strains identified in nodules of the bait experiment *in vitro*.

4.3.2 Identification of candidate QA biosynthetic genes and housekeeping genes in *L. x watereri* 'Vossii' and *L. arboreus*

LDC emerged by gene duplication of ODC and is reported to be involved in QA biosynthesis (Bunsupa et al. 2012a). Due to their bacterial origin, the gDNA of the enzymes do not contain any introns. Employing various PCR techniques, primer combinations and cDNA as well as gDNA as template, putative homologs of *ldc* and *odc* were successfully amplified from *Lawa* and *Luar*. For this purpose, available sequence read archives (SRAs) of *Laburnum anagyroides* genome and *Lupinus arboreus* transcriptome on NCBI were used for the search. Detailed amplification strategies are summarized in Figure 4 and Supplemental Table S4.

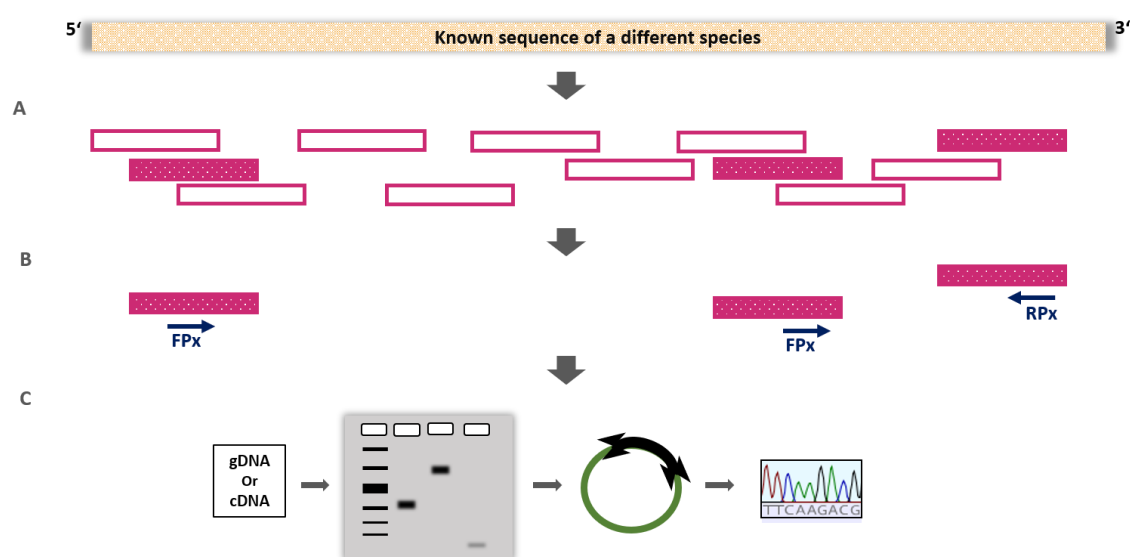


Figure 4. Approach to identify sequences of candidate genes that might be involved in QA biosynthesis from *Laburnum x watereri* 'Vossii' and *Lupinus arboreus*. Known L/ODC (comparable to LDC) and ODC sequences of *Lupinus angustifolius* served as reference. **A** Available genome (Accession: ERX147333/ERX147334 of *Laburnum anagyroides*) and transcriptome data on NCBI (Accession: SRX1721965 for *Lupinus arboreus*) were screened using BLAST. Illustration of the short overlapping BLAST SRAs hits from the database of interest after blast with the known sequence. Empty boxes represent SRA hits which were not used for primer design, while filled boxes were used. **B** Specific primer pairs were designed for each species and gene of interest (FPx/RPx) for amplification of the gene or transcript from which the fragments identified from SRA resulted. **C** The genes of interest sequences were amplified of the respective species using either gDNA or cDNA, cloned into a vector system and used for control sequencing.

The open reading frames (ORFs) of the sequences encoding putative ODC and LDC from *Lawa* are both 1302 bp long and encode 433 amino acids, while those from *Luar* have a length of 1302 bp and 1335 bp, encoding 433 amino acids and 444 amino acids,

respectively. The identified sequences share a high degree of identity with that of *Lawa* sharing a pairwise identity of 83.0% on nucleic acid and 81.1% on amino acid levels. For the sequences identified from *Luar* identities are slightly lower with 75.6% and 73.6% on nucleic acid and amino acid level, respectively.

The identification of housekeeping genes as references for RT-qPCR approaches was successful using degenerated primers and cDNA preparations of nodules and leaves of *Lawa* and *Luar*, respectively (Supplemental Table S4). For *Lawa* partial sequences of about 500 bp of the genes encoding EF1 α and ubiquitin have been identified. For *Luar*, this approach resulted in the identification of partial sequences encoding EF1 α (~520 bp), ubiquitin (~430 bp), and actin (~627 bp).

4.3.3 ODC and LDC of *L. x watereri* 'Vossii' and *L. arboreus* show both bi-functionality *in vitro*

To verify the biochemical function of putative *Lawa*ODC, *Lawa*LDC, *Luar*ODC, and *Luar*LDC the complete ORFs were cloned with a C-terminal 6xhistidine (HIS)-tag into the modified pET21d expression vector. The resulting proteins were purified by metal chelate affinity chromatography and checked for their predicted sizes of 46.777-, 46.912-, 46.340- and 47.955 kDa for *Lawa*ODC, *Lawa*LDC, *Luar*ODC and *Luar*LDC, respectively on SDS-PAGE (Supplemental Figure S1).

To analyze the enzymatic activities, the method was optimized with respect to the HPLC-based separation and detection of the derivatized substrates and products of this enzyme assays. For this purpose, standards of the individual substances were measured via HPLC in preliminary tests in order to be able to assign them based on their retention time. If the retention time was similar, the program was adapted to achieve an accurate separation. Subsequently, a mixture of the four standards was used (Figure 5, red chromatogram). The peaks of the substrates (1,2) and products (4,5) show a clear separation from each other and can be, due to the high sensitivity of the assay, precisely quantified based on their respective peak area in relation to the peak area of the internal standard diaminoheptane (DAH). The black chromatogram summarizes the result of the controls, showing detection only for piperidine, which intercept the remaining FMOC groups after derivatization, and the internal standard DAH.

To estimate the amino acid decarboxylase activities of the affinity-purified recombinant enzymes, they have been incubated with the substrates L-ornithine and L-lysine (each 10 mM) and the polyamine products were quantified via HPLC-UV as fluorenylmethoxycarbonyl (Fmoc)-derivatives using a method described previously (Kaltenegger et al. 2021).

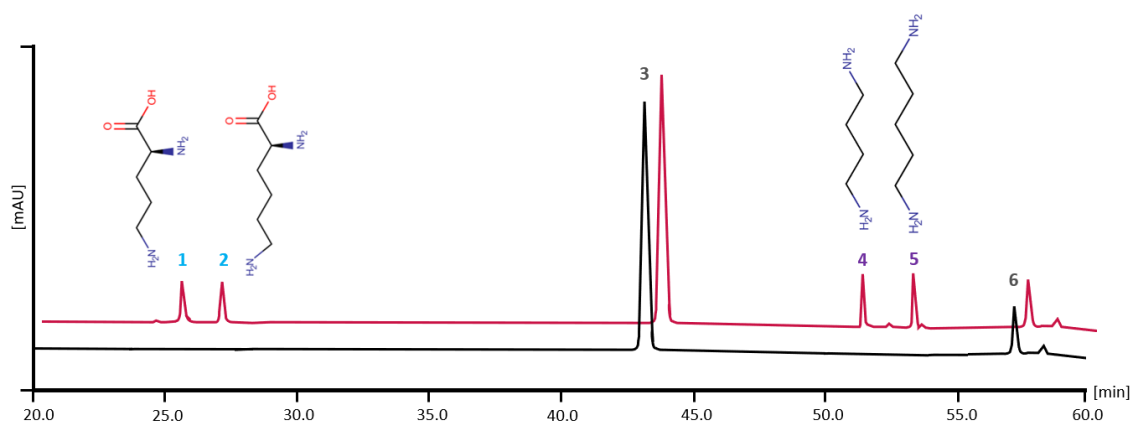
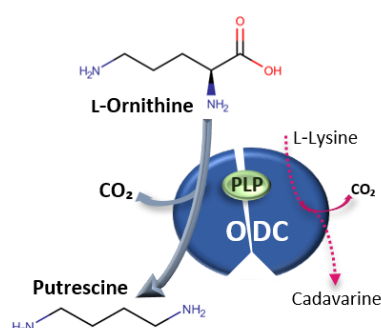


Figure 5. Separation of substrates and products of ODC and LDC enzyme assays by HPLC. Chromatograms show the controls where each of the four tested proteins was assayed without substrates (black) and a mixture of standards of used substrates and products (red). 1, L-ornithine (RT 24.749 min); 2, L-lysine (RT 26.792 min); 3, piperidine (RT 43.375 min); 4, putrescine (RT 51.086 min); 5, cadaverine (RT 52.929 min); 6, internal standard 1,7-Diaminoheptane (DAH, RT 57.383 min). Measured substrates and products were Fmoc-derivates. RT, retention time; Fmoc, fluorenylmethoxycarbonyl.

Both ODCs converted L-ornithine to putrescine with a specific activity of 133.31 ± 25.60 nkat \cdot mg $^{-1}$ (*Lawa*ODC) and 353.45 ± 92.80 nkat \cdot mg $^{-1}$ (*Luar*ODC) (Table 2A, Figure 6A and C). In contrast, the activity of these enzymes to produce cadaverine from L-lysine was about 100-fold lower (*Lawa*ODC 0.95 ± 0.13 nkat \cdot mg $^{-1}$; *Luar*ODC 3.53 ± 0.01 nkat \cdot mg $^{-1}$) (Table 2A, Figure 6A and C). Moreover, if the enzymes are exposed to substrate competition, both accept exclusively ornithine over lysine and produce putrescine only with a slightly lower specific activity than with ornithine as the sole substrate (*Lawa*ODC 108.87 ± 1.53 nkat \cdot mg $^{-1}$; *Luar*ODC 286.47 ± 26.59 nkat \cdot mg $^{-1}$) (Table 2A, Figure 7A, C). In contrast, both LDCs converted L-lysine to cadaverine with a specific activity of 274.78 ± 42.92 nkat \cdot mg $^{-1}$ (*Lawa*LDC) and 114.76 ± 48.36 nkat \cdot mg $^{-1}$ (*Luar*LDC), while the activity of these enzymes to produce putrescine from L-ornithine was about 10-fold lower (*Lawa*LDC 29.51 ± 4.04 nkat \cdot mg $^{-1}$; *Luar*LDC 8.75 ± 0.74 nkat \cdot mg $^{-1}$) (Table 2B, Figure 6B and D). If the LDCs are exposed to substrate competition they showed a lower substrate

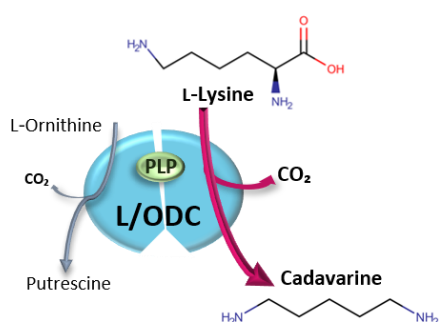
specificity than the ODCs as they converted both substrates (Figure 7B and D), but with a preference for lysine. According to that, the activities were 26.40 ± 1.23 nkat*mg⁻¹ for putrescine and 158.11 ± 7.12 nkat*mg⁻¹ for lysine of *Lawa*LDC, while for *Luar*LDC 10.13 ± 3.69 nkat*mg⁻¹ with putrescine and 47.27 ± 14.80 nkat*mg⁻¹ with lysine were measured (Table 2). Based on the data, we consider from now on *Lawa*ODC and *Luar*ODC are as ODCs and *Lawa*LDC and *Luar*LDC as functionally LDCs with an ODC side activity.

A ODC activity



Protein	Substrate [10 mM]	Specific Activity [nkat*mg ⁻¹]	
		Putrescine	Cadavarine
<i>Lawa</i> ODC	Orni	133.31 ± 25.60	—
	Lys	—	0.95 ± 0.13
	Orni + Lys	108.87 ± 1.53	n.d.
<i>Luar</i> ODC	Orni	353.45 ± 92.80	—
	Lys	—	3.53 ± 0.01
	Orni + Lys	286.47 ± 26.59	n.d.

B LDC activity



Protein	Substrate [10 mM]	Specific Activity [nkat*mg ⁻¹]	
		Putrescine	Cadavarine
<i>Lawa</i> LDC	Orni	29.51 ± 4.04	—
	Lys	—	274.78 ± 42.92
	Orni + Lys	26.40 ± 1.23	158.11 ± 7.12
<i>Luar</i> LDC	Orni	8.75 ± 0.74	—
	Lys	—	114.76 ± 48.36
	Orni + Lys	10.13 ± 3.69	47.27 ± 14.80

Table 2. Specific activities of *Lawa*ODC, *Lawa*LDC, *Luar*ODC, and *Luar*LDC tested with the substrates L-ornithine and L-lysine. Product formation was quantified after FMOC-derivatization and separation by HPLC. For each assay, technical replicates (n=3 independent enzyme assays) were implemented. Used time points to determine the specific activity are labelled in the following Figures (6 and 7). **A** Illustration of the protein function of an ODC with a potential bi-functionality and the measured specific activities of *Lawa*ODC and *Luar*ODC with the respective substrates. **B** Illustration of the protein function of an LDC with a potential bi-functionality and the measured specific activities of *Lawa*LDC and *Luar*LDC. *Lawa*, *L. watereri* x '*Vossii*'; *Luar*, *L. arboreus*; LDC, lysine decarboxylase; Lys, L-lysine; ODC, ornithine decarboxylase; Orni, L-ornithine; PLP, pyridoxal-5'-phosphate.

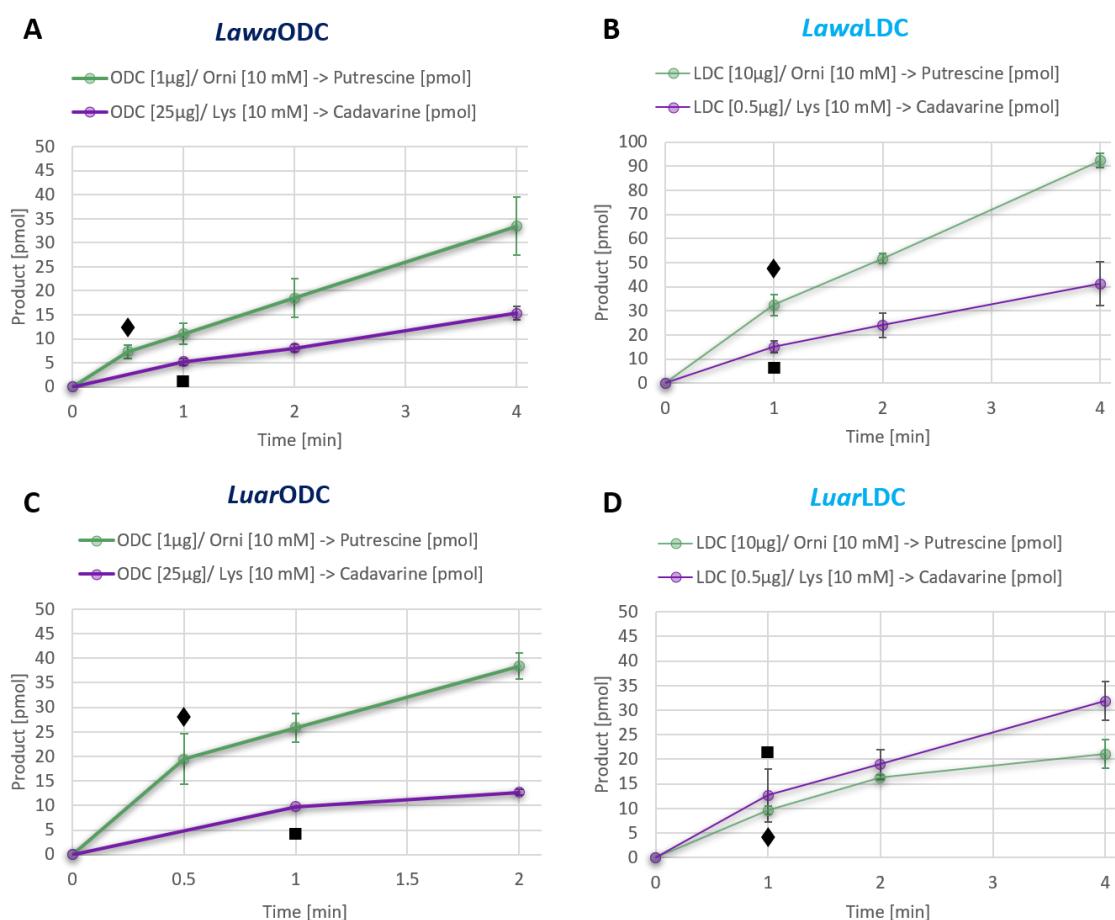


Figure 6. *In vitro* activity assays of ornithine decarboxylase (ODC) and lysine decarboxylase (LDC) of the species *L. x watereri* 'Vossii' (Lawa) and *L. arboreus* (Luar) with two different substrates, L-ornithine and L-lysine [each 10 mM]. Product was quantified at various time points to ensure linearity of the enzymatic conversion. **A** LawaODC with L-ornithine and with L-lysine as substrates (1 μg and 50 μg enzyme, respectively). **B** LawaLDC with L-ornithine and with L-lysine as substrates (10 μg and 0.5 μg enzyme, respectively). **C** LuarODC with L-ornithine and with L-lysine as substrates (1 μg and 25 μg enzyme, respectively). **D** LuarLDC with L-ornithine and with L-lysine as substrates (10 μg and 0.5 μg enzyme, respectively). ♦/■, time points which were taken to determine the specific activity in Table 2; n=3.

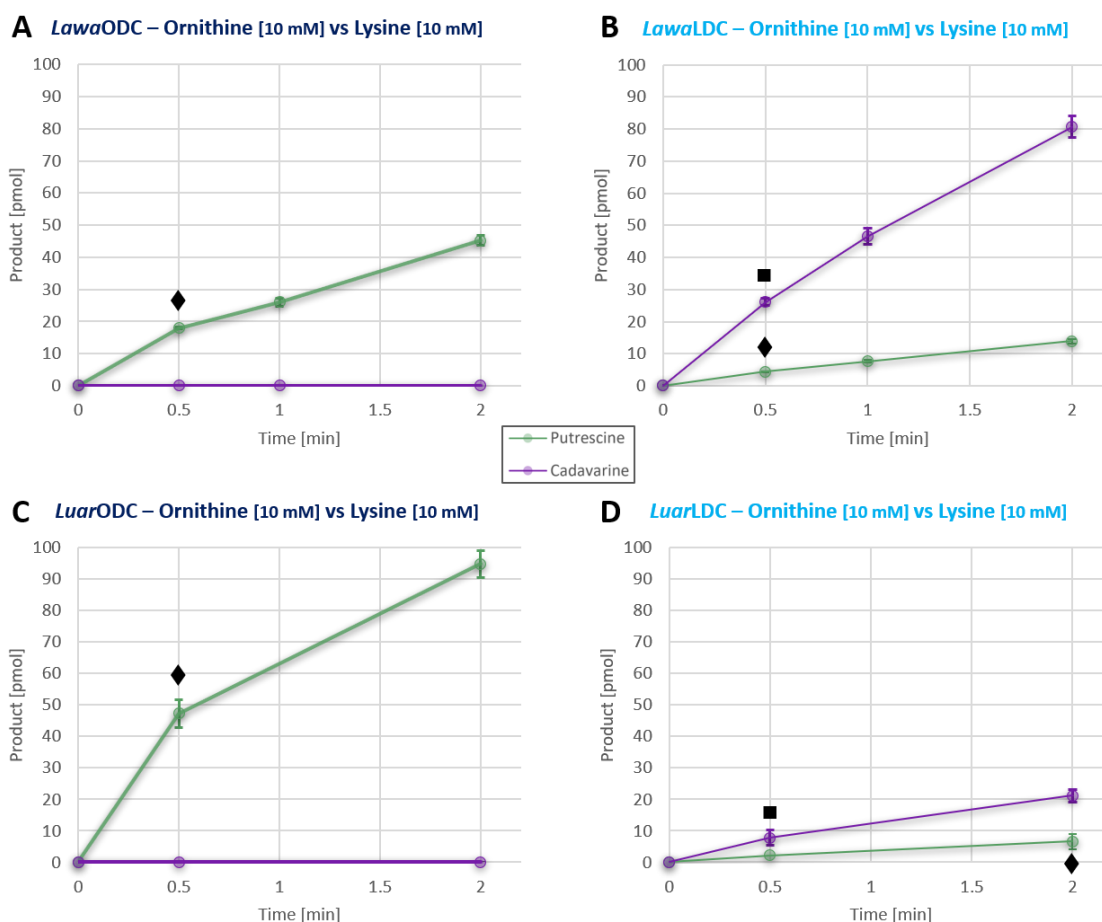


Figure 7. Substrate competition tests of L-ornithine [10 mM] and L-lysine [10 mM] with ODC and LDC [each 3 μ g] of *L. x watereri* 'Vossii' (Lawa) and *L. arboreus* (Luar). A LawaODC. B LawaLDC. C LuarODC. D LuarLDC. ♦/■, time points which were taken to determine the specific activity in Table 2; n=3.

4.3.4 Phylogenetic classification based on sequence similarities supports their tested functions of the identified LDCs and ODCs

Phylogenetic analyses were used to give a hint for potential function of the characterized LDCs (LawaLDC and LuarLDC) and ODCs (LawaODC and LuarODC). Therefore, they were compared, based on an alignment of cDNA sequences (ORFs), with known LDCs and ODCs of various species within the Fabaceae (Figure 8). Species from different tribes, which are described to produce either QAs (Genisteae and Sophoreae) or PAs (only the genera *Crotalaria* and *Lotononis* within Crotalarieae) or lacking QAs as well as PAs (Cicereae, Loteae, Phaseoleae and Trifolieae) (Wink 2013), were used. The identified sequences

which are considered to be ODCs and LDCs of *L. x watereri* 'Vossii' and *L. arboreus* according to their biochemical activity tested in this project, are clustering with in literature described ODCs and LDCs, respectively, within the Genisteae tribe. This supports their function and the hypothesis that both paralogs (one encoding an ODC and one encoding an LDC) are present in both *L. x watereri* 'Vossii' and *L. arboreus* genomes.

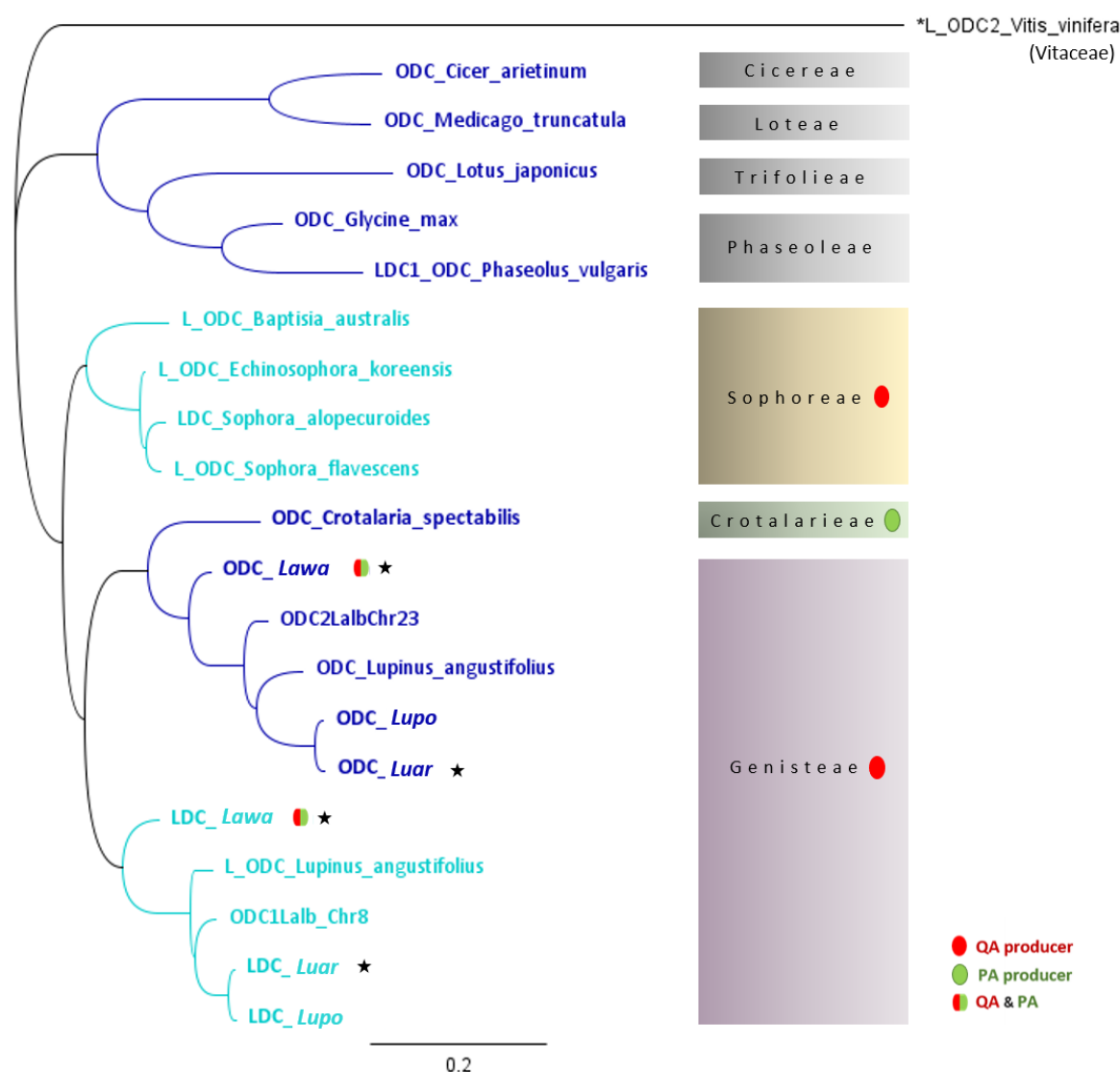


Figure 8. Phylogenetic tree of ODCs and LDCs encoding sequences (ORF or partial fragments) of selected species of the Fabaceae representing the different tribes (Cicereae, Crotalarieae, Genisteae, Loteae, Phaseoleae, Sophoreae, Trifolieae). Groups that are known to produce alkaloids are labelled with red (QA producer) or green (PA producer) dots. *Laburnum*, located within the Genisteae tribe, feature both QAs and PAs. L/ODC of the grapevine (*Vitis vinifera*, Family: Vitaceae) served as outgroup. Asterisks marked sequences were experimentally determined in this study by assays for their protein function.

4.3.5 Non-infected and infected (nodulated) *in vitro* grown plants contain several QAs with different patterns

Alkaloid extracts of various plant parts of *L. x watereri* 'Vossii', *L. arboreus* and *L. polyphyllus* were analyzed via GC-MS for the presence of QAs using lupinine (Figure 10; peak 1) or heliotrine (Figure 10; peak 11) as internal standards for quantification. Detected QAs were identified via Kovat's retention indexes (RI) and their characteristic ions m/z (Supplemental Table S6). Hereby, *in vitro* grown infected and non-infected plants in different stages were either analyzed as complete individual or dissected into the different organs. Up to nine different QAs were detectable in the measured plant tissues (Supplemental Table S1). Final concentration of QAs was calculated by adding the amounts of QA detected in the individual organs (Figure 11). *L. x watereri* 'Vossii' contain as major QA cytosine (Figure 10; peak 10) as well the QA *N*-methylcytosine/caulophylline (Figure 10; peak 9) in lower amounts. In total six non-infected plants of 2.5-, 5-, 9-, 10- and 11-months were investigated and contained between 123 μg and 304 μg QA per individual fresh weight (Figure 11A). Investigations of in total six infected 9-, 10-, 11- and 14-months old nodule possessing plants exhibited QAs in an amount ranging from 108 μg to 1055 μg per individual fresh weight (Figure 11A). To investigate the alkaloid patterns of developing seedlings, for *L. x watereri* 'Vossii' six seeds, cotyledons of a germinated seedling and a one-month-old *in vitro* grown non-infected seedling were examined for QAs (Figure 9). While within the seeds as main QA cytosine occurred (Figure 9A), the patterns changed during germination. Cotyledons already contained beside cytosine the QA *N*-methylcytosine/caulophylline (Figure 9B). The ratio was even more shifted from cytosine to *N*-methylcytosine/caulophylline in the one-month-old grown seedling (Figure 9C). This observation supposes a transformation of cytosine into *N*-methylcytosine/caulophylline during germination.

Analyzed *L. arboreus* exhibited up to six QAs (dehydrolupanine, lupanine, nuttalline, 13 α -hydroxylupanine, 3 β ,13 α -dihydroxylupanine and sparteine). The major QA lupanine (Figure 10; peak 4) was present in all investigated samples, while the other five detected QAs occurred widespread in traces (Supplemental Table S1). Overall, ten infected, eight non-infected and three seeds were examined for QAs (Figure 11B). First nodules of infected *L. arboreus* were visible after 2-months. In total ten infected plants were obtained of 2-, 3-,

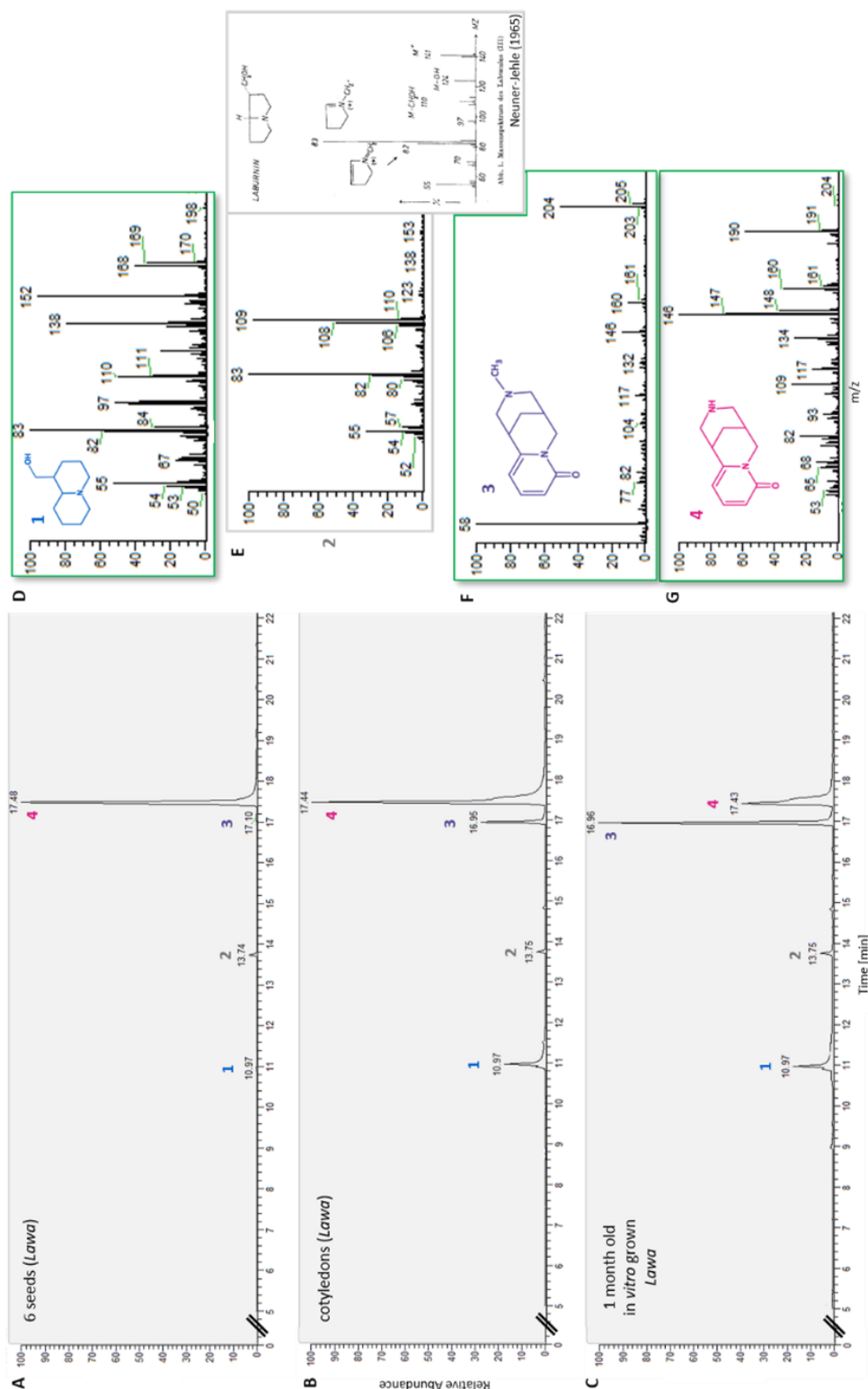


Figure 9. Development of the alkaloid pattern during germination in *L. x watereri* 'Vossii'. Shown are chromatograms of GC-MS analysis (A-C) and mass spectra (MS) of the detected alkaloids within the samples (D-G). The main alkaloid in *Lawa* is the QA cytisine (peak 4) which apparently being transformed into *N*-methylcytisine (peak 3) during germination process. Peak 1 is equivalent to the used internal standard lupinine and the detected compound in peak 2 belongs to a PA. **A** Seeds. **B** Cotyledons. **C** One month old *in vitro* grown seedling. **D** QA MS of lupinine. **E** MS of PA compound. **F** QA MS of *N*-methylcytisine. **G** QA MS of cytisine. *Lawa*, *L. x watereri* 'Vossii'; PA, pyrrolizidine alkaloid; QA, quinolizidine alkaloid; n=1.

and 4-months, whereby two 4 months old plants (Figure 11B, B15* and B16*) did not develop nodules after infection. All ten plants contained distinct amount of QAs, ranging from 689.40 μg (Figure 11B, B6(+), 4 months) to 3431.58 μg (Figure 11B, B3(+), 2 months) per individual dry weight. Likewise, all eight non-infected plants showed considerable amount of QAs, ranging from 520.76 μg (Figure 11B, B12(-), 7 months) to 3080.41 μg (Figure 11B, B1(-), 4 months) per individual dry weight. Interestingly, the oldest investigated plants were 7 months old as well as non-infected and contained the lowest concentration of QAs per individual dry weight. Variations of QAs are also visible in the seeds. The lowest measured concentration was 1237 μg in one seed (Figure 11B, B19(S)) while the highest concentration within one seed was 2368.74 (Figure 11B, B21(S)).

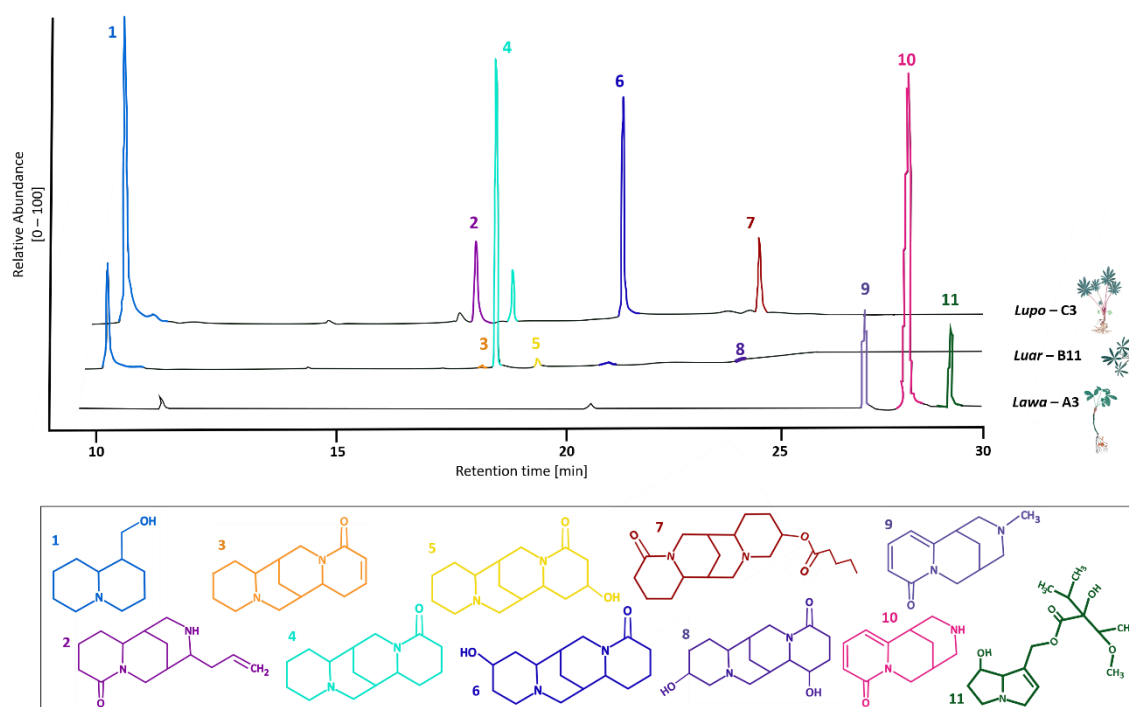


Figure 10. GC-MS chromatograms of QA analyses of *in vitro* grown plants. An internal standard (1, *Luar* and *Lupo*; 10, *Lawa*) conducted for quantification within each sample. Samples investigated of *L. polyphyllus* (*Lupo*), *L. arboreus* (*Luar*) and *L. x watereri* 'Vossii' (*Lawa*). 1, internal standard lupinine (RI 1384); 2, angustifoline (RI 2072); 3, dehydrolupanine (RI 2128); 4, lupanine (RI 2147); 5, nuttalline (RI 2244); 6, 13 α -hydroxylupanine (RI 2401); 7, 13 α -isovaleroyloxylupanine (RT 2675); 8, 3 β ,13 α -dihydrolupanine (RI 2493); 9, *N*-methylcytisine/caulophylline (RI 1952); 10, cytisine (RI 1984); 11, internal standard heliotrine.

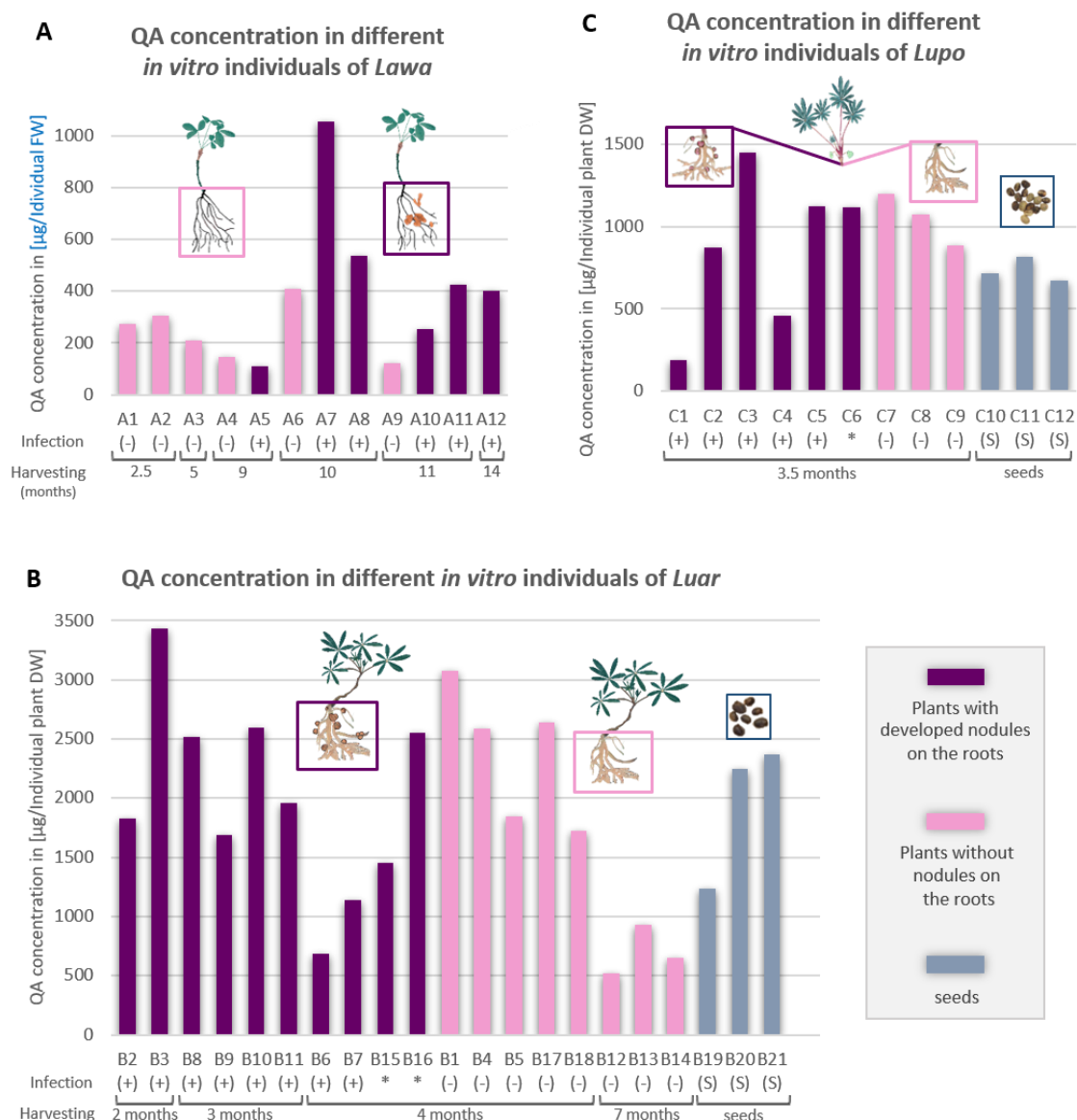


Figure 11. Analyses of total QA concentration per individual of (A) *L. x watereri* 'Vossii' (*Lawa*, FW), (B) *L. arboreus* (*Luar*, DW) and (C) *L. polyphyllus* (*Lupo*, DW). QA concentrations in seeds, non-infected and infected *in vitro* grown plants of different ages were compared. (+), infected plants with developed nodules; *, infected plants without developed nodules; (-), non-infected plants were free of nodules; (S), seeds; DW, dry weight; FW, fresh weight. $n=1$.

For *L. polyphyllus* in total five infected nodule developing plants (C1-C5), one of these infected plants did not develop nodules (C6*), and three non-infected (C7-C9) 3.5-months old plants were successfully grown in jars (Figure 11C). One single QA can not to be named as major QAs since an unequal distribution was detected within the samples (Supplemental Table S1). However, four QAs angustifoline, lupanine, 13 α -hydroxylupanine and 13 α -isovaleroyloxylupanine (Figure 10; peaks 2,4, 6 and 7) were almost present in all plants, whereas the two QAs dehydrolupanine and nuttalline (Figure 9; peaks 3 and 5) were only

detected in traces in the plants C1, C4 and C5. The amounts of detected QAs ranging from 187.86 μg (Figure 11C, C1(+), 3.5 months) to 1452.64 μg (Figure 11C, C3(+), 3.5 months) in infected *L. polyphyllus* individuals per dry weight. Non-infected individuals of the same age contained averaging more steady amounts of QAs. The individual with the lowest amount of QAs contained 886.96 μg (Figure 11C, C9(-), 3.5 months) per dry weight and the individual with the highest amount 1200.43 μg (Figure 11C, C7(-), 3.5 months). QAs concentration in seeds ranged from 670.18 μg to 818.80 μg (Figure 11C, C10 and C12). Only two infected plants (C1, C4) were below the lowest measured seed QA concentration, indicating that a new production of QAs happened probably already during growing independently of nodulation. Nevertheless, detected ups and downs of QAs in all samples led to the decision to test the impact of nodulation on QA biosynthesis additionally on the transcript level of the involved QA gene *ldc*.

4.3.6 *ldc* transcripts are detectable in plants with and without nodules

To analyze the tissue-specific expression of the gene encoding LCD as the first specific enzyme of QA biosynthesis in *L. arboreus* and *L. x watereri* 'Vossii', RT-qPCR experiments were performed. The tissues have been collected from plants in the field in the Botanic Gardens Kiel as well as from *in vitro* cultures.

Quantitative real-time PCR analyses using *ubiquitin* (Figure 12) and *ef1a* (Supplemental Figure S5) as reference genes showed that transcripts of *ldc* were detectable in almost every tissue of *L. arboreus* grown in the botanical garden. For comparison, the transcript level to the paralogue of *ldc*, *odc* was analyzed, which was constantly transcribed in all tissues of in-field grown and *in vitro* grown plants (Figure 12C, F and Figure 13F). The consistent detection of *odc* transcripts confirms intact cDNA and functioning RT-qPCR analyses. Highest transcript levels of *ldc* were found in young unevolved leaves (Figure 12; B3/12, E16). Further above ground organs such as stems (Figure 12; B9), mature leaves (Figure 12; E17) and green pods (Figure 12; E24/25) also contained a considerable amount of *ldc* transcripts but almost half as much as unevolved leaves. In contrast, hardly any *ldc* transcript was found in unripe inflorescences and in single flower buds or open flowers (Figure 12; E19-21). Also, in the roots and nodules no *ldc* transcript was detectable (Figure 12; B14/15; E22/23).

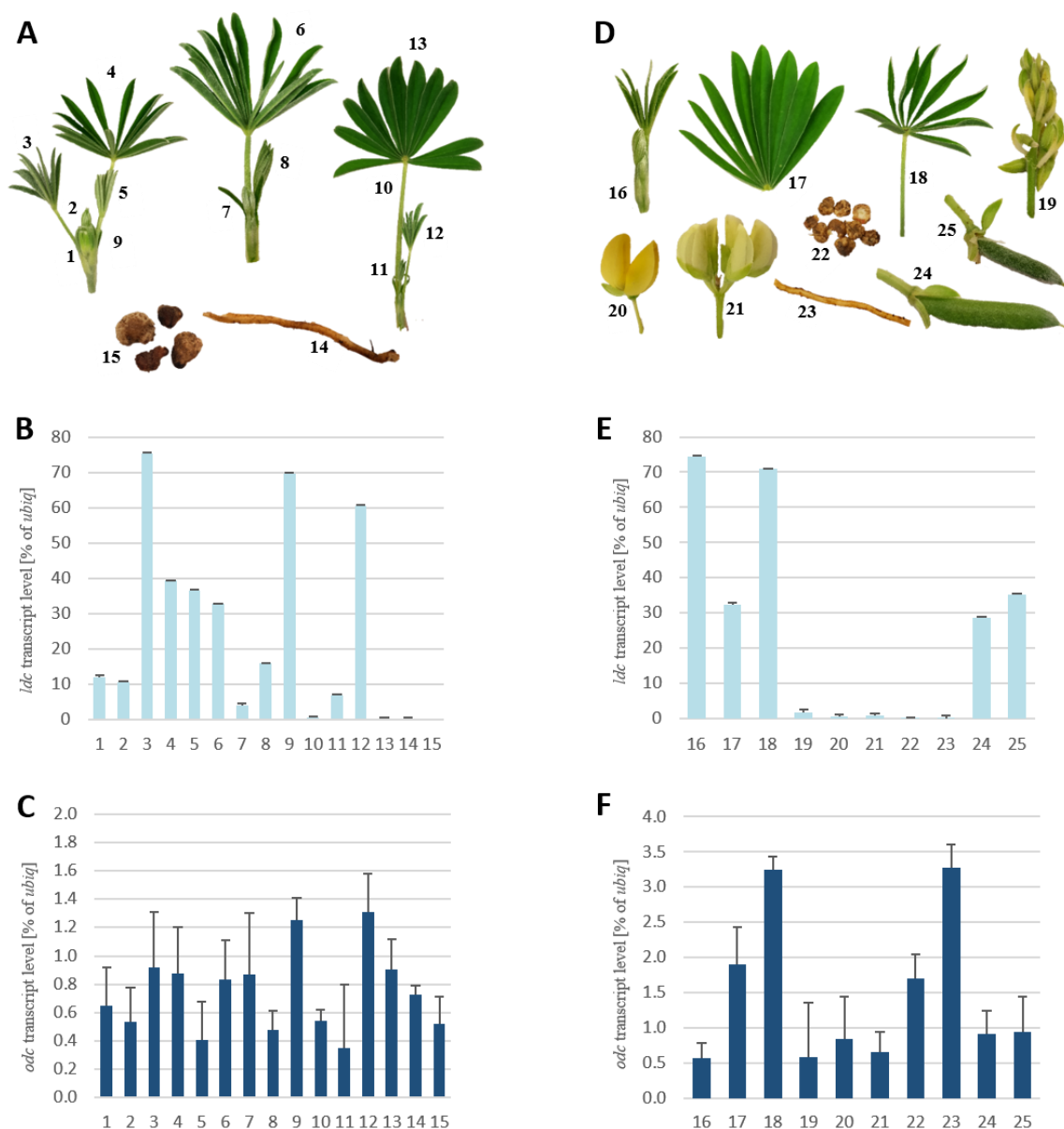


Figure 12. Relative transcript levels of *Idc* and *odc* ($2^{-\Delta CT}$) in various tissues of field-grown *L. arboreus* plants using the gene encoding ubiquitin as reference [%]]. Samples were collected in two different seasons (**A-C**; harvested April 27th, 2019), **D-F**; harvested June 14th, 2019). **A** Different tissue harvested the April 27th, 2019. **B** *Idc* transcript levels of samples given in **A**. **C** *odc* transcript levels of samples given in **A**. **D** Different tissues harvested the June 14th, 2019. **E** *Idc* transcript levels of samples given in **D**. **F** *odc* transcript levels of samples given in **D**. 1 = leaf bud; 2 = unevolved leaf; 3 = unfolding leaf; 4 = mature unfurled leaf; 5 = unevolved leaf; 6 = unfurled leaf; 7 = two unevolved leaves; 8 = unevolved leaf; 9 = petiole of samples (3-5); 10 = petiole; 11 = unevolved leaf; 12 = unevolved leaf; 13 = mature leaf; 14 = root; 15 = nodules; 16 = unevolved leaves plus larger unevolved leaf; 17 = mature leaf; 18 = leaf; 19 = inflorescence with flower buds; 20 = open flower; 21 = flower buds; 22 = nodules; 23 = root; 24 and 25 = single green pod; n=1 (tested in three technical replicates).

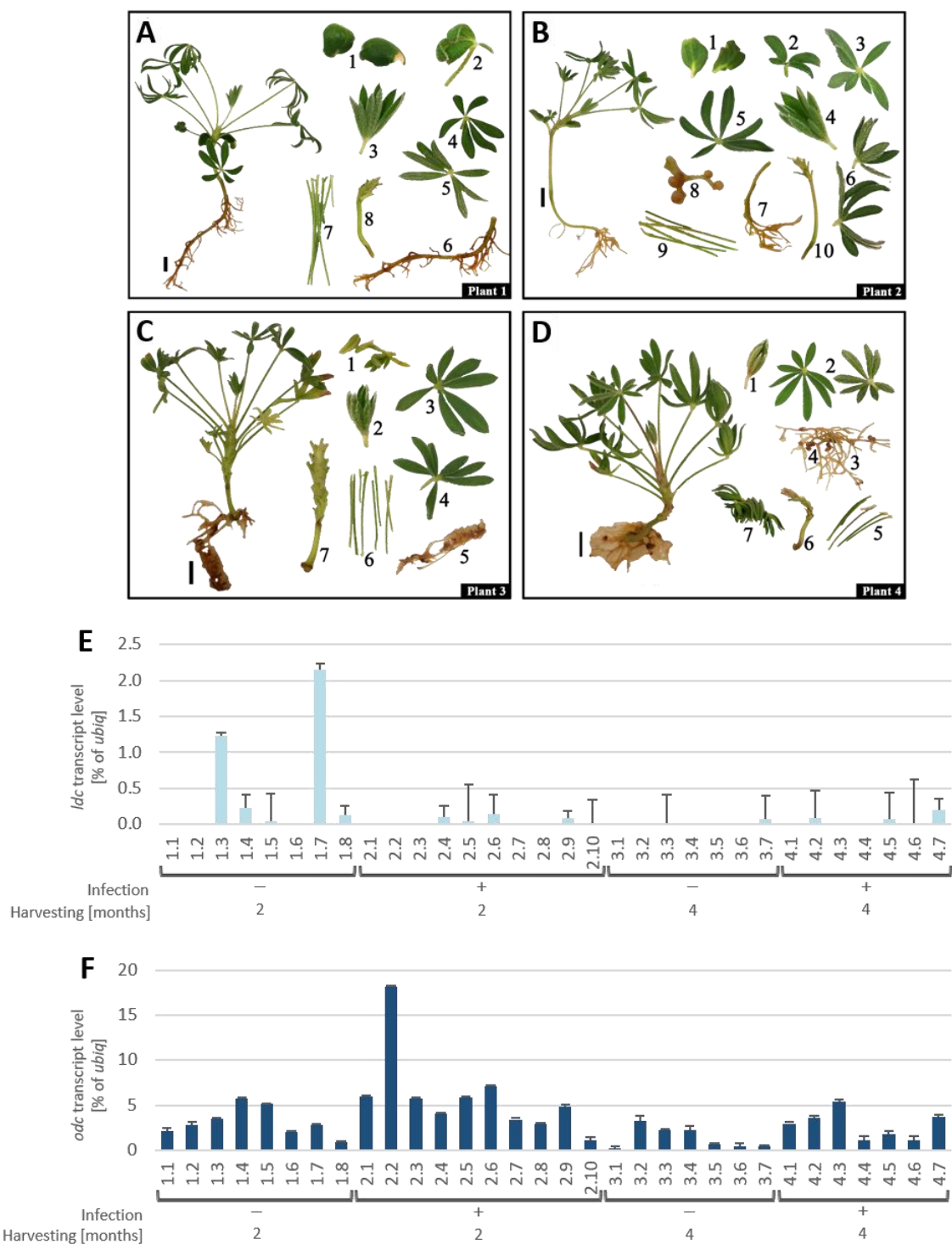


Figure 13. Transcript level of *ldc* and *odc* ($2^{-\Delta CT}$ relative transcript level of the target gene in relation to the reference gene *ubiquitin* [%]) in various tissues of 2 months and 4 months old *in vitro* grown non-infected and infected *L. arboreus*. **A Plant 1 (2 months, non-infected): 1.1 = cotyledons; 1.2 = leaf; 1.3 = unevolved leaf; 1.4 = leaf; 1.5 = leaf; 1.6 = root; 1.7 = petioles; 1.8 = main stem. **B** Plant 2 (2 months, infected): 2.1 = cotyledons; 2.2 = leaf; 2.3 = leaf; 2.4 = unevolved leaf; 2.5 = leaf; 2.6 = two leaves; 2.7 = root; 2.8 = nodules; 2.9 = petioles; 2.10 = main stem. **C** Plant 3 (4 months, non-infected): 3.1 = leaves; 3.2 = unevolved leaf; 3.3 = leaf; 3.4 = leaf; 3.5 = root; 3.6 = petioles; 3.7 = main stem. **D** Plant 4 (4 months, infected): 4.1 = unevolved leaf; 4.2 = leaves; 4.3 = root; 4.4 = nodules; 4.5 = petioles; 4.6 = main stem; 4.7 = remaining leaves. **E** *ldc* transcript level. **F** *odc* transcript level. Scale = 1cm; n=1 (tested in three technical replicates).**

To test for an effect of the *in vitro* culture on the transcript levels we also analyzed various tissues of *in vitro*-grown plants. We notice that *in vitro* plants generally have a significantly lower transcript level of *ldc* than infield grown plants, whereas *odc* shows higher transcription level by a factor of 15 in *in vitro* grown plants (Figure 13E, F). Here, a non-infected plant of 2 months showed the highest *ldc* transcript level (Figure 13E). In general, organs such as younger leaves, petioles, and more developed leaves show the highest *ldc* transcript levels, a transcription pattern similar to that of the field-grown plants. Due to the fact that *ldc* transcripts are found in organs of both nodulated and non-nodulated *in vitro* plants, an effect of nodulation on QA biosynthesis can be ruled out.

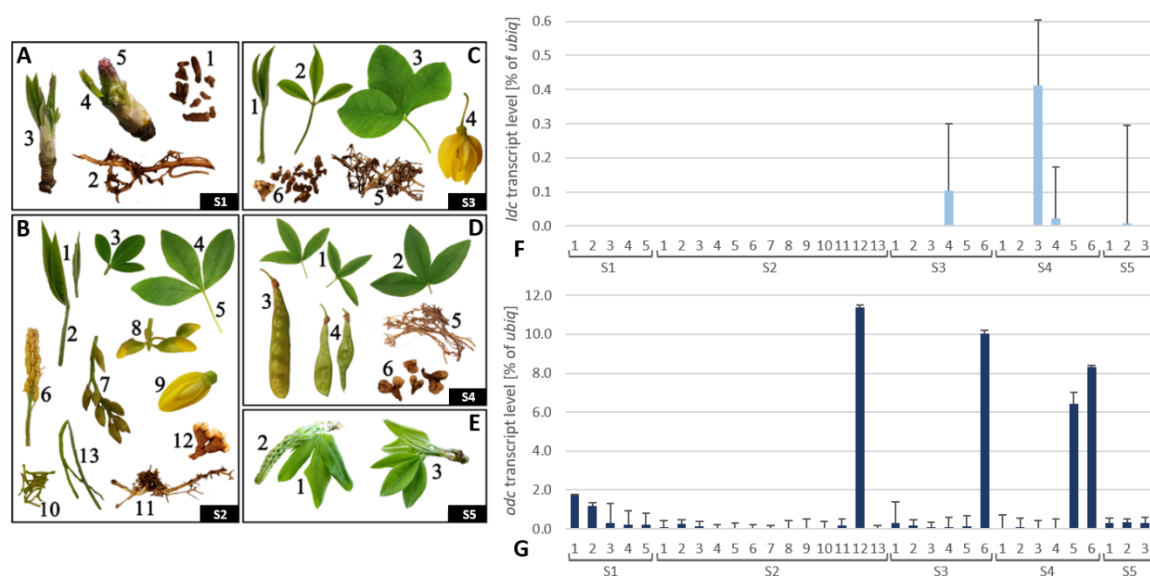


Figure 14. Transcript level of the genes *ldc* and *odc* ($2^{-\Delta CT}$ relative transcript level of the respective target gene in relation to the reference gene *ubiquitin* [%]) in various tissues (sampled at different seasons every time around 5 p.m.) of *L. x watereri* 'Vossii' grown in the Botanical Garden, Kiel (A - D) and in Molfsee (E), Germany. **A Sampling 1** (harvested April 25th, 2019): 1 = nodules; 2 = root; 3 = leaf bud; 4 = leaves of flower bud; 5 = young flower. **B Sampling 2** (harvested May 14th, 2019): 1 = unevolved leaves; 2 = petioles; 3 = leaf; 4 = mature leaf; 5 = petiole; 6 = unripened inflorescence; 7 = green enclosed flowers; 8 = green enclosed flower buds; 9 = single open flower; 10 = petioles; 11 = root; 12 = nodules; 13 = petioles. **C Sampling 3** (harvested May 27th, 2019): 1 = unevolved leaf; 2 = mature leaf; 3 = mature leaf; 4 = single open flower; 5 = root; 6 = nodules. **D Sampling 4** (harvested June 27th, 2019): 1 = mature leaves; 2 = mature leaf; 3 = green seedpod; 4 = two green seedpods; 5 = root; 6 = nodules. **E Sampling 5** (harvested April 10th, 2019): 1 = leaf; 2 = green inflorescence; 3 = leaves. **F** *ldc* transcript level. **G** *odc* transcript level; n=1 (tested in three technical replicates).

Investigations of different field-grown *L. x watereri* 'Vossii' tissues, harvested at different seasons were analyzed via RT-qPCR for transcripts of *ldc* and its paralogue *odc* referring to the reference genes *ubiquitin* (Figure 14) and *ef1a* (Supplemental Figure S6). Of tissues collected early in spring (S5), we could detect tiny amounts of *ldc* transcript only in green inflorescences, but in none of the investigated leaves taken at the same time (Figure 14; E/F; S5). In tissues collected still during spring, 15 days later (S1) and one month later (S2) compared to S5, no *ldc* transcript was detected in any of the investigated tissues (Figure 14; A/B/F; S1/S2). Two weeks after S2 further samples were collected (S3). Here, only a single open flower contained a distinct amount of *ldc* transcript (Figure 14; C4/F4; S3). The last sampling (S4) was taken one month later during summertime and the only tissue with detectable *ldc* transcript were the seedpods (Figure 14; D3/D4/F3 and 4; S4). Surprisingly in all samplings none of the other taken tissues like any kind of leaf, petioles, green closed flowers, roots or nodules showed any amount of *ldc* transcript. The analyzed paralogue *odc* showed extremely low transcripts, except for the nodules.

Comparing these results with *in vitro* grown non-infected and infected *L. x watereri* 'Vossii' with different ages, again, *ldc* transcript was barely detectable in the investigated tissues (Figure 15A). Mostly roots and petioles, sometimes leaves too, contained either more or less transcript of *ldc* in both non-infected and infected plants. Nevertheless, investigation of a whole seedling (containing young leaves, stems and root) contained already a distinct transcript of *ldc* (Figure 15; C1), while picking partial parts (marked leaves in Figure 15C) of seedlings with the same age led to no *ldc* detection (Figure 15; C2/C3). In general, *ldc* transcription seems to be little and not detectable in all tissues taken at different developmental stages of *L. x watereri* 'Vossii'. However, since *ldc* transcript is already present in non-infected seedlings, as well as in older *in vitro* grown non-infected and infected plants, the assumption is very likely, like for *L. arboreus*, that QA biosynthesis might not depend on nodulation.

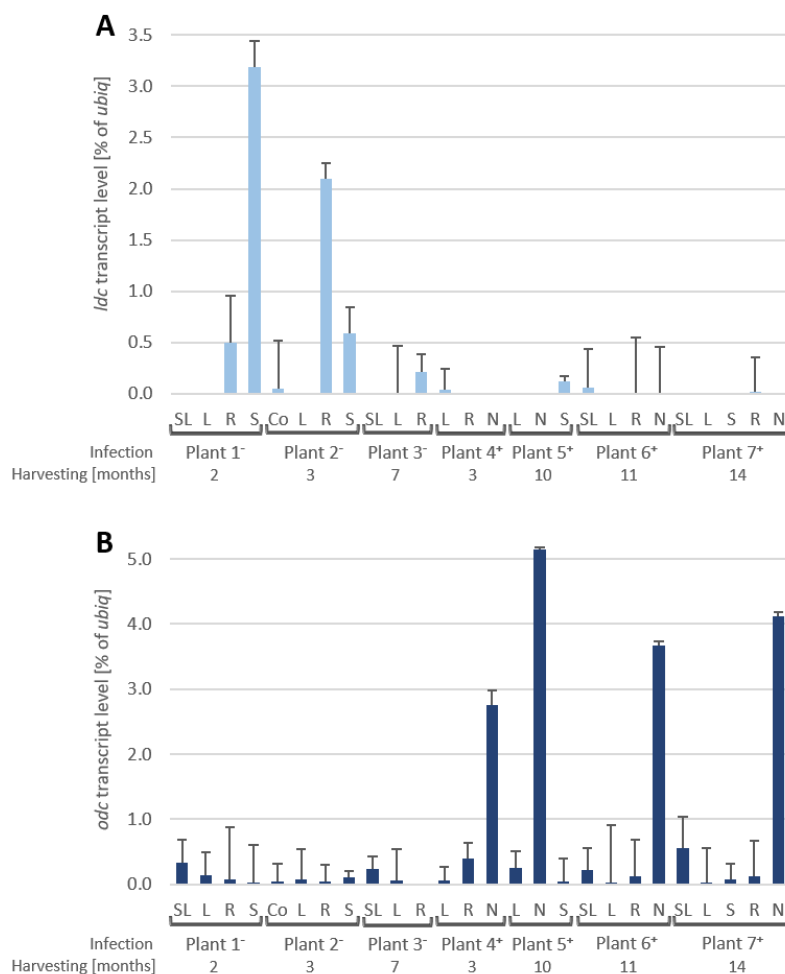


Figure 15. Transcript level of *ldc* and *odc* ($2^{-\Delta CT}$ relative transcript level of the target gene in relation to the housekeeping gene *ubiquitin* [%]) in various tissues of *in vitro* grown non-infected (-) and infected (+) *Laburnum x watereri* 'Vossii'. **A** *ldc* transcript level. **B** *odc* transcript level. **C** *ldc* and *odc* transcript level in noninfected germ buds. **Plant 1⁻**: 2 months; **Plant 2⁻**: 3 months; **Plant 3⁻**: 7 months; **Plant 4⁺**: 3 months; **Plant 5⁺**: 10 months; **Plant 6⁺**: 11 months; **Plant 7⁺**: 14 months. Co = cotyledons; L = leaf; N = nodule; R = root; S = stem; SL = small leaf; 1 = complete germ bud; 2 and 3 = analyzed only black circled leaves; n=1 (tested in three technical replicates).

4.4 DISCUSSION

4.4.1 Isolation of plant-specific rhizobial interaction partners

Fabaceae are known for their symbiosis with *N*-fixing rhizobia, which can give them a tremendous advantage over other plant species at least in habitats with nitrogen limitation. To address the question of whether nodulation affects the presence of QAs like it does for PAs in *C. spectabilis* (Irmer et al. 2015), we developed a protocol to grow, under comparable conditions, infected and non-infected *in vitro* plants of *L. x watereri* 'Vossii' and *L. arboreus* as model system.

For this purpose, nodules of field-grown plants were used to isolate species-specific rhizobia, since an ordered strain (*Rhizobium lupini*) from a database failed in previous experiments with *L. polyphyllus*. The legume-rhizobia interaction is described to be either very specific (some types of *Medicago*, *Vicia* or *Trifolium* host only one rhizobia species) or alternatively quite unspecific, in which case several rhizobial species are harbored by one host e.g. in *Cytisus scoparius* or *Lotus corniculatus* (De Meyer et al. 2011; Fisher and Long 1992). The formation of symbiosis between plant and rhizobia is influenced by a number of factors. Making the first move, plants release flavones via their roots, which are perceived by the rhizobia and result in the activation of the rhizobial *nod* genes. These nod genes synthesizing a large variety of lipochitooligosaccharides (nod-factors) that are very specific (Sajnaga et al. 2001; Tan et al. 2001; Moulin et al. 2004).

In this study the bacterial isolates were identified based on 16S rRNA gene and belonged to the genera *Rhizobium*, *Mesorhizobium* or *Phyllobacterium*. Comparing this distribution with a large-scale study by (De Meyer et al. 2011), *Rhizobium* is named as the most common rhizobia as symbiotic partner with several plant species. They examined also the two species *L. polyphyllus* and *Laburnum anagyroides*. For *L. polyphyllus* they describe four rhizobia species as symbiotic partner (*Bradyrhizobium* sp., *Bradyrhizobium japonicum*, *Rhizobium leguminosarum* and *Rhizobium* sp.). The study of Ryan-Salter et al. (2014) described mostly rhizobia from the genera *Bradyrhizobium* as the most present symbiosis partner for *L. polyphyllus*. In this study we found also different rhizobia species (*Mesorhizobium huakuii* and *Phyllobacterium* sp.) for *L. polyphyllus*, which belonged to two different genera as compared with the studies of De Meyer et al. (2011) and Ryan-Salter et al. (2014).

The bacterial isolates of *L. x watereri* 'Vossii' we obtained in our study were from the genus *Rhizobium* (*R. leguminosarum* and *R. sp.*), which dissent from the findings for *L. anagyroides* of De Meyer et al. (2011). In their study they were able to only isolate one rhizobium that was moreover from a different genus (*Bradyrhizobium sp.*).

No data were found about rhizobia that are specifically entering in a symbiosis with *L. arboreus*. During the process of isolation species-specific rhizobia of *L. arboreus* in this study, a different rhizobium (*Rhizobium sp.*) was obtained after re-isolation of an *in vitro* infected and nodule developing plant with *Mesorhizobium sp.* These findings reveal the fact that many factors play a role in the isolation of rhizobia from nodules, as well as the interaction to establish successful a symbiosis. It is possible that we were only able to identify a small proportion of rhizobia successfully during the isolation process. In this instance it could be an issue that some rhizobia genera are known as fast grower or slow grower (Bromfield and Kumar Rao 1983; Sadowsky and Bohlool 1986). Because of this, some picked colonies could have been a mixture of different rhizobia species. This might be an explanation for the different re-isolated rhizobia in *L. arboreus*.

4.4.2 Influencing factors on QA biosynthesis

QA analyses of our model plants *L. x watereri* 'Vossii', *L. arboreus* and *L. polyphyllus* with and without nodulation did not lead to an answer to our research question. The total QA concentration varied conspicuous within the individuals of infected and non-infected plants so that no clear influence on the QAs could be attributed to nodulation. Before extraction, some plants were divided into their tissues. All investigated tissues such as cotyledons, leaves, shoots, roots as well as nodules contained a similar number of QAs (Supplemental Table S1). In case of a nodule dependency, the highest concentration relative to the weight would have been expected in the nodule, like it has been observed for PAs in nodules of *C. spectabilis* (Irmer et al. 2015). Especially the cotyledons contained an enormous number of QAs, which could still be residual QAs from the seeds or already new synthesized ones depending on their stage. It has been reported that two weeks old cotyledons after germination of *Lupinus albus* were almost empty of QAs, but when they were fully enlarged and green the overall alkaloid content increased again within the growing plant by probably *de novo* synthesis (Wink and Witte 1985). Wink and Witte (1985) also investigated the

alkaloid patterns of developing seedlings of nine species from the genus *Lupinus*, *Baptisia*, *Laburnum*, *Spartium* and *Cytisus*. They observed in case of lupins that the main alkaloid lupanine decreased while an ester of 13-hydroxylupanine increased. For *Laburnum anagyroides*, *Baptisia australis* and *Spartium junceum* the main alkaloid in seeds cytosine dropped rapidly by being transformed into *N*-methylcytosine during germination (Wink and Witte 1985) which corresponds to our observations in *L. x watereri* 'Vossii' germination process (Figure 9). Furthermore, Wink and Witte (1985) monitored the alkaloid content during different developmental stages concluding that QAs serve as nitrogen source for seedlings, since QA content decrease fast after germination and then increase to a higher QA content compared with output contents of seeds. QAs would not be the only compounds that degrade so that their nitrogen can be used by growing seedlings. Non-protein amino acids have been reported to serve as nitrogen compounds in legumes and will be mobilized during seed germination and the continuing development (Polhill and Raven 1981; Rosenthal 1982). The QA observations in non-infected and infected *L. x watereri* 'Vossii', *L. arboreus* and *L. polyphyllus* of different ages in this study showed variations as well but assume that both non-infected and infected individuals produced *de novo* QAs comparing with seed QA concentrations. Thus, QA biosynthesis might not be affected by nodulation. However, the synthesis of QAs is also reported to be light-dependent and thus, higher during the day (Wink and Hartmann 1982). To proof in another manner whether biosynthesis of QAs depends on nodulation or not, the transcript levels of *odcs* and *ldcs* were examined in a wide variety of plant organs from field grown and *in vitro* plants, since the *hss* transcript in PA producing *C. spectabilis* occurred exclusively in nodules (Irmer et al. 2015). To date, studies on LDC, the first specific enzyme in QA biosynthesis, and ODC (important for plant growth) in lupins have been conducted exclusively on field grown plants that are assumed to have developed nodules (Bunsupa et al. 2012a; Frick et al. 2017). However, mainly leaves and roots were the preferred examined tissues, but nodules were never mentioned. Studies with the bitter cultivar (contains contrary to sweet lupins QAs) of *Lupinus angustifolius* showed the highest transcript for *l/odc* in young leaves compared to mature leaf, cotyledon, hypocotyl and root (Bunsupa et al. 2012a). Former studies already mentioned in general leaves and the therein located chloroplasts as site of QA biosynthesis (Schütte 1969; Hartmann et al. 1980). This observation fits with our field

grown *L. arboreus*, where the green plant parts showed the highest *ldc* transcript levels while it could not be detected in roots and nodules.

Surprisingly, the observation deviates completely infield grown *L. x watereri* 'Vossii'. Here, *ldc* transcript could not be detected even in minor traces in any of the harvested tissues such as leaves, shoots, some inflorescences, roots or nodules. Only in one opened flower, green pods and one green inflorescence *ldc* transcript could be detected in minor traces. Other factors we do not know about may have an important influence on the regulation of QA production and thus on the transcript level, too. Nevertheless, the yield of RNA and the associated cDNA was quite low in some samples and might be the reason that detection of the transcripts was limited due to the sensitivity of the used method.

A similar observation was made within the *in vitro* grown plants where the detected transcript level of *ldc* is several times lower particularly in *L. arboreus* compared to infield grown plant tissues. In *L. x watereri* 'Vossii' *in vitro* grown plants *ldc* transcripts were low too, but detectable in more tissues than infield grown tissues. More importantly, *ldc* transcript was already distinct present in a non-infected seedling. Hence, the observed differences of *ldc* transcript are not associated with nodulation. This observation is additionally supported by 2 months old infected as well as uninfected plants where *ldc* is detectable in leaves and shoots of *L. arboreus*, while in 4 months old infected and uninfected plants only minor traces of *ldc* transcript was found.

4.4.3 Substrate preferences and activity of LDCs and ODCs

To confirm the function of the *ldc* and *odc* transcripts analyzed in this study, recombinant proteins were examined for their biochemical activity, i.e., the decarboxylation of the amino acids lysine and ornithine. Up to the present day, measurements have been made based on the method of Gaines et al. (1988), where only the CO₂ gas, which is released during the reactions, can be quantified. To make clear statements regarding substrate and product identification as well as quantification, we developed a new method that allowed to distinguish the peaks of the used substrates and the formed products (Figure 5). Due to the high sensitivity of the assay, it allowed us to quantify even minor amounts of product increase and substrate decrease over the time in relation to the used internal standard. Furthermore, it allowed a clear assignment of the substances in the competition assay by

testing an enzyme with both substrates at the same time. Due to the previous mentioned analyses, we can confirm the assignment of our amplified sequences.

In this study we identified two ODCs (*LawaODC*; *LuarODC*) and two LDCs (*LawaLDC*; *LuarLDC*) from QA-producing plants. ODCs have been reported to accept only ornithine (Fuell et al. 2010) as substrate. Here, the tested *LawaODC* and *LuarODC* behaved similarly. Rapid conversion was achieved with L-ornithine, while L-lysine was only slightly converted and was only detectable when high concentrations of the ODC enzyme were used. Moreover, when both substrates were added in equal amounts in a competition assay, a clear preference was observed with only L-ornithine being accepted and converted by the ODCs.

In contrast, LDCs have already been described as L/ODCs, since they are able to decarboxylate both L-ornithine and L-lysine with quite similar (Bunsupa et al. 2012a). It is assumed that the catalytic site of L/ODC fit for both substrates despite their different side chain constitution. This was shown by the L/ODC of the bacterium *Selenomonas ruminantium* (Liao et al. 2008), L/ODC of *Lupinus angustifolius* (Bunsupa et al. 2012a) and the ODC of *Nicotiana glutinosa* (Lee and Cho 2001). In this study, *LawaLDC* and *LuarLDC* had a higher preference for L-lysine. However, in addition to L-lysine, L-ornithine was also converted in the competition assay, albeit at a lower rate than L-lysine. Based on these biochemical properties, we consider the enzymes as LDC, even so they are also able to catalyze L-ornithine. Due to their signal peptides, enzymes can be used in different parts of the cell. The compartmentalization could also be an exclusion for some substrates. *LuarODC* possesses a signal peptide for the cytosol while *LuarLDC* possesses a chloroplastic signal peptide according to WolfPSORT.

4.4.4 Phylogenetic classification

QAs are widespread in some phylogenetically related tribes of the Fabaceae (Fuell et al. 2010; Feitoza and Lima 2021; Wink 2013), but they also occur in some unrelated species like *Osyris alba* L. from the family Santalaceae (Woldemichael and Wink 2002).

Since L/ODC was proved to be the first enzyme in steps of QA biosynthesis (Bunsupa et al. 2012a), all QA containing plants should feature an LDC. While Bunsupa et al. (2012a) named the first responsible enzyme in QA biosynthesis L/ODC because of accepting L-lysine as well

as L-ornithine equally, we decided to just name it an LDC, because these two tested enzymes prefer univocally L-lysine over L-ornithine. In this study all identified LDC and ODC sequences were compared with other genes of related species to get a deeper insight in the evolution of this plant enzyme. Considering already the clustering of the LDCs and ODCs of *L. arboreus*, *L. x watereri 'Vossii'* and *L. polyphyllus* it coincides with known LDCs and ODCs of other QA producing representatives which presage their presumed function.

The identification of the recent mentioned LDCs supports the assumption that plant LDCs (*Lal*/ODC; Bunsupa et al. 2012a) are responsible for the production of cadaverine from lysine, which has been speculated since the 1980s (Pegg and McGill 1979; Hartmann et al. 1980).

Enzymes with function in secondary metabolism are often hypothesized to be originated by gene duplication of an enzyme of primary metabolism. Nucleotide mutations might result in different amino acids which in turn affect substrate specificity that implicate a new function. A very well studied example would be the homospermidine synthase, which is the first specific enzyme in PA biosynthesis and arose from the primary metabolic enzyme deoxyhypusine synthase (Hartmann and Ober 2000; Ober and Kaltenegger 2009; Irmer et al. 2015). After gene duplication, homospermidine synthase lost the ability of binding the eIF5A precursor protein and maintained the former deoxyhypusine synthase side activity, synthesizing homospermidine, as main activity (Ober and Hartmann 1999b).

The sequence similarity between LDC and ODC within one species is high (~ 85 % amino acid). Furthermore, the achieved results from the activity assays from LDCs and ODCs of *L. arboreus* and *L. x watereri 'Vossii'* with L-lysine and L-ornithine as substrates supporting the assumption that LDC also arose from a gene duplication of the primary ODC.

Conclusion/Outlook

In this study we could show that nodulation has no direct impact on the QA biosynthesis like it has been described for PA biosynthesis of *C. spectabilis*. However, the symbiosis is mostly known for nitrogen fixation by rhizobia which trade nitrogen for sugar from the plant. Further studies might be interesting in how much nitrogen is actually taken from the symbiosis to produce QAs and thus, the nodulation might have a bigger impact in this case after all. The established *in vitro* model system of this study is needful for further upcoming research where controlled conditions are required. The new developed assay in this study allowed us to detect and distinguish the substrates and products (amino acids and polyamines) of these PLP depending enzymes in the most careful way and to make a clear statement about their activity.

4.5 EXPERIMENTAL

4.5.1 Plant Material

Laburnum x watereri 'Vossii' was purchased from "Garten Baumschule Dittmann" (Gettorf, Germany) and further cultivated in Kiel Botanic Gardens (Kiel University, Germany). For one-time realtime sampling (S5), we used a *L. x watereri* 'Vossii' located in Molfsee, Germany. *Lupinus arboreus* and *Lupinus polyphyllus* are part of the living plant collection of Kiel Botanical Gardens. Samples were harvested at different seasons for infield grown *L. x watereri* 'Vossii' (timepoints in year 2019: 10th April, 25th April, 14th May, 27th May, 27th June) and infield grown *L. arboreus* (timepoints in year 2019: 27th April, 14th June). All samples of infield grown as well as *in vitro* grown plants were always harvested around 5 p.m. To establish *in vitro* cultures, seeds were surface sterilized by soaking them in 70% (v/v) ethanol (20 min), followed by 35% (v/v) hydrogen peroxide (10 min) and 96% (v/v) sulfuric acid (40 min) at 28°C/130rpm. After washing twice with sterilized water, seeds were transferred to solid NOD media (pH 6.5) containing 5 mM KNO₃, 1.14 mM CaCl₂xH₂O, 0.5 mM KH₂PO₄, 0.33 mM K₂HPO₄, 10.08 µM Na/Fe(III)-EDTA, 0.25 mM MgSO₄x7H₂O, 29.6 µM MnSO₄xH₂O, 5.2 µM ZnSO₄x7H₂O, 24.26 µM H₃BO₃, 2.26 µM KI, 0.52 µM Na₂MoO₄x2H₂O, 0.29 µM CuSO₄x5H₂O and 0.53 µM CoCl₂x6H₂O. Germinating seeds were transferred to squared petri dishes (when radicle reached at least 5 mm) covered with filter paper as described by Barbulova and Chiurazzi (2005) and either stayed uninfected or were inoculated with species-specific rhizobia strains, isolated in this study. Rhizobia cultivation and infection of *in vitro* grown plants was performed as described in Irmer et al. (2015) except that for infection, the rhizobium suspension was rinsed alongside the roots by pipetting. Well-developed plants were transferred into glass jars (Weck®, Wehr, Germany) containing solidified 5 mM N NOD media (agar 0.8%, Carl Roth® GmbH, Germany) for further cultivation. *In vitro* seedlings and plants were cultivated in a climate chamber at 24°C with a 16-h light/8-h dark cycle (average illumination 100-500 µE m⁻² s⁻¹).

4.5.2 Isolation and identification of N-fixing bacteria from root nodules

To isolate species-specific rhizobia, nodules were collected from the roots of the plants grown in Kiel Botanic Gardens and washed with water to remove residual soil. Bacteria isolation was guided by Hassen et al. (2012) and cultivation was carried out on TY medium

(Beringer 1974). Surface sterilization of rinsed nodules was either done by washing in 70% ethanol or a short flame sterilization, before they were cut with a sterile scalpel into two halves. One-half was dabbed with the cut surface onto the TY-plate, while the bacteria of the other half were absorbed by pipetting and streaked on a TY-plate. After incubation for three to eight days at 28°C, colorless and milky appearing colonies were picked, resuspended in 1 ml sterile water, and streaked out on new TY-plates to isolate individual bacterial cells. For identification, 16S rRNA gene sequencing was used. Single milky colonies were resuspended in 100 µl sterile water and 0.5 to 2 µl were used as template for PCR. PCR was performed with Phusion® Hot Start II High-Fidelity DNA-Polymerase (Thermo Scientific) under the terms of manufacturer's instructions with the primer pair P1/P2 (Supplemental Table S2) modified according to Weisburg et al. (1991). PCR products (~1500bp) were monitored by agarose gel electrophoresis and sequenced (Eurofins Genomics, Ebersberg, Germany). Sequences showed good quality in the range of 660 - 850bp and were used as query to search the NCBI data library via the basic local alignment search tool (BLAST; <https://blast.ncbi.nlm.nih.gov/Blast.cgi>) to determine the identity of the isolates. Isolates belonging to the group of *N*-fixing rhizobia were cultured and stored at -80°C containing 60% (m/v) glycerol until further use. Symbiont isolation and characterization was repeated with nodules that formed after controlled infection of the plant under *in vitro* conditions with the isolates resulting from the field-grown plants.

4.5.3 Nucleic acid extraction and cDNA synthesis

gDNA was extracted from fresh leaves with the Phire Plant Direct PCR Kit (Thermo Scientific) according to the manufacturer.

For total RNA isolation, fresh plant tissues up to 100 mg were homogenized in liquid nitrogen, mixed with 5 mg of Polyclar AT (SERVA, Heidelberg, Germany) and extracted with 0.5 – 1 ml Trizol (Carl Roth® GmbH, Germany). After one round of chloroform extraction (200 µl), RNA was purified from the aqueous phase with Direct-zol™ RNA MiniPrep Kit (Zymo Research Europe GmbH, Freiburg, Germany) according to the manufacturer's instructions. Purity and integrity of total RNA were analyzed by agarose gel electrophoresis and 260/230 nm ratio measurements via NanoDrop® ND2000 UV/VIS spectrometer with which the concentration was also determined. 0,5 – 1 µg purified RNA was used for reverse

transcription with RevertAid® Reverse Transcriptase (Thermo Scientific) and an Oligo(dT)₁₇ primer (Supplemental Table S4).

4.5.4 Identification of *ldc*, *odc* and housekeeping genes

To identify candidate *ldc* and *odc* sequences of *L. x watereri* 'Vossii' and *L. arboreus*, we used sequence read archive (SRA) files from not assembled genomes on NCBI (Acc. No. ERX147333/ERX147334 of *Laburnum anagyroides*, SRX1721965 of *Lupinus arboreus*, respectively). Sequences of *ldc* and *odc* from *Lupinus angustifolius* (Acc. No. AB560664 and XM_019582537.1, respectively) were used for a BLAST search within the Sequence Read Archives (SRAs). Based on the BLAST hits, species-specific primers were designed to amplify the predicted full open reading frames (ORF). To identify candidate *ldc* and *odc* sequences of *L. polyphyllus* illumina sequencing with leaves, roots and nodules were performed (unpublished data). For 3' prime rapid amplification of cDNA ends (3'RACE) via PCR of different reference genes (encoding ubiquitin and elongation factor 1 α) in *L. x watereri* 'Vossii' and *L. arboreus* degenerate primers were used. PCRs were either performed with Go-taq (Promega) or a Hot Start (Phire/Phusion II, ThermoScientific) polymerase due to manufactures protocol. Amplification strategies are summarized in Supplemental Table S4. PCR products were gel purified (NucleoSpin®Gel and PCR Clean-up, MACHEREY-NAGEL, Düren, Germany), A-tailed if necessary, cloned into pGEM T-easy vector system (Promega), and sequenced at Eurofins Genomics (Germany).

4.5.5 Cloning and heterologous expression of sequences encoding putative LDC and ODC

The ORFs of *LawaLDC*, *LawaODC*, *LuarLDC* and *LuarODC*, were amplified by PCR using Phusion® HS II Polymerase (Thermo Scientific) with gene specific primers featuring an overhang with restriction sites (Supplemental Table S3). For each sequence a total reaction mixture of 20 μ l was composed of 4 μ l 5x Phusion HF Buffer, 0.4 μ l dNTPs [10 mM], 0.2 μ l Phusion® HS II DNA Polymerase [2U/ μ l], 1 μ l of each forward and reverse primer [10 pmol/ μ l] and 1 μ l plasmid DNA (5 – 25 ng/ μ l) containing the ORF. Cycling conditions were adjusted to manufactures instructions. PCR products were then purified using NucleoSpin®Gel and PCR Clean-up (MACHEREY-NAGEL, Düren, Germany), before digested

(200 ng DNA) with 1 μ l BbsI to generate sticky ends which are compatible with the XhoI and NcoI (FastDigest, Thermo Fisher Scientific) generated overhangs of the used expression vector to ensure directed ligation with T4 DNA Ligase (Thermo Fisher Scientific) with an insert to vector ratio 1:3 at 16°C overnight. The used expression vector is a modified pET21d that contains a kanamycin resistance, the suicide gene *ccdB* and a C-terminal HIS tag for later protein purification. After transformation of ligation products in *E. coli* TOP10 (Invitrogen), resulting expression constructs were sequenced and transformed into *E. coli* BL21 (DE3) for heterologous protein expression. Protein expression was induced with 0.2 mM isopropyl β -D-1-thiogalactopyranoside (IPTG) at an OD₆₀₀ of 0.6-0.8 and incubated at 16°C for 16 hours. The HIS-tagged recombinant proteins were purified via nickel-nitrilotriacetic acid-agarose (Ni-NTA; Qiagen, Hilden, Germany) according to the manufacturer's instructions under native conditions in a batch procedure. Purified proteins were concentrated and rebuffed in LDC/ODC-assay buffer (50 mM potassium phosphate buffer, 1 mM ethylenediaminetetraacetic acid, 4 mM dithiothreitol, 5 μ M pyridoxal-phosphate (PLP), pH 7.4) and kept overnight at 4°C or stored in aliquots at -80°C until further use. Protein concentration was estimated following the method of (Bradford 1976) and protein purity was monitored by sodium dodecyl sulfate polyacrylamide gel electrophoresis (SDS-PAGE) using 10 % gels (Supplemental Figure S1).

4.5.6 Activity assays of recombinant LDCs and ODCs

To quantify the enzymes ability to decarboxylate L-lysine (LDC assay) and L-ornithine (ODC assay), enzymatic reactions contained a total volume of 200 μ l with 0.5-50 μ g enzyme and 10 mM lysine or ornithine as substrate in LDC/ODC assay buffer. The reaction mixtures were incubated at 30°C and 30 μ l aliquots were withdrawn after 1 to 16 minutes to guarantee linearity of the enzymatic conversion. To stop the reaction and to precipitate the enzyme, aliquots were immediately mixed with 60 μ l acetonitrile containing 5 mM diaminoheptane (DAH) as internal standard (ISTD) and placed on ice. To improve protein precipitation, samples were preserved at -20°C for 20 minutes. After centrifugation for 10 min at 21 000 g at room temperature, the supernatant was taken for quantification of the reaction products according to a method described previously Kaltenegger et al. (2021). Briefly, for derivatization of the diamines resulting from decarboxylation with

fluorenylmethoxycarbonyl protecting group (FMOC), 20 µl borate buffer (0.6 M, pH 8), 24 µl sample, 48 µl FMOC (5 mM) were incubated for 5 minutes at room temperature. 3 µl piperidine (40 mM) was added to react with excess FMOC. After incubation, 40 µl of a solution containing acetonitrile, sodium acetate buffer (400 mM, pH 5), tetrahydrofuran, and *N,N*-dimethylformamide in a ratio (v/v) of 80/40/10/10 was added to adjust the pH for subsequent HPLC analyses and to ensure solubility of FMOC-derivatives. The stated concentrations are the added stock solutions and not the final concentration within the initial solution. Finally, 50 µl tetrahydrofuran were added to further improve the solubility of the FMOC derivatives. Technical replicates (n=3) were assayed from each enzyme batch. To exclude false signals due to the respective protein, each of the four proteins was assayed without substrates as a control.

HPLC analyses for quantification of diamines were performed as described by Kaltenegger et al. (2021) with a modified gradient profile as follows: 80% B to 60% B in 15 min, to 50% B in 10 min, 50% B for 14 min, to 30% B in 12 min, to 10% B in 6 min, and to 5% B in 0 min, 5% B for 10 min.

4.5.7 Data base retrieval and gene tree

In total, 20 identified ODC and L/ODC homologs (Supplemental Table S5) from Fabaceae were analyzed. As outgroup, one ODC encoding sequence from *Vitis vinifera* genome was included and retrieved from the PLAZA 3.0 databank.

Selection criteria for the outgroup sequence were: it should be from a species, which is phylogenetically basal to the Fabaceae and which is not known to have experienced lineage specific whole genome amplifications.

On the Plaza platform, protein coding genes are stored in gene families based on sequence similarity inferred through BLAST (basic local). ODCs fall into the HOM03D002804 gene family and from *Vitis vinifera*, three genes fall into this gene family. Two are annotated as ODC and organized as tandem repeats but differ in the length of the encoded ORF. VV11G05710 (NCBI GenBank accession number AM479355), which encodes an ORF (1113 bp) comparable to the length of ODCs from Fabaceae, was used as outgroup for phylogenetic reconstructions. The second copy only encodes a 543 bp long ORF and was not included.

The ORFs of these sequences were aligned by using the MUSCLE v5 (Edgar 2004) algorithm implemented in the Geneious software package with the default settings. Based on the resulting multiple sequence a maximum likelihood phylogenetic tree was constructed by using PhyML 3.3 (nucleotide substitution model: GTR+GAMMA, equilibrium nucleotide frequencies estimated using maximum likelihood) (Guindon et al. 2010). Approximate likelihood branch supports were estimated with three tests: i) approximate Bayes (aBayes); ii) approximate likelihood test (aLRT); iii) Shimodaira Hasegawa aLRT (SH-aLRT). All three tests were congruent concerning branch support.

4.5.8 Quantitative Real-Time PCR (RT-qPCR) and primer design

Total RNA extraction and cDNA synthesis was done as previously described above. To exclude contaminations of the cDNA with genomic DNA, “no-reverse-transcription” (-rt) control reactions were set up for every sample (Supplemental Figure S3 and S4).

Design of real-time PCR primers, RT-qPCR conditions and final analyses were done as described in chapter A and chapter C with the following modifications: genes of interest were *ldc* and *odc* of both *L. x watereri* ‘Vossii’ and *L. arboreus*; genes encoding ubiquitin (*ubiq*) and elongation factor 1-alpha (*ef1a*) were used as reference for the calculation of the relative transcript level; applied template DNA ranged from 3.75 ng to 12.5 ng, depending on the yield of the respective individual cDNA tissue (n=1). Technical replicates (n=3) were achieved due to pipetting three RT-qPCR runs for determination the transcript level. Primer sequences are given in Supplemental Table S2. To exclude unspecific binding of these primers due to the high similarity of the cDNA encoding LDC and ODC, plasmids containing the LDC- and ODC-coding sequences were used as template in control PCRs that were analyzed via agarose gel electrophoresis using 3% gels (Supplemental Figure S2).

4.5.9 QA extraction and analytics by GC-MS

Plant samples of lupins were freeze-dried, weighed, then ground to fine powder and weighed again, before ~ 10 mg from this powder were used for the following extraction. To each sample of *L. arboreus* and *L. polyphyllus* a fixed amount of internal standard of QA lupinine (125 µg/ per sample) was added. For *L. x watereri* ‘Vossii’ plant material was collected and immediately frozen. QA and PA were extracted from fresh plant material

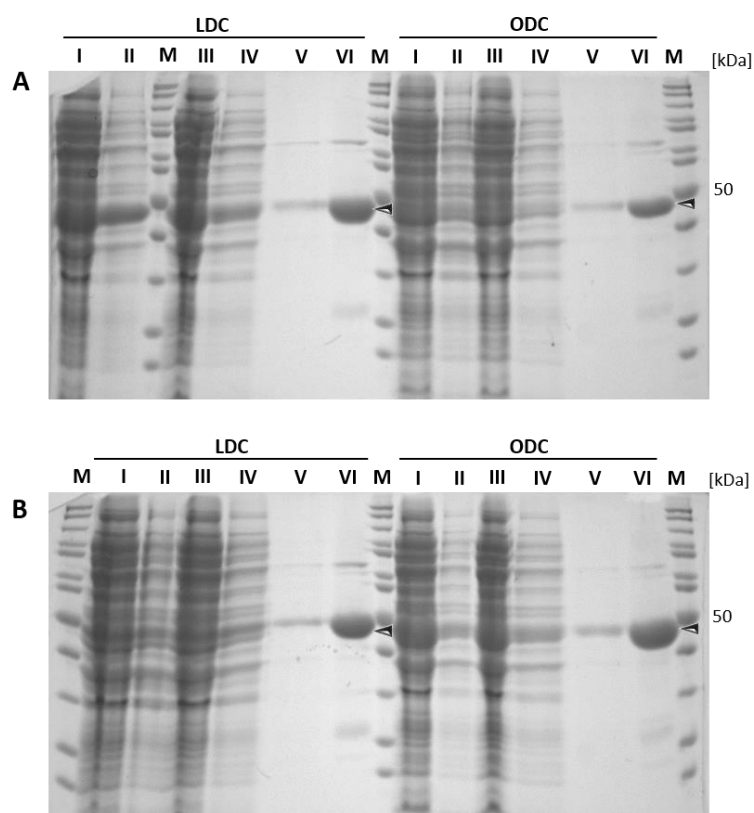
without freeze drying. 10 µg heliotrine (pyrrolizidine alkaloid) was added per 100 mg fresh weight. Weight of the samples varied from 295 – 909 mg for total plants, and 40 – 400 mg for individual plant organs. In case of GC-MS analysis of *L. x watereri* 'Vossii' germination procedure, lupinine was used as internal standard.

QAs and PAs within this study were extracted just as the described PA extraction by Kruse et al. (2017). For lupines, which do not produce PAs, reduction with zinc was excluded. GC-MS analyses were performed with Focus GC-DSQ II (ThermoFisher Scientific) equipped with a TraceGOLD™ TG-5MS Amine column (30 m × 0.25 mm × 0.5 µm; ThermoFisher Scientific, Dreieich, Germany) with a 5M Safeguard guard column, and a TRACE GC1310-TSQ Duo (ThermoFisher Scientific) and TG-1MS capillary columns (30 m × 0.25 mm × 0.25 µm; ThermoFisher Scientific).

Helium was used as carrier gas with a flow rate of 1 mL min⁻¹ (TRACE GC ULTRA-DSQ) or 1.2 mL min⁻¹ (TRACE GC1310-TSQ); injection volume of 1 µL, split 1:10 transfer line was set at 280°C and the ion source of the mass spectrometer was operated at 280°C and 70 eV for ionization.



The temperature program used was: initial 3 min at 100°C, then increasing by 6°C min⁻¹ to 300°C, followed by 10 min at 300°C. The data processing was performed by using Xcalibur™ software (ThermoFisher Scientific). The internal standard, QAs and PAs were identified via comparison with in-house and literature reference data of mass spectra and retention indexes (Wink et al. 1995) were calculated with a reference set of co-injected hydrocarbons (Sigma-Aldrich).


4.6 SUPPLEMENTAL DATA

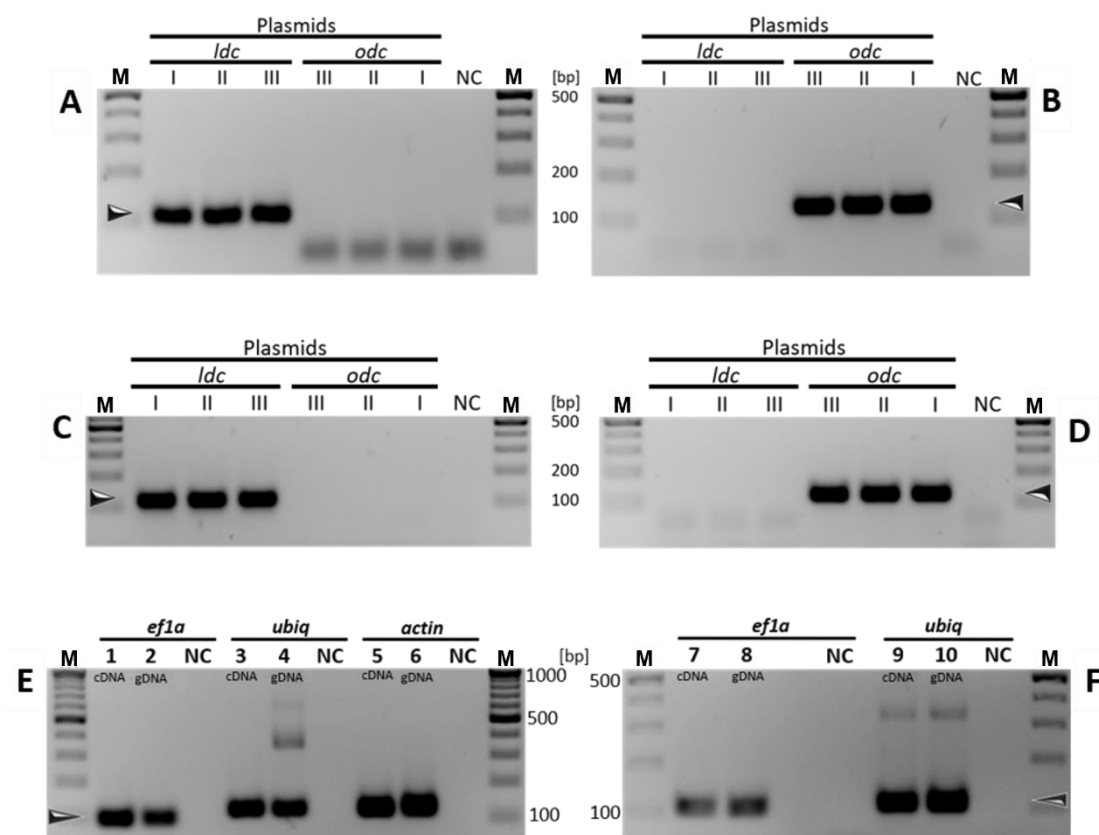


Supplemental Figure S1. SDS-PAGEs of the two enzymes lysine decarboxylase (LDC) and ornithine decarboxylase (ODC), after protein expression and purification, of the three species: (A) *L. x watereri* 'Vossii' (LDC = 46.912 kDa; ODC = 46.777 kDa) and (B) *Lupinus arboreus* (LDC = 47.955 kDa; ODC = 46.340 kDa). Arrowhead indicates expected size of the respective purified protein. I, supernatant; II, pellet; III, flow; IV, wash buffer step; V, repeating wash buffer step; VI, purified protein [2 μ g]; kDa, kilodalton; M, Protein ladder (Thermo Scientific).

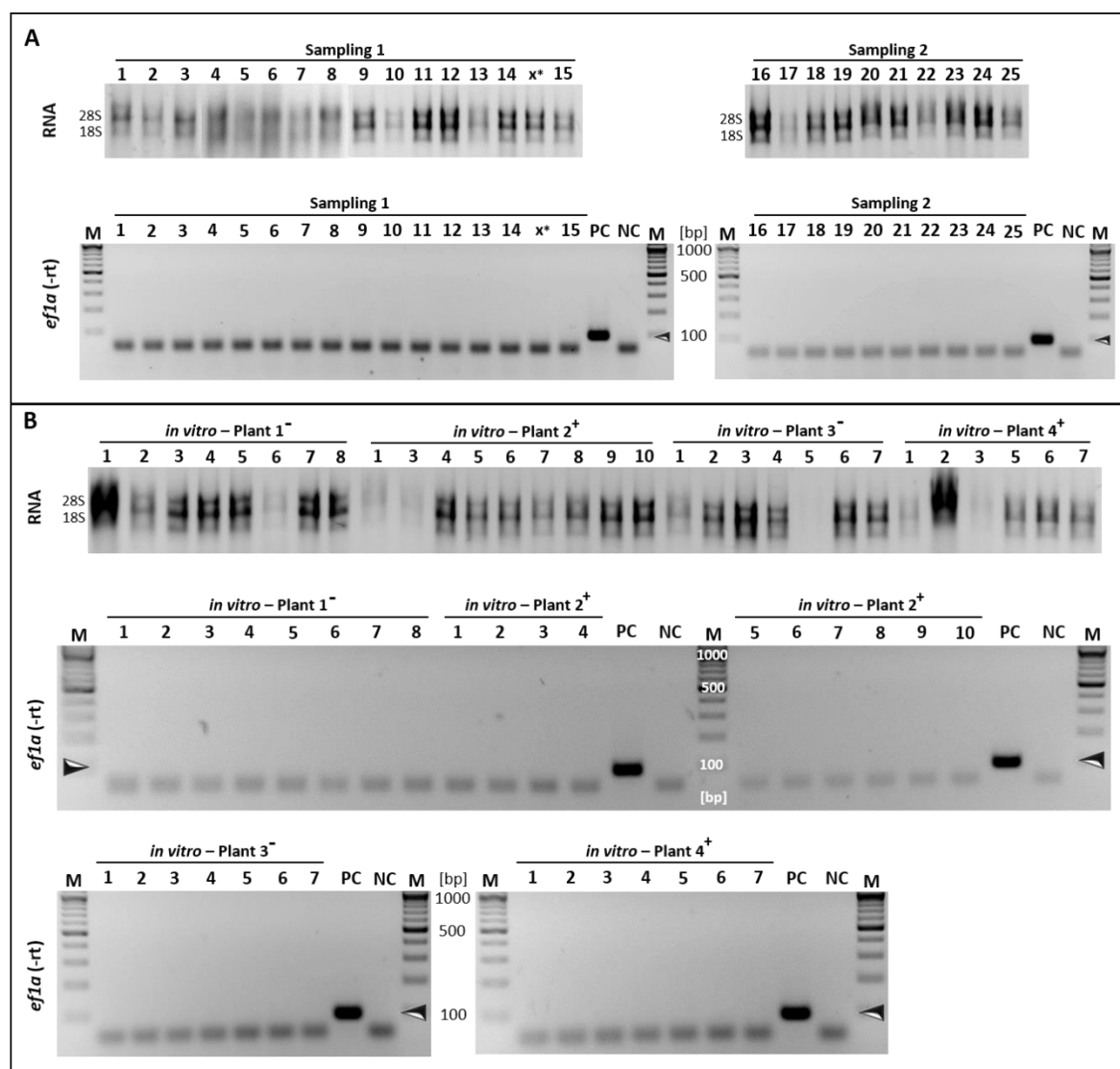
Supplemental Table S1. Detailed distribution of various QAs in the investigated infected and non-infected *in vitro* grown plants of *L. x watereri* 'Vossii', *L. arboreus* and *L. polyphyllus*

Organism	Plant	Nodules	Tissue	QA [$\mu\text{g}/100\text{mg}$] FW								Total amount within this tissue		
				sparteine	caulophylline	cytisine	angustifoline	dehydro-lupanine	lupanine	nuttalline	13-hydroxy lupanine		13 α -isovaleroyl-oxy-lupanine	3 β ,13 α -dihydro-lupanine
 <i>L. x watereri</i> 'Vossii'	A1	–	complete		4.20	93.19								97.39
	A2	–	complete		14.01	92.05								106.06
	A3	–	complete		8.46	60.37								68.83
	A4	–	complete		12.32	16.63								28.95
	A5	+	complete		3.59	21.98								25.57
	A6	+	complete		2.40	108.15								110.55
	A7	+	complete		8.67	94.50								103.16
	A8	+	complete		2.43	113.17								115.61
	A9	–	complete		4.01	14.32								18.33
	A10	+	complete		2.65	35.82								38.48
	A11	–	complete		3.38	56.60								59.98
	A12	+	complete		1.53	51.13								52.66
 <i>Lupinus polyphyllus</i>	C1	+	leaves + roots leaf + cotyledon				1.00	0.12	1.43		0.50	0.22		2.76
	C2	+	complete				0.92		1.12		2.86	0.09		0.62
	C3	+	complete				2.22		1.03		5.21	2.15		4.99
	C4	+	leaves				0.45		0.19		2.90	0.35		10.6
			roots				1.00	0.06	1.23	4.00	0.14		3.88	
	C5	+	nodules						0.55					6.43
			Leaves				1.20		0.87	2.36	1.47			0.55
	C6	+	roots + nodules				0.42		0.40	0.11	0.15	0.31		5.9
			nodules				2.28		0.72	0.38	0.43			1.39
	C6	*	complete				1.10		0.13		0.99	4.68		3.81
	C7	–	complete				0.68		0.30		1.40	2.16		6.91
	C8	–	complete				1.91		1.53		5.31			4.55
C9	–	complete				0.85		0.49		1.89	2.11		10.86	

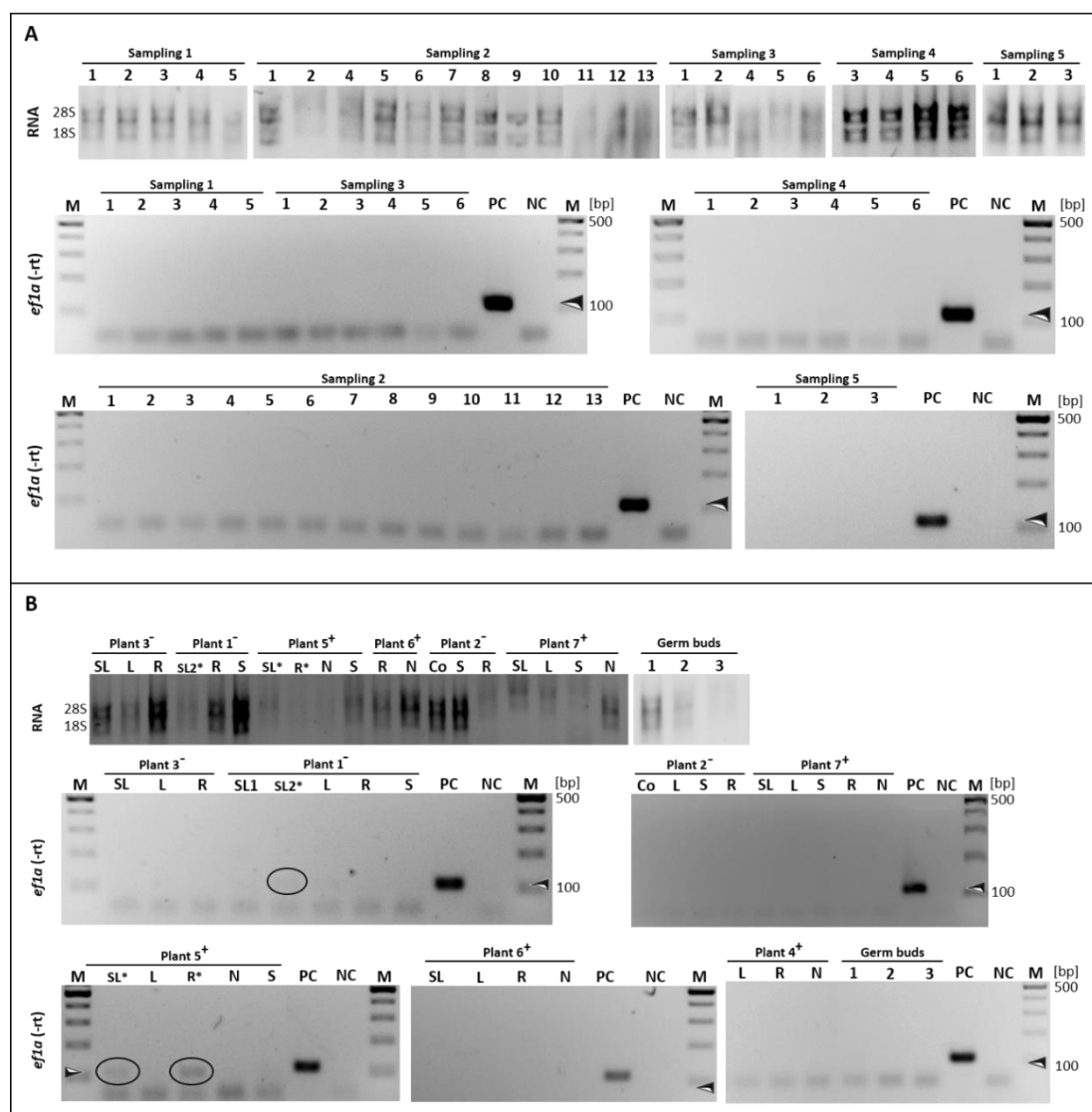
Organism	Plant	Nodules	Tissue	QA [µg/mg] DW										Total amount within this tissue
				sparteine	caulophilline	cytisine	angustifoline	dehydro-lupanine	lupanine	nuttalline	13-hydroxy lupanine	13α-isovaleroyl-oxy-lupanine	3β,13α-dihydro-lupanine	
 <i>L. arboreus</i>	B1	+	leaves					0.44	9.96				2.64	13.03
			roots					1.26	10.08		2.78		3.67	14.12
			stem					0.34	4.82		3.21		1.68	8.37
	B2	+	cotyledons					0.37	61.53	1.05				62.95
			complete					2.05	63.93				1.77	67.74
	B3	+	complete					1.86	64.14		1.25		1.38	68.63
	B4	-	leaves					0.72	22.09		1.36		1.53	25.70
			roots					0.09	4.84	0.30	0.51			5.74
	B5	-	complete					0.21	19.52	0.29	0.38		0.12	20.51
	B6	+	complete						2.12				1.71	3.83
	B7	+	complete						5.62		0.25		0.63	6.49
			leaves	0.19				0.19	24.53					24.91
			roots					0.18	8.29	1.39	1.32			11.17
	B8	+	nodules						4.68	1.39				6.07
			leaves	0.06				0.49	20.55	0.69	0.30		0.42	22.51
	B9	+	roots					0.24	5.57	2.01	0.56		0.34	8.39
			nodules						2.61					2.61
	B10	+	leaves						1.58					1.58
roots							0.23	5.05	0.51				5.78	
nodules								2.96					2.96	
B11	+	complete					0.14	19.24	0.52	0.17		0.13	20.20	
B12	-	complete					0.10	1.71		0.23		0.87	2.91	
B13	-	complete					0.06	2.42		0.23		0.38	3.09	
B14	-	complete						2.56		0.21		0.48	3.24	
B15	*	complete					0.06	12.31	0.14	0.34		0.33	13.19	
B16	*	complete					0.22	15.20	0.10	0.86		0.18	16.55	
B17	-	complete					0.40	19.46	0.13	1.31		0.09	21.39	
B18	-	complete					0.21	17.45	0.54	0.39		0.19	18.78	



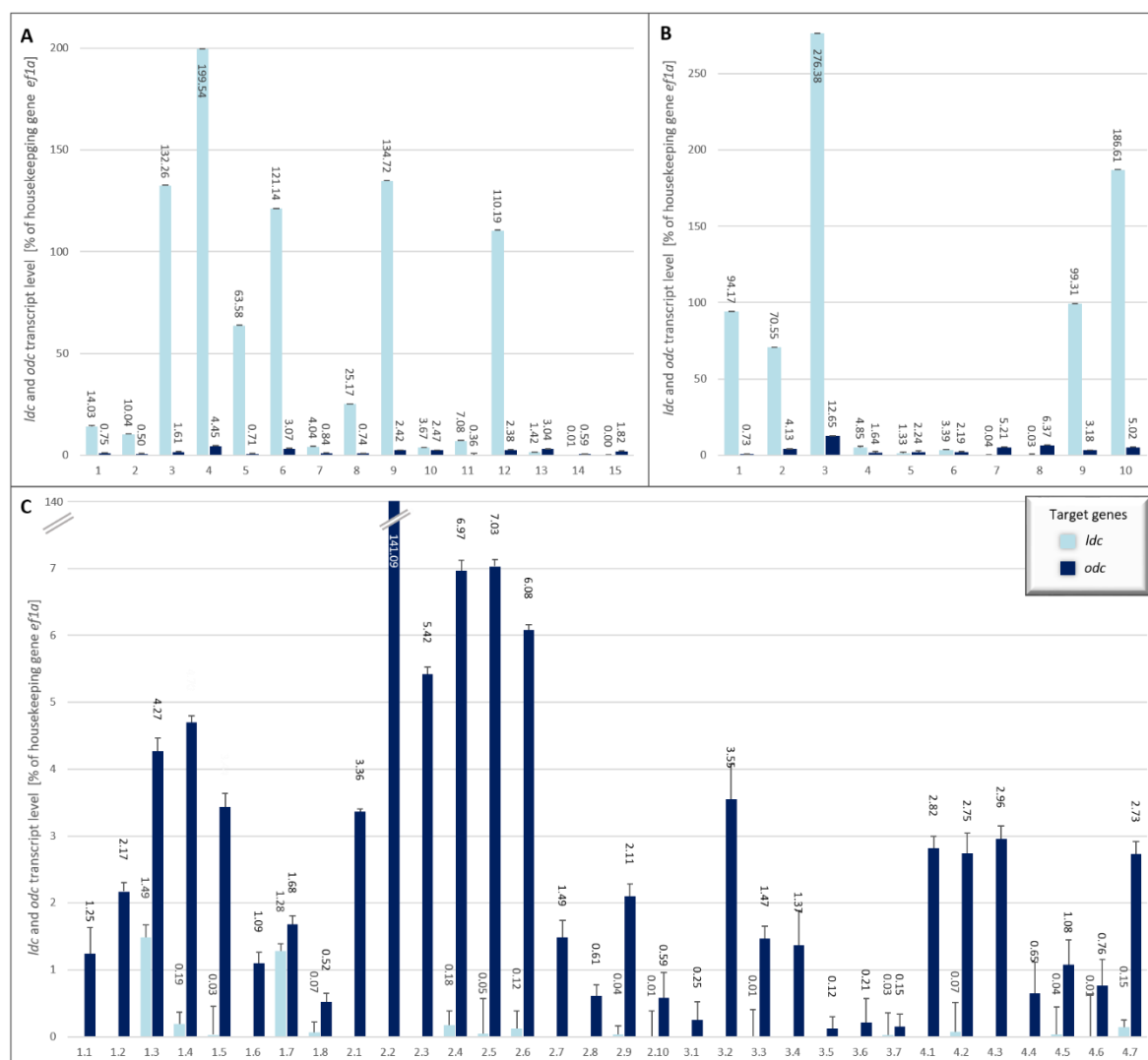
Supplemental Figure S2. Specificity tests of the primer pairs used for transcript quantification of *Ldc*, *odc* or housekeeping genes of *L. arboreus* and *L. x watereri* 'Vossii' for RT-qPCR. Due to high sequence similarity between *Ldc* and *odc*, unspecific binding of primers was ruled out by testing them with *Ldc* and *odc*-containing plasmids as template. **A** Test of *Ldc* primer pair (P11/P12, 110 bp) and **B** *odc* primer pair (P9/P10, 128 bp) for *L. arboreus*. **C** Test of *Ldc* primer pair (P19/P20, 116 bp) and **D** *odc* primer pair (P17/P18, 126 bp) for *L. x watereri* 'Vossii'. **E** For each housekeeping gene one primer combination was tested for *L. arboreus*. **1-2**, Primer pair for *ef1a* (P5/P6, 96 bp); **3-4**, Primer pair for *ubiquitin* (P3/P4, 115 bp); **5-6**, Primer pair for *actin* (P7/P8, 117 bp, not used for final RT-qPCR analysis in this study). **F** Housekeeping genes test for *L. x watereri* 'Vossii'. **7-8**, Primer pair for *ef1a*, used in PCRs to test -rt samples for gDNA contamination (P21/22, 109 bp).; **9-10**, Primer pair for *ubiquitin*, used in RT-qPCRs within this study (P13/14, 108 bp). Arrow heads indicate the size of the specific products after amplification with GoTaq DNA polymerase (annealing temperature of 60°C). bp, base pair; M, GeneRuler 100 bp Plus DNA Ladder (Thermo Scientific); I, 25 ng of plasmid DNA; II, 10 ng of plasmid DNA; III, 5 ng of plasmid DNA; NC, no-template control.



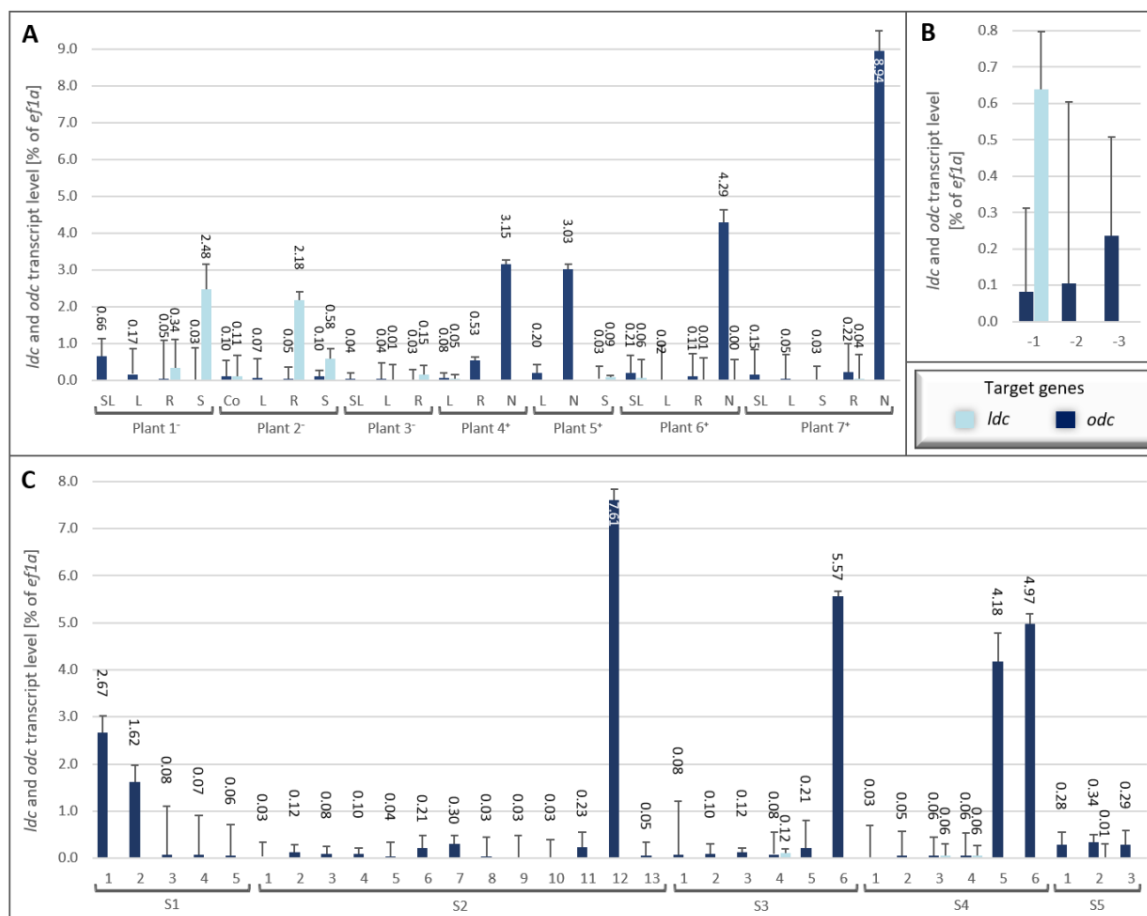
Supplemental Figure S3. Quality tests of RNA extractions used for reverse transcription and gDNA contamination in cDNA samples of infield grown and infected nodule developing (+) and non-infected (-) *in vitro* grown *L. arboreus*. Total RNA and PCR reactions of (-rt)-controls have been separated by agarose gel electrophoresis. Arrowhead indicates expected product size of 96 bp for the housekeeping gene *ef1a*, as pictured in the positive control with leaf cDNA template, with primer pair P5/P6 (Supplemental Table S2). **A Samples of sampling 1 and 2 of infield grown plants.** 1 = leaf bud; 2 = unevolved leaf; 3 = unfolding leaf; 4 = mature unfurled leaf; 5 = unevolved leaf; 6 = unfurled leaf; 7 = two unevolved leaves; 8 = unevolved leaf; 9 = petiole of samples (3-5); 10 = petiole; 11 = unevolved leaf; 12 = unevolved leaf; 13 = mature leaf; 14 = root; 15 = nodules; 16 = unevolved leaves plus larger unevolved leaf; 17 = mature leaf; 18 = leaf; 19 = inflorescence with flower buds; 20 = open flower; 21 = flower buds; 22 = nodules; 23 = root; 24 and 25 = single green pod. **B Samples of infected nodule developing (+) and non-infected (-) *in vitro* grown plants.** **Plant 1** (2 months, non-infected): 1.1 = cotyledons; 1.2 = leaf; 1.3 = unevolved leaf; 1.4 = leaf; 1.5 = leaf; 1.6 = root; 1.7 = petioles; 1.8 = main stem. **Plant 2** (2 months, infected): 2.1 = cotyledons; 2.2 = leaf; 2.3 = leaf; 2.4 = unevolved leaf; 2.5 = leaf; 2.6 = two leaves; 2.7 = root; 2.8 = nodules; 2.9 = petioles; 2.10 = main stem. **Plant 3** (4 months, non-infected): 3.1 = leaves; 3.2 = unevolved leaf; 3.3 = leaf; 3.4 = leaf; 3.5 = root; 3.6 = petioles; 3.7 = main stem. **Plant 4** (4 months, infected): 4.1 = unevolved leaf; 4.2 = leaves; 4.3 = root; 4.4 = nodules; 4.5 = petioles; 4.6 = main stem; 4.7 = remaining leaves. PC, positive control; NC, no-template control; bp, base pair; M, DNA ladder (GeneRuler 100 bp Plus DNA Ladder, Thermo Scientific).



Supplemental Figure S4. Tests of RNA used for reverse transcription and for gDNA contamination in cDNA samples of in field and in vitro grown *L. x watereri* 'Vossii'. Agarose gel electrophoresis of total RNA and PCR products resulting from RNA prepared without reverse transcription (-rt). Contamination of RNA with gDNA would result in fragments as pictured in the positive controls amplified with leaf cDNA (PC). PCR was implemented according to the manufacturer with GoTaq polymerase and annealing temperature of 60°C. Arrow heads indicate expected product size of 109 bp for the housekeeping gene *ef1a* with primers (P21/P22; Supplemental Table S2). **A Samples of sampling 1-5 of in field grown plants.** **S 1:** 1 = nodules; 2 = root; 3 = leaf bud; 4 = leaves of flower bud; 5 = young flower. **S 2:** 1 = unevolved leaves; 2 = petioles; 3 = leaf; 4 = mature leaf; 5 = petiole; 6 = unripened inflorescence; 7 = green enclosed flowers; 8 = green enclosed flower buds; 9 = single open flower; 10 = petioles; 11 = root; 12 = nodules; 13 = petioles. **S 3:** 1 = unevolved leaf; 2 = mature leaf; 3 = mature leaf; 4 = single open flower; 5 = root; 6 = nodules. **S 4:** 1 = mature leaves; 2 = mature leaf; 3 = green seedpod; 4 = two green seedpods; 5 = root; 6 = nodules. **S 5:** 1 = leaf; 2 = green inflorescence; 3 = leaves. **B Samples of infected nodule developing (+) and non-infected (-) in vitro grown plants.** Plant 1⁻: 2 months; Plant 2⁻: 3 months; Plant 3⁻: 7 months; Plant 4⁺: 3 months; Plant 5⁺: 10 months; Plant 6⁺: 11 months; Plant 7⁺: 14 months. Co = cotyledons; L = leaf; N = nodule; R = root; S = stem; SL = smaller appearing leaf. 1, complete germ bud; 2 and 3, germ buds analyzed only leaves. PC, positive control; NC, no-template control; bp, base pair; M, DNA ladder (GeneRuler 100 bp Plus DNA Ladder, Thermo Scientific). *labelled tissue was not used in RT-qPCR because of containing gDNA. RNA concentration of the following tissues was too low for both reverse transcription and performing an RNA gel (Plant 1⁻: SL1 and L; Plant 2⁻: L; Plant 4⁺: L, R and N; Plant 5⁺: L; Plant 6⁺: SL, L; Plant 7⁺: R).



Supplemental Figure S5. Tissue-specific analysis of relative transcript levels ($2^{-\Delta CT}$) of *Idc* and *odc* in *L. arboreus*. Various tissues of field-grown (A and B) and *in vitro*-grown (C) plants with and without infection with rhizobia using the *ef1a* gene as reference. **A Sampling 1 and B Sampling 2.** 1 = leaf bud; 2 = unevolved leaf; 3 = unfolding leaf; 4 = mature unfurled leaf; 5 = unevolved leaf; 6 = unfurled leaf; 7 = two unevolved leaves; 8 = unevolved leaf; 9 = petiole of samples (3-5); 10 = petiole; 11 = unevolved leaf; 12 = unevolved leaf; 13 = mature leaf; 14 = root; 15 = nodules; 16 = unevolved leaves plus larger unevolved leaf; 17 = mature leaf; 18 = leaf; 19 = inflorescence with flower buds; 20 = open flower; 21 = flower buds; 22 = nodules; 23 = root; 24 and 25 = single green pod. **C In vitro grown plants. Plant 1** (2 months, non-infected): 1.1 = cotyledons; 1.2 = leaf; 1.3 = unevolved leaf; 1.4 = leaf; 1.5 = leaf; 1.6 = root; 1.7 = petioles; 1.8 = main stem. **Plant 2** (2 months, infected): 2.1 = cotyledons; 2.2 = leaf; 2.3 = leaf; 2.4 = unevolved leaf; 2.5 = leaf; 2.6 = two leaves; 2.7 = root; 2.8 = nodules; 2.9 = petioles; 2.10 = main stem. **Plant 3** (4 months, non-infected): 3.1 = leaves; 3.2 = unevolved leaf; 3.3 = leaf; 3.4 = leaf; 3.5 = root; 3.6 = petioles; 3.7 = main stem. **Plant 4** (4 months, infected): 4.1 = unevolved leaf; 4.2 = leaves; 4.3 = root; 4.4 = nodules; 4.5 = petioles; 4.6 = main stem; 4.7 = remaining leaves; n=1 (tested in three technical replicates).



Supplemental Figure S6. Tissue-specific analysis of $2^{-\Delta CT}$ relative transcript level of the target genes *ldc* and *odc* in *L. x watereri* 'Vossii'. Various tissues of *in vitro* grown infected and non-infected (A and B) and infield grown (C) plants were analyzed by using the housekeeping gene *ef1a* as reference. **A** *In vitro* grown infected (+) and non-infected (-) plants with different age. Plant 1⁻: 2 months; Plant 2⁻: 3 months; Plant 3⁻: 7 months; Plant 4⁺: 3 months; Plant 5⁺: 10 months; Plant 6⁺: 11 months; Plant 7⁺: 14 months. Co = cotyledons; L = leaf; N = nodule; R = root; S = stem; SL = small leaf. **B** Non-infected germ buds. 1 = complete germ bud; 2 and 3 = analyzed only black circled leaves. **C** Sampling S 1-5. **S 1**: 1 = nodules; 2 = root; 3 = leaf bud; 4 = leaves of flower bud; 5 = young flower. **S 2**: 1 = unevolved leaves; 2 = petioles; 3 = leaf; 4 = mature leaf; 5 = petiole; 6 = unripened inflorescence; 7 = green enclosed flowers; 8 = green enclosed flower buds; 9 = single open flower; 10 = petioles; 11 = root; 12 = nodules; 13 = petioles. **S 3**: 1 = unevolved leaf; 2 = mature leaf; 3 = mature leaf; 4 = single open flower; 5 = root; 6 = nodules. **S 4**: 1 = mature leaves; 2 = mature leaf; 3 = green seedpod; 4 = two green seedpods; 5 = root; 6 = nodules. **S 5**: 1 = leaf; 2 = green inflorescence; 3 = leaves; n=1 (tested in three technical replicates).

Supplemental Table S2. Sequences of Primers and their expected product size used for 16S RNA gene and RT-qPCR to investigate different tissues regarding to the transcript level of the genes *ldc* and *odc*. Additional housekeeping gene primer pairs which were either not used for final RT-qPCR (*¹ P7/P8) or only used in PCRs to check for gDNA contamination in –rt samples (*² P21/P22).

Organism	Primer	Sequence 5' -> 3'	Product size
Rhizobia	P1	16S forward	AGAGTTTGATCCTGGCTCAG
	P2	16S reverse	AGAGTTTGATCCTGGCTCAG
<i>Lupinus arboreus</i>	P3	UBQ forward	AGTCTACCCTTCATCTTGTGCTG
	P4	UBQ reverse	ACATTATCAATTGTGTCAGAGCTTTCC
	P5	Ef1a forward	GAATGTTGCGGTGAAAGATCTCAA
	P6	Ef1a reverse	ATAACTTGGGATGTGAAGCTAGCA
	P7* ¹	ACT forward	TGAATCCGGTCCATCGATTGTG
	P8* ¹	ACT reverse	TCATCACTCCAACAATAGAACAACATG
	P9	ODC forward	CGATGGGATCTATGGCTCTATGAA
	P10	ODC reverse	CTGTTGAACCGTACTTTTTCACTTCT
	P11	LDC forward	GTCGTTATTTTGCAGAGTCACCTT
	P12	LDC reverse	AAGAGAACCGTAAATCCCATCATCAA
	P13	UBQ forward	GGAGGAATGCAGATCTTTGTGAAG
	P14	UBQ reverse	CTCCTTGTCTGGATTTTTGCTTT
<i>Laburnum x watereri</i> , <i>Vossii</i>	P15	Ef1a forward_2	TAAGGAGATGGAGAAGGAGCCC
	P16	Ef1a reverse_2	TCTCTGACAGCAAAACGACCAA
	P17	ODC forward	CCCCTGCCTTATTGAAATTGAAGT
	P18	ODC reverse	TAGTCCAGATATCTTCCTTTTATGGCC
	P19	LDC forward	CAGTTGTGGTGTTCGCTAGAGTAT
	P20	LDC reverse	CCCATGCAGATATTATTGAGTTCCC
	P21* ²	Ef1a forward_1	GTGGTTGAAACTTTTGCCGAGTA
	P22* ²	Ef1a reverse_1	TAGGATCCTTCTTCTCCACACTCT

Supplemental Table S3. Primer pairs (annealing 70°C) and restriction sites for generating protein expressions constructs of putative *ldc*'s and *odc*'s via Golden-Gate-Vector system. Primer sequences were extended with an overhang (green marked) which includes a recognition site for BbsI (= Bpil) for successful cloning. The start codons and the last amino acid before the stops are shown in bold type.

Organism	Gene	Primer	Sequence 5' -> 3'
<i>Laburnum x watereri</i> , <i>Vossii</i>	<i>ldc</i>	P23-forward	TATATGAAGACTACATGGCAACACTACTCCTTACCGAGG
		P24-reverse	TATATGAAGACTATCGAGCACAAATGGGATTTGAATATGCAAGGTAGG
	<i>odc</i>	P25-forward	TATATGAAGACTACATGGTTGCTGAGGCATCATTCCG
		P26-reverse	TATATGAAGACTATCGAGGAACATAGTTTGAGCTCTCCCG
<i>Lupinus arboreus</i>	<i>ldc</i>	P27-forward	TATATGAAGACTACATGCCTTCACTACTTCTGACCGAGG
		P28-reverse	TATATGAAGACTATCGAGGAACATAGATTGTTCCCGCGCGAT
	<i>odc</i>	P29-forward	TATATGAAGACTACATGGTTGCTCATGCATCACTTCAAA
		P30-reverse	TATATGAAGACTATCGAGGAACATAGTCTGCAGGTCTCCCACT

Supplemental Table S4. Listed are primers, expected product sizes, used tissues and the amplified sequence part of putative *Idc's*, *odc's* and housekeeping genes (*ubiquitin*, *ef1a*) of *Laburnum x watereri* 'Vossii' and *Lupinus arboreus*. PCRs were performed with either Go-taq (3'RACE) or a Hot Start polymerase (Internal fragment, ORF) according due to the manufacture protocols. *Oligo_(dT) conducted as reverse primer for all 3'RACE amplifications. Letters in bold display the base position where different bases could match due to degeneration of the primer.

Organism	Gene	Primer (5' -> 3')		Expected Fragment/ Tissue	Amplified Sequence Part
<i>Laburnum x watereri</i> 'Vossii'	<i>odc</i>	P31-f	GTGTGGGTGTCAATGTTACAACATTTGATTCC	~740 bp gDNA leaf	Internal fragment
		P32-r	CCAATCATTAATTTGCAGTTCGGTAGCAG		
	<i>Idc</i>	P33-f	TGCACTCGCAGCACTCGGTTC	~916 bp gDNA leaf	
		P34-r	CCGTCGTATAAGCACCCATATTCGG		
	<i>odc</i>	P35-f	TTCCAAGGAAGAGATTCAAAAGATTAGAA	~712 bp cDNA leaf	3'RACE*
	<i>Idc</i>	P36-f	GATATGGCTTCTAACGAACTAGGC	~493 bp cDNA germ bud	
	<i>odc</i>	P37-f	ATGGTTGCTGAGGCATCATTCC	~1454 bp gDNA fresh leaf	Fragment containing ORF
		P38-r	TAGTCCAGATATCTTCTTTTATGGCC		
	<i>Idc</i>	P39-f	ATGGCAACACTACTCCTTACCG	~1450 bp gDNA fresh leaf	Fragment containing ORF
		P40-r	CAGTTGTGGTGTTCGCTAGAGTAT		
	<i>ubiq</i>	P41-f	GTCTGAGGGGAGGAATGCAG	~500 bp cDNA nodule	3'RACE*
	<i>ef1a</i>	P42-f	AARGARATGARAARGARCC		
<i>Lupinus arboreus</i>	<i>odc</i>	P43-f	GGAAGAGATTCAAAAGATTAGAAAATGGCA	~700 bp gDNA leaf	Internal fragment
		P44-r	CCAATCATTAATTTGCAGTTCGGTAGCAG		
	<i>Idc</i>	P45-f	ACTGCGCCAGCCGAGCCGAAAT	~888 bp gDNA leaf	
		P46-r	CCGTCGTATAAGCACCCATATTCGG		
	<i>odc</i>	P47-f	ATGGTTGCTCATGCATCACTTCAA	1302 bp cDNA young leaf	ORF
		P48-r	CTAGAACATAGTCTGCAGGTCTCCC		
	<i>Idc</i>	P49-f	ATGCCTTCACTACTTCTGACCGA	1335 bp cDNA young leaf	
		P50-r	TTAGAACATAGATTGTTCCCGCGC		
	<i>ubiq</i>	P51-f	GCTGATTAYAAYATYCARAAGGAGTC	~430 bp cDNA young leaf	3'RACE*
	<i>ef1a</i>	P52-f	AARTCTGTYGAAATGCACCATGAAGC	~520 bp cDNA young leaf	
	<i>actin</i>	P53-f	TATGCMCTCCCYCATGCCATCCT	~627 bp cDNA young leaf	
* Oligo _(dT) P54 GTCGACTCGAGAATTC(T)17					

Supplemental Table S5. Origin and lengths of the aligned sequences used in the phylogenetic tree of LDCs and ODCs. ■ Full ORF sequences were used, except for *B. australis* and *C. spectabilis*. *These 4 genes were then characterized in more detail by assays for their protein function. ^a (Hufnagel et al. 2020) and (www.whitelupin.fr). Other sequences can be found by their accession number on NCBI.

Organism	cDNA/Gene	ORF length [bp]	Accession number/ Reference
<i>Vitis vinifera</i>	LDC ODC	1113 bp	AM479355
<i>Baptisia australis</i>	LDC ODC	864 bp [■]	AB647177
<i>Cicer arietinum</i>	ODC	1284 bp	XM_004500845
<i>Crotalaria spectabilis</i>	ODC	1211 bp [■]	unpublished Jacky and Ober
<i>Echinosophora koreans</i>	LDC ODC	1368 bp	AB561139
<i>Glycine max</i>	ODC	1404 bp	XM_003523182
<i>Laburnum watereri ,Vossii'</i>	LDC	1302 bp	This study*
	ODC	1302 bp	
<i>Lotus japonicus</i>	ODC	1269 bp	AJ575746
<i>Lupinus angustifolius</i>	L/ODC	1323 bp	AB560664
	ODC	1302 bp	XM_019582537.1
<i>Lupinus albus</i>	ODC2 (ODC)	1230 bp	Lalb_Ch23g0265921 ^a
	ODC1 (LDC)	1320 bp	Lalb_Ch08g0246321 ^a
<i>Lupinus arboreus</i>	LDC	1335 bp	This study*
	ODC	1302 bp	
<i>Lupinus polyphyllus</i>	LDC	1332 bp	This study (Transcriptomic data unpublished)
	ODC	1302 bp	
<i>Medicago truncatula</i>	ODC	1287 bp	XM_003603797
<i>Phaseolus vulgaris</i>	LDC1 ODC	1356 bp	XM_007136069
<i>Sophora alopecuroides</i>	LDC	1368 bp	KM249871
<i>Sophora flavescens</i>	LDC ODC	1374 bp	AB561138

Supplemental Table S6. QAs from the infected and non-infected *in vitro* grown plants of *L. x watereri* 'Vossii', *L. arboreus* and *L. polyphyllus*. GC-MS measurements were performed on a TG-1MS column and received RIs were compared with literature (Wink et al. 1995^a and Witte et al. 1992^b) for identification. RI, Kovat's retention index; M⁺, molecular ion.

	Alkaloid	RI TG-1MS/Ref.	M ⁺	MS data: characteristic ions m/z (% relative abundance)	Ref.
1	Lupinine	1384/1420	169	152 (81), 169 (84), 138 (76), 97 (70), 83 (100)	a
2	Angustifoline	2072/2083	234	193 (100), 112 (85), 150 (15), 55 (20), 94 (11)	a
3	Dehydrolupanine	2128/2133	246	150 (100), 246 (80), 136 (80), 134 (40), 217 (10)	a
4	Lupanine	2147/2165	248	136 (100), 149 (60), 248 (40), 150 (34), 219 (8)	a
5	Nuttalline	2244/2250	264	136 (100), 264 (97), 150 (61), 134 (61), 247 (38)	a
6	13 α -Hydroxylupanine	2401/2400	264	152 (100), 165 (40), 264 (40), 246 (40), 134 (30)	a
7	13 α - Isovaleroyloxylupanine	2675/2680	348	246 (100), 134 (50), 148 (25), 112 (30), 348 (5)	a
8	3 β ,13 α - Dihydroxylupanine	2493/2508	280	152 (100), 280 (96), 165 (43), 134 (35), 262 (34)	a
9	Caulophylline	1952/1955	204	58 (100), 204 (30), 146 (10), 160 (10)	a
10	Cytisine	1984/1990	190	146 (100), 147 (80), 190 (65), 160 (25), 134 (25)	a
12	Sparteine	1761/1785	234	137 (100), 98 (90), 234 (44), 193 (25), 84 (10)	a

5. CHAPTER C

Unexpected findings in terms of pyrrolizidine alkaloid biosynthesis in the ornamental plant *Laburnum x watereri* ‘Vossii’ and an additional deeper insight in the localization of the homospermidine synthase and their origin within the genistoid clade (Fabaceae)

Nadine Jacky ^a, Elisabeth Kaltenegger ^a, and Dietrich Ober ^a

^a Botanical Institute and Botanic Gardens, Kiel University, Kiel, Germany

Detailed author contributions are listed at the end of the thesis.

5.1 ABSTRACT

Homospermidine synthase (HSS) is reported to have evolved several times independently in the plant kingdom from a duplication of a gene encoding deoxyhypusine synthase (DHS) of primary metabolism and catalyzes the first step in the biosynthesis of pyrrolizidine alkaloids (PAs). In this study, we investigated several species of the family Fabaceae, particularly representatives from the Genistoid clade that produce either PAs or quinolizidine alkaloids (QAs) to get a deeper insight into HSS evolution within this clade. Fabaceae are known for developing root-nodules to host their symbiosis partner, *N*-fixing rhizobia. A previous study showed that nodules are the site for *hss* transcription in *Crotalaria spectabilis*. Here we show via reverse transcription quantitative PCR (RT-qPCR) that *hss* transcript was present even in nodules of *Cytisus scoparius*, a species not producing PAs. For *Laburnum x watereri* 'Vossii', a species described to produce PAs and QAs, two sites (nodules and pods) were identified containing *hss* transcript. To locate the cells expressing HSS, polyclonal antibodies against the HSS of *C. spectabilis* were produced and used for the tissue-specific immunolocalization within the root-nodules of *C. spectabilis* and *L. x watereri* 'Vossii'. The nodule parenchyma cells and the nodule endodermis were identified as sites of HSS expression in *C. spectabilis*. Due to the high sequence identity of the two HSS of *C. spectabilis* and *L. x watereri* 'Vossii', the polyclonal antibodies were also used to localize HSS in nodules of *L. x watereri* 'Vossii' again in the nodule parenchyma cells. For further studies regarding nodule dependency for PAs in *L. x watereri* 'Vossii', PAs were extracted from *in vitro* grown infected and non-infected plants. In total four known PAs, (-)-trachelanthamidine or its enantiomer (+)-laburnine, (-)-isoretronecanol, (-)-turneforcidine and chysin A, and one unknown PA were found. The mass spectra of the unknown PA suggest a necine base of the trachelanthamidine-type as its core structure. Surprisingly, the PAs were not restricted to nodule developing plants, since all non-nodulated plants contained PAs. Thus, the regulation of PA biosynthesis in *L. x watereri* 'Vossii' appears to be quite different than in *C. spectabilis* where the biosynthesis of PAs depends on nodulation.

5.2 INTRODUCTION

Pyrrolizidine alkaloids (PAs) are secondary metabolites produced by some plants within the angiosperms as toxins for protection against herbivores. They consist of a nitrogen-containing bicyclic ring system, the necine base, that can be esterified with one or more necine acids (Hartmann and Toppel 1987; Hartmann and Witte 1995; Moll et al. 2002). This results in over 400 already known compounds which are widely distributed in the plant families Asteraceae (Senecioneae and Eupatorieae), Boraginaceae, Orchidaceae, Convolvulaceae, Poaceae and in some genera of the Apocynaceae (Hartmann and Witte 1995; Jenett-Siems et al. 2005; Reimann et al. 2004; Kaltenegger et al. 2013). Within the Fabaceae only the genera *Crotalaria*, *Laburnum* and a few species of *Lotononis* are described as PA producers (Wink and Mohamed 2003; Wink 2013; Irmer et al. 2015; Neuner-Jehle et al. 1965).

Predominantly present in the plant is the hydrophilic non-toxic form of PAs, the *N*-oxide, which is storable and transportable. The toxic tertiary form causes cell toxicity and is formed by the conversion of the ingested *N*-oxide by herbivores like insects or invertebrates (Robins 1986; Frei et al. 1992; Lindigkeit et al. 1997). Only PAs with a double bond at position (1,2) are bioactive and therefore toxic to organisms, while saturated PAs are regarded as not bioactive and thus as non-toxic (Fu et al. 2004).

The first step in PA biosynthesis is catalyzed by the enzyme homospermidine synthase (HSS), which is derived from duplications of the gene encoding deoxyhypusine synthase (DHS) of primary metabolism, a scenario that occurred several times independently in the PA-producing lineages within the plant kingdom (Hartmann and Ober 2000; Ober and Kaltenegger 2009). While HSS lost the ability of binding the precursor protein eIF5A (eukaryotic initiation factor 5A), it evolved instead the activity to catalyze the synthesis of homospermidine that serves as precursor for the necine base. The HSS transfers the 4-aminobutyl moiety of spermidine to putrescine in an NAD⁺-depending reaction (Ober et al. 2003; Ober and Kaltenegger 2009).

The plant family of the Fabaceae is one of the largest plant families with more than 18 000 species (Käss and Wink 1997). Various representatives within the Genistoid clade are characterized by producing quinolizidine alkaloids (QAs) with the exception of some species

belonging to the tribe Crotalarieae and one species belonging to the tribe Genisteae that contain PAs (Wink 2013).

Crotalaria has a pantropical distribution with Africa as a core area, occurs in the form of herbs or shrubs and is used as green manure, fiber or fodder (Sy et al. 2001; Fletcher et al. 2009). In *C. spectabilis*, the main PA is monocrotaline and within the study of (Irmer et al. 2015), *hss* transcript could have been only detected in root-nodules, considering PA biosynthesis in *Crotalaria* as nodule dependent. However, *Laburnum* belongs to the tribe Genisteae and is a popular ornamental plant in European gardens featuring both alkaloid types (QAs and PAs) and develop root-nodules as well. So far, only non-toxic PAs, which have a saturated necine base, have been described in *Laburnum* spec. (Neuner-Jehle et al. 1965; Schade and Jockusch 2018; Greinwald et al. 1990).

The symbiosis with free ground-dwelling nitrogen-fixing α -proteobacteria (so-called rhizobia) is unique for legumes, which form root-nodules as additional organs only for harboring their partner. The successful establishment of the symbiosis is based on the exchange of chemical signals, whereby plants secrete flavones, which in turn lead to the activation of nodulation genes (Nod) in bacteria. The three nod genes *nodA*, *nodB*, and *nodC* control the synthesis of the core structure of lipochitooligosaccharides, so-called Nod factors, and are present in all rhizobia (Sajnaga et al. 2001; Tan et al. 2001; Moulin et al. 2004).

The perception of these Nod factors leads to the reprogramming of root cells, which ensures the entry of bacteria. Different mechanisms are described for rhizobia invading plants roots, the probably best studied one is via root hair curling with formation of infection tubes (Callaham and Torrey 1981; Gage 2004). The bacteria end up in the middle of the nodule (infected zone) where they convert to their nitrogen-fixing form (bacteroides). At this point they reduce atmospheric nitrogen to ammonia using the enzyme complex nitrogenase (Bergersen and Goodchild 1973; Ferguson et al. 2010; Sy et al. 2001). In exchange, the host supplies the symbiont with carbon compounds (Brear et al. 2013).

In this study, the focus was on the first specific enzyme, HSS, of PA biosynthesis and the influence of nodulation. It was hypothesized that in *L. x watereri* 'Vossii' (PA and QA

producer) as well as in three QA producing species of the Genisteae (*Cytisus scoparius*, *Spartium junceum*, and *Ulex europaeus*) *hss* might be under nodulation control. For this purpose, RT-qPCRs of different tissues were performed for *hss*. Furthermore, *in vitro* grown infected (nodulated) with non-infected (lacking nodules) *L. x watereri* 'Vossii' plants were analytically compared for the presence of PAs. For tissue localization of the HSS enzyme within nodules, antibodies against the HSS of *C. spectabilis* were prepared, purified, and tried in nodule tissue sections of both *C. spectabilis* and *L. x watereri* 'Vossii' for labeling.

5.3 RESULTS

5.3.1 Identification of putative *hss*, *dhs* and housekeeping genes in *L. x watereri* 'Vossii' and selected non-PA producing Genisteae

To investigate the transcript levels of *dhs* and *hss* in different tissues and under different conditions (nodulated vs. non-nodulated) using RT-qPCR, the respective transcript sequences were identified. We used partial genomic sequences containing the start-ATG and with known exon/intron interfaces of HSS and DHS from *L. x watereri* 'Vossii', *Cytisus scoparius*, *Spartium junceum*, and *Ulex europaeus* that have previously identified (Milewski and Ober, unpublished). Amplification strategy and primers used are listed in Supplemental Table S2. For the DHS and HSS of *L. x watereri* 'Vossii', as well as the HSS of *C. scoparius*, 3'-ends were amplified using the rapid amplification of cDNA ends (RACE) strategy. The obtained cDNA amplification for the DHS of *L. x watereri* 'Vossii' was 1524 bp long and included the ORF with 1116 bp and the 3'UTR with 408 bp. Amplifying the 3'-end of HSS of *L. x watereri* 'Vossii' on cDNA level was at first associated with difficulties. Two approaches with internal located forward oriented primers were used in combination with P25 (Oligo_(dT)) and lead to the successful amplification of the two cDNAs (1288 bp and 622 bp) in which both included the sequence information about the so far unknown ending of the ORF and the 262 bp long 3'UTR. The newly obtained sequence information for the ending part of the ORF of *L. x watereri* 'Vossii' HSS was used to verify the complete ORF in one piece and was in total 1098 bp long. For *C. scoparius* a completion of the ORF (known till Exon 8) and the amplification of the 3'UTR (213 bp) was successful. For the HSS of *S. junceum* and *U. europaeus*, no amplicon could be obtained on cDNA basis, giving a hint that in these two species the *hss* gene might not be transcribed. Nevertheless, to be able to perform RT-qPCR analysis, the known gDNA sequences were used for primer design. The housekeeping genes *ef1a* and *ubiquitin* for *L. x watereri* 'Vossii' have been amplified previously (chapter B).

Due to the close relationship between *L. x watereri* 'Vossii', *C. scoparius*, *S. junceum* and *U. europaeus*, the housekeeping gene forward primers for *ef1a* and *ubiquitin* of *L. x watereri* 'Vossii' were used to amplify the 3'-ends in *C. scoparius*, *S. junceum*, and *U. europaeus*. The combination of primers P3/P25 (Supplemental Table S2) resulted in the successful amplification of the 3'-ends of the *ef1a* transcript of *C. scoparius* (450 bp),

S. junceum (541 bp), and *U. europaeus* (483 bp), whereas amplification of the 3'ends of *ubiquitin* failed in all three species. Subsequently, the RT-qPCR primers P1/P2 for *ubiquitin* and P3/P4 for *ef1a* of *L. x watereri* 'Vossii' were used in *C. scoparius*, *S. junceum* and *U. europaeus* to test for potential specific binding. Here, gDNA was used as template to assure that the primers are not binding at an exon/intron interface, because otherwise no transcript could be amplified on cDNA level in the RT-qPCR analysis. The PCR showed specific bands for both investigated reference genes in each species (Figure1), additionally cloning and sequencing confirmed the identity. Thus, for *C. scoparius*, *S. junceum* and *U. europaeus*, no new housekeeping gene primers were designed for RT-qPCR, but those from *L. x watereri* 'Vossii' were used.

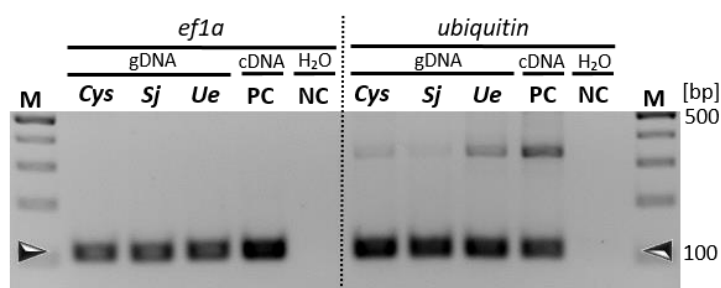


Figure 1. Tests of binding of the RT-qPCR primers of the two reference genes *ef1a* and *ubiquitin* of *L. x watereri* 'Vossii' in the related species *C. scoparius*, *S. junceum* and *U. europaeus* of the tribe Genisteae. Primers (P3/P4) were used to amplify the gene *ef1a* and (P1/P2) to amplify the gene *ubiquitin*. PCR was implemented with GoTaq DNA polymerase (Promega) and an annealing temperature of 60°C. Resulting PCR products were separated on a 3% agarose gel. Arrow heads indicate the expected product size of 109 bp for *ef1a* and 108 bp for *ubiquitin* according to the EF1a-encoding cDNA of *L. x watereri* 'Vossii' that served as positive control. Cys, *Cytisus scoparius* gDNA; Sj, *Spartium junceum* gDNA; Ue, *Ulex europaeus* gDNA; PC, positive control; NC, no-template control; M, DNA ladder (GeneRuler 100 bp Plus DNA Ladder, Thermo Scientific); bp, base pair.

5.3.2 Levels of *hss* transcript are restricted to nodules and pods in *L. x watereri* 'Vossii'

To investigate the influence of nodulation on PA biosynthesis in *L. x watereri* 'Vossii', RT-qPCR analyses were performed with tissues of field grown plants and of nodulated and non-nodulated plants grown *in vitro*. cDNA of leaves, buds, pods, flowers, roots and nodules were used to quantify the transcript level of *hss* and in comparison, to that of the *dhs* gene using *ubiquitin* and *ef1a* as reference genes.

While the transcript of *dhs* was present in all tissues relatively consistently at low levels (up to 3.5 % in relation to *ubiquitin*), *hss* transcript was detected almost exclusively in nodules with up to 500 % in relation to *ubiquitin*. Moreover, *hss* transcript was also detected in the pods at extremely low intensity with about 1 % in relation to *ubiquitin* (Figure 2). To exclude unspecific binding of primers resulting in a false amplification, the PCR product was applied to a gel showing clear bands (Figure 3) and subsequently sequenced for verification. Here, the evaluation of the sequence confirmed that the found transcript within the pods is equivalent to *hss*. This suggests that besides the nodules as the main tissue for *hss* transcription, a second tissue exists. Infected and non-infected *in vitro* grown plants show almost exclusively *hss* transcript in the nodules of infected plants with up to 300 % in relation to *ubiquitin*, except for Plant5+ (Figure 4A). Plant5+ possess nodules and contain additionally to the nodules also low *hss* transcript (about 0.3 % in relation to *ubiquitin*) in the investigated smaller appearing leaf. The small sporadic detected *hss* transcript within roots of nodulated plants are very likely ascribable to residues of detached nodules. Nevertheless, none of the investigated non-infected plants, which lack nodules, contained any *hss* transcript. Again, for comparison the *dhs* transcript was examined, as before in tissues of the field grown plant, and was present with a constant value (about 0.5 % to 7 % in relation to *ubiquitin*) in all tissues of *in vitro* grown plants (Figure 4B). Early investigated stages, i.e., germ buds, were free of *hss* transcript but contained about 1 % transcript of *dhs* in relation to *ubiquitin* (Figure 4C). Comparable results regarding the transcript levels of *hss* and *dhs* in the investigated tissues of infield grown as well *in vitro* grown *L. x watereri* 'Vossii' were achieved with the reference gene *ef1a* and are shown in the Supplemental Figure S4.

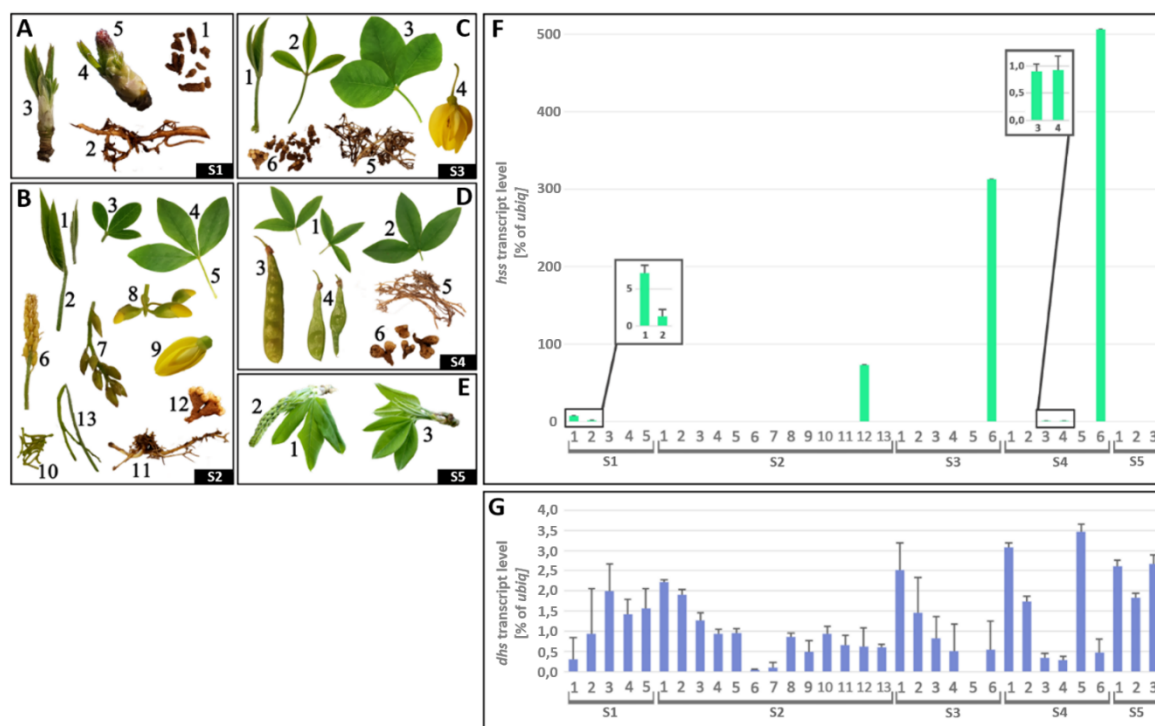


Figure 2. Transcript level of the genes *hss* and *dhs* ($2^{-\Delta CT}$ relative transcript level of the respective target gene in relation to the housekeeping gene *ubiquitin* [%]) in various tissues (sampled at different seasons every time around 5 p.m.) of *L. x watereri* 'Vossii' grown in the Botanical Garden, Kiel (A - D) and in Molfsee (E), Germany. **A Sampling 1** (harvested April 25th, 2019): 1 = nodules; 2 = root; 3 = leaf bud; 4 = leaves of flower bud; 5 = young flower. **B Sampling 2** (harvested May 14th, 2019): 1 = unevolved leaves; 2 = petioles; 3 = leaf; 4 = mature leaf; 5 = petiole; 6 = unripened inflorescence; 7 = green enclosed flowers; 8 = green enclosed flower buds; 9 = single open flower; 10 = petioles; 11 = root; 12 = nodules; 13 = petioles. **C Sampling 3** (harvested May 27th, 2019): 1 = unevolved leaf; 2 = mature leaf; 3 = mature leaf; 4 = single open flower; 5 = root; 6 = nodules. **D Sampling 4** (harvested June 27th, 2019): 1 = mature leaves; 2 = mature leaf; 3 = green seedpod; 4 = two green seedpods; 5 = root; 6 = nodules. **E Sampling 5** (harvested April 10th, 2019): 1 = leaf; 2 = green inflorescence; 3 = leaves. **F** *hss* transcript level. **G** *dhs* transcript level. S= sampling; n=1 (tested in three technical replicates).

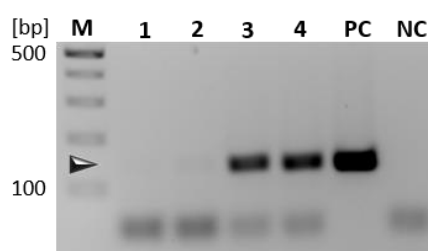


Figure 3. Verification of the transcript, amplified from RT-qPCR, for *hss* in immature pods of sampling S 4 in *L. x watereri* 'Vossii'. The two samples for immature pods show a positive signal for *hss* with the right size. For confirmation, the PCR products were additionally sequenced. Arrowhead indicates the expected product size of 142 bp. 1, mature leaves; 2, mature leaf; 3, green seedpod; 4, two green seedpods; PC, positive control (cDNA nodule); NC, no-template control; M, DNA ladder (GeneRuler 100 bp Plus DNA Ladder, Thermo Scientific); bp, base pair; gDNA, genomic DNA.

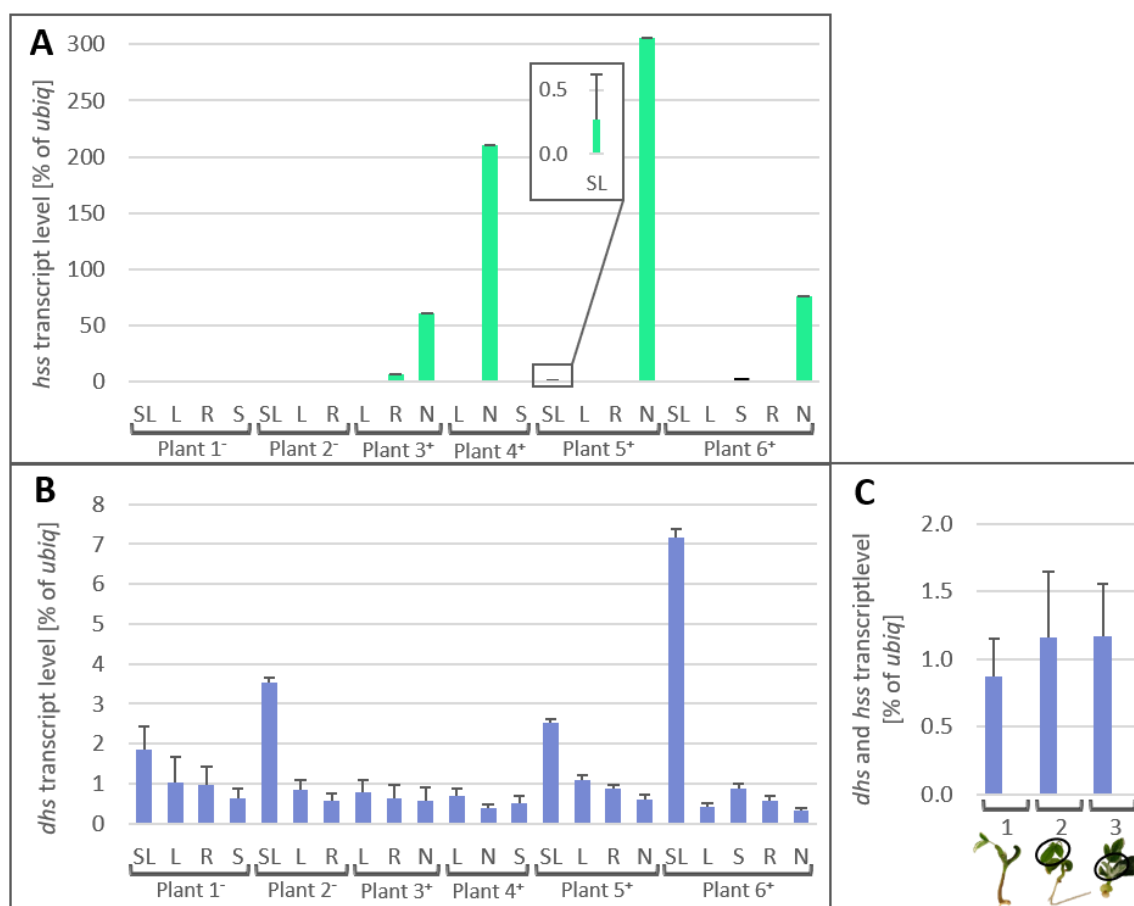


Figure 4. Transcript level of *hss* and *dhs* ($2^{-\Delta CT}$ relative transcript level of the target gene in relation to the reference gene *ubiquitin* [%]) in various tissues of *in vitro* grown non-infected (lacking nodules) and infected (nodule possessing) *L. x watereri* 'Vossii'. **A** *hss* transcript level. **B** *dhs* transcript level. **C** *dhs* and *hss* transcript level in non-infected germ buds. **Plant 1⁻**: 2 months; **Plant 2⁻**: 7 months; **Plant 3⁺**: 3 months; **Plant 4⁺**: 10 months; **Plant 5⁺**: 11 months; **Plant 6⁺**: 14 months. L = leaf; N = nodule; R = root; S = stem; SL = smaller appearing leaf; 1 = complete germ bud; 2 and 3 = analyzed only black circled leaves; - = non-infected plant; + = infected plant; n=1 (tested in three technical replicates).

5.3.3 The first specific enzyme in PA biosynthesis – HSS – is expressed in the parenchyma of *C. spectabilis* and *L. x watereri* 'Vossii' root-nodules

In both Fabaceae, *Crotalaria spectabilis* and *Laburnum x watereri* 'Vossii', the *hss* transcript was previously detected via RT-qPCR almost exclusively in the nodules. Subsequently, the HSS protein of *C. spectabilis* was heterologously expressed in *E. coli*, affinity-purified, and used for polyclonal antibody production.

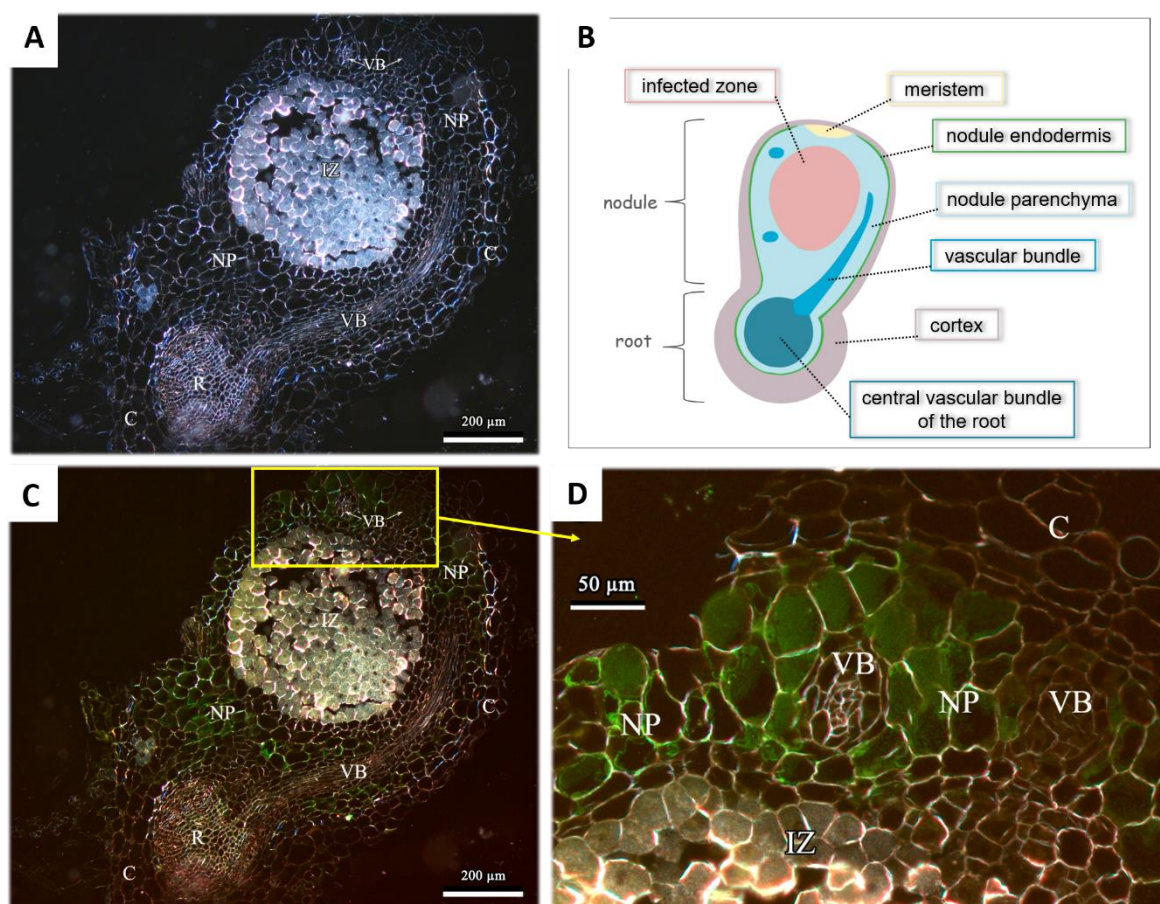


Figure 5. Longitudinal section of an indetermined root nodule of *C. spectabilis* with vascular bundle ensuing from the central cylinder of the root. To locate the cells of HSS expression, sections were treated with a first (HSS) and second antibody (Alexa Fluor 488) A Phase contrast exposure. B Schematic nodule structure. C Same section as A shows green labeled cells within the nodule parenchyma indicating HSS expression. D Detail of picture C with labelled cells surrounding a vascular bundle with unlabeled cells. C, cortex; HSS, homospermidine synthase; IZ, infected zone with bacteroides; NP, nodule parenchyma; R, root; VB, vascular bundle.

Both species form indeterminate nodules, which means that the infected zone with the bacteria is located inside and is surrounded by the nodule parenchyma in which the vascular bundles occur unevenly netlike distributed. The nodule parenchyma is enclosed by a thin nodule endodermis and the cortex to the outside. The nodule arises from dividing root cells and remains attached to the root. At the spire, a located meristem enables the growth of elongated and branched appearing nodules (Figure 5B).

The recent RT-qPCR insights point out the nodules as the tissue with the highest *hss* transcript. Therefore, only the nodules were initially investigated for the localization of the HSS protein. Thin sections from different nodules of both *C. spectabilis* and *L. x watereri* 'Vossii' were labeled with the specific antibodies against HSS of *C. spectabilis*. Different sectioning planes were selected so that as many structures as possible come into view.

For *C. spectabilis*, a distinct immuno labeling could be detected in the nodule parenchyma (Figure 5 and Figure 6A-C) with a used HSS antibody concentration of 0.0097 mg/ml. Figure 5D shows an enlarged longitudinal section of the nodule that is shown in Figure 5C with a clear green label in the cells of the nodule parenchyma where the HSS protein seems to be localized. However, the vascular bundles which occur unregular distributed within the nodule parenchyma are not labeled and thus indicating no HSS expression in these cells. A second nodule shown in Figure 6 also shows a clear labeling around the infected zone within the nodule parenchyma.

The HSS-encoding cDNA sequence of *C. spectabilis* and *L. x watereri* 'Vossii' have a sequence identity of 86.9 % on nucleotide and 87.2 % on amino acid level. For this reason, the existing HSS antibody of *C. spectabilis* was tested in nodules of *L. x watereri* 'Vossii', too. Here, the HSS antibody of *C. spectabilis* seemed to be less sensitive since a concentration of 0.0194 mg/ml proved to be a good detectable signal for the *L. x watereri* 'Vossii' HSS. Figure 6D shows a longitudinal section of a *L. x watereri* 'Vossii' nodule. The outer brownish appearing cells are the terminating cortex cells. This is followed by a narrow strip of smaller cells representing the endodermis. The signal in the nodule endodermis is inconclusive to confirm HSS expression in these cells, whereas the following cells have a green marking, which corresponds to the HSS localization in the nodule parenchyma of *C. spectabilis*. The following densely packed cells are bacterioid cells of the infected zone.

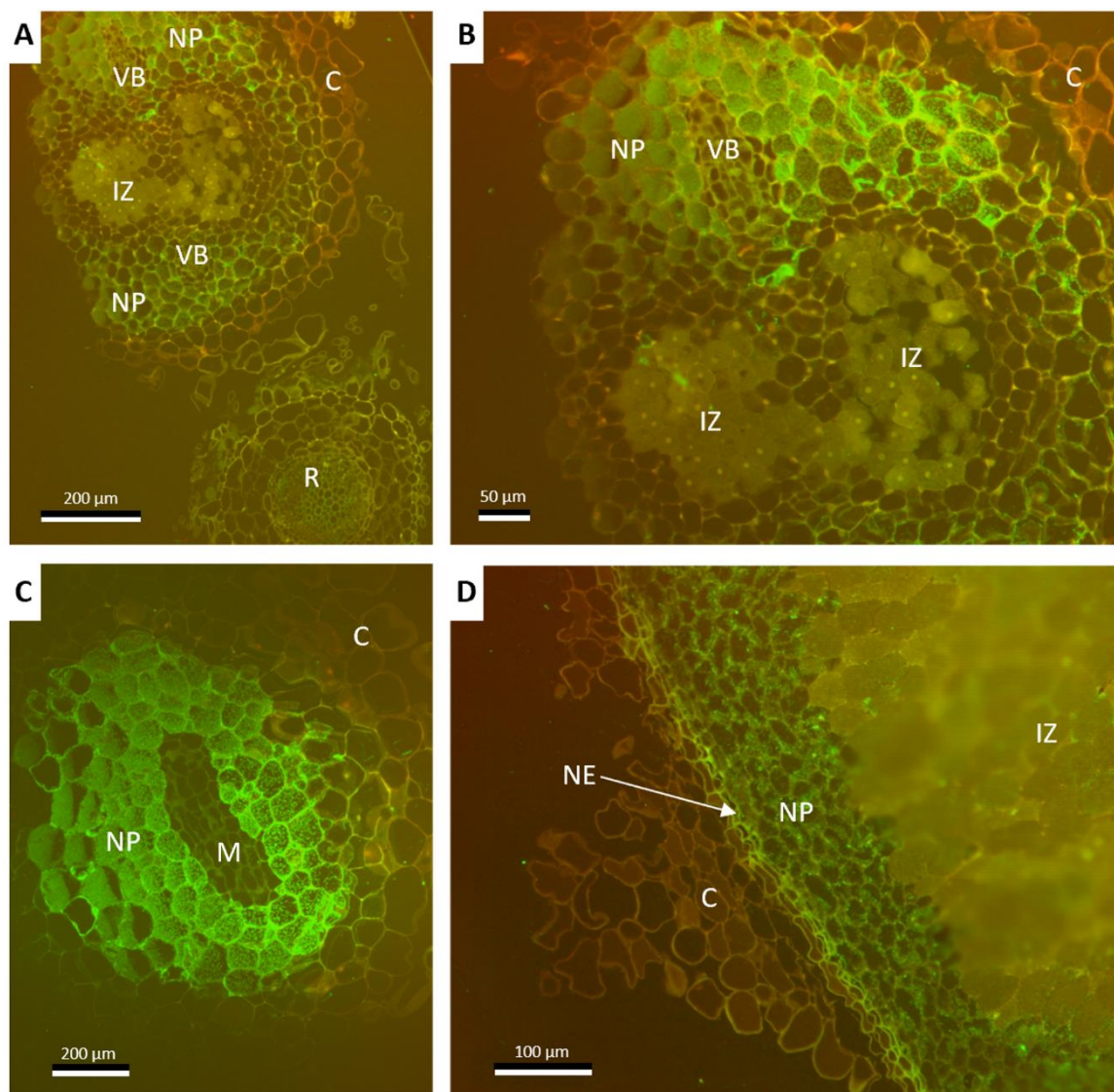


Figure 6. Thin longitudinal sections and a transverse section of different indetermined root nodules from *C. spectabilis* (A-C) and *L. x watereri* 'Vossii' (D). Sections were labeled with the first (HSS) and second antibody (Alexa Fluor 488) to identify the responsible cells for HSS expression, which resulted in a green signal exclusively in the nodule parenchyma cells and the nodule endodermis. A Full depiction of a nodule longitudinal section that is still attached to the root. B Magnification of the section shown in A. C Transverse section displaying the spire on the margin of the nodule just below the cortex surface, where the infected zone could not be reached at this point. D Partial nodule section from the middle part of a nodule. C, cortex; HSS, homospermidine synthase; IZ, infected zone with bacteroides; M, meristem; NE, nodule endodermis; NP, nodule parenchyma; R, root; VB, vascular bundle.

5.3.4 Nodule free plants of *L. x watereri* 'Vossii' contain several PAs

The parallels from *L. x watereri* 'Vossii' to *Crotalaria* regarding the common occurrence of the *hss* transcript almost exclusively in nodules as well as the labeling of the HSS protein within the nodule parenchyma imply the possibility that plants of *L. x watereri* 'Vossii' that lack nodules should also be PA free. To verify the hypothesis that PA biosynthesis in *L. x watereri* 'Vossii' is exclusively dependent on nodulation, infected and non-infected plants were grown *in vitro* and then analyzed for the presence of PAs by GC-MS.

The following GC-MS analysis of PAs and the interpretation of the results were done by E. Kaltenegger and the results then exchanged and discussed.

In total, 10 plants of different ages (2.5 to 14 months) were analyzed either completely (plants 1 - 7) or subdivided before into their tissues (plants 9 - 12) (Figure 7; Supplemental Table S3). Five saturated PAs were generally found ((-)-trachelanthamidine or the enantiomer (+)-laburnine, (-)-isoretronecanol, unknown necine base (PA), (-)-turneforcidine and chysin A (Table 1). The exact distribution of PAs within each individual and their tissues are listed in Supplemental Table S3. Due to their properties, they behave differently on the GC-column, so that the extracts were measured underivatized and derivatized with *N*-methyl-*N*-(trimethylsilyl)trifluoroacetamide (MSTFA) resulting in a trimethylsilyl-group (TMS) at freely accessible hydroxyl groups. While almost exclusively chysin A was detected in the underivatized samples, the other four PAs only became visible after derivatization. Therefore, the quantification of PAs within the plants was based on the four PAs without chysin A and the PA concentration was given in µg/individual fresh weight (Figure 7). The dispersion of the five detected PAs varies within each tested individual and their tissues (Supplemental Table S3). Briefly, it was found that (-)-turneforcidine and the unknown necine base (PA) were the most present PAs in all individuals except in two leaves of plant 11 and plant 12. Chysin A was likewise detectable with the exception of few tissues in plants 9, 10 and 12, but with a remarkable lower concentration than (-)-turneforcidine and the unknown necine base (PA). The stereoisomers (-)-trachelanthamidine (or the enantiomer (+)-laburnine) and (-)-isoretronecanol were less common compared to the previously three stated PAs. Nevertheless, (-)-trachelanthamidine was present in higher concentrations than (-)-isoretronecanol. Surprisingly, PAs could be found in all investigated individuals (infected

and non-infected) in either more or less amount ranging from 8.20 μg (Figure 7, Plant 6, infected, 10 months) for infected and 8.86 μg (Figure 7, Plant 3, non-infected, 5 months) for non-infected up to 480.95 μg for infected (Figure 7, Plant 10, infected, 11 months) and 410.05 μg (Figure 7, Plant 11, non-infected, 9 months) for non-infected *in vitro* grown individuals per fresh weight. These results implicate that PA biosynthesis in *L. x watereri* 'Vossii' might not depend on the formation of root-nodules.

The unknown necine base (PA) could not be assigned to a described PA by means of retention index and mass spectrometry like the other four PAs (Table 1). However, considering the mass spectrum (Figure 8C) and comparing this with the derivatized (-)-turneforcicine-2xTMS (Figure 8A) and trachelanthamidine-1xTMS (Figure 8B) it shows fragments (73; 82; 83; 110) of a necine base core structure (Figure 8D). Main mass fragments are 73 (silyl-moiety indicating successful derivatization of the compound), 82 and 83 (decay fragments of the necine base core structure), 110 (suggesting cleavage of a $\text{C}_4\text{H}_{11}\text{OSi}$), 143 (is unassignable and could be specific for the unknown PA structure). Thus, the necine base core structure could resemble the trachelanthamidine or its stereoisomers (Figure 8B and 8C). A further indication are the total masses. The total masses of the unknown PA ($\text{M}^{[+]} 227$, without 1xTMS $\text{M}^{[+]} 155$) and trachelanthamidine ($\text{M}^{[+]} 213$, without 1xTMS $\text{M}^{[+]} 141$) show a mass difference of 12, which could correspond exactly to an additional $-\text{CH}_2$ molecule that is pictured in the derivatized side chain. Also, the absence of the fragments 124 and 185 implies that the side chain of the unknown PA could contain one more $-\text{CH}_2$ molecule. The structure in question with the total mass of $\text{M}^{[+]} 227$ is represented in the turquoise box with a question mark (Figure 8C).

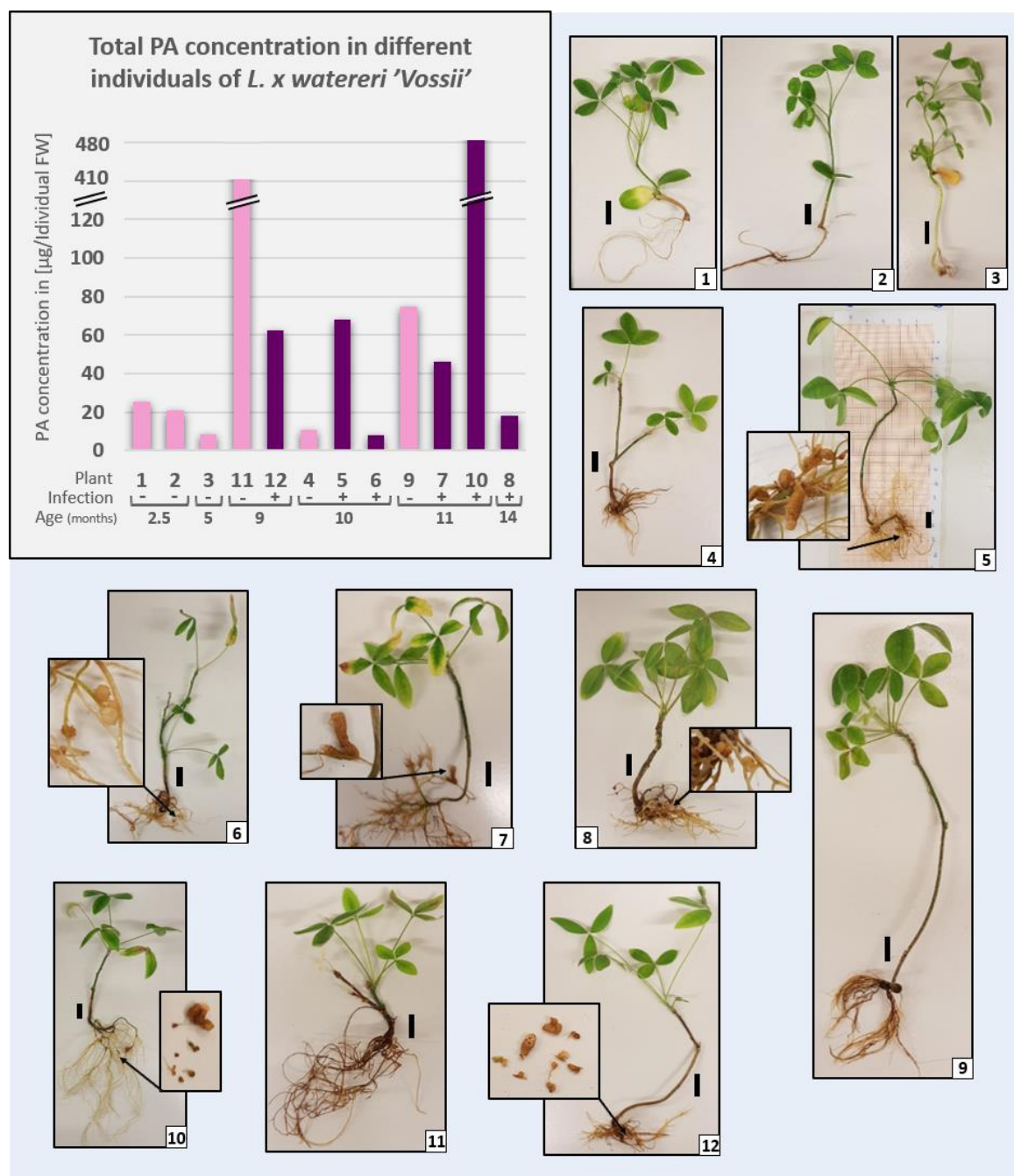
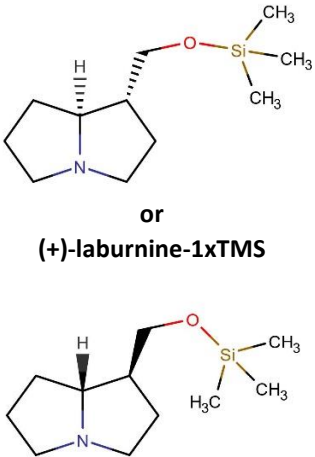
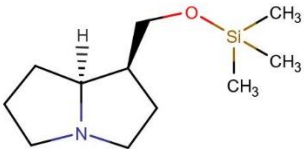
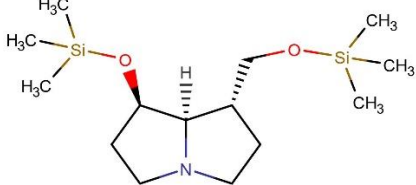
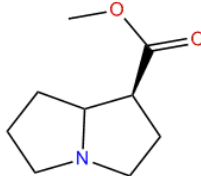


Figure 7. GC-MS analyses of PAs of *in vitro* grown infected (with fully developed nodules; +) and non-infected (lacking nodules; -) *L. x watereri* 'Vossii' of different ages. The quantification of the total PA amount per individual is based on the four PAs ((-)-trachelanthamidine or the enantiomer (+)-laburnine, (-)-isoretronecanol, unknown necine base (PA) and (-)-turneforcidine). **Plant 1 and 2**, Ten weeks non-infected plants; **Plant 3**, Five months non-infected plant; **Plant 4**, Ten months non-infected plant; **Plant 5 and 6**, Ten months infected plants; **Plant 7 and 10**, Eleven months infected plants; **Plant 8**, Fourteen months infected plant; **Plant 9**, Eleven months non-infected plant; **Plant 11**, Nine months non-infected plant; **Plant 12**, Nine months infected plant; **FW**, fresh weight; scale bar, 1 cm; $n = 1$.

Table 1. PAs detected within *in vitro* grown infected and non-infected *L. x watereri* 'Vossii' plants. Retention indexes (RI) on TG-1MS column were compared with literature (Ref.) for identification where the same column was used (Hartmann et al. 2005^a, Woldemichael and Wink 2002^b). Samples were measured without and with derivatization (- and + MSTFA). MS data are taken from the literature for the derivatized PAs and the non-derivatized chysin A. PA structures are shown as derivatized form (+ TMS group) which has been added at the hydroxy group (-OH). RI, Kovat's retention index; M⁺, molecular ion; TMS, trimethylsilyl.

	(-)-trachelanthamidine- 1xTMS	(-)-isoretronecanol- 1xTMS	unknown necine base- 1xTMS	(-)-turneforcidine- 2xTMS	chysin A
Alkaloid	 <p>or (+)-laburnine-1xTMS</p>		?		
RI measured on TG-1MS¹/ compared to Ref.²	1350 ¹ /1350 ²	1380 ¹ /1377 ²	1421 ¹ / ? ²	1579 ¹ /1569 ²	1295 ¹ /1283 ²
M⁺	213	213	227	301	169
MS data: characteristic ions m/z (% relative abundance)	213(27), 212(14), 198(24), 185(27), 124(12), 122(13), 110(23), 84(19), 83(100), 82(36)	213(25), 212(14), 198(21), 185(27), 110(23), 84(19), 83(100), 82(38), 73(14), 55(13)		301(7), 286(10), 212(4), 211(17), 187(3), 186(9), 185(74), 83(5), 82(100), 73(15)	169(35), 154(8), 138(21), 119(13), 83(100), 82(68), 70(13), 55(44), 42(14)
Ref.	a				b

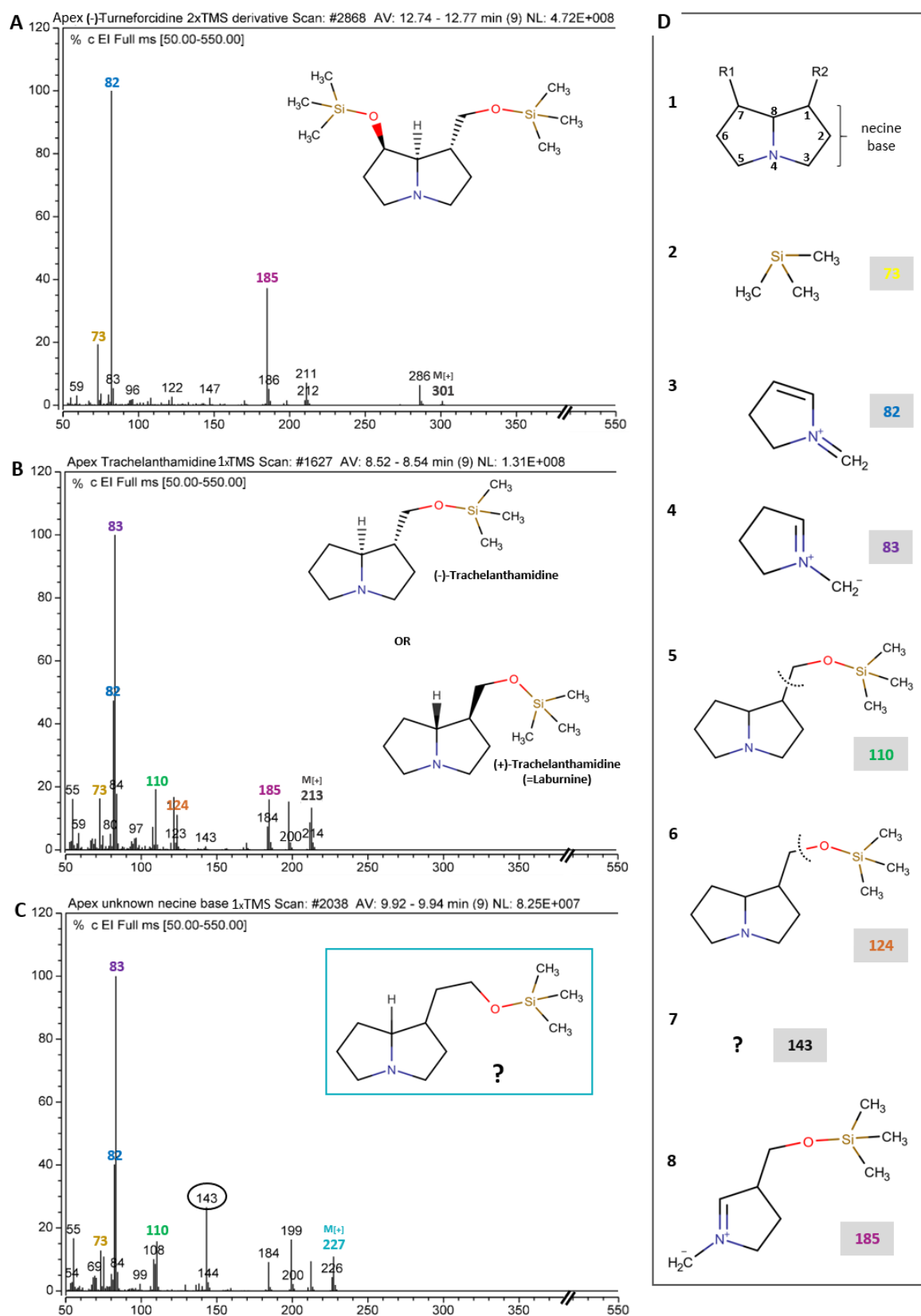


Figure 8. Mass spectra of three out of the five found PAs in infected (nodule possessing) and non-infected (nodule lacking) *in vitro* grown *L. x watereri* 'Vossii'. **A** (-)-turneforcidine-2xTMS. **B** (-)-trachelanthamidine or its enantiomer (+)-trachelanthamidine (laburnine). **C** Unknown necine base. **D** Necine base core structure and possible resulting mass fragments with their corresponding mass. TMS, trimethylsilyl-group.

5.3.5 Level of *hss* transcript was detectable in nodules of a non-PA producing plant

After *Crotalaria*, *L. x watereri* 'Vossii' is the second species in which the first specific enzyme (HSS) for the production of PAs was shown to be primarily nodule dependent. This raised the question of whether non-PA-producing Genisteae also have a *hss* transcript in nodules, since they have an encoding HSS gene in their genomes with the same suspected origin as *C. spectabilis* (unpublished Milewski and Ober). For this purpose, the non-PA producing species *C. scoparius*, *S. junceum* and *U. europaeus* were investigated. For this purpose, RT-qPCR was performed to investigate the transcripts of *hss* and *dhs* in comparison to the reference genes *ubiquitin* (Figure 9) and *ef1a* (Supplemental Figure S3). Leaves, roots and nodules were examined in each species. In all tissues, the *dhs* was distinct detectable. Whereas the *hss* transcript could be found exclusively in the nodules of *C. scoparius*. In both *S. junceum* and *U. europaeus*, no *hss* transcript was present in any of the analyzed tissues. Surprisingly the amount of *hss* transcript is notable lower compared to the *dhs* transcript in nodules of *C. scoparius*, whereas a large distinction between *hss* and *dhs* transcript were detected in the nodules of *L. x watereri* 'Vossii' (Figure 2 and Figure 4).

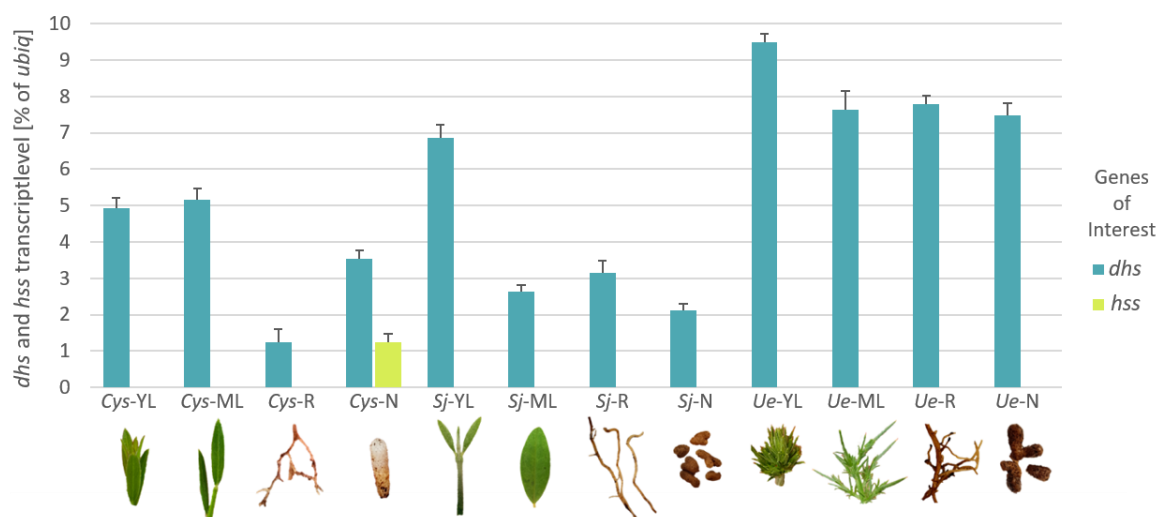


Figure 9. Transcript level of *hss* and *dhs* ($2^{-\Delta CT}$ relative transcript level of the target gene in relation to the housekeeping gene *ubiquitin* [%]) in various tissues of the three species *C. scoparius*, *S. junceum* and *U. europaeus* of the Genisteae grown in the botanical garden Kiel. *Cys*, *Cytisus scoparius*; *Sj*, *Spartium junceum*; *Ue*, *Ulex europaeus*; YL, young leaf; ML, mature leaf; R, root; N, nodule; n=1 (tested in three technical replicates).

5.4 DISCUSSION

5.4.1 The origin of an HSS copy in the Genistoids

HSS arose several times independently by duplication of the gene encoding DHS and is considered to be the first pathway-specific enzyme in PA biosynthesis (Hartmann and Witte 1995; Ober et al. 2003; Kaltenegger et al. 2013; Irmer et al. 2015). In *C. spectabilis*, PA biosynthesis is nodule-dependent, since the *hss* transcript was detected exclusively in nodules and nodule-free plants lacked PAs (Irmer et al. 2015). In this study, we identified additional species, *L. x watereri* 'Vossii' and *C. scoparius*, with *hss* transcripts in the nodule. For *L. x watereri* 'Vossii' which contains both, PAs as well as QAs, even two sites with *hss* transcript could be identified, whereas the nodule immensely stood out containing the highest amount of *hss* transcript level compared to the pods. A comparison of the sequences of DHS and HSS of *C. spectabilis* with those of *L. x watereri* 'Vossii' showed high similarities on nucleotide level which may indicate a common origin of HSS in these two species. Also, the HSS localization within the nodule parenchyma in both *C. spectabilis* and *L. x watereri* 'Vossii' give hints about HSS evolution and the feasible involvement in PA biosynthesis. In addition to the just mentioned general similarities on nucleotide level, *L. x watereri* 'Vossii' HSS sequence also exhibited a "HSS motif" on amino acid level (VRAMD; position 265-269 in exon 6/7) that has been described very detailed in species of the Convolvulaceae and which seems to be important for the HSS function (Kaltenegger et al. 2013).

Most representatives of the Genistoid clade are QA producers and thus not dependent on an HSS. In some species however, an HSS copy could be found on the genomic level (Milewski and Ober, unpublished), which suggests a gene duplication within the lineages from a common ancestor. Nevertheless, the found *hss* genes on genomic level can be pseudogenes which will not be transcribed and then translated into a functional protein. While for *S. junceum* and *U. europaeus* no *hss* transcript could be found, for *C. scoparius* a *hss* transcript was detected exclusively in the nodules of the investigated tissues. This finding is consistent with *C. spectabilis* and *L. x watereri* 'Vossii' where *hss* transcript was almost restricted to the nodules. Reasons why no *hss* transcript could be detected for *S. junceum* and *U. europaeus* at all in any investigated tissue are possibly due to not successful functioning PCRs. However, since every amplification worked for *dhs* and the

two reference genes in all three species, it is possible that just no *hss* transcript was present. *S. junceum* contain in exon 2 already an early STOP Codon, whereby no translation of the full sequence can be implemented. Whereas *U. europaeus* shows no abnormalities on genomic DNA that translation might not take place (Milewski and Ober, unpublished). *C. scoparius*, *S. junceum* and *U. europaeus* are described as QA producers (Greinwald et al. 1990; Gresser et al. 1996; Hornoy et al. 2012). Further studies on other species of this group are needed to understand when the *hss* arose, how and why it came under "nodule control" and whether it has been inactivated over time in some species. An answer to all these questions could be that the QAs have already acquired an optimized function in herbivorous defense and thus, there has been no selection pressure in the other species to refine the PA biosynthetic pathway.

5.4.2 *L. x watereri* 'Vossii' has two sites for the synthesis of homospermidine via HSS

For a long time it was assumed that only one site exists for the synthesis of PAs in plants (Moll et al. 2002), but for *Symphytum officinale* (Boraginaceae) (Niemüller et al. 2012; Kruse et al. 2017) and the *Phalaenopsis* hybrids (Orchidaceae) (Anke et al. 2008) two sites were reported to be involved in PA biosynthesis. The two sites of PA synthesis in *S. officinale* are roots and young leaves under the inflorescence while within *Phalaenopsis* hybrids root tips and young flower buds are the two PA producing sites. For the Fabaceae *C. spectabilis*, Irmer et al. (2015) provided evidence that there is just one site for PA production since the *hss* transcript was exclusively detected in the nodules. In this study the authors also described the generation of PA free plants by cultivating *C. spectabilis* *in vitro* in the absence of rhizobia. However, the only analyzed tissues of plants cultivated under these conditions, have been leaves, shoots, roots, and nodules. Therefore, it remains open whether there might be additional sites for PA production in *Crotalaria* like flower buds, open flowers, or developing fruits. This initially led to the hypothesis that PA biosynthesis is also linked to nodules in *L. x watereri* 'Vossii'. The first studies on *in vitro* grown *L. x watereri* 'Vossii' clearly showed *hss* transcript in the nodules. Subsequently, antibodies targeting HSS in *C. spectabilis* were also tested in *L. x watereri* 'Vossii'. For both species, the HSS was localized within the same nodule tissue, the nodule parenchyma, supporting the previous assumption that the two species have at least one identical site of PA biosynthesis.

It has been hypothesized that the proximity of HSS expressing cells to vascular bundles might be of importance for the transportation of PAs within the plant, since the phloem has been shown to be the transporting tissue for PAs in *Senecio vernalis* and for QAs in *Lupinus albus* and *Lupinus angustifolius* (Sander and Hartmann 1989; Lee et al. 2007). In this study the proximity of HSS expressing cells to the vascular bundles creates the impression that it might have the same mission for transporting the PAs within *C. spectabilis* and *L. x watereri 'Vossii'*. Further research is needed to prove this assumption. Surprisingly, further studies on infield grown *L. x watereri 'Vossii'* showed pods and with exception one leaf as further sites with present *hss* transcript in addition to nodules. Considering PAs being an important factor in the plants defense (Hartmann and Ober 2000), multiple sites for production are advantageous to ensure sufficient protection. Comparing other biosynthetic pathways for secondary metabolites like the one for QAs, different tissues are stated to be involved in the biosynthesis. Here the first enzyme a lysine decarboxylase is present in all chloroplastic associated tissues such as leaves and shoots (Bunsupa et al. 2012a; chapter B). Nevertheless, the last step in QA biosynthesis is described to take place in different tissues (roots and hypocotyls) and is catalyzed by an *O*-tigloyltransferase (Okada et al. 2005).

5.4.3 Nodules are not necessary for the production of PAs in *L. x watereri 'Vossii'*

Following earlier findings in *C. spectabilis*, it has been hypothesized that PA biosynthesis may also be nodule-dependent in the Fabaceae *L. x watereri 'Vossii'*. Analytical studies regarding the occurrence of PAs in infected (nodule possessing) and non-infected (nodule lacking) *in vitro* grown *L. x watereri 'Vossii'* plants clearly showed a nodule-independent biosynthesis of PAs. Infected plants with developed nodules as well as non-infected plants without nodules of different ages contained PAs. There are two scenarios that could explain the occurrence of PAs in plants not expressing HSS:

First, transcription and translation of *hss*/HSS might be switched on at other time points than those that have been investigated in this study. Different developmental stages especially of leaves in *L. x watereri 'Vossii'* could provide unexpected outcomes, since one single leaf (Figure 4 A) of *in vitro* grown *L. x watereri 'Vossii'* showed very low *hss* transcript levels. Compared to the *hss* transcript in nodules and pods, the leaves did not appear to be

a potential site. However, now that it has been shown that non-infected *L. x watereri* 'Vossii' contain PAs, further investigations of different leaves for the presence of *hss* transcript could provide deeper insight if leaves are an actual tissue for homospermidine production via HSS.

The second possibility is that the DHS may have a good HSS activity. The main function of DHS is the activation of the eIF5A precursor protein and shows the homospermidine production only as side activity (Park et al. 1997; Ober et al. 2003). After gene duplication, the HSS maintained the former side activity to synthesize homospermidine as main activity and lost the ability to bind the eIF5A precursor protein (Ober and Hartmann 1999b). Examination of the activities from the *L. x watereri* 'Vossii' DHS and HSS by heterologous expression with subsequent activity assays could provide a deeper insight. The DHS is a vital primary metabolic enzyme for the plant and ubiquitously found in all tissues (Irmer et al. 2015; Kruse et al. 2017; Park et al. 2010). Therefore, homospermidine might be available in other organs as well of *L. x watereri* 'Vossii' and would provide in this way a basis for a possible biosynthesis of PAs.

Aside from that the question arises why *L. x watereri* 'Vossii' possesses a *hss* transcript in nodules although there are no indications that nodulated plants contain more PAs than non-nodulated ones. A possibility is that the *hss* has another yet unknown function within this plant or is only a relic of the PA producing ancestor. This might be also the case for the present *hss* transcript in the PA free plant *C. scoparius*. This phenomenon of plants being PA free but come up with an HSS-like sequence has been reported in earlier studies. Especially in species within the Convolvulaceae gain and loss of HSS-like sequences are reported to be associated with sporadic occurrence of PAs (Ober and Kaltenegger 2009). Here, the species *Ipomoea purpurea* and *Convolvulus tricolor* do not produce PAs but still possess a *hss* gene on genomic DNA with indications for pseudogenization like it is as well assumed for *S. junceum* from this study. However, in the PA free Convolvulaceae *Ipomoea alba* a functional HSS-like sequence was found on genomic DNA as well as on transcription basis.

To clarify whether HSS is involved in the PA biosynthesis of *L. x watereri* 'Vossii' assuredly, *in vitro* grown plants should be transformed by carrying a CRISPR/Cas9 construct for targeting the *hss* gene to create knockout mutants.

5.4.4 Speculative structure of the found unknown necine base

First descriptions of PAs detected in *Laburnum anagyroides* date back to the 1950s. In that study, QAs like cytosine and methylcytosine as well as exclusively saturated PAs like platynecine, laburnine and laburnamine were described (Galinovsky et al. 1949; Neuner-Jehle et al. 1965). Within the genus *Laburnum* there are two known hybrids: *L. watereri* (*L. anagyroides* x *L. alpinum*) and *Laburnocytisus adamii* (*L. anagyroides* x *Cytisus purpureus*). For both hybrids little is known about their alkaloid patterns. The latter one contains 14 alkaloids, mostly QAs (main QAs were cytosine, *N*-methylcytosine and anagyrine) but also piperidyl alkaloids and only one PA (the laburnamine) which represents a mix of the two crossed species and corresponds with some of the above mentioned alkaloids in *L. anagyroides* (Greinwald et al. 1991).

The coincident occurrence of both alkaloid types within one species (QA and PA) is rare. Another species that has both QAs and PAs is *Osyris alba* L. from the family Santalaceae (Woldemichael and Wink 2002). In contrast to *Laburnum* spec., this plant shows a more complex pattern of both alkaloid classes. Despite the great diversity of QAs and PAs together in *Laburnocytisus adamii* and *O. alba* L. our unknown PA from this study in *L. x watereri* 'Vossii' cannot be identified by comparing the mentioned mass spectra.

The unknown PA shows typical fragments of a PA core structure. The assumption that it could be a loline alkaloid with a similar core structure can be excluded by the fragment pattern. The main fragment of the loline alkaloids is 82, while 83 (which has our unknown necine base) is completely absent (Justus et al. 1997). The described laburnamine does not fit as possible structure has for the unknown PA, since the side chain is connected via an additional nitrogen not oxygen, thus the total mass of the laburnamine molecule ($C_{12}H_{22}N_2O$) would be too large.

However, the substrate specificity of the HSS of *L. x watereri* 'Vossii' could provide further insight here. Quite recently a HSS of *Ipomoea alba* was described to accept just as well cadavarine as a substrate (Prakashrao et al. 2022). In this catalytic step, not a 4-aminobutyl residue is transferred from spermidine as usually described (Ober et al. 2003; Ober and Kaltenegger 2009), but an 5-aminopentyl residue from cadavarine to putrescine. If this product (4-aminobutyl-5-aminopentyl-amine) would be accepted by further enzymes of PA biosynthesis, a side chain could be formed with one -CH₂ (mass increment of 12) more than

in trachelanthamidine. Further studies are needed to investigate the activity of the HSS and DHS of *L. x watereri* 'Vossii' which could lead to more knowledge how PA biosynthesis works in this species. Especially to test the ability of HSS to accept cadaverine to catalyze 4-aminobutyl-5-aminopentyl-amine, since *L. x watereri* 'Vossii' is one of the species in which PAs and QAs coexists, it has the necessary cadaverine, which is catalyzed by the first specific enzyme of QA biosynthesis (Bunsupa et al. 2012a), a lysine decarboxylase.

5.5 MATERIAL AND METHODS

5.5.1 Plant material and culturing

Cultivation of *L. x watereri* 'Vossii' and *C. spectabilis* *in vitro* plants were processed as described in Chapter A and Chapter B of this study. The investigated species *C. scoparius*, *S. junceum* and *U. europaeus* were grown in the field in Kiel Botanic Gardens.

5.5.2 Preparation and affinity purification of polyclonal antibodies

Polyclonal antibodies against the HSS of *C. spectabilis* have been prepared previously (Jacky 2015). Briefly, heterologous expression of HSS of *C. spectabilis* was implemented as described in Irmer et al. (2015). Purified recombinant HSS protein was freeze dried and 1 mg was used to produce polyclonal antibodies by immunization of rabbits by bj-diagnostik GmbH (Göttingen, Germany). Two injections were carried out, first with 500 µg and the second with 250 µg. For affinity purification of the antibody, 1 mg of purified recombinant HSS was coupled to CNBr-activated Sepharose™ 4B (GE Healthcare), according to the manufacturer's protocol. Removing of lipids from the serum was achieved by filtration over fiberglass before incubation of the serum with the matrix for 17 h at room temperature under constant shaking to guarantee a sufficient antigen-antibody binding. Following this, the matrix was washed with 0.1 M sodium acetate containing 0.5 M NaCl (pH 4.8) and eluted with 0.2 M sodium acetate containing 0.5 M NaCl (pH 2.5). The purified antibodies were rebuffed in 1.5 M Tris/HCl (pH 8.8), concentrated, mixed with 0.02% (m/v) sodium azide (NaN₃) and stored at -80°C until further use.

5.5.3 Immuno histochemical localization

For the immunohistochemical detection of HSS of *C. spectabilis* and *L. x watereri* 'Vossii' different stages of nodules were harvested, and some larger nodules were already partly divided into smaller pieces since complete fixation of bigger nodules have been difficult. Fixation was executed as described by (Anke et al. 2004) for 2 h on ice under reduced pressure (0.3 bar). Subsequently, fixated tissues were washed twice for 5 min with 1x PBS (8 g/l NaCl, 0.2 g/l KCl, 1.44 g/l Na₂HPO₄, 0.24 g/l KH₂PO₄), followed by an ascending alcohol series (30%, 50%, 70%, 90% and 3 x 100%) each for 30 min. After dehydration, the sections were embedded in Technovit 7100 resin (Kulzer) in four steps. First, sections were

incubated for 60 min in Technovit 7100 and 100% ethanol (1:1), then for 60 min in pure Technovit 7100 at 4°C. Afterwards, the sections were incubated overnight in hardener I + Technovit 7100 [10 mg/ 1 ml] before final embedding (10 mg hardener I/ 1 ml Technovit 7100 mixed with 330 µl hardener II). Samples were oriented and polymerization took place overnight at room temperature. For microscopic analysis, embedded tissues were cut to 4 µm sections on a microtome (HM 355 S, MICROM International GmbH, Walldorf) and mounted on coated object slides (Thermo Scientific, Menzel Gläser SuperFrost®Plus). Cut sections were washed at 37°C with 50 mM NH₄Cl and 50 mM glycine (20 min each) before blocking unspecific binding sites for 1 h at 37°C (1% BSA + 0.1% fish gelatin in 1x PBS). Slices were washed with 1x PBS (3 x 5 min) and incubated with the affinity-purified primary antibody specific for the HSS of *C. spectabilis* [4.858 mg/ml]. Therefore, 30-50 µl of diluted first antibody (dilution 1:500 for *C. spectabilis* resulting in [0.0097 mg/ml] and dilution 1:250 for *L. x watereri* 'Vossii' resulting in [0.0194 mg/ml]) was pipetted on each section and incubated overnight at 4°C. Washing steps with 1x PBS were repeated three times for 10 min. To allow UV detection, a second antibody (goat anti-rabbit AlexaFluor488, 1:100, Invitrogen) was applied onto the sections that were incubated for 1 h at 37°C under exclusion of light. Subsequently three washing steps each 15 min with 1x PBS were executed, followed by one step with water. Air dried sections were covered with mounting medium (ROTI®Mount FluorCare, Carl Roth, Germany), to reduce bleaching, before microscopic analysis (Zeiss, Axioskop2plus linked with AxioCam HRc) using the software AxioVision Release 4.8.2 for recording images.

5.5.4 Identification of putative *dhs*, *hss* and housekeeping genes in *L. x watereri* 'Vossii' and of further species of Genisteae

RNA extraction and cDNA synthesis are the same as described in chapter B. Identification of housekeeping genes *ubiquitin* and *ef1a* on cDNA level was already performed for *L. x watereri* 'Vossii' in chapter B. PCR conditions, cloning and sequencing for the identifications of the encoding cDNAs of DHS and HSS of *L. x watereri* 'Vossii' are equal to the identifications of encoding cDNAs of LDC and ODC of *L. x watereri* 'Vossii', and the two lupins *L. arboreus* and *L. polyphyllus* (chapter B). Partial gDNA sequences of *hss* and *dhs* of *L. x watereri* 'Vossii', *C. scoparius*, *S. junceum* and *U. europaeus* (Milewski and Ober

unpublished) were used for completion and identification on cDNA basis. Housekeeping genes *ubiquitin* and *ef1a* of *C. scoparius*, *S. junceum* and *U. europaeus* were amplified by using realtime primers of *L. x watereri* 'Vossii' and Oligo_(dt) described in the results and Supplemental Table S2.

5.5.5 Quantitative realtime PCR (RT-qPCR)

For analyses of the transcript levels of *dhs* and *hss* in *L. x watereri* 'Vossii', the same plants and tissues were used as for the investigations of the transcript levels of *ldc* and *odc* (chapter B). For *C. scoparius*, *S. junceum* and *U. europaeus* new samples were taken from infield grown plants. Briefly, the extracted RNA was transcribed into cDNA and to exclude cDNA contaminations with genomic DNA, "no-reverse-transcription" (-rt) control reactions were set up for every sample (Supplemental Figure S1), except for infield grown *L. x watereri* 'Vossii' samples (chapter B, Supplemental Figure S4 A). The considered parameters for the design of real-time primers are described in chapter A. Due to the high similarity of the cDNA encoding HSS and DHS, unspecific binding of these primers was tested for *L. x watereri* 'Vossii' in control PCRs with plasmids, which contained HSS- and DHS-coding sequences, as template (Supplemental Figure S2). For *C. scoparius*, *S. junceum* and *U. europaeus* no plasmids with the corresponding cDNAs were available. The specificity tests were therefore implemented via RT-qPCR and based on the resulting melting curves. RT-qPCR tests were done in a Rotor-Gene® Q System (Qiagen, Hilden, Germany) with the following RT-qPCR settings. In a total volume of 20 µl for each amplification reaction: 10 µl GoTaq® qPCR Master Mix (Promega), 0.125 pmol of each primer, 4 µl RNase-free water and 5 µl template cDNA. The applied template cDNA depended on the yield of the respective sample and ranged from 3.75 ng to 12.5 ng. Cycling conditions ensued by the two-step variant: one cycle 95°C for 2 min; 40 cycles with 95°C for 15 s and 60°C for 60 s. Calculation of the relative transcript level ($2^{-\Delta CT}$) of each gene of interest (*hss* and *dhs*) was performed using the two reference genes *ubiquitin* (*ubiq*) and elongation factor 1-alpha (*ef1a*) (Schmittgen and Livak, 2008). Technical replicates (n=3) were achieved due to pipetting three RT-qPCR runs of individual cDNA (n=1) for determination the transcript level of each gene of interest. Evaluation and interpretation of the results was done under consideration of resulting melting curves. In cases of

ambiguity, PCR products were additionally checked on agarose gels and sequenced. Real-time primer sequences are given in Supplemental Table S1.

5.5.6 PA analytics in *L. x watereri* 'Vossii'

The same plants were checked for PAs as before for QAs. The same GC-MS device was used as well as the already in chapter B described settings and temperature program for analysis. Fresh plant material was collected and immediately frozen before ground. Weight of the samples varied from 295 – 909 mg for total plants, and 40 – 400 mg for individual plant organs. PAs were extracted following the protocol described by Kruse et al. (2017). 10 µg heliotrine was added per 100 mg fresh weight as internal standard. For detection of PAs, the samples were after first measurement in GC-MS additionally derivatized with *N*-methyl-*N*-(trimethylsilyl)trifluoroacetamide (MSTFA). Samples derivatization with MSTFA was carried out by first evaporating the sample and then dissolving the residue in 50 µl MSTFA and heated at 60°C for 30 min. The samples were evaporated again and resuspended in 30 µl methanol for the second measurement. Settings and temperature program remained as used for the first measurement. Identification of detected PAs was done via comparison of retention indices with the literature (Woldemichael and Wink 2002; Hartmann et al. 2005) and their MS pattern.

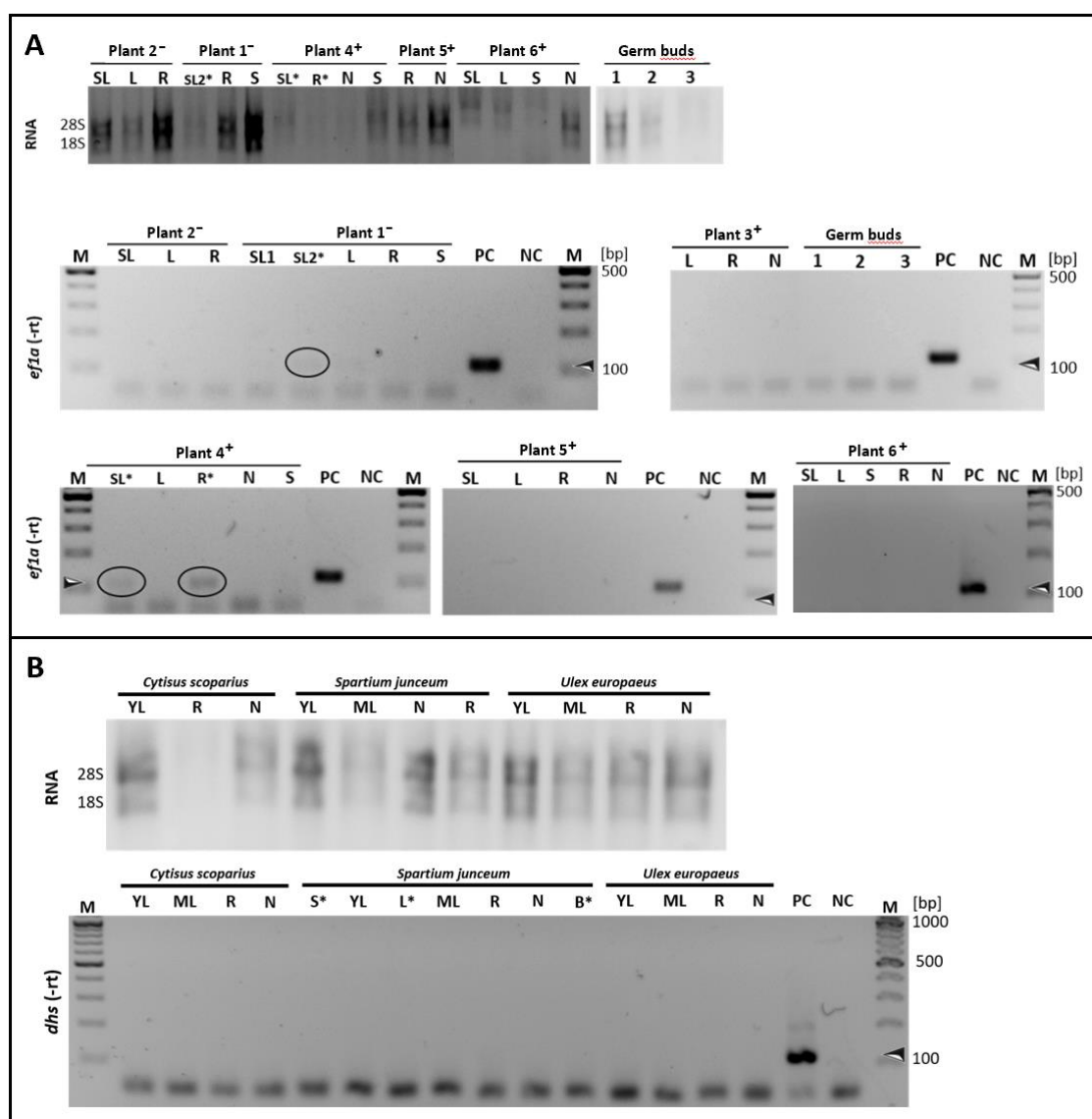
5.6 SUPPLEMENTAL DATA

Supplemental Table S1. Sequences of primers and the expected product size for each investigated gene of interest in RT-qPCR analysis for *L. x watereri* 'Vossii', *C. scoparius*, *S. junceum* and *U. europaeus*. *Cys*, *Cytisus scoparius*; *Lxw*, *Laburnum x watereri* 'Vossii'; *Sj*, *Spartium junceum*; *Ue*, *Ulex europaeus*.

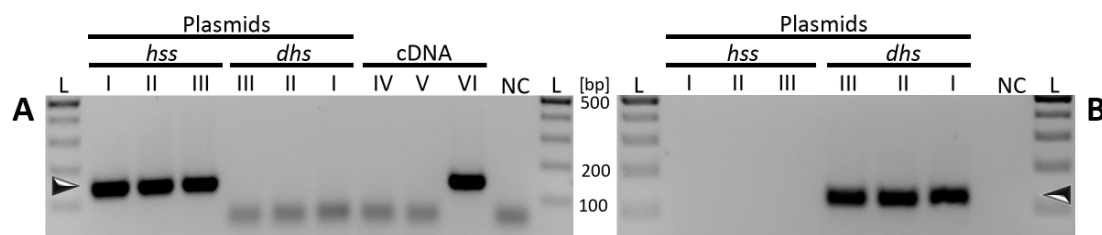
Primer	Sequence 5' -> 3'	Product size
P1 UBQ forward (<i>Lxw</i> , <i>Cys</i> , <i>Sj</i> , <i>Ue</i>)	GGAGGAATGCAGATCTTTGTGAAG	108 bp
P2 UBQ reverse (<i>Lxw</i> , <i>Cys</i> , <i>Sj</i> , <i>Ue</i>)	CTCCTTGTCCTGGATTTTGTCTT	
P3 EF1a forward (<i>Cys</i> , <i>Sj</i> , <i>Ue</i>)	GTGGTTGAACTTTGCCGAGTA	109 bp
P4 EF1a reverse (<i>Cys</i> , <i>Sj</i> , <i>Ue</i>)	TAGGATCCTTCTTCTCCACACTCT	
P5 EF1a forward2 (<i>Lxw</i>)	TAAGGAGATGGAGAAGGAGCCC	132 bp
P6 EF1a reverse2 (<i>Lxw</i>)	TCTCTGACAGCAAAACGACCAA	
P7 DHS forward (<i>Lxw</i>)	CAACTATCGCTTTTCCTCTGCTT	120 bp
P8 DHS reverse (<i>Lxw</i>)	GCAAGATCAACAGGACTAGAAAATGC	
P9 DHS forward (<i>Cys</i> , <i>Sj</i> , <i>Ue</i>)	GGGCTTAACGGATGGCTCATT	117 bp
P10 DHS reverse (<i>Cys</i> , <i>Sj</i> , <i>Ue</i>)	GCATGTACAGCTTCACCATTTCATG	
P11 HSS forward (<i>Lxw</i>)	GAATGAGGGAAATGAAAGTGGTGAT	142 bp
P12 HSS reverse (<i>Lxw</i>)	CATGATAAGCTGAGGATAATCAACACC	
P13 HSS forward (<i>Cys</i>)	GCCAATAGAGATTTACTACCAATTGCAT	144 bp
P14 HSS reverse (<i>Cys</i>)	GCCCTCACAATATGCAAGTTTTATTATGA	
P15 HSS forward (<i>Sj</i>)	TCCAGGATTAACAGATGGGTCATTA	110 bp
P16 HSS reverse (<i>Sj</i>)	CAACATCATCCATTGCCCTTACAT	
P17 HSS forward (<i>Ue</i>)	AGGATTAACAGATGGCTCATTAGGG	108 bp
P18 HSS reverse (<i>Ue</i>)	ACTTCATCATCCATTGCCCTTACAT	

Supplemental Table S2. Listed are primers, amplified product sizes, used tissues and the amplified sequence part of *hss*'s, *dhs*'s and the reference genes (*ubiquitin*, *ef1a*) of *L. x watereri* 'Vossii', *C. scoparius*, *S. junceum* and *U. europaeus*. PCRs were performed with Phusion Hot Start polymerase (Thermofisher Scientific) according due to the manufacture protocols. *Oligo_(dT) conducted as reverse primer for all 3'RACE amplifications.

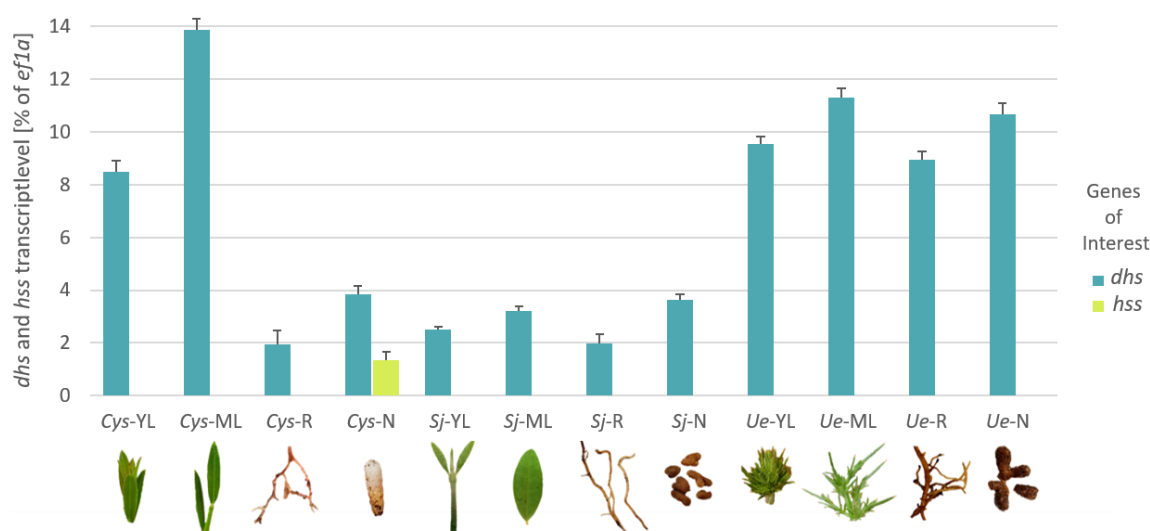
Organism	Gene	Primer (5' -> 3')	Amplified Product Size/ Tissue	Amplified Sequence Part
<i>L. x watereri</i> 'Vossii'	<i>dhs</i>	P19-f (binds at Start-ORF) ATGAATTATACGGTAAAGGAAACAGCTAGTG	1524 bp cDNA leaf	ORF + 3'UTR *
	<i>hss</i>	P20-f (binds in Exon 1) CTKGAAGGAAARTGYGCCAAG	1288 bp cDNA nodule	Internal fragment *
	<i>hss</i>	P21-f D168 (binds in Exon 6)	622 bp cDNA nodule	3'RACE *
	<i>hss</i>	P22-f (binds at Start-ORF) ATGAATGAGGGAAATGAAAGTGGTGA	1098 bp cDNA nodule	ORF
		P23-r (binds at Stop-ORF) TCAAGGTTTCACTCTTGTGGCAAAA		
<i>C. scoparius</i>	<i>hss</i>	P24-f (binds at intersection point Exon 6/7) AGATGTAAGGGCAATGGATGATGA	523 bp cDNA nodule	3'RACE *
<i>C. scoparius</i> <i>S. junceum</i> <i>U. europaeus</i>	<i>ef1a</i>	P3 (Exon binding unknown) GTGGTTGAACTTTTGCCGAGTA	450 bp (<i>Cs</i>) 541 bp (<i>Sj</i>) 483 bp (<i>Ue</i>) cDNA leaf each	3'RACE *
* Oligo _(dT) P25 GTCGACTCGAGAATTC(T)17				



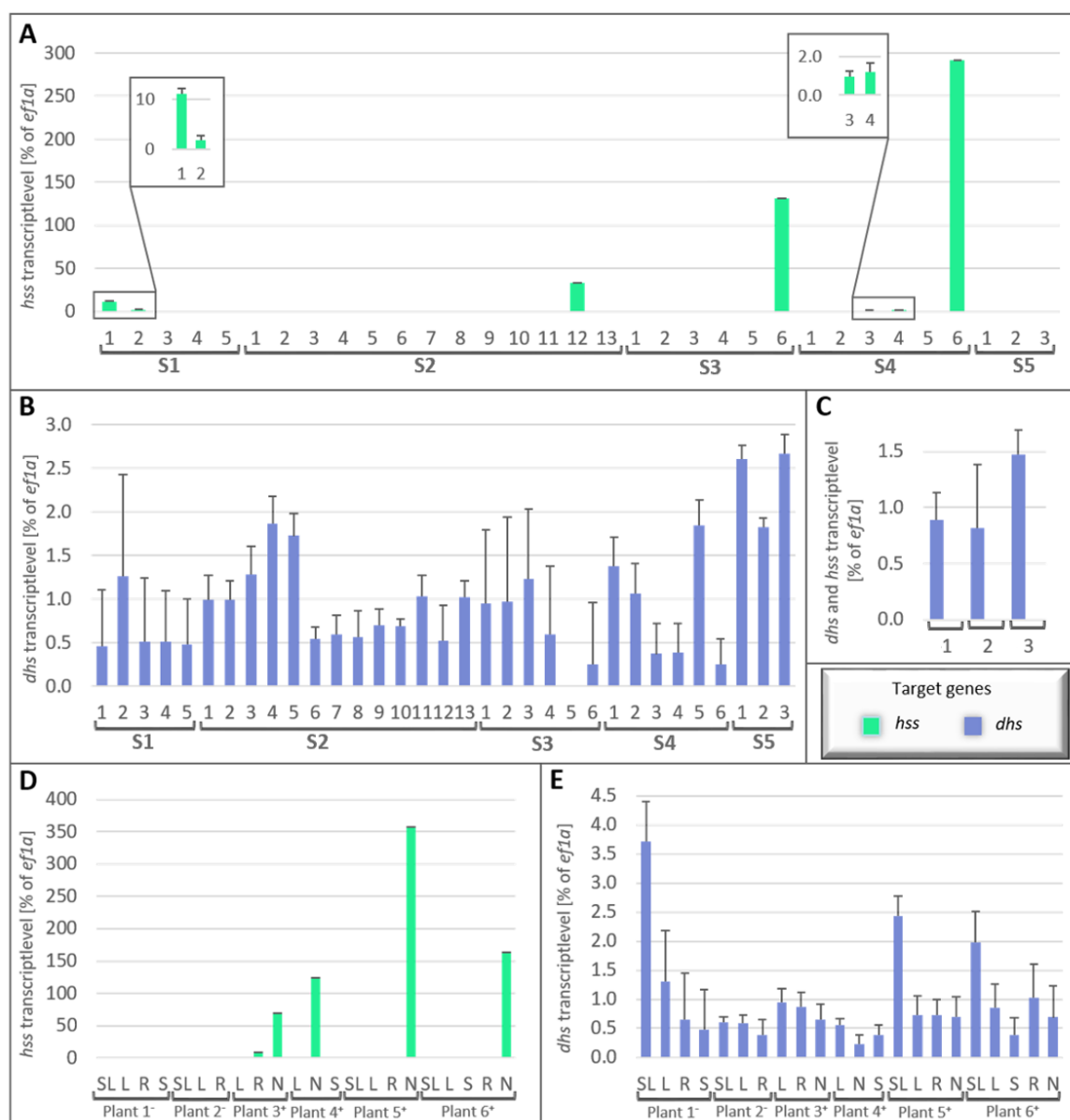
Supplemental Figure S1. Tests of RNA used for reverse transcription and for gDNA contamination in cDNA samples of *in vitro* grown *L. x watereri* 'Vossii' (A) and the three infield grown species *C. scoparius*, *S. junceum* and *U. europaeus* of the tribe Genisteae (B). Agarose gel electrophoresis of total RNA and PCR products resulting from RNA prepared without reverse transcription (-rt). **A Contamination of RNA with gDNA would result in a fragment of 109 bp as it is amplified by the primer pair P3/P4 for *ef1a* in the positive control. Plant 1⁻: 2 months; Plant 2⁻: 7 months; Plant 3⁺: 3 months; Plant 4⁺: 10 months; Plant 5⁺: 11 months; Plant 6⁺: 14 months. 1, complete germ bud; 2 and 3, germ buds analyzed only leaves. **B** Contamination of RNA with gDNA would result in a fragment of 204 bp due to an intron, that exist within the amplified area for the *dhs* gene with primer pair P9/P10. On cDNA level the expected product size is 117 bp as shown in the positive control. PCRs were implemented with GoTaq polymerase and annealing temperature of 60°C. Arrowhead indicates expected product as mentioned, respectively. M, DNA ladder (GeneRuler 100 bp Plus DNA Ladder, Thermo Scientific); bp, base pair; B, flower; Co, cotyledons; YL, young leaf; L, leaf; ML, mature leaf; R, root; S, stem; SL, smaller appearing leaf; N, nodule; PC, positive control of leaf cDNAs; NC, no-template control. *Labeled tissue cDNA was not used in RT-qPCR. RNA concentration of the mature leaf of *C. scoparius* as well Plant 3⁺ of *L. x watereri* 'Vossii' was too low for both reverse transcription and performing an RNA gel.**



Supplemental Figure S2. Specificity tests of the RT-qPCR primer pairs for homospermidine synthase (*hss*) and deoxyhypusine synthase (*dhs*) of *L. x watereri* 'Vossii' for tissue specific analysis. Due to gene duplication and high sequence similarity, unspecific binding of primers was tested through plasmid DNA containing the respective genes. **A** Test of *hss* primer pair P9/P10 against *hss* and *dhs* plasmids as well as cDNA of different tissues. **B** Test of *dhs* primer pair P5/P6 against *hss* and *dhs* plasmids. Arrow head indicates expected PCR product size (*hss* = 142 bp; *dhs* = 120 bp) with GoTaq polymerase and annealing temperature of 60°C. L, ladder (GeneRuler 100 bp Plus DNA Ladder, Thermo Scientific); bp, base pair; I, 25 ng of plasmid DNA; II, 10 ng of plasmid DNA; III, 5 ng of plasmid DNA; IV, cDNA of a germ bud; V, cDNA of leaf; VI, cDNA of nodule; NC, no-template control.




Supplemental Figure S3. Transcript level of *hss* and *dhs* (2^{-ΔCT} relative transcript level of the target gene in relation to the housekeeping gene *ef1a* [%]) in various tissues of the three species *C. scoparius*, *S. junceum* and *U. europaeus* of the Genisteae grown in the botanical garden Kiel. Cys, *Cytisus scoparius*; Sj, *Spartium junceum*; Ue, *Ulex europaeus*; YL, young leaf; ML, mature leaf; R, root; N, nodule; n=1 (tested in three technical replicates).



Supplemental Figure S4. Tissue-specific analysis of $2^{-\Delta CT}$ relative transcript level of the target genes *hss* and *dhs* in *L. x watereri* 'Vossii'. Various tissues of infield grown (plant with root-nodules) (**A** and **B**) and *in vitro* grown infected (nodule possessing; +) and non-infected (lacking nodules; -) plants (**C-E**) were analyzed by using the housekeeping gene *ef1a* as reference. **A** *hss* transcript level in tissues of infield grown plants (sampling S1-S5). **B** *dhs* transcript level in tissues of infield grown plants (sampling S1-S5). **C** *dhs* and *hss* transcript level in non-infected germ buds. **D** *hss* transcript level in tissues of *in vitro* grown infected (+) and non-infected (-) plants with different age. **E** *dhs* transcript level in tissues of *in vitro* grown infected (+) and non-infected (-) plants with different age. **Sampling 1:** 1 = nodules; 2 = root; 3 = leaf bud; 4 = leaves of flower bud; 5 = young flower. **Sampling 2:** 1 = unevolved leaves; 2 = petioles; 3 = leaf; 4 = mature leaf; 5 = petiole; 6 = unripened inflorescence; 7 = green enclosed flowers; 8 = green enclosed flower buds; 9 = single open flower; 10 = petioles; 11 = root; 12 = nodules; 13 = petioles. **Sampling 3:** 1 = unevolved leaf; 2 = mature leaf; 3 = mature leaf; 4 = single open flower; 5 = root; 6 = nodules. **Sampling 4:** 1 = mature leaves; 2 = mature leaf; 3 = green seedpod; 4 = two green seedpods; 5 = root; 6 = nodules. **Sampling 5:** 1 = leaf; 2 = green inflorescence; 3 = leaves. S1-S5 = sampling; **Plant 1⁺:** 2 months; **Plant 2⁺:** 7 months; **Plant 3⁺:** 3 months; **Plant 4⁺:** 10 months; **Plant 5⁺:** 11 months; **Plant 6⁺:** 14 months. L = leaf; N = nodule; R = root; S = stem; SL = smaller appearing leaf; 1 = complete germ bud; 2 and 3 = analyzed only black circled leaves; n=1 (tested in three technical replicates).

Supplemental Table S3. Detailed distribution of the detected PAs in the investigated infected (nodule possessing) and non-infected (nodule lacking) *in vitro* grown plants of *L. x watereri* 'Vossii'. For better detection of PAs, derivatization with *N*-methyl-*N*-(trimethylsilyl)trifluoroacetamide (MSTFA) resulted in a trimethylsilyl-group (TMS) at accessible hydroxyl groups.

Organism	Plant	Nodules	Tissue	PA [$\mu\text{g}/100\text{mg}$] FW				
				(-)-Trachelanthamidine-1xTMS	(-)-Isoretronecanol-1xTMS	unknown necine base-1xTMS	(-)-Turnefordicine-2xTMS	Chysin A
 <i>L. x watereri</i> 'Vossii'	1	-	complete	0.411	0.086	0.996	1.589	0.279
	2	-	complete	2.034	0.064	4.374	3.132	0.509
	3	-	complete	0.473		6.573	1.087	1.381
	4	-	complete			1.397	1.658	0.337
	5	+	complete	1.730	0.131	1.156	4.513	0.385
	6	+	complete	0.589		0.716	0.468	0.166
	7	+	complete	3.585	0.177	1.063	2.309	0.297
	8	+	complete	1.764	0.039	0.493	0.459	0.101
	9	-	leaves			1.274	0.638	0.631
			stem			3.595	5.726	0.575
			roots			1.136	11.345	
	10	+	leaves			22.323	2.134	1.542
			stem	69.997	4.013	40.397	186.715	1.646
			roots			53.367	92.482	
	11	-	nodules	14.178		20.172	51.882	
			leaves				72.290	0.389
			stem			56.350	15.636	1.033
			roots	3.417		132.299	4.412	2.325
	12	+	leaves					
			stem	0.239		5.790	2.920	
			roots	5.707		2.536	5.333	0.313
			nodules	145.997		8.334	43.072	1.702

6.

MISCELLANEOUS CHAPTER D

Study of CuAOs in the Fabaceae golden chain as potential involved enzymes in the biosynthesis of PAs

6.1 INITIAL POSITION AND GOAL SETTING

Copper-dependent amine oxidases (CuAOs) have been postulated for quite a long time to be involved in PA biosynthesis (Böttcher et al. 1993; Frölich et al. 2007) and are described playing a role in QA biosynthesis (Yang et al. 2017). Recently, studies in *Heliotropium indicum* (Zakaria et al. 2022) and *Crotalaria spectabilis* (chapter A) proofed for the first time the involvement of CuAOs in PA biosynthesis.

The Fabaceae *Laburnum* spec. is also a PA producing plant, consisting of PAs with no 1,2-double bound in the necine base (Neuner-Jehle et al. 1965). For the past years several PA representatives have been investigated for the presence of the first specific enzyme within PA biosynthesis, a homospermidine synthase (HSS) (Ober and Hartmann 1999b; Ober et al. 2000; Reimann et al. 2004; Kaltenegger et al. 2013; Irmer et al. 2015). Within this project (chapter C) reverse transcription quantitative PCR analyses (RT-qPCR) of *Laburnum x watereri* 'Vossii' showed clearly the nodules as *hss* transcript-containing tissue and additionally with minor detectable amounts the pods.

To investigate CuAOs as further enzymes that could be involved in the pathway of PAs, an unassembled genome of *L. anagyroides* on NCBI (chapter C) was compared with the five identified *cuaos* sequences of *C. spectabilis* (chapter A). The identified sequence parts of the five *cuaos* were then used to perform RT-qPCR analyses for the tissue determination of their transcripts.

6.2 RESULTS

6.2.1 Sequence identification of five *cuaos* in *L. x watereri* 'Vossii'

To identify potential *cuaos* in *L. x watereri* 'Vossii', the known five *cuaos* of *C. spectabilis* were used for a comparison with a *L. anagyroides* genome on NCBI (Acc. No. ERX147333/ERX147334). In this process, the five gene encoding cDNA sequence parts of *C. spectabilis* CuAOs were compared with the sequence read archives (SRAs) of the *L. anagyroides* genome. The identified reads of each CuAO for *L. anagyroides* were used for primer construction. Subsequently, RNA was extracted from leaves and nodules of a field-grown *L. x watereri* 'Vossii' plant and transcribed into cDNA. This cDNA served as template. The following PCR-based strategy to extend the sequence information with primers build

on the reads is listed in Supplemental Table S1. In total five *cuaos* partial sequences were identified (1953 bp for *cuaa1*, 1934 bp for *cuaa2*, 1269 bp for *cuaa3*, 2102 bp for *cuaa4* and 1938 bp for *cuaa5*). For all five *cuaos* PCR products were purified, A-tailed and cloned. For each *cuaa* two positive clones were picked, sequenced and compared. In case for *cuaa1*, both clones were identical in their sequence information, except that clone-1 contained additionally the 3'UTR (in total 1953 bp). The fragment with the primer pair FP1/RP1 resulted in 1742 bp and was equivalent to clone-2. It is possible that the remaining Oligo_(dt) in the template cDNA, which was used before for reverse transcription, conducted as reverse primer during the PCR. Because of this, not only the 3'UTR was amplified but also the missing part starting from primer RP1 towards the end of the ORF, which is 211 bp long. For *cuaa2*, *cuaa3* and *cuaa4* the sequence parts do not include the complete ORF. Nevertheless, in *cuaa4* it seems that only the stop codon is missing when comparing with *cuaa4* from *C. spectabilis*. The identified sequence of *cuaa5* starts with ATG but the part including the stop codon is missing, while for *cuaa1* only the sequence information for the start is missing. A complementation of the sequences within this study was time-wise not any longer realizable. The identified sequences were sufficing for the phylogenetic classification and performing RT-qPCR analyses.

6.2.2 Phylogenetic classification

Transcript sequences of 57 CuAO-like proteins were used for phylogenetic analysis to classify the five identified CuAOs of *L. x watereri* 'Vossii'. By using the Geneious software package (Geneious Prime®, Biomatters, Ltd., Auckland, New Zealand) a sequence alignment, based on nucleotide level, and the phylogenetic tree were obtained. The Geneious Tree Builder consists of two settings: 1. pairwise alignment options for building a distance matrix which includes the alignment type: global alignment with free end gaps and the cost matrix: 65% similarity (5.0/-4.0). 2. tree builder options which includes the genetic distance model: Tamura-Nei; the tree build method: Neighbor-Joining and the outgroup: no outgroup. The origin of the used 57 CuAO sequences can be taken from the Supplemental Table S2. Up to now, three main clusters exist in which the CuAOs from plants are divided (Figure 1). Comparing the five partial *cuaos* sequences of *L. x watereri* 'Vossii'

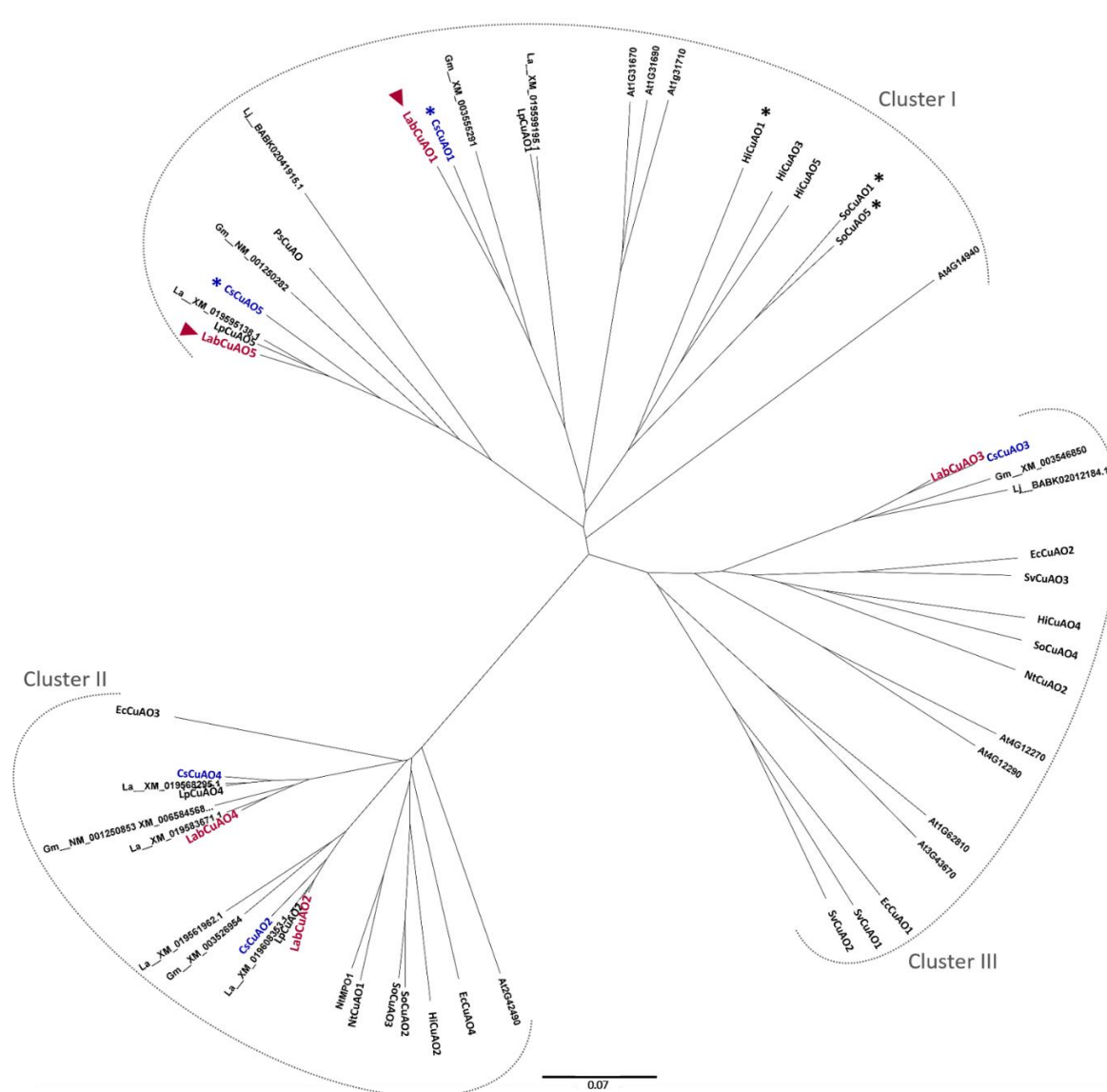


Figure 1. Neighbor-joining tree of cDNA sequences encoding CuAOs of various species of the plant kingdom. The CuAOs of *L. x watereri* 'Vossii' identified in this study are labeled in red. Red arrows point to the two presumed CuAOs involved in PA biosynthesis in *L. x watereri* 'Vossii'. Blue and black asterisks label the CuAOs of the three species *C. spectabilis*, *H. indicum* and *S. officinale* that have been identified recently as being involved in PA biosynthesis. Note that not all used nucleotide sequences contained the whole ORF information (Supplemental Table S2).

on nucleotide level with known *cuaos* from PA-producing and non-PA-producing plants it is conspicuous that the sequences of *L. x watereri* 'Vossii' and *C. spectabilis* always lie in pairs close together. A closer look at the three existing clusters shows that cluster I stands out by including the following CuAOs which have already been confirmed so far to be involved in the biosynthesis of PAs: *HiCuAO1* from *Heliotropium indicum* (Zakaria et al. 2022), *SoCuAO1* and *SoCuAO5* from *Symphytum officinale* (Zakaria unpublished), as well as

the two from *Crotalaria spectabilis* (CsCuAO1 and CsCuAO5) (chapter A). The phylogeny now shows that two of the identified CuAOs (*LabCuAO1* and *LabCuAO5*) of *L. x watereri* 'Vossii' are also located in Cluster I and thus presume a similar function in terms of involvement in PA biosynthesis.

6.2.3 Only one *cuao* is co-transcribed with *hss* in nodules

Since the first specific enzyme of PA biosynthesis (HSS) was almost exclusively detected in the nodules of *L. x watereri* 'Vossii', the five identified *cuao*s of *L. x watereri* 'Vossii' were investigated for co-transcription with *hss* via realtime quantitative PCR (RT-qPCR) in different tissues, whereas nodules remained as most interesting tissue because of the high level of *hss* transcript. The genes *ubiquitin* and *ef1a* were used as reference and have been identified before (chapter B). The samples for RNA extraction, cDNA synthesis and PCR conditions are the same as previously used for RT-qPCR for *Idc*, *odc* and *hss*, *dhs* (chapters B and C). Primer specificity tests excluded unspecific binding between the five CuAOs (Supplemental Figure S1). The used primers for RT-qPCR are listed in Supplemental Table S3. For RT-qPCR analyses, the transcript level of five *cuao*s in different tissues of infield grown (Figure 2) and *in vitro* grown (Figure 3) *L. x watereri* 'Vossii' were compared. The analyses using *ubiquitin* and *ef1a* as reference genes showed both that the *cuao2*, *cuao3*, and *cuao4* are transcribed in all tested tissues of infield grown and *in vitro* grown *L. x watereri* 'Vossii' (Figure 2, Figure 3, Supplemental Figure S2 and S3). Due to their omnipresence in all tissues, it is assumed that these three *cuao*s might be essential for the plant development and growth and do not have any impact on PA biosynthesis. Whereas *cuao1* and *cuao5* transcripts are almost exclusively detectable in nodules, like *hss*. Only minor traces of *cuao1* and *cuao5* transcripts were found in seedpods (Figure 2 I, K; Supplemental Figure S2 A, E) of an infield grown plant like it is similar shown for the *hss* transcript (Figure 2 G; Supplemental Figure S2 F). However, analyses of *in vitro* grown infected (nodule possessing) and non-infected (nodule lacking) plants gives some surprising insight. It was found that *cuao5* has deviations from the transcription pattern of *hss*, whereas this is not the case for *cuao1* which is the only exclusively co-transcribed CuAO with *hss* and present in nodules (Figure 3 A; Supplemental Figure S3 A). The transcript of

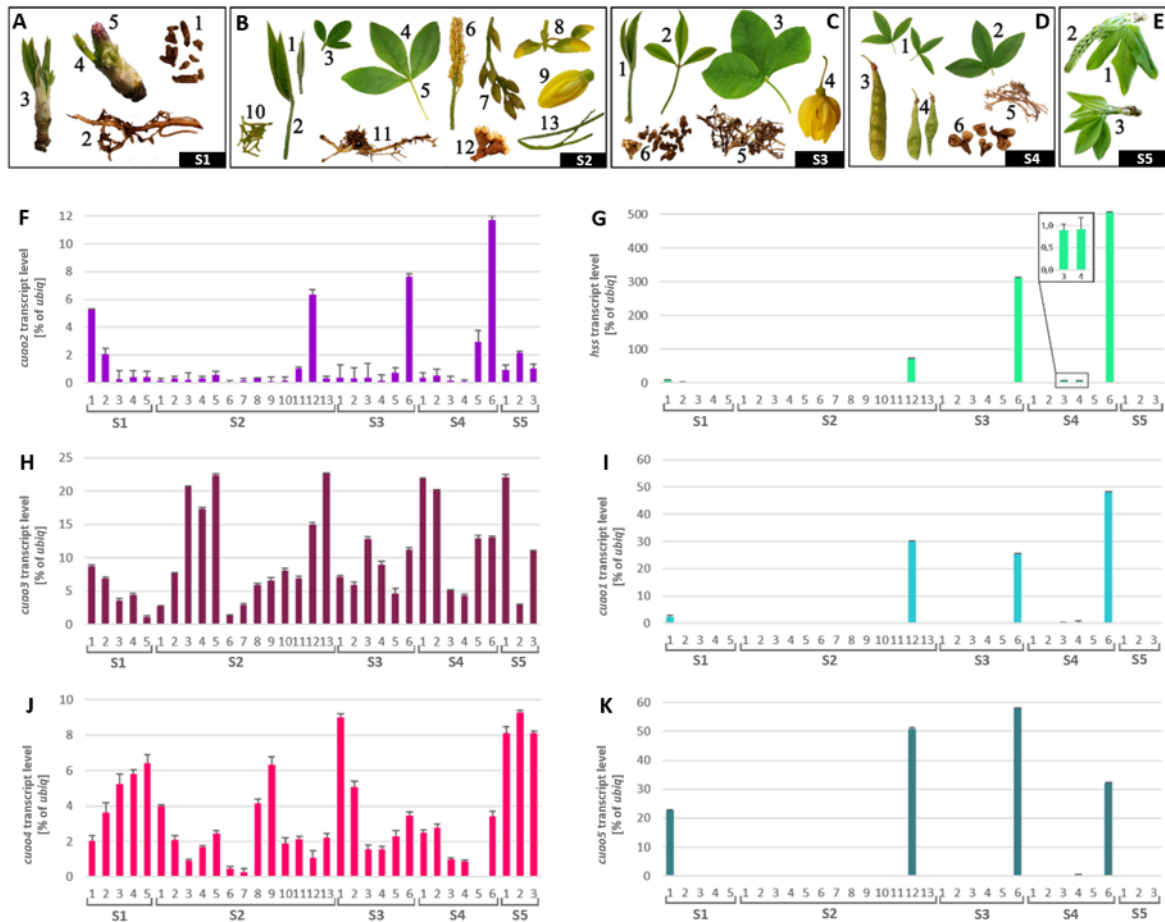


Figure 2. Transcript level of the genes *hss* and *cuao1-5* ($2^{-\Delta CT}$ relative transcript level of the respective target gene in relation to the housekeeping gene *ubiquitin* [%]) in various tissues (sampled at different seasons every time around 5 p.m.) of *L. x watereri* 'Vossii' grown in the Botanical Garden, Kiel (A - D) and in Molfsee (E), Germany. **A Sampling 1** (harvested April 25th, 2019): 1 = nodules; 2 = root; 3 = leaf bud; 4 = leaves of flower bud; 5 = young flower. **B Sampling 2** (harvested May 14th, 2019): 1 = unevolved leaves; 2 = petioles; 3 = leaf; 4 = mature leaf; 5 = petiole; 6 = unripened inflorescence; 7 = green enclosed flowers; 8 = green enclosed flower buds; 9 = single open flower; 10 = petioles; 11 = root; 12 = nodules; 13 = petioles. **C Sampling 3** (harvested May 27th, 2019): 1 = unevolved leaf; 2 = mature leaf; 3 = mature leaf; 4 = single open flower; 5 = root; 6 = nodules. **D Sampling 4** (harvested June 27th, 2019): 1 = mature leaves; 2 = mature leaf; 3 = green seedpod; 4 = two green seedpods; 5 = root; 6 = nodules. **E Sampling 5** (harvested April 10th, 2019): 1 = leaf; 2 = green inflorescence; 3 = leaves. **F** *cuao2* transcript level. **G** *hss* transcript level. **H** *cuao3* transcript level. **I** *cuao1* transcript level. **J** *cuao4* transcript level. **K** *cuao5* transcript level. S= sampling; n=1 (tested in three technical replicates).

cuao5 was instead additionally detected in one leaf, shoot and a germ bud of non-infected plants (Figure 3 E, F; Supplemental Figure S3 E, F) assuming that CuAO5 might not be essentially for the production of PAs. The minor traces of *cuao1* and *cuao5* transcripts in roots can be attributed to the fact, that the nodules are adhered to the roots, since in none of the non-infected roots were any *hss* or *cuao1* transcript detectable. To verify the traces

in seedpods as the right product, the melting curves of the RT-qPCR run were checked and a gel was additionally prepared. A distinct clear band in the right size supports specific binding of primers with resulting in the right amplificat.

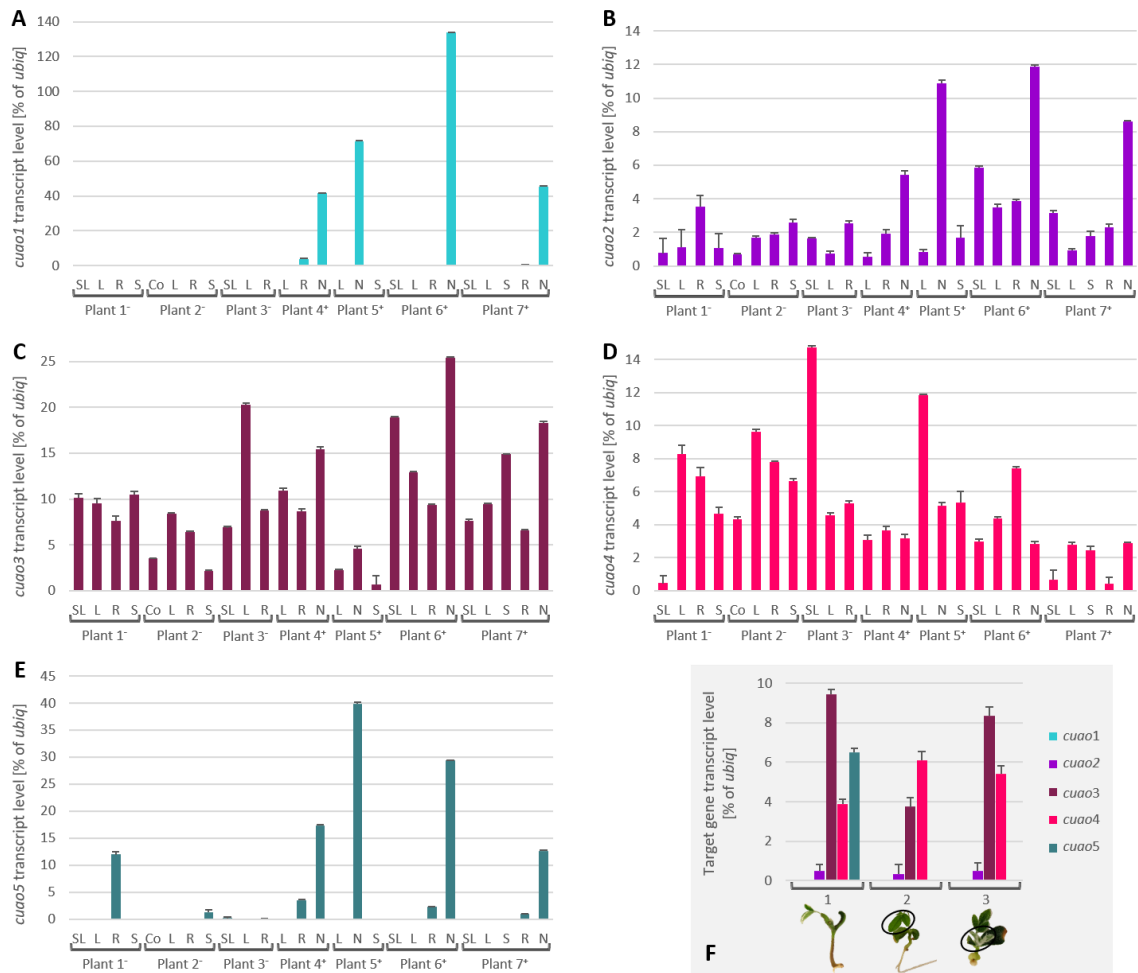


Figure 3. Transcript level of *cuao1-5* ($2^{-\Delta CT}$ relative transcript level of the target gene in relation to the housekeeping gene *ubiquitin* [%]) in various tissues of *in vitro* grown non-infected (nodule lacking; -) and infected (nodule possessing; +) *L. x watereri* 'Vossii'. **A** *cuao1* transcript level. **B** *cuao2* transcript level. **C** *cuao3* transcript level. **D** *cuao4* transcript level. **E** *cuao5* transcript level. **F** Transcript level of displayed target genes in noninfected germ buds. **Plant 1-**: 2 months; **Plant 2-**: 3 months; **Plant 3-**: 7 months; **Plant 4+**: 3 months; **Plant 5+**: 10 months; **Plant 6+**: 11 months; **Plant 7+**: 14 months. Co = cotyledons; L = leaf; N = nodule; R = root; S = stem; SL = smaller appearing leaf; 1 = complete germ bud; 2 and 3 = analyzed only black circled leaves; n=1 (tested in three technical replicates).

6.3 SUMMARY/OUTLOOK

Five partial cDNA encoding sequences of CuAOs were successfully identified and amplified for *L. x watereri* 'Vossii'. The results of RT-qPCR assume, that *cuao1* might play a key role within the production of PAs in nodules. Also, *cuao5* is predominantly transcribed in nodules and could be still a potential candidate gene. For *H. indicum* only one CuAO, called homospermidine oxidase (HSO), forms a bicyclic structure, 1-formylpyrrolizidine, by oxidizing the two primary amino groups of homospermidine (Zakaria et al. 2022). In *C. spectabilis*, whereas two CuAOs are involved in forming the bicycle structure 1-formylpyrrolizidine. Here CsCuAO5 accepts homospermidine as substrate and forms a monocyclic intermediate, which in turn conduces as substrate for CsCuAO1 forming 1-formylpyrrolizidine (chapter A). Aside from that the *cuao1* and *cuao5* are also co-transcribed with *hss* in minor traces in seedpods. This tissue should be kept in mind even though the transcript levels differ enormously from the nodules. In *Symphytum officinale*, a well-known PA producing plant, two tissues with *hss* transcript lead to the discovery of two sites (roots and leaves under the inflorescence) for the synthesis of PAs (Kruse et al. 2017). The completion of the five partial cDNA encoding sequences of *L. x watereri* 'Vossii' CuAOs on cDNA and genomic DNA could pave the way for characterization the proteins and creating knockout mutants via CRISPR/Cas9. The transformation protocol of *in vitro* grown *C. spectabilis* could serve as model establishing one for *L. x watereri* 'Vossii'. This would provide deeper insight in the PA pathway of *L. x watereri* 'Vossii' and add novel knowledge to a better understanding in the biosynthesis of PAs in general.

6.4 SUPPLEMENTAL DATA

Supplemental Table S1. PCR strategy to extend the sequence information from *Laburnum x watereri* 'Vossii' CuAOs. Listed are primers, amplified fragments and the used tissues as template DNA. PCRs were performed with a Hot Start polymerase under stated conditions.

Organism	Primer (5' -> 3')			Amplified Fragment/ Tissue
	Primer	Labor Primer Name	Primer Sequence	
<i>Laburnum x watereri</i> 'Vossii'	FP1	NJ_Lab_DAO1-f1	TCGTCATTGCCCCGCTTCCAAAA	1953 bp
	RP1	NJ_Lab_DAO1-rev1	GTCCAAACAGCTAAAGTATCATCGCC	cDNA nodule
	FP2	NJ_Lab_DAO2-f1	ACCCTTTGGACCCTTTATCTGCT	1934 bp
	RP2	NJ_Lab_DAO2-rev1	TACTGGCATAACAGGCCAATCTTC	cDNA nodule
	FP3	NJ_Lab_DAO3-f1	CAATTGATGGGAACCTTGGTGAAATGG	1269 bp
	RP3	NJ_Lab_DAO3-rev1	GCCTTGCAAACAGGTAAATCATCTT	cDNA leaf
	FP4	NJ_Lab_DAO4-f1	ATGAGAGCTCAAACCTGCCACC	2102 bp
	RP4	NJ_Lab_DAO4-rev1	GAGCTTGGCAATCAGCCCATTCT	cDNA leaf
	FP5	NJ_Lab_DAO5-f1	ATGAGTTCCACTATGAAACTTATGCTCT	1938 bp
	RP5	NJ_Lab_DAO5-rev1	CCTCAACTCAAATCCAGTGCTCAA	cDNA nodule
PCR Conditions (Phusion Hot Start Polymerase, Thermo Scientific)				
Initial Denaturation		98°C	30 s	1 cycle
Denaturation		98°C	10 s	35 cycles
Primer Annealing		65°C	30 s	
Elongation		72°C	1 min 30 s	
Final Elongation		72°C	5 min	1 cycle
Hold		4°C	∞	

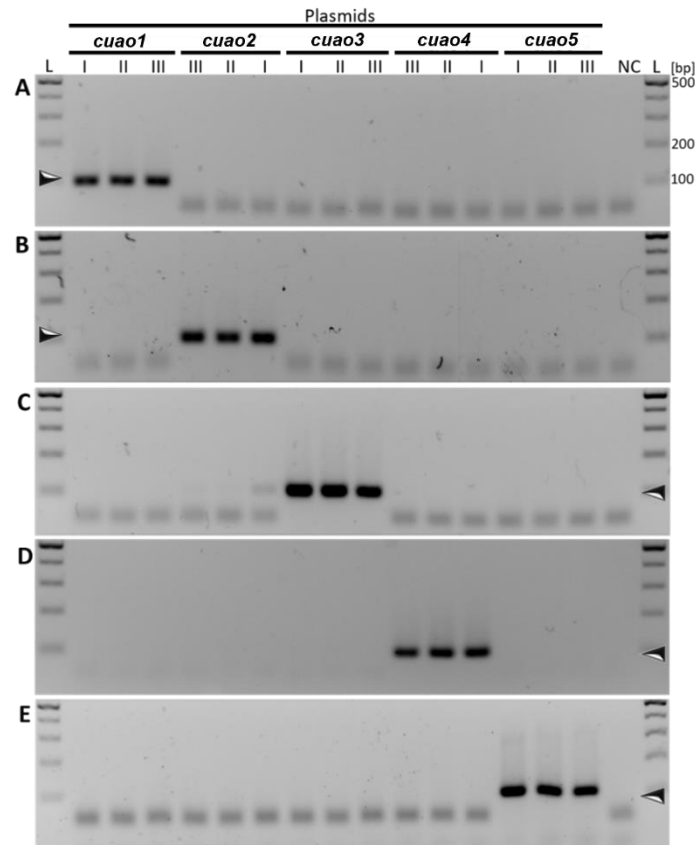
Supplemental Table S2. Sequence origins for the phylogenetic analysis. *Sequences were taken from GenBank. ■Not the complete ORF.

Organism	Gene	ORF length [bp]	Accession number / Reference*
<i>Arabidopsis thaliana</i>	At1G31670	2226	At1G31670 /*
	At1G31690	2034	At1G31690 /*
	At1g31710	2046	At1g31710 /*
	At1G62810	2139	At1G62810/*
	At2G42490	2331	At2G42490/*
	At3G43670	2064	At3G43670/*
	At4G12270	1383	At4G12270/*
	At4G12290	2226	At4G12290/*
	At4G14940	1953	At4G14940/*
<i>Crotalaria spectabilis</i>	CsCuAO1	2022	Jacky and Ober, unpublished (Chapter A)
	CsCuAO2	2262	
	CsCuAO3	2214	
	CsCuAO4	2103	
	CsCuAO5	2073	
<i>Eupatorium cannabinum</i>	EcCuAO1	2148	Ober, unpublished

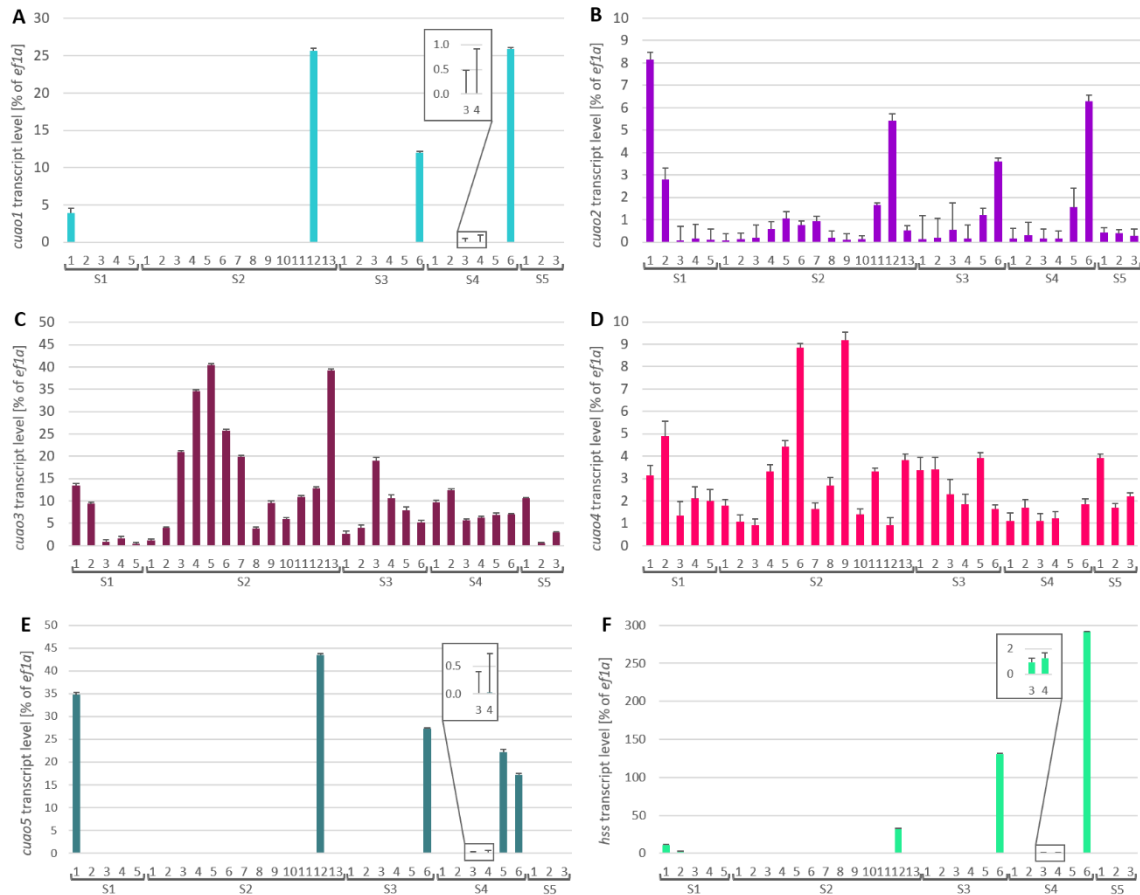
	EcCuAO2	2184	
	EcCuAO3	2313	
	EcCuAO4	2316	
<i>Glycine max</i>	Gm__NM_001250282	2025	NM_001250282/*
	Gm__NM_001250853.2	2301	NM_001250853.2/*
	Gm__XM_003526954	2325	XM_003526954/*
	Gm__XM_003546850	2199	XM_003546850/*
	Gm__XM_003555291	2049	XM_003555291/*
<i>Heliotropium indicum</i>	HiCuAO1	1986	MT597432/Zakaria et al. 2022
	HiCuAO2	2304	MT627598/Zakaria et al. 2022
	HiCuAO3	1980	MT627599/Zakaria et al. 2022
	HiCuAO4	2250	MT627600/Zakaria et al. 2022
	HiCuAO5	1983	MT627601/Zakaria et al. 2022
	LabCuAO1	1953[■]	
	LabCuAO2	1934[■]	
<i>Laburnum x watereri 'Vossii'</i>	LabCuAO3	1269[■]	This study
	LabCuAO4	2102[■]	
	LabCuAO5	1958[■]	
<i>Lotus japonicus</i>	Lj__BABK02012184.1	1322 [■]	Lotus Base*
	Lj__BABK02041915.1	702 [■]	
<i>Lupinus angustifolius</i>	La__XM_019561962.1	2122	XM_019561962.1/*
	La__XM_019568295.1	2036 [■]	XM_019568295.1/*
	La__XM_019583671.1	2036 [■]	XM_019583671.1/*
	La__XM_019595138.1	2015 [■]	XM_019595138.1/*
	La__XM_019599195.1	1648	XM_019599195.1/*
	La__XM_019608353.1	2262	XM_019608353.1/*
<i>Lupinus polyphyllus</i>	LpCuAO1	1977 [■]	Jacky and Ober, unpublished
	LpCuAO2	2009 [■]	
	LpCuAO4	2066 [■]	
	LpCuAO5	2012 [■]	
<i>Nicotiana tabacum</i>	NtCuAO1	2373	DQ873385.1/*
	NtCuAO2	2301	AB289457.1/*
	NtCuAO3	2172	KJ730259.1/*
<i>Pisum sativum</i>	PsCuAO	2025	L39931.1/*
<i>Senecio vernalis</i>	SvCuAO1	2157 [■]	Ober unpublished
	SvCuAO2	2121 [■]	
	SvCuAO3	2175*	
<i>Symphytum officinale</i>	SoCuAO1	2025	Zakaria, Kruse, and Ober, unpublished
	SoCuAO2	2253	
	SoCuAO3	2181	
	SoCuAO4	2169	
	SoCuAO5	2004	

Supplemental Table S3. Sequences of Primers and their expected product size used for RT-qPCR to investigate the co-transcription of five different *cuaos* with *hss* in *Laburnum x watereri* 'Vossii'.

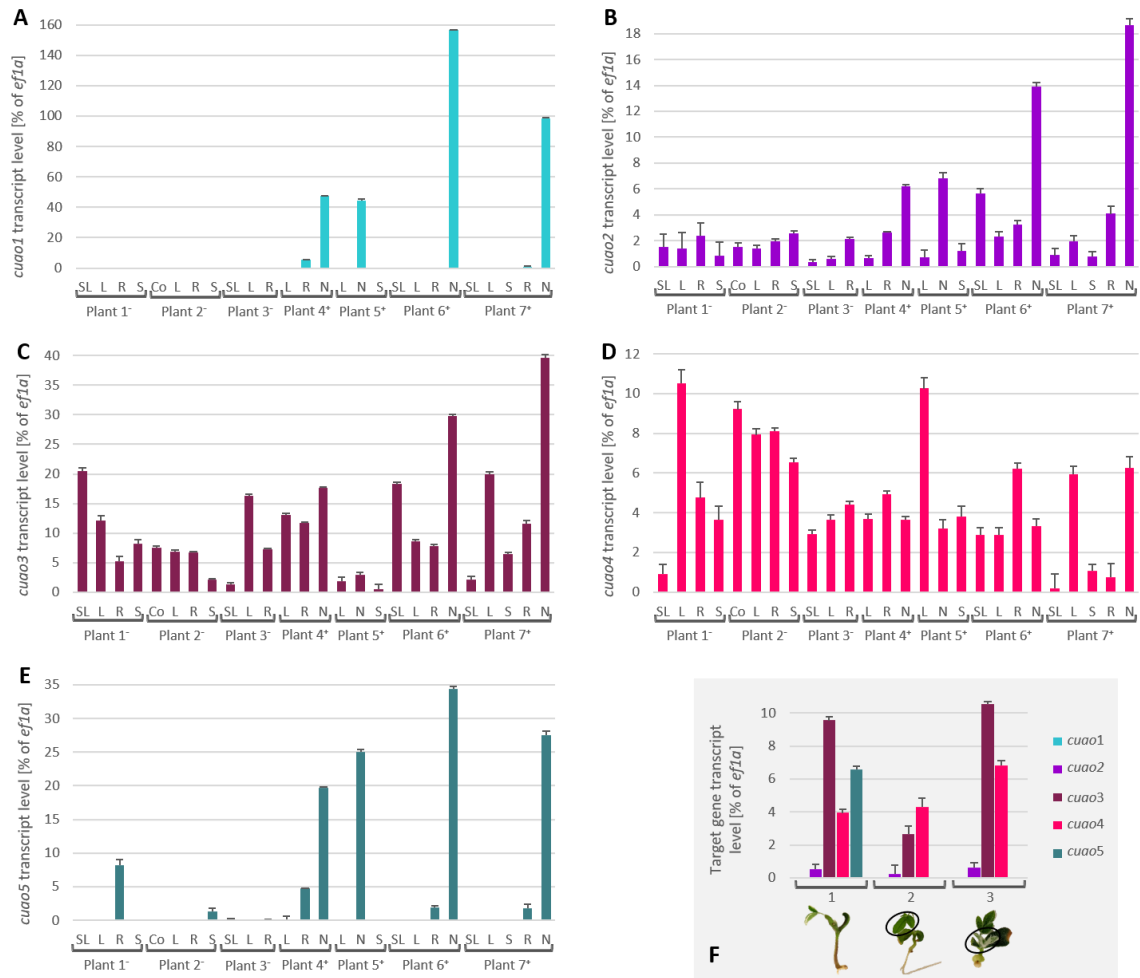
Primer	Gene	Sequence 5' -> 3'	Product size
P1	<i>ubiquitin</i>	NJ_Lab_Ubiq_RT_for	108 bp
P2		NJ_Lab_Ubiq_RT_rev	
P3	<i>ef1a</i>	NJ_Lab_EF1a_RT_for2	132 bp
P4		NJ_Lab_EF1a_RT_rev2	
P5	<i>hss</i>	NJ_Lab_HSS_RT_forA	142 bp
P6		NJ_Lab_HSS_RT_revA	
P7	<i>cua1</i>	NJ_Lab_DAO1_RT_f1	97 bp
P8		NJ_Lab_DAO1_RT_rev1	
P9	<i>cua2</i>	NJ_Lab_DAO2_RT_f1	91 bp
P10		NJ_Lab_DAO2_RT_rev1	
P11	<i>cua3</i>	NJ_Lab_DAO3_RT_f1	104 bp
P12		NJ_Lab_DAO3_RT_rev1	
P13	<i>cua4</i>	NJ_Lab_DAO4_RT_f2	98 bp
P14		NJ_Lab_DAO4_RT_rev2	
P15	<i>cua5</i>	NJ_Lab_DAO5_RT_f1	104 bp
P16		NJ_Lab_DAO5_RT_rev1	



Supplemental Figure S1. Specificity tests of the primers for RT-qPCR analysis in *Laburnum x watereri* 'Vossii'. For the five tested copper depending amine oxidases (CuAOs) each primer pair was tested against the remaining four CuAOs to exclude unspecific binding and implicating a false positive signal. As template different concentrations of plasmids containing one CuAO each was used. **A** Testing primer pair of *cuao1* (P7/P8). **B** Testing primer pair of *cuao2* (P9/P10). **C** Testing primer pair of *cuao3* (P11/P12). **D** Testing primer pair of *cuao4* (P13/P14). **E** Testing primer pair of *cuao5* (P15/P16). PCR was implemented with GoTaq polymerase due to manufacturer protocol and an annealing temperature of 60°C for the primers. Arrowhead indicates expected PCR product size (*cuao1* = 97 bp; *cuao2* = 91 bp; *cuao3* = 104 bp; *cuao4* = 100 bp; *cuao5* = 104 bp). L, ladder (GeneRuler 100 bp Plus DNA Ladder, Thermo Scientific); I, 25 ng of plasmid DNA with the respective gene of interest; II, 10 ng of plasmid DNA with the respective gene of interest; III, 5 ng of plasmid DNA with the respective gene of interest; NC, no-template control.



Supplemental Figure S2. Transcript level of the genes *hss* and *cuao*s 1-5 ($2^{-\Delta CT}$ relative transcript level of the respective target gene in relation to the housekeeping gene *ef1a* [%]) in various tissues (sampled at different seasons every time around 5 p.m.) of *L. x watereri* 'Vossii' grown in the Botanical Garden, Kiel (S1-4) and in Molfsee, Germany (S5). **A** *cuao1* transcript level. **B** *cuao2* transcript level. **C** *cuao3* transcript level. **D** *cuao4* transcript level. **E** *cuao5* transcript level. **F** *hss* transcript level. **S1** (harvested April 25th, 2019): 1 = nodules; 2 = root; 3 = leaf bud; 4 = leaves of flower bud; 5 = young flower. **S2** (harvested May 14th, 2019): 1 = unevolved leaves; 2 = petioles; 3 = leaf; 4 = mature leaf; 5 = petiole; 6 = unripened inflorescence; 7 = green enclosed flowers; 8 = green enclosed flower buds; 9 = single open flower; 10 = petioles; 11 = root; 12 = nodules; 13 = petioles. **S3** (harvested May 27th, 2019): 1 = unevolved leaf; 2 = mature leaf; 3 = mature leaf; 4 = single open flower; 5 = root; 6 = nodules. **S4** (harvested June 27th, 2019): 1 = mature leaves; 2 = mature leaf; 3 = green seedpod; 4 = two green seedpods; 5 = root; 6 = nodules. **S5** (harvested April 10th, 2019): 1 = leaf; 2 = green inflorescence; 3 = leaves. S= sampling; n=1 (tested in three technical replicates).



Supplemental Figure S3. Tissue-specific analysis of $2^{-\Delta CT}$ relative transcript level of the target genes *cuao 1-5* in *L. x watereri* 'Vossii'. Various tissues of *in vitro* grown infected (nodule possessing; +) and non-infected (nodule lacking; -) plants were analyzed by using the housekeeping gene *ef1a* as reference. **A** *cuao1* transcript level. **B** *cuao2* transcript level. **C** *cuao3* transcript level. **D** *cuao4* transcript level. **E** *cuao5* transcript level. **F** Transcript level of displayed target genes in non-infected germ buds. **Plant 1⁻**: 2 months; **Plant 2⁻**: 3 months; **Plant 3⁻**: 7 months; **Plant 4⁺**: 3 months; **Plant 5⁺**: 10 months; **Plant 6⁺**: 11 months; **Plant 7⁺**: 14 months. Co = cotyledons; L = leaf; N = nodule; R = root; S = stem; SL = smaller appearing leaf; 1 = complete germ bud; 2 and 3 = analyzed only black circled leaves; n=1 (tested in three technical replicates).

7.

CONCLUSION AND OUTLOOK

The results obtained from this work add novel knowledge in the fields of pyrrolizidine alkaloid and quinolizidine alkaloid biosynthesis in general and especially within representatives from the legumes (Fabaceae) related to nodulation.

Alkaloids have ever since produced by plants as a defense against herbivores, whereby being produced constantly or after induction of the plant by herbivore attack (Schaller 2008). This can be related to the costs and benefits that these two options entails. Having a constant high level of defense substances means high costs to the plant, especially nitrogen is costly in the case of alkaloids, while with induced defense the cost only is made when attacked. However, in the case of a strong attack, production of effective concentrations could take too long and would thus potentially represent a negative impact on plant survival (Heil and Baldwin 2002; Wittstock and Gershenzon 2002). Another noteworthy aspect is that not all plants might have key advantages due to the constant production of defense molecules. (Purrington 2000) reviewed that plants where less visited by common pollinators when producing abundant defense substrates and this state can

lead sustainable to reduced seed production. A further disadvantage of constant produced substrates is the possibility for specialized herbivores to adapt to the high concentrations of the defense substrates and continue feeding on the plant. For example, specialized insects have been reported to accumulate toxic PAs from the plants to support their own defense by becoming toxic for their own predators (T. Hartmann 1994; Wang et al. 2012). It seems that the alkaloids are constantly present in *Crotalaria spectabilis* (PAs), *Laburnum x watereri 'Vossii'* (PAs & QAs), *Lupinus arboreus* (QAs) and *Lupinus polyphyllus* (QAs). While *C. spectabilis* (chapter A) only produce monocrotaline (PA), *L. arboreus* (QAs) and *L. polyphyllus* (chapter B) usually contain a number of different QAs that have more or less toxic effects on predators. *Laburnum x watereri 'Vossii'* (chapter B and C) even has both, PAs and QAs, which matches with the presumed theory that plants relay not only on one defense mechanism. Understanding the production of defense substrates, whether constantly or induced after attack, seems more complicated and complex (Freeman, B. and Beattie 2008).

The four mentioned species belong to the Fabaceae. It is assumed that these plants only occur nodulated in nature, meaning that they form a symbiosis with atmospheric nitrogen-fixing bacteria. This gives the plants a clear advantage compared to other plant species in terms of the nitrogen required for alkaloid production.

In the past, it was shown that the first pathway-specific enzymes, HSS and LDC of PA-and QA biosynthesis, respectively, can be differently regulated and localized (Anke et al. 2008; Bunsupa et al. 2012a; Niemüller, Reimann, and Ober 2012; Irmer et al. 2015; Kruse et al. 2017). Investigations of LDC in various lupin species have been limited predominantly to leaves, since LDC has been postulated to be a plastid enzyme (Schütte 1969; Wink and Hartmann 1981). To investigate the influence of nodulation on QA biosynthesis (chapter B), tissues of (*L. x watereri 'Vossii'* and *Lupinus arboreus*) of infield and *in vitro* grown plants (*L. x watereri 'Vossii'* and *Lupinus arboreus*) were examined. This revealed that *ldc* is transcribed in all green plant parts, not only in leaves, and independent of nodulation. Furthermore, analytics of nodule-free plants as well as nodulated plants exhibited QAs. Thus, nodulation does not appear to be a determining factor in switching on the QA biosynthesis. The established *in vitro* model system within this work might be helpful to

study further questions under controlled conditions in the connections with nodulation. In literature, the exchange of nitrogen from bacteria to the plant and carbon from the plant to bacteria has been mostly described (White et al. 2007). But, what about further substance exchange possibilities? Or, in what way will the received nitrogen be used (regarding the production of PAs/QAs)? Is it feasible that rhizobia and their host trade more substances than just the above mentioned? The trade of the polyamine homospermidine is at least in *C. spectabilis* excluded (chapter A). *C. spectabilis hss* knockouts do not produce PAs anymore, even though they exhibit a small amount of rhizobia homospermidine in their nodules. Apparently, no transporters exist and thus, the homospermidine produced by rhizobia remain within the infected zone (Figure 5B; chapter C).

To verify the assumed activity of the LDC and the primary counterpart ODC of *L. arboreus* and *L. x watereri 'Vossii'* enzyme, activity assays were performed. Here, both LDCs showed a clearly optimized function towards LDC, in contrast to the described L/ODC of *L. angustifolius* (Bunsupa et al. 2012a). In this way, we were able to establish a new assay that allows substrates and products of PLP depending enzymes to be accurately detected and distinguished from each other (amino acids and polyamines).

This thesis provides the basis for future research questions referring to PA biosynthesis because of the presence of *hss* transcripts in both, a PA producing plant (*L. x watereri 'Vossii'*; chapter C) and a non-PA producing plant (*Cytisus scoparius*; chapter C). For *C. spectabilis*, the nodules have been described as the site of PA biosynthesis, since *hss* transcript has been detected exclusively in nodules and nodule-free plants lacked PAs (Irmer et al. 2015).

We studied the PA mechanism regarding a nodule dependency in *L. x watereri 'Vossii'* (chapter C), a close relative of *Crotalaria* that contains both PAs and QAs. Realtime-PCR analyses (chapter C) showed distinct *hss* transcript in nodules and only minor *hss* transcript in green pods, suggesting a similar mechanism as in *C. spectabilis* and an additionally second site of homospermidine production. The produced HSS antibodies of *C. spectabilis* showed the cells of nodule parenchyma as the site of HSS expression in *C. spectabilis* and *L. x watereri 'Vossii'* nodules. At this point, the PA mechanism of the two plants is still similar, but surprisingly both, the *in vitro* grown infected and non-infected plants of

L. x watereri 'Vossii', contained PAs. This indicates that PA biosynthesis depends not only on nodulation initially as assumed. The knowledge on PAs in *Laburnum spec.* is mainly based on older studies (Neuner-Jehle et al. 1965). Therefore, further analysis with today's capabilities would certainly be informative. Further studies on the enzyme activities of HSS and DHS is an option since the HSS originated from a gene duplication of the primary metabolic enzyme DHS (Hartmann and Ober 2000; Ober and Kaltenegger 2009). The DHS in *L. x watereri* 'Vossii' could possibly have a significantly higher side activity of homospermidine formation than other species and thus catalyze the production of PAs sufficiently. The DHS of a non-related species *Ipomoea alba* showed HSS activity (Prakashrao et al. 2022). In *L. x watereri* 'Vossii' *dhs* transcript was shown via RT-qPCR analyses to be present in all tested tissues and could provide according to that homospermidine for PA production. Excluding other homospermidine producing enzymes that might be involved in PA biosynthesis, would be provided by generating *hss* knockout mutants via genome editing with CRISPR/Cas9, which will then be tested for the presence of PAs via GC-MS. Furthermore, within this study, we were able to detect a PA that could not be assigned to a previously described PA based on its RI, mass and fragment pattern. Thus, a structural elucidation could possibly shed light on this.

To gain a better understanding of the evolution of HSS in general and specifically in the Fabaceae, three other relatives (*Cytisus scoparius*, *Spartium junceum* and *Ulex europaeus*) representing QA and not PA producers were examined (chapter C). All three species have an HSS copy on gDNA level and surprisingly, only for *C. scoparius* we detected *hss* transcripts in the nodules. Detecting *hss* transcript does not secure the production of a functioning protein. Production of HSS antibodies from *C. scoparius* for immunolocalization within nodules will give a clear answer. In the case that HSS protein is detectable in *C. scoparius* nodules, the question arises, which other function HSS might have than the involvement in PA biosynthesis.

The occurrence of *hss* transcript in a non-PA producing plant (chapter C) shows once more that the first step is important but further enzymes have to be involved to produce a complete PA. However, little progress has been made in recent years on other enzymes involved in PA biosynthesis. In chapter A and chapter D, we used *C. spectabilis* and

L. x watereri 'Vossii' as object for further research in this field. CuAOs have been postulated as potential enzymes involved in the PA pathway for a long time. In this study, it was possible to identify five CuAOs for both species. Further experiments on *C. spectabilis* showed, that two of them, CsCuAO1 and CsCuAO5, are exclusively co-transcribed with the HSS in nodules. Using CRISPR/Cas9 and establishing a protocol to generate transgenic plants, the involvement of the enzymes CsCuAO1 and CsCuAO5 in PA biosynthesis could be identified due to the received and tested knockout mutants.

The tested plants showed different mutations and were PA free. Furthermore, the polyamine content of homospermidine was measured, showing that only CsCuAO5-KO mutants accumulate homospermidine. It is very likely that this enzyme accepts homospermidine as a substrate and the resulting product, *N*-(4-aminobutyl)pyrrolinium ion, which stagnates at CsCuAO1-KO mutants, in turn serves as a substrate for CsCuAO1. To date, this finding has never been considered or described before, because it was assumed that a CuAO accepts homospermidine and directly generates a bicyclic in one step and not in two steps as shown here for *C. spectabilis*. To prove this assumption, heterologous expression and characterization of the activity of the enzymes, CsCuAO5 and CsCuAO1, should be tested in further experiments. For *in planta* expression, constructs have been already cloned. Further experiments include the tissue-specific localization of CsCuAO5 and CsCuAO1 in comparison to the expression pattern and the cell-type with HSS. Heterologously expressed and purified protein can serve for the production of polyclonal antibodies. Already prepared thin sections of embedded nodules, where CsHSS protein was detectable within the nodule parenchyma cells (chapter D), can be used.

While the first step in PA biosynthesis, the production of homospermidine via HSS, seems to be consistent in all species studied so far, the second step, however, varies and seems to be individual for each species. Just recently, in *Heliotropium indicum*, an HSO catalyzing homospermidine to 1-formylpyrrolizidine (bicyclic) was identified as the second step in PA biosynthesis (Zakaria et al. 2022). The already uncovered two different mechanisms of formation of the bicyclic PA backbone in *C. spectabilis* and *H. indicum* suggest how variable, individual and complex the PA biosynthesis may be in distinct species.

Early and late steps of PA synthesis in *C. spectabilis* are suggested to take part in different organs of the plant, since feeding experiments with detached nodules (without plant)

ended with the detection of only the free necine base trachelanthamidine and lacking the completed PA monocrotaline (chapter A). Irmer et al. (2015) however, showed that monocrotaline had the highest in concentration per dry weight in nodules and suggested a PA dependency on nodules. Those nodules were still attached to the plant before analyses, speculating that the free necine base have been transported to a different organ for completing the PA monocrotaline. The finished PA monocrotaline was then most likely transported back to the nodules. To test the ability of synthesizing monocrotaline with the help of other tissues than the nodules, a feeding experiment with nodules that are still attached to the plant can be carried out. A better understanding how this pathway works could help to use PA containing plants that also serve as medicinal plants, e.g. *Symphytum* and *Petasites* (Salehi et al. 2019; Borlak et al. 2022), more efficient and with less safety concern. New and simpler possibilities to remove PAs successfully might be discovered.

This valuable new data within this thesis provides many aspects for further research within these two pathways and is a strong encouragement to attempt to identify other candidate genes. Similar experiments based on CRISPR/Cas9 approaches can be used to test further possibly candidate genes for their involvement in certain PA or even QA biosynthesis steps. Additionally, biochemical analyses might confirm the involvement of postulated enzymes, when knockout plants are alkaloid free.

8. CONTRIBUTIONS

The presented study in **CHAPTER A** was designed by **Nadine Jacky**, Mahmoud M. Zakaria, and Dietrich Ober. **Nadine Jacky** did the sampling and the RT-qPCR analysis as well designing the CRISPR/Cas9 constructs with the selected protospacer sequences that conducted as target sites within each candidate gene (*cscuao1* and *cscuao5*). Anna-Lena Sprick carried out cloning the CRISPR/Cas9 constructs for the two CsCuAOs and established the stable transformation of *C. spectabilis* during her Master thesis under the guidance of **Nadine Jacky** and Britta Milewski. Knockout mutants for CsCuAO1 and CsCuAO5 were created by **Nadine Jacky**. Anna-Lena Sprick and Britta Milewski obtained by an independent CRISPR/Cas9 approach knockout mutants for the gene encoding CsHSS that have been investigated in this study. PCR screening of transgenic plants for mutations of the genes encoding CsCuAO1 and CsCuAO5 were done by **Nadine Jacky** with the assistance of Brigitte Schemmerling. PA analytics for possible knockouts was done by **Nadine Jacky**. Plant *in vitro* culturing of transformed *C. spectabilis* was done by **Nadine Jacky** and Brigitte Schemmerling. Further GC-MS and HPLC analytics were implemented by **Nadine Jacky** and Mahmoud M. Zakaria. Feeding experiments and structure elucidation were carried out by Mahmoud M. Zakaria. The manuscript was written by **Nadine Jacky**, Mahmoud M. Zakaria

and Dietrich Ober. The prepared figures are created by **Nadine Jacky** and Mahmoud M. Zakaria and attributable to the respective experimenter.

The study described in **CHAPTER B** was designed by **Nadine Jacky**, Elisabeth Kaltenegger, and Dietrich Ober. Rhizobia isolation, culture optimizing of nodulated and non-nodulated *in vitro* grown plants, sequence identifications, RT-qPCR analyses, GC-MS analyses as well as cloning of the LDC and ODC expression constructs were done by **Nadine Jacky**. Brigitte Schemmerling performed heterologous protein expression, and Sebastian Fritz assisted by isolating the RNAs from the investigated tissues for the above-mentioned RT-qPCR analyses in this study. Phylogenetic tree calculation was done by Elisabeth Kaltenegger. The enzyme assays for LDC and ODC activities were established by **Nadine Jacky** and Elisabeth Kaltenegger. The data of the assays were analyzed and interpreted by Elisabeth Kaltenegger and **Nadine Jacky**. **Nadine Jacky**, Elisabeth Kaltenegger, and Dietrich Ober discussed the data. **Nadine Jacky** prepared the figures and wrote the final version of the manuscript together with Elisabeth Kaltenegger and Dietrich Ober. Dietrich Ober commented on the manuscript.

The study of **CHAPTER C** was designed by **Nadine Jacky**, Elisabeth Kaltenegger, and Dietrich Ober. Experiments were done by **Nadine Jacky** and results were discussed by **Nadine Jacky** and Dietrich Ober. The illustration of the HSS immunolocalization in sections of *L. x watereri* 'Vossii' was prepared by Linnea Rule during her Bachelor thesis under the guidance of **Nadine Jacky**. RNA isolation of the same used tissues for RT-qPCR analyses, as mentioned above in the contributions for Chapter B, were done with the help of Sebastian Fritz. PA analytics and interpretation of these results were done by Elisabeth Kaltenegger. Susanne Klocke assisted PA analytics by extracting the PAs from the samples. Figures were prepared by **Nadine Jacky** who also wrote the manuscript. Dietrich Ober commented on the manuscript.

The study of the miscellaneous **CHAPTER D** was designed by **Nadine Jacky** and Dietrich Ober. **Nadine Jacky** carried out the experiments using RNA preparations of Sebastian Fritz for RT-qPCR experiments. **Nadine Jacky** prepared the figures and wrote the draft. Dietrich Ober commented on the manuscript.

LIST OF ABBREVIATIONS

1-cbp	1-(carboxybutyl)pyrrolidine
1-mcbp	Methyl ester of 1-(carboxybutyl)pyrrolidine
2,4-D	2,4-Dichlorophenoxyacetic acid
3'	3' end of cDNA
5'	5' end of cDNA
16S	16S rRNA gene
°C	Degree Celsius
%	Percent
% (m/v)	Mass/Volume percent
% (v/v)	Volume percent
<i>A. tumefaciens</i>	<i>Agrobacterium tumefaciens</i>
ACT	Gene encoding actin
bp	Base pairs
BSA	Bovine serum albumin
<i>B. JAPAN</i>	<i>Bradyrhizobium</i> strain 'JAPAN'
c	Concentration
Cad	Cadavarine
Cas9	CRISPR-associated endonuclease and ribonucleoprotein
cDNA	Complementary DNA
CL	Control line

<i>C. scoparius</i>	<i>Cytisus scoparius</i>
<i>C. spectabilis</i>	<i>Crotalaria spectabilis</i>
Cs	<i>Crotalaria spectabilis</i>
CRISPR	Clustered regularly interspaced short palindromic repeats
<i>cuao</i>	Gene encoding copper amine-dependent oxidase
CuAO	Protein copper amine-dependent oxidase
DAH	Diaminoheptane
Del.	Deletion
<i>dhs</i>	Gene encoding deoxyhypusine synthase
DHS	Protein deoxyhypusine synthase
DNA	Deoxyribonucleic acid
dNTPs	Deoxynucleoside triphosphate
DW	Dry weight
<i>E. coli</i>	<i>Escherichia coli</i>
EF1a	Elongation factor 1-alpha
<i>ef1a</i>	Gene encoding elongation factor 1-alpha
eIF5A	Eukaryotic initiation factor 5A
eIF5A(Dhp)	Deoxyhypusine eIF5A – intermediate
eIF5A(Lys)	Lysine containing eIF5A – precursor
eIF5A(Hyp)	Hypusine containing eIF5A
Fmoc	Fluorenylmethoxycarbonyl (-protecting group)
FW	Fresh weight
GABA	γ -aminobutyric acid
gDNA	Genomic DNA
GC-MS	Gas chromatography – mass spectrometry
GC-TIC	Gas chromatography – total ion chromatogram
H ₂ O ₂	Hydrogen peroxide
H ₂ SO ₄	Sulfuric acid
HCL	Hydrogen chloride
<i>H. indicum</i>	<i>Heliotropium indicum</i>
HIS-taq	Polyhistidine-taq

HPLC	High pressure liquid chromatography
<i>hss</i>	Gene encoding homospermidine synthase
HSS	Protein homospermidine synthase
HSO	Protein homospermidine oxidase
Hspd	Homospermidine
infected	nodule possessing plants
Ins.	Insertion
IPTG	Isopropyl- β -thiogalactopyranoside
IS/ ISTD	Internal standard
<i>in vivo</i>	carried out in the living organism
<i>in vitro</i>	carried out in the test tube
kDA	Kilodalton
KO	Knockout
<i>Lawa</i>	<i>Laburnum x watereri</i> , Vossii'
<i>Luar</i>	<i>Lupinus arboreus</i>
<i>Lupo</i>	<i>Lupinus polyphyllus</i>
<i>L. alpinum</i>	<i>Laburnum alpinum</i>
<i>L. anagyroides</i>	<i>Laburnum anagyroides</i>
<i>L. arboreus</i>	<i>Lupinus arboreus</i>
<i>L. polyphyllus</i>	<i>Lupinus polyphyllus</i>
<i>L. x watereri</i> , Vossii'	<i>Laburnum x watereri</i> , Vossii'
LCO	Lipochoitoligosaccharide
<i>ldc</i>	Gene encoding lysine decarboxylase
LDC	Protein lysine decarboxylase
MOPS	3-(<i>N</i> -morpholino)propanesulfonic acid
mRNA	Messenger RNA
MSTFA	<i>N</i> -methyl- <i>N</i> -(trimethylsilyl)trifluoroacetamide
MS20	Murashige and Skoog medium
N	Nitrogen
NaOH	Sodium hydroxide
NC	No-template control

NCBI	National Center for Biotechnology Information
NE	No effect
NH ₄ NO ₃	Ammonium nitrate
NOD medium	Nodulation medium
Nod factors	Nodulation factors
<i>nod</i>	Nodulation gene
non-infected	plants without nodules
nt	Nukleotide
<i>odc</i>	Gene encoding ornithine decarboxylase
ODC	Protein ornithine decarboxylase
ORF	Open reading frame
PA	Pyrrolizidine alkaloid
PAM	Protospacer adjacent motif
PBS	Phosphate-buffered saline
PC	Positive control
PCR	Polymerase chain reaction
pH	Capability of hydrogen
PLP	Pyridoxal-5'-phosphate
Put	Putrescine
p.m.	Post meridiem
QA	Quinolizidine alkaloid
RACE	Rapid amplification of cDNA-ends
RI	Kovat's retention index
RNA	Ribonucleic acid
RNase	Ribonuclease
rpm	Rounds per minute
rRNA	Ribosomal RNA
RT	Retention time
RT-qPCR	Reverse transcription quantitative polymerase chain reaction
SDS-PAGE	Sodium dodecyl sulfate – polyacrylamide gel electrophoresis
sgRNA	Single guide RNA

SIC	Single ion chromatogram
<i>S. junceum</i>	<i>Spartium junceum</i>
<i>S. officinale</i>	<i>Symphytum officinale</i>
Spd	Spermidine
Spm	Spermine
SRA	Sequence read archive
Sub.	Substitution
TMS	Trimethylsilyl
TRis/HCL	Tris(hydroxymethyl)aminomethane/hydrochloride
<i>ubiq</i>	Gene encoding ubiquitin
UBQ	Protein ubiquitin
<i>U. europaeus</i>	<i>Ulex europaeus</i>
UTR	Untranslated region
WT	Wild type
YEB	Yeast extract beef

One letter code for nucleic acids:

A	Adenine	C	Cytosine
T	Thymine	G	Guanine
R (purine)	A or G	S (strong)	G or C
Y (pyrimidine)	T or C	W (weak)	A or T
M (amino)	A or C	K (keto)	G or T
H	not G	B	not A
D	not C	V	not T
N (any base)	A or C or G or T		

One-letter/ three-letter code for amino acids:

A / Ala	Alanine	M / Met	Methionine
C / Cys	Cysteine	N / Asn	Asparagine
D / Asp	Aspartic acid	P / Pro	Proline
E / Glu	Glutamate	Q / Gln	Glutamine
F / Phe	Phenylalanine	R / Arg	Arginine
G / Gly	Glycine	S / Ser	Serine
H / His	Histidine	T / Thr	Threonine
I / Ile	Isoleucine	V / Val	Valine
K / Lys	Lysine	W / Trp	Tryptophan
L / Leu	Leucine	Y / Tyr	Tyrosine

Genetic code (degenerate):

1 st position (5' end)	2 nd position				3 rd position (3' end)
	T	C	A	G	
T	TTT Phe	TCT Ser	TAT Tyr	TGT Cys	T
	TTC	TCC	TAC	TGC	C
	TTA Leu	TCA	TAA Stop	TGA Stop	A
	TTG	TCG	TAG Stop	TGG Trp	G
C	CTT Leu	CCT Pro	CAT His	CGT Arg	T
	CTC	CCC	CAC	CGC	C
	CTA	CCA	CAA Gln	CGA	A
	CTG	CCG	CAG	CGG	G
A	ATT Ile	ACT Thr	AAT Asn	AGT Ser	T
	ATC	ACC	AAC	AGC	C
	ATA	ACA	AAA Lys	AGA Arg	A
	ATG Met*	ACG	AAG	AGG	G
G	GTT Val	GCT Ala	GAT Asp	GGT Gly	T
	GTC	GCC	GAC	GGC	C
	GTA	GCA	GAA Glu	GGA	A
	GTG	GCG	GAG	GGG	G

Tab. Genetic code (degenerate): yellow, unpolare/hydrophobic amino acid residues; blue, alkaline amino acid residues; red, aspartic acid amino acid residues; purple, polar/neutral amino acid residues; green, unpolare amino acid = Start codon; white, triplet amino acids = Stop codon.

REFERENCES

- Abraham, Eleni M, Ioannis Ganopoulos, Panagiotis Madesis, Athanasios Mavromatis, Photini Mylona, Irini Nianiou-Obeidat, Zoi Parissi, Alexios Polidoros, Eleni Tani, and Dimitrios Vlachostergios. 2019. "The Use of Lupin as a Source of Protein in Animal Feeding: Genomic Tools and Breeding Approaches." *Int. J. Mol. Sci.*, 27.
- Aïnouche, A., R. J. Bayer, P. Cubas, and Marie-Thérèse Misset. 2003. "Phylogemetoc relationships within tribe genisteae (Papiliondeae) with special reference to genus *Ulex*." *Advances in Legume Systematics, Part 10, Higher Level Systematics Royal Botanic Gardens, Kew.*, 239–52.
- Albrecht, C. 1999. "Legume Nodulation and Mycorrhizae Formation; Twoextremes in Host Specificity Meet." *The EMBO Journal* 18 (2): 281–88. <https://doi.org/10.1093/emboj/18.2.281>.
- Almagro Armenteros, Jose Juan, Marco Salvatore, Olof Emanuelsson, Ole Winther, Gunnar von Heijne, Arne Elofsson, and Henrik Nielsen. 2019a. "Detecting Sequence Signals in Targeting Peptides Using Deep Learning." *Life Science Alliance* 2 (5): e201900429. <https://doi.org/10.26508/lsa.201900429>.
- Almagro Armenteros, José Juan, Konstantinos D. Tsirigos, Casper Kaae Sønderby, Thomas Nordahl Petersen, Ole Winther, Søren Brunak, Gunnar von Heijne, and Henrik Nielsen. 2019b. "SignalP 5.0 Improves Signal Peptide Predictions Using Deep Neural Networks." *Nature Biotechnology* 37 (4): 420–23. <https://doi.org/10.1038/s41587-019-0036-z>.
- Aniszewski, Tadeusz. 2007. *Alkaloids - Secrets of Life: Alkaloid Chemistry, Biological Significance, Applications and Ecological Role*. Elsevier.
- Anjos, Bruno Leite, Verônica M.T. Nobre, Antônio F.M. Dantas, Rosane M.T. Medeiros, Temístocles S. Oliveira Neto, Russell J. Molyneux, and Franklin Riet-Correa. 2010. "Poisoning of Sheep by Seeds of *Crotalaria retusa*: Acquired Resistance by Continuous Administration of Low Doses." *Toxicon* 55 (1): 28–32. <https://doi.org/10.1016/j.toxicon.2009.06.028>.
- Anke, Sven, Daniela Gondé, Elisabeth Kaltenegger, Robert Hänsch, Claudine Theuring, and Dietrich Ober. 2008. "Pyrrolizidine Alkaloid Biosynthesis in Phalaenopsis Orchids: Developmental Expression of Alkaloid-Specific Homospermidine Synthase in Root Tips and Young Flower Buds." *Plant Physiology* 148 (2): 751–60.
- Anke, Sven, Daniel Niemüller, Stefanie Moll, Robert Hänsch, and Dietrich Ober. 2004. "Polyphyletic Origin of Pyrrolizidine Alkaloids within the Asteraceae. Evidence from Differential Tissue Expression of Homospermidine Synthase." *Plant Physiology* 136 (4): 4037–47.
- Baldwin, Ian T., Eric A. Schmelz, and Thomas E. Ohnmeiss. 1994. "Wound-Induced Changes in Root and Shoot Jasmonic Acid Pools Correlate with Induced Nicotine Synthesis in *Nicotiana glauca* Spegazzini and Comes." *Journal of Chemical Ecology* 20 (8): 2139–57. <https://doi.org/10.1007/BF02066250>.
- Barbulova, Ani, and Maurizio Chiurazzi. 2005. "A Procedure for in Vitro Nodulation Studies." In *Lotus Japonicus Handbook*, edited by Antonio J. Márquez, 83–86. Berlin/Heidelberg: Springer-Verlag. https://doi.org/10.1007/1-4020-3735-X_5.

- Becerra-Rivera, Victor A, and Michael F Dunn. 2019. "Polyamine Biosynthesis and Biological Roles in Rhizobia." *FEMS Microbiology Letters* 366 (7): fnz084. <https://doi.org/10.1093/femsle/fnz084>.
- Bergersen, Fj, and Dj Goodchild. 1973. "Cellular Location and Concentration of Leghaemoglobin in Soybean Root Nodules." *Australian Journal of Biological Sciences* 26 (4): 741. <https://doi.org/10.1071/B19730741>.
- Beringer, J. E. 1974. "R Factor Transfer in *Rhizobium leguminosarum*." *Microbiology* 84 (1): 188–98. <https://doi.org/10.1099/00221287-84-1-188>.
- Bond, Lora. 1948. "Origin and Development Morphology of Root Nodules of *Pisum sativum*." *Botanical Gazette* 109 (4): 411–34. <https://doi.org/10.1086/335494>.
- Borlak, Jürgen, Hans-Christoph Diener, Johanna Kleeberg-Hartmann, Karl Messlinger, and Stephen Silberstein. 2022. "Petasites for Migraine Prevention: New Data on Mode of Action, Pharmacology and Safety. A Narrative Review." *Frontiers in Neurology* 13 (April): 864689. <https://doi.org/10.3389/fneur.2022.864689>.
- Botha, Christo J., Alex Lewis, Elizabeth C. du Plessis, Sarah J. Clift, and Mark C. Williams. 2012. "Crotalariaiosis equorum ('Jaagsiekte') in Horses in Southern Mozambique, a Rare Form of Pyrrolizidine Alkaloid Poisoning." *Journal of Veterinary Diagnostic Investigation* 24 (6): 1099–1104. <https://doi.org/10.1177/1040638712460673>.
- Böttcher, Frank, Ralf-Dieter Adolph, and Thomas Hartmann. 1993. "Homospermidine Synthase, the First Pathway-Specific Enzyme in Pyrrolizidine Alkaloid Biosynthesis." *Phytochemistry* 32 (3): 679–89.
- Bouchereau, A, A Aziz, F Larher, and J Martin-Tanguy. 1999. "Polyamines and Environmental Challenges: Recent Development." *Plant Science* 140 (2): 103–25. [https://doi.org/10.1016/S0168-9452\(98\)00218-0](https://doi.org/10.1016/S0168-9452(98)00218-0).
- Bradford, M. M. 1976. "A Rapid and Sensitive Method for the Quantitation of Microgram Quantities of Protein Utilizing the Principle of Protein-Dye Binding." *Analytical Biochemistry* 72 (May): 248–54. <https://doi.org/10.1006/abio.1976.9999>.
- Brear, Ella M., David A. Day, and Penelope M. C. Smith. 2013. "Iron: An Essential Micronutrient for the Legume-Rhizobium Symbiosis." *Frontiers in Plant Science* 4. <https://doi.org/10.3389/fpls.2013.00359>.
- Bromfield, E. S. P., and J. V. D. K Kumar Rao. 1983. "Studies on Fast and Slow Growing *Rhizobium* spp. Nodulating *Cajanus cajan* and *Cicer arietinum*," no. 102: 485–93.
- Bunsupa, Somnuk, Kousuke Hanada, Akira Maruyama, Kaori Aoyagi, Kana Komatsu, Hideki Ueno, Madoka Yamashita. 2016. "Molecular Evolution and Functional Characterization of a Bifunctional Decarboxylase Involved in Lycopodium Alkaloid Biosynthesis." *Plant Physiology* 171 (4): 2432–44. <https://doi.org/10.1104/pp.16.00639>.
- Bunsupa, Somnuk, Kae Katayama, Emi Ikeura, Akira Oikawa, Kiminori Toyooka, Kazuki Saito, and Mami Yamazaki. 2012a. "Lysine Decarboxylase Catalyzes the First Step of Quinolizidine Alkaloid Biosynthesis and Coevolved with Alkaloid Production in Leguminosae." *The Plant Cell* 24 (3): 1202–16. <https://doi.org/10.1105/tpc.112.095885>.
- Bunsupa, Somnuk, Mami Yamazaki, and Kazuki Saito. 2012b. "Quinolizidine Alkaloid Biosynthesis: Recent Advances and Future Prospects." *Frontiers in Plant Science* 3. <https://doi.org/10.3389/fpls.2012.00239>.
- Callaham, Dale A. and Torrey, John G. 1981. "The Structural Basis for Infection of Root Hairs of *Trifolium repens* by *Rhizobium*," no. 59: 1647–64.

- Cardoso, D., R.T. Pennington, L.P. de Queiroz, J.S. Boatwright, B.-E. Van Wyk, M.F. Wojciechowski, and M. Lavin. 2013. "Reconstructing the Deep-Branching Relationships of the Papilionoid Legumes." *South African Journal of Botany* 89 (November): 58–75. <https://doi.org/10.1016/j.sajb.2013.05.001>.
- Cardoso, Domingos, Luciano P. de Queiroz, R. Toby Pennington, Haroldo C. de Lima, Émile Fonty, Martin F. Wojciechowski, and Matt Lavin. 2012. "Revisiting the Phylogeny of Papilionoid Legumes: New Insights from Comprehensively Sampled Early-Branching Lineages." *American Journal of Botany* 99 (12): 1991–2013. <https://doi.org/10.3732/ajb.1200380>.
- Chang, Antje, and Thomas Hartmann. 1998. "Solubilization and Characterization of a Senecionine N-Oxygenase from *Crotalaria scassellatii* Seedlings." *Phytochemistry* 49 (7): 1859–66. [https://doi.org/10.1016/S0031-9422\(98\)00396-3](https://doi.org/10.1016/S0031-9422(98)00396-3).
- Conant, Gavin C., and Kenneth H. Wolfe. 2008. "Turning a Hobby into a Job: How Duplicated Genes Find New Functions." *Nature Reviews Genetics* 9 (12): 938–50. <https://doi.org/10.1038/nrg2482>.
- Corby, H.D.L. 1988. "Types of rhizobial nodules and their distribution among the leguminosae." JSTOR; Kirka (Vol. 13, No. 1): 53-123 (72 pages).
- De Meyer, Sofie E., Koenraad Van Hoorde, Bram Vekeman, Tamara Braeckman, and Anne Willems. 2011. "Genetic Diversity of Rhizobia Associated with Indigenous Legumes in Different Regions of Flanders (Belgium)." *Soil Biology and Biochemistry* 43 (12): 2384–96. <https://doi.org/10.1016/j.soilbio.2011.08.005>.
- Douglas, A E. 1998. "Host Benefit and the Evolution of Specialization in Symbiosis." *Heredity* 81 (6): 599–603. <https://doi.org/10.1046/j.1365-2540.1998.00455.x>.
- Downie, J Allan, and Simon A Walker. 1999. "Plant Responses to Nodulation Factors." *Current Opinion in Plant Biology* 2 (6): 483–89. [https://doi.org/10.1016/S1369-5266\(99\)00018-7](https://doi.org/10.1016/S1369-5266(99)00018-7).
- Edgar, R. C. 2004. "MUSCLE: Multiple Sequence Alignment with High Accuracy and High Throughput." *Nucleic Acids Research* 32 (5): 1792–97. <https://doi.org/10.1093/nar/gkh340>.
- Eisner, T, and J Meinwald. 1995. "The Chemistry of Sexual Selection." *Proceedings of the National Academy of Sciences* 92 (1): 50–55. <https://doi.org/10.1073/pnas.92.1.50>.
- Elma, Fatmanur, Hüseyin ÇetiN, Mustafa Yorgancilar, and Ramazan Acar. 2021. "Metabolite Content of Local Bitter White Lupin Seeds (*Lupinus albus* L.) and Acaricidal and Insecticidal Effects of Its Seed Extract." *Tarım Bilimleri Dergisi*, December. <https://doi.org/10.15832/ankutbd.622123>.
- Erb, Matthias, and Daniel J. Kliebenstein. 2020. "Plant Secondary Metabolites as Defenses, Regulators, and Primary Metabolites: The Blurred Functional Trichotomy." *Plant Physiology* 184 (1): 39–52. <https://doi.org/10.1104/pp.20.00433>.
- Feitoza, Rodrigo B.B., and Helena R.P. Lima. 2021. "Chemosystematic and Evolutionary Trends of the Genistoid Clade Ssensu Stricto (Papilionoideae, Fabaceae)." *Phytochemistry* 183 (March): 112616. <https://doi.org/10.1016/j.phytochem.2020.112616>.
- Ferguson, Brett J., Arief Indrasumunar, Satomi Hayashi, Meng-Han Lin, Yu-Hsiang Lin, Dugald E. Reid, and Peter M. Gresshoff. 2010. "Molecular Analysis of Legume Nodule Development and Autoregulation." *Journal of Integrative Plant Biology* 52 (1): 61–76. <https://doi.org/10.1111/j.1744-7909.2010.00899.x>.

- Fisher, Robert F., and Sharon R. Long. 1992. "Rhizobium–Plant Signal Exchange." *Nature* 357 (6380): 655–60. <https://doi.org/10.1038/357655a0>.
- Fletcher, Mary T., Ross A. McKenzie, Barry J. Blaney, and Keith G. Reichmann. 2009. "Pyrrolizidine Alkaloids in *Crotalaria* Taxa from Northern Australia: Risk to Grazing Livestock." *Journal of Agricultural and Food Chemistry* 57 (1): 311–19. <https://doi.org/10.1021/jf8026099>.
- Freeman, B., and G. Beattie. 2008. "An Overview of Plant Defenses against Pathogens and Herbivores." *The Plant Health Instructor*. <https://doi.org/10.1094/PHI-I-2008-0226-01>.
- Frei, Hansjörg, Jürg Lüthy, Julia Brauchli, Ulrich Zweifel, Friedrich E. Würigler, and Christian Schlatter. 1992. "Structure/Activity Relationships of the Genotoxic Potencies of Sixteen Pyrrolizidine Alkaloids Assayed for the Induction of Somatic Mutation and Recombination in Wing Cells of *Drosophila melanogaster*." *Chemico-Biological Interactions* 83 (1): 1–22. [https://doi.org/10.1016/0009-2797\(92\)90088-3](https://doi.org/10.1016/0009-2797(92)90088-3).
- Frick, Karen M., Lars G. Kamphuis, Kadambot H. M. Siddique, Karam B. Singh, and Rhonda C. Foley. 2017. "Quinolizidine Alkaloid Biosynthesis in Lupins and Prospects for Grain Quality Improvement." *Frontiers in Plant Science* 8 (January). <https://doi.org/10.3389/fpls.2017.00087>.
- Frölich, Cordula, Dietrich Ober, and Thomas Hartmann. 2007. "Tissue Distribution, Core Biosynthesis and Diversification of Pyrrolizidine Alkaloids of the Lycopsamine Type in Three Boraginaceae Species." *Phytochemistry* 68 (7): 1026–37. <https://doi.org/10.1016/j.phytochem.2007.01.002>.
- Fu, Peter P., Qingsu Xia, Ge Lin, and Ming W. Chou. 2004. "Pyrrolizidine Alkaloids—Genotoxicity, Metabolism Enzymes, Metabolic Activation, and Mechanisms." *Drug Metabolism Reviews* 36 (1): 1–55. <https://doi.org/10.1081/DMR-120028426>.
- Fuell, Christine, Katherine A. Elliott, Colin C. Hanfrey, Marina Franceschetti, and Anthony J. Michael. 2010. "Polyamine Biosynthetic Diversity in Plants and Algae." *Plant Physiology and Biochemistry* 48 (7): 513–20. <https://doi.org/10.1016/j.plaphy.2010.02.008>.
- Fujihara, Shinsuke. 2009. "Biogenic Amines in Rhizobia and Legume Root Nodules." *Microbes and Environments* 24 (1): 1–13. <https://doi.org/10.1264/jsme2.ME08557>.
- Fujihara, Shinsuke, Hiroto Abe, Yasuo Minakawa, Shoichiro Akao, and Tadakatsu Yoneyama. 1994. "Polyamines in Nodules from Various Plant-Microbe Symbiotic Associations." *Plant and Cell Physiology* 35 (8): 1127–34. <https://doi.org/10.1093/oxfordjournals.pcp.a078705>.
- Furbank, Robert T., and John E. Lunn. 1997. "Localisation of Sucrose-Phosphate Synthase and Starch in Leaves of C 4 Plants." *Planta* 202 (1): 106–11. <https://doi.org/10.1007/s004250050108>.
- Gage, Daniel J. 2004. "Infection and Invasion of Roots by Symbiotic, Nitrogen-Fixing Rhizobia during Nodulation of Temperate Legumes." *Microbiology and Molecular Biology Reviews* 68 (2): 280–300. <https://doi.org/10.1128/MMBR.68.2.280-300.2004>.
- Gaines, Dennis W., Leonard Friedman, and Peter P. McCann. 1988. "Apparent Ornithine Decarboxylase Activity, Measured by ¹⁴CO₂ Trapping, after Frozen Storage of Rat Tissue and Rat Tissue Supernatants." *Analytical Biochemistry* 174 (1): 88–96. [https://doi.org/10.1016/0003-2697\(88\)90522-2](https://doi.org/10.1016/0003-2697(88)90522-2).

- Galinovsky, F., H. Goldberger, and M. Pöhm. 1949. "Über Das Laburnin, Ein Alkaloid Aus *Cytisus laburnum*." *Monatshefte Für Chemie Und Verwandte Teile Anderer Wissenschaften*, no. 80: 550–54.
- Gamo, T, A. Itoh, A. Sawazaki, I. J. Manguiat, and D. M. Mendoza. 1991. "Rhizobia Collected from Leguminous Plants in the Philippines." *Rhizobia Collected from Leguminous Plants in the Philippines*, no. 6: 111–29.
- Gerdes, Hans Joachim, and Eckhard Leistner. 1979. "Stereochemistry of Reactions Catalysed by L-Lysine Decarboxylase and Diamine Oxidase." *Phytochemistry* 18 (5): 771–75. [https://doi.org/10.1016/0031-9422\(79\)80011-4](https://doi.org/10.1016/0031-9422(79)80011-4).
- Graham, Peter H., and Carroll P. Vance. 2003. "Legumes: Importance and Constraints to Greater Use." *Plant Physiology* 131 (3): 872–77. <https://doi.org/10.1104/pp.017004>.
- Greinwald, Roland, Gabriele Lurz, Ludger Witte, and Franz-Christian Czygan. 1990. "A Survey of Alkaloids in *Spartium junceum* L. (Genisteae-Fabaceae)." *Zeitschrift Für Naturforschung C* 45 (11–12): 1085–89. <https://doi.org/10.1515/znc-1990-11-1202>.
- Greinwald, Roland, Wulf Schultze, and Franz-Christian Czygan. 1990. "Über die Alkaloidzusammensetzung der oberirdischen Teile von *Laburnum watereri* (Kirchn.) Dipp." *Biochemie und Physiologie der Pflanzen* 186 (1): 1–10. [https://doi.org/10.1016/S0015-3796\(11\)80282-9](https://doi.org/10.1016/S0015-3796(11)80282-9).
- Greinwald, Roland, Michael Wink, Ludger Witte, and Franz-Christian Czygan. 1991. "Das Alkaloidmuster Der Pfropfchimäre *Laburnocytisus adamii* (Fabaceae)." *Biochemie Und Physiologie Der Pflanzen* 187 (5): 385–91. [https://doi.org/10.1016/S0015-3796\(11\)80044-2](https://doi.org/10.1016/S0015-3796(11)80044-2).
- Gremigni, P., J. Hamblin, D. Harris, and W. A. Cowling. 2003. "The Inter- Action of Phosphorus and Potassium with Seed Alkaloid Concentrations, Yield and Mineral Content in Narrow-Leafed Lupin (*Lupinus angustifolius* L.)." *Plant and Soil* 253 (2): 413–27. <https://doi.org/10.1023/A:1024828131581>.
- Gresser, Gabriele, Ludger Witte, Victor P Dedkov, and Franz-Christian Czygan. 1996. "A Survey of Quinolizidine Alkaloids and Phenylethylamine Tyramine in *Cytisus scoparius* (Leguminosae) from Different Origins." *Zeitschrift Für Naturforschung C* 51 (11–12): 791–801. <https://doi.org/10.1515/znc-1996-11-1205>.
- Groß, Felicitas, Eva-Esther Rudolf, Björn Thiele, Jörg Durner, and Jeremy Astier. 2017. "Copper Amine Oxidase 8 Regulates Arginine-Dependent Nitric Oxide Production in *Arabidopsis thaliana*." *Journal of Experimental Botany* 68 (9): 2149–62. <https://doi.org/10.1093/jxb/erx105>.
- Grotewold, Erich. 2005. "Plant Metabolic Diversity: A Regulatory Perspective." *Trends in Plant Science* 10 (2): 57–62. <https://doi.org/10.1016/j.tplants.2004.12.009>.
- Guindon, Stéphane, Jean-François Dufayard, Vincent Lefort, Maria Anisimova, Wim Hordijk, and Olivier Gascuel. 2010. "New Algorithms and Methods to Estimate Maximum-Likelihood Phylogenies: Assessing the Performance of PhyML 3.0." *Systematic Biology* 59 (3): 307–21. <https://doi.org/10.1093/sysbio/syq010>.
- Gull, Audil, Ajaz Ahmad Lone, and Noor Ul Islam Wani. 2019. "Biotic and Abiotic Stresses in Plants." In *Abiotic and Biotic Stress in Plants*, edited by Alexandre Bosco de Oliveira. IntechOpen. <https://doi.org/10.5772/intechopen.85832>.

- Hamana, Koei, and Shigeru Matsuzaki. 1992. "Polyamines As A Chemotaxonomic Marker in Bacterial Systematics." *Critical Reviews in Microbiology* 18 (4): 261–83. <https://doi.org/10.3109/10408419209113518>.
- Handa, Avtar K., Tahira Fatima, and Autar K. Mattoo. 2018. "Polyamines: Bio-Molecules with Diverse Functions in Plant and Human Health and Disease." *Frontiers in Chemistry* 6 (February): 10. <https://doi.org/10.3389/fchem.2018.00010>.
- Hartmann, T. 1994. "Pyrrolizidine Alkaloids between Plants and Insects: A New Chapter of an Old Story." *Chemoecology* 5-6 (3-4): 139–46.
- Hartmann, T., G. Schoofs, and M. Wink. 1980. "A Chloroplast-Localized Lysine Decarboxylase of *Lupinus polyphyllus*: The First Enzyme in the Biosynthetic Pathway of Quinolizidine Alkaloids." *FEBS Letters* 115 (1): 35–38. [https://doi.org/10.1016/0014-5793\(80\)80721-6](https://doi.org/10.1016/0014-5793(80)80721-6).
- Hartmann, T., C. Theuring, T. Beuerle, E.A. Bernays, and M.S. Singer. 2005. "Acquisition, Transformation and Maintenance of Plant Pyrrolizidine Alkaloids by the Polyphagous Arctiid *Grammia geneura*." *Insect Biochemistry and Molecular Biology* 35 (10): 1083–99. <https://doi.org/10.1016/j.ibmb.2005.05.011>.
- Hartmann, T. 1996. "Diversity and Variability of Plant Secondary Metabolism: A Mechanistic View." *Entomologia Experimentalis et Applicata* 80 (1): 177–88. <https://doi.org/10.1111/j.1570-7458.1996.tb00914.x>.
- Hartmann, T. 1999. "Chemical Ecology of Pyrrolizidine Alkaloids." In *Planta*, 207:483–95. Springer. <https://www.jstor.org/stable/23385595>.
- Hartmann, T. and Dierich, B. 1998. "Chemical Diversity and Variation of Pyrrolizidine Alkaloids of the Senecionine Type: Biological Need or Coincidence?" *Planta* 206 (3): 443–51. <https://doi.org/10.1007/s004250050420>.
- Hartmann, Thomas, Adelheid Ehmke, Udo Eilert, Kirsten von Borstel, and Claudine Theuring. 1989. "Sites of Synthesis, Translocation and Accumulation of Pyrrolizidine Alkaloid *N*-Oxides in *Senecio vulgaris* L." *Planta* 177 (1): 98–107. <https://doi.org/10.1007/BF00392159>.
- Hartmann, T. and Ober, D. 2000. "Biosynthesis and Metabolism of Pyrrolizidine Alkaloids in Plants and Specialized Insect Herbivores." In *Biosynthesis*, 207–43. Springer.
- Hartmann, T. and Ober, D. 2008. "Defense by Pyrrolizidine Alkaloids: Developed by Plants and Recruited by Insects." In *Induced Plant Resistance to Herbivory*, edited by Andreas Schaller, 213–31. Dordrecht: Springer Netherlands. https://doi.org/10.1007/978-1-4020-8182-8_10.
- Hartmann, T. and Toppel, G. 1987. "Senecionine *N*-Oxide, the Primary Product of Pyrrolizidine Alkaloid Biosynthesis in Root Cultures of *Senecio vulgaris*." *Phytochemistry* 26 (6): 1639–43. [https://doi.org/10.1016/S0031-9422\(00\)82261-X](https://doi.org/10.1016/S0031-9422(00)82261-X).
- Hartmann, T. and Witte, L. 1995. "Chapter Four - Chemistry, Biology and Chemoecology of the Pyrrolizidine Alkaloids." In *Alkaloids: Chemical and Biological Perspectives*, edited by S. William Pelletier, 9:155–233. Pergamon. <https://doi.org/10.1016/B978-0-08-042089-9.50011-5>.
- Hashimoto, T., K. Tamaki, K.-i. Suzuki, and Y. Yamada. 1998. "Molecular Cloning of Plant Spermidine Synthases." *Plant and Cell Physiology* 39 (1): 73–79. <https://doi.org/10.1093/oxfordjournals.pcp.a029291>.
- Hashimoto, T. and Y. Yamada. 1994. "Alkaloid Biogenesis: Molecular Aspects." *Annual Review of Plant Physiology and Plant Molecular Biology* 45 (1): 257–85. <https://doi.org/10.1146/annurev.pp.45.060194.001353>.

- Hashimoto, Takashi, Akira Mitani, and Yasuyuki Yamada. 1990. "Diamine Oxidase from Cultured Roots of *Hyoscyamus niger*: Its Function in Tropane Alkaloid Biosynthesis." *Plant Physiology* 93 (1): 216–21. <https://doi.org/10.1104/pp.93.1.216>.
- Hassen, Ahmed Idris, Francina Lebogang Bopape, Johannes Habig, and Sandra Christina Lamprecht. 2012. "Nodulation of Rooibos (*Aspalathus linearis* Burm. f.), an Indigenous South African Legume, by Members of Both the α -Proteobacteria and β -Proteobacteria." *Biology and Fertility of Soils* 48 (3): 295–303. <https://doi.org/10.1007/s00374-011-0628-3>.
- Heil, M, and Baldwin, Ian T. 2002. "Fitness Costs of Induced Resistance: Emerging Experimental Support for a Slippery Concept." *Trends in Plant Science* 7 (2): 61–67. [https://doi.org/10.1016/S1360-1385\(01\)02186-0](https://doi.org/10.1016/S1360-1385(01)02186-0).
- Heim, William G., Katie A. Sykes, Sherry B. Hildreth, Jian Sun, Rong-He Lu, and John G. Jelesko. 2007. "Cloning and Characterization of a *Nicotiana tabacum* Methylputrescine Oxidase Transcript." *Phytochemistry* 68 (4): 454–63. <https://doi.org/10.1016/j.phytochem.2006.11.003>.
- Herridge, David F., Mark B. Peoples, and Robert M. Boddey. 2008. "Global Inputs of Biological Nitrogen Fixation in Agricultural Systems." *Plant and Soil* 311 (1–2): 1–18. <https://doi.org/10.1007/s11104-008-9668-3>.
- Hirsch, Ann M. 1992. "Developmental Biology of Legume Nodulation." *New Phytologist* 122 (2): 211–37. <https://doi.org/10.1111/j.1469-8137.1992.tb04227.x>.
- Hood, Elizabeth E., Stanton B. Gelvin, Leo S. Melchers, and Andre Hoekema. 1993. "New *Agrobacterium* Helper Plasmids for Gene Transfer to Plants." *Transgenic Research* 2 (4): 208–18. <https://doi.org/10.1007/BF01977351>.
- Hornoy, Benjamin, Anne Atlan, Michèle Tarayre, Sébastien Dugravot, and Michael Wink. 2012. "Alkaloid Concentration of the Invasive Plant Species *Ulex europaeus* in Relation to Geographic Origin and Herbivory." *Naturwissenschaften* 99 (11): 883–92. <https://doi.org/10.1007/s00114-012-0970-9>.
- Houen, Gunnar, Casper Struve, Roar Søndergaard, Tina Friis, Uffe Anthoni, Per H. Nielsen, Carsten Christophersen, Bent O. Petersen, and Jens Ø. Duus. 2005. "Substrate Specificity of the Bovine Serum Amine Oxidase and in Situ Characterisation of Aminoaldehydes by NMR Spectroscopy." *Bioorganic & Medicinal Chemistry* 13 (11): 3783–96. <https://doi.org/10.1016/j.bmc.2005.03.020>.
- Hufnagel, Bárbara, André Marques, Alexandre Soriano, Laurence Marquès, Fanchon Divol, Patrick Dumas, Erika Sallet, et al. 2020. "High-Quality Genome Sequence of White Lupin Provides Insight into Soil Exploration and Seed Quality." *Nature Communications* 11 (1): 492. <https://doi.org/10.1038/s41467-019-14197-9>.
- Ibáñez, Fernando, Luis Wall, and Adriana Fabra. 2016. "Starting Points in Plant-Bacteria Nitrogen-Fixing Symbioses: Intercellular Invasion of the Roots." *Journal of Experimental Botany*, October, erw387. <https://doi.org/10.1093/jxb/erw387>.
- Innan, Hideki, and Fyodor Kondrashov. 2010. "The Evolution of Gene Duplications: Classifying and Distinguishing between Models." *Nature Reviews Genetics* 11 (2): 97–108. <https://doi.org/10.1038/nrg2689>.
- Irmer, Simon, Nora Podzun, Dorothee Langel, Franziska Heidemann, Elisabeth Kaltenegger, Brigitte Schemmerling, Christoph-Martin Geilfus, Christian Zörb, and Dietrich Ober. 2015. "New Aspect of Plant–Rhizobia Interaction: Alkaloid Biosynthesis in *Crotalaria* Depends on Nodulation." *Proceedings of the National Academy of Sciences* 112 (13): 4164–69. <https://doi.org/10.1073/pnas.1423457112>.

- Jacky, Nadine. 2015. "Biosynthesis of Alkaloids as a Function of Nodulation in Selected Species of the Fabaceae." Masterthesis.
- Jansen, Gisela, Hans-Ulrich Juergens, Edgar Schliephake, Sylvia Seddig, and Frank Ordon. 2015. "Effects of Growing System and Season on the Alkaloid Content and Yield of Different Sweet *L. angustifolius* Genotypes." PDF. *Journal of Applied Botany and Food Quality*; 88; 1-4. <https://doi.org/10.5073/JABFQ.2015.088.001>.
- Jansen, Gisela, Hans-Ulrich Jürgens, Edgar Schliephake, and Frank Ordon. 2012. "Effect of the Soil PH on the Alkaloid Content of *Lupinus angustifolius*." *International Journal of Agronomy* 2012: 1–5. <https://doi.org/10.1155/2012/269878>.
- Jenett-Siems, Kristina, Sonja C. Ott, Thomas Schimming, Karsten Siems, Frank Müller, Monika Hilker, Ludger Witte, Thomas Hartmann, Daniel F. Austin, and Eckart Eich. 2005. "Ipangulines and Minalobines, Chemotaxonomic Markers of the Infrageneric Ipomoea Taxon Subgenus Quamoclit, Section Mina." *Phytochemistry* 66 (2): 223–31. <https://doi.org/10.1016/j.phytochem.2004.11.019>.
- Johnson, A. Earl, Russell J. Molyneux, and Glory B. Merrill. 1985. "Chemistry of Toxic Range Plants. Variation in Pyrrolizidine Alkaloid Content of *Senecio*, *Amsinckia*, and *Crotalaria* Species." *Journal of Agricultural and Food Chemistry* 33 (1): 50–55. <https://doi.org/10.1021/jf00061a015>.
- Johnson, Stuart K., Jonathan Clements, Casiana Blanca J. Villarino, and Ranil Coorey. 2017. "Lupins: Their Unique Nutritional and Health-Promoting Attributes." In *Gluten-Free Ancient Grains*, 179–221. Elsevier. <https://doi.org/10.1016/B978-0-08-100866-9.00008-X>.
- Jungmayr, Apothekerin Dr. Petra. 2015. "Goldregen Zur Raucherentwöhnung Cytisin Punktet Im Vergleich Mit Nicotin," Deutsche Apotheker Zeitung, , no. DAZ 2015, Nr. 5, S. 32 (January). <https://www.deutsche-apotheker-zeitung.de/daz-az/2015/daz-5-2015/goldregen-zur-raucherentwoehnung>.
- Justus, Matthias, Ludger Witte, and Thomas Hartmann. 1997. "Levels and Tissue Distribution of Loline Alkaloids in Endophyte-Infected *Festuca pratensis*." *Phytochemistry* 44 (1): 51–57. [https://doi.org/10.1016/S0031-9422\(96\)00535-3](https://doi.org/10.1016/S0031-9422(96)00535-3).
- Kaltenegger, Elisabeth, Eckart Eich, and Dietrich Ober. 2013. "Evolution of Homospermidine Synthase in the Convolvulaceae: A Story of Gene Duplication, Gene Loss, and Periods of Various Selection Pressures." *The Plant Cell* 25 (4): 1213–27. <https://doi.org/10.1105/tpc.113.109744>.
- Kaltenegger, Elisabeth, Arunraj S. Prakashrao, Serhat S. Çiçek, and Dietrich Ober. 2021. "Development of an Activity Assay for Characterizing Deoxyhypusine Synthase and Its Diverse Reaction Products." *FEBS Open Bio* 11 (1): 10–25. <https://doi.org/10.1002/2211-5463.13046>.
- Käss, Ernst, and Michael Wink. 1997. "Phylogenetic Relationships in the Papilionoideae (Family Leguminosae) Based on Nucleotide Sequences of CpDNA (Rbcl) and NcDNA (ITS 1 and 2)." *Molecular Phylogenetics and Evolution* 8 (1): 65–88. <https://doi.org/10.1006/mpev.1997.0410>.
- Katoh, Akira, Hiroyuki Ohki, Koji Inai, and Takashi Hashimoto. 2005. "Molecular Regulation of Nicotine Biosynthesis." *Plant Biotechnology* 22 (5): 389–92. <https://doi.org/10.5511/plantbiotechnology.22.389>.
- Katoh, Akira, Tsubasa Shoji, and Takashi Hashimoto. 2007. "Molecular Cloning of N - Methylputrescine Oxidase from Tobacco." *Plant and Cell Physiology* 48 (3): 550–54. <https://doi.org/10.1093/pcp/pcm018>.

- Kelly, Henry A., and David J. Robins. 1988. "Evidence for an Immonium Ion Intermediate in Pyrrolizidine Alkaloid Biosynthesis." *Journal of the Chemical Society, Chemical Communications*, no. 5 (January): 329–30. <https://doi.org/10.1039/C39880000329>.
- Kern, A. D., M. A. Oliveira, P. Coffino, and M. L. Hackert. 1999. "Structure of Mammalian Ornithine Decarboxylase at 1.6 Å Resolution: Stereochemical Implications of PLP-Dependent Amino Acid Decarboxylases." *Structure (London, England: 1993)* 7 (5): 567–81. [https://doi.org/10.1016/S0969-2126\(99\)80073-2](https://doi.org/10.1016/S0969-2126(99)80073-2).
- Khan, Hassan A., and David J. Robins. 1985. "Pyrrolizidine Alkaloid Biosynthesis. Synthesis of 14 C-Labelled Homospermidines and Their Incorporation into Retronecine." *Journal of the Chemical Society, Perkin Transactions 1*, 819–24.
- Kraker, Jan-Willem de, and Jonathan Gershenzon. 2011. "From Amino Acid to Glucosinolate Biosynthesis: Protein Sequence Changes in the Evolution of Methylthioalkylmalate Synthase in *Arabidopsis*." *The Plant Cell* 23 (1): 38–53. <https://doi.org/10.1105/tpc.110.079269>.
- Krossa, Sebastian, Annette Faust, Dietrich Ober, and Axel J. Scheidig. 2016. "Comprehensive Structural Characterization of the Bacterial Homospermidine Synthase—an Essential Enzyme of the Polyamine Metabolism." *Scientific Reports* 6 (1): 19501. <https://doi.org/10.1038/srep19501>.
- Kruse, Lars H., Thomas Stegemann, Christian Sievert, and Dietrich Ober. 2017. "Identification of a Second Site of Pyrrolizidine Alkaloid Biosynthesis in Comfrey to Boost Plant Defense in Floral Stage." *Plant Physiology* 174 (1): 47–55.
- Kumar, Vinay, David M Dooley, Hans C Freeman, J Mitchell Guss, Ian Harvey, Michele A McGuirl, Matthew CJ Wilce, and Vilma M Zubak. 1996. "Crystal Structure of a Eukaryotic (Pea Seedling) Copper-Containing Amine Oxidase at 2.2 Å Resolution." *Structure* 4 (8): 943–55. [https://doi.org/10.1016/S0969-2126\(96\)00101-3](https://doi.org/10.1016/S0969-2126(96)00101-3).
- Lacroix, Benoît, and Vitaly Citovsky. 2019. "Pathways of DNA Transfer to Plants from *Agrobacterium tumefaciens* and Related Bacterial Species." *Annual Review of Phytopathology* 57 (August): 231–51. <https://doi.org/10.1146/annurev-phyto-082718-100101>.
- Laguerre, Gisèle, Sarah M. Nour, Valérie Macheret, Juan Sanjuan, Pascal Drouin, and Noëlle Amarger. 2001. "Classification of Rhizobia Based on NodC and NifH Gene Analysis Reveals a Close Phylogenetic Relationship among *Phaseolus vulgaris* Symbionts." *Microbiology* 147 (4): 981–93. <https://doi.org/10.1099/00221287-147-4-981>.
- Lee, M. J., J. S. Pate, D. J. Harris, and C. A. Atkins. 2007. "Synthesis, Transport and Accumulation of Quinolizidine Alkaloids in *Lupinus albus* L. and *L. angustifolius* L." *Journal of Experimental Botany* 58 (5): 935–46. <https://doi.org/10.1093/jxb/erl254>.
- Lee, Yong-Sun, and Young-Dong Cho. 2001. "Identification of Essential Active-Site Residues in Ornithine Decarboxylase of *Nicotiana glutinosa* Decarboxylating Both L-Ornithine and L-Lysine." *Biochemical Journal* 360 (3): 657. <https://doi.org/10.1042/0264-6021:3600657>.
- Li, Dapeng, Sven Heiling, Ian T. Baldwin, and Emmanuel Gaquerel. 2016. "Illuminating a Plant's Tissue-Specific Metabolic Diversity Using Computational Metabolomics and Information Theory." *Proceedings of the National Academy of Sciences* 113 (47): E7610–18. <https://doi.org/10.1073/pnas.1610218113>.
- Li, Rongbao, Judith P Klinman, and F Scott Mathews. 1998. "Copper Amine Oxidase from *Hansenula Polymorpha*: The Crystal Structure Determined at 2.4 Å Resolution

- Reveals the Active Conformation." *Structure* 6 (3): 293–307. [https://doi.org/10.1016/S0969-2126\(98\)00033-1](https://doi.org/10.1016/S0969-2126(98)00033-1).
- Liao, Shaofu, Phuntip Poonpairaj, Kyong-Cheol Ko, Yumiko Takatuska, Yoshihiro Yamaguchi, Naoki Abe, Jun Kaneko, and Yoshiyuki Kamio. 2008. "Occurrence of Agmatine Pathway for Putrescine Synthesis in *Selenomonas ruminatium*." *Bioscience, Biotechnology, and Biochemistry* 72 (2): 445–55. <https://doi.org/10.1271/bbb.70550>.
- Lichman, Benjamin R. 2021. "The Scaffold-Forming Steps of Plant Alkaloid Biosynthesis." *Natural Product Reports* 38 (1): 103–29. <https://doi.org/10.1039/D0NP00031K>.
- Lindigkeit, Rainer, Andreas Biller, Markus Buch, Hans-Martin Schiebel, Michael Boppré, and Thomas Hartmann. 1997. "The Two Faces of Pyrrolizidine Alkaloids: The Role of the Tertiary Amine and Its *N*-Oxide in Chemical Defense of Insects with Acquired Plant Alkaloids." *European Journal of Biochemistry* 245 (3): 626–36. <https://doi.org/10.1111/j.1432-1033.1997.00626.x>.
- Liu, Ji-Hong, Wei Wang, Hao Wu, Xiaoqing Gong, and Takaya Moriguchi. 2015. "Polyamines Function in Stress Tolerance: From Synthesis to Regulation." *Frontiers in Plant Science* 6. <https://www.frontiersin.org/article/10.3389/fpls.2015.00827>.
- López-Gómez, Miguel, Libertad Cobos-Porras, Jürgen Prell, and Carmen Lluch. 2016. "Homospermidine Synthase Contributes to Salt Tolerance in Free-Living *Rhizobium tropici* and in Symbiosis with *Phaseolus vulgaris*." *Plant and Soil* 404 (1–2): 413–25. <https://doi.org/10.1007/s11104-016-2848-7>.
- Lunelli, Michele, Maria Luisa Di Paolo, Marianna Biadene, Vito Calderone, Roberto Battistutta, Marina Scarpa, Adelio Rigo, and Giuseppe Zanotti. 2005. "Crystal Structure of Amine Oxidase from Bovine Serum." *Journal of Molecular Biology* 346 (4): 991–1004. <https://doi.org/10.1016/j.jmb.2004.12.038>.
- Lunn, John E. 2007. "Compartmentation in Plant Metabolism." *Journal of Experimental Botany* 58 (1): 35–47. <https://doi.org/10.1093/jxb/erl134>.
- Lynch, Michael, and Allan Force. 2000. "The Probability of Duplicate Gene Preservation by Subfunctionalization." *Genetics* 154 (1): 459–73. <https://doi.org/10.1093/genetics/154.1.459>.
- Martínez-Romero, Esperanza. 2009. "Coevolution in *Rhizobium* -Legume Symbiosis?" *DNA and Cell Biology* 28 (8): 361–70. <https://doi.org/10.1089/dna.2009.0863>.
- McKey, D. 1979. "The Distribution of Secondary Compounds within Plants." *Herbivores-Their Interaction with Secondary Plant Metabolites*, 55–134. <https://cir.nii.ac.jp/crid/1574231874860006784>.
- Medda, Rosaria, Andrea Bellelli, Pavel Pec, Rodolfo Federico, Alessandra Cona, Giovanni Floris, and B. Mondovì. 2009. "Copper Amine Oxidases from Plants." Vol. 4. Taylor and Francis Group, CRC Press: Boca Raton, FL, USA.
- Moll, Stefanie, Sven Anke, Uwe Kahmann, Robert Hänsch, Thomas Hartmann, and Dietrich Ober. 2002. "Cell-Specific Expression of Homospermidine Synthase, the Entry Enzyme of the Pyrrolizidine Alkaloid Pathway in *Senecio vernalis*, in Comparison with Its Ancestor, Deoxyhypusine Synthase." *Plant Physiology* 130 (1): 47–57.
- "Monocrotaline." 1976. *IARC Monographs on the Evaluation of the Carcinogenic Risk of Chemicals to Man* 10: 291–302.
- Morton, Julia F. 1983. "Rooibos Tea, *Aspalathus linearis*, a Caffeineless, Low-Tannin Beverage." *Economic Botany* 37 (2): 164–73. <https://doi.org/10.1007/BF02858780>.

- Mosjidis, J.A., and M.L. Wang. 2011. "Crotalaria." In *Wild Crop Relatives.* In *Genomic and Breeding Resources*, 63–69. Industrial Crops. C. Kole, ed., Springer, Berlin, Heidelberg.
- Moulin, Lionel, Gilles Béna, Catherine Boivin-Masson, and Tomasz Stępkowski. 2004. "Phylogenetic Analyses of Symbiotic Nodulation Genes Support Vertical and Lateral Gene Co-Transfer within the Bradyrhizobium Genus." *Molecular Phylogenetics and Evolution* 30 (3): 720–32. [https://doi.org/10.1016/S1055-7903\(03\)00255-0](https://doi.org/10.1016/S1055-7903(03)00255-0).
- Murashige, Toshio, and Folke Skoog. 1962. "A Revised Medium for Rapid Growth and Bio Assays with Tobacco Tissue Cultures." *Physiologia Plantarum* 15 (3): 473–97. <https://doi.org/10.1111/j.1399-3054.1962.tb08052.x>.
- Naconsie, Maliwan, Keita Kato, Tsubasa Shoji, and Takashi Hashimoto. 2014. "Molecular Evolution of N-Methylputrescine Oxidase in Tobacco." *Plant and Cell Physiology* 55 (2): 436–44. <https://doi.org/10.1093/pcp/pct179>.
- Nakajima, K, T Hashimoto, and Y Yamada. 1993. "Two Tropinone Reductases with Different Stereospecificities Are Short-Chain Dehydrogenases Evolved from a Common Ancestor." *Proceedings of the National Academy of Sciences* 90 (20): 9591–95. <https://doi.org/10.1073/pnas.90.20.9591>.
- Neuner-Jehle, N., H. Nesvadba, and G. Spiteller. 1965. "Anwendung der Massenspektrometrie zur Strukturaufklärung von Alkaloiden, 6. Mitt.: Pyrrolizidinalkaloide aus dem Goldregen." *Monatshefte fuer Chemie* 96 (2): 321–38. <https://doi.org/10.1007/BF00909439>.
- Niemüller, Daniel, Andreas Reimann, and Dietrich Ober. 2012. "Distinct Cell-Specific Expression of Homospermidine Synthase Involved in Pyrrolizidine Alkaloid Biosynthesis in Three Species of the Boraginales." *Plant Physiology* 159 (3): 920–29. <https://doi.org/10.1104/pp.112.195024>.
- Ober, D., R. Harms, L. Witte, and T. Hartmann. 2003. "Molecular Evolution by Change of Function. Alkaloid-Specific Homospermidine Synthase Retained All Properties of Deoxyhypusine Synthase except Binding the EIF5A Precursor Protein." *The Journal of Biological Chemistry* 278 (15): 12805–12.
- Ober, D., and T. Hartmann. 1999a. "Deoxyhypusine Synthase from Tobacco. CDNA Isolation, Characterization, and Bacterial Expression of an Enzyme with Extended Substrate Specificity." *The Journal of Biological Chemistry* 274 (45): 32040.
- Ober, D., and T. Hartmann. 1999b. "Homospermidine Synthase, the First Pathway-Specific Enzyme of Pyrrolizidine Alkaloid Biosynthesis, Evolved from Deoxyhypusine Synthase." *Proceedings of the National Academy of Sciences* 96 (26): 14777–82. <https://doi.org/10.1073/pnas.96.26.14777>.
- Ober, Dietrich, Lutz Gibas, Ludger Witte, and Thomas Hartmann. 2003. "Evidence for General Occurrence of Homospermidine in Plants and Its Supposed Origin as By-Product of Deoxyhypusine Synthase." *Phytochemistry* 62 (3): 339–44.
- Ober, Dietrich, Reiner Harms, and Thomas Hartmann. 2000. "Cloning and Expression of Homospermidine Synthase from *Senecio vulgaris*: A Revision." *Phytochemistry* 55 (4): 305–9. [https://doi.org/10.1016/S0031-9422\(00\)00267-3](https://doi.org/10.1016/S0031-9422(00)00267-3).
- Ober, Dietrich, and Thomas Hartmann. 2000. "Phylogenetic Origin of a Secondary Pathway: The Case of Pyrrolizidine Alkaloids." *Plant Molecular Biology* 44 (4): 445–50. <https://doi.org/10.1023/A:1026597621646>.

- Ober, Dietrich, and Elisabeth Kaltenecker. 2009. "Pyrrolizidine Alkaloid Biosynthesis, Evolution of a Pathway in Plant Secondary Metabolism." *Phytochemistry* 70 (15–16): 1687–95.
- Ober, Dietrich, Dorothea Tholl, William Martin, and Thomas Hartmann. 1996. "Metabolism of *Escherichia coli*" 42: 9.
- Ohmiya, Shigeru, Kazuki Saito, and Isamu Murakoshi. 1995. "Chapter 1 Lupine Alkaloids." In *The Alkaloids: Chemistry and Pharmacology*, 47:1–114. Elsevier. [https://doi.org/10.1016/S0099-9598\(08\)60153-4](https://doi.org/10.1016/S0099-9598(08)60153-4).
- Okada, Taketo, Masami Yokota Hirai, Hideyuki Suzuki, Mami Yamazaki, and Kazuki Saito. 2005. "Molecular Characterization of a Novel Quinolizidine Alkaloid O-Tigloyltransferase: CDNA Cloning, Catalytic Activity of Recombinant Protein and Expression Analysis in *Lupinus* Plants." *Plant and Cell Physiology* 46 (1): 233–44. <https://doi.org/10.1093/pcp/pci021>.
- Osorio, Claudia E., and Bradley J. Till. 2022. "A Bitter-Sweet Story: Unraveling the Genes Involved in Quinolizidine Alkaloid Synthesis in *Lupinus albus*." *Frontiers in Plant Science* 12 (January): 795091. <https://doi.org/10.3389/fpls.2021.795091>.
- Panchy, Nicholas, Melissa Lehti-Shiu, and Shin-Han Shiu. 2016. "Evolution of Gene Duplication in Plants." *Plant Physiology* 171 (4): 2294–2316. <https://doi.org/10.1104/pp.16.00523>.
- Park, M. H., K. Nishimura, C. F. Zanelli, and S. R. Valentini. 2010. "Functional Significance of EIF5A and Its Hypusine Modification in Eukaryotes." *Amino Acids* 38 (2): 491–500. <https://doi.org/10.1007/s00726-009-0408-7>.
- Park, M. H., E. C. Wolff, and J. E. Folk. 1993. "Hypusine: Its Post-Translational Formation in Eukaryotic Initiation Factor 5A and Its Potential Role in Cellular Regulation." *BioFactors (Oxford, England)* 4 (2): 95–104.
- Park, Myung Hee, Young Bok Lee, and Young Ae Joe. 1997. "Hypusine Is Essential for Eukaryotic Cell Proliferation." *Neurosignals* 6 (3): 115–23. <https://doi.org/10.1159/000109117>.
- Pegg, Anthony E. 2006. "Regulation of Ornithine Decarboxylase." *Journal of Biological Chemistry* 281 (21): 14529–32. <https://doi.org/10.1074/jbc.R500031200>.
- Pegg, Anthony E., and Shirley McGill. 1979. "Decarboxylation of Ornithine and Lysine in Rat Tissues." *Biochimica et Biophysica Acta (BBA) - Enzymology* 568 (2): 416–27. [https://doi.org/10.1016/0005-2744\(79\)90310-3](https://doi.org/10.1016/0005-2744(79)90310-3).
- Peter, J., W. Young, and Kaisa E. Haukka. 1996. "Diversity and Phylogeny of Rhizobia." *New Phytologist* 133 (1): 87–94. <https://doi.org/10.1111/j.1469-8137.1996.tb04344.x>.
- Philippi, Jasmin, Edgar Schliephake, Hans-Ulrich Jürgens, Gisela Jansen, and Frank Ordon. 2015. "Feeding Behavior of Aphids on Narrow-Leafed Lupin (*Lupinus angustifolius*) Genotypes Varying in the Content of Quinolizidine Alkaloids." *Entomologia Experimentalis et Applicata* 156 (1): 37–51. <https://doi.org/10.1111/eea.12313>.
- Pichersky, Eran, and David R Gang. 2000. "Genetics and Biochemistry of Secondary Metabolites in Plants: An Evolutionary Perspective." *Trends in Plant Science* 5 (10): 439–45. [https://doi.org/10.1016/S1360-1385\(00\)01741-6](https://doi.org/10.1016/S1360-1385(00)01741-6).
- Pichersky, Eran, and Efraim Lewinsohn. 2011. "Convergent Evolution in Plant Specialized Metabolism." *Annual Review of Plant Biology* 62 (1): 549–66. <https://doi.org/10.1146/annurev-arplant-042110-103814>.
- Polhill, R. M., and P. H. Raven. 1981. *Advances in Legume Systematics. Vol. 1 and 2*. Royal bot. Garden Kew.

- Prakashrao, Arunraj Saranya, Till Beuerle, Ana Rita G. Simões, Christina Hopf, Serhat Sezai Çiçek, Thomas Stegemann, Dietrich Ober, and Elisabeth Kaltenegger. 2022. "The Long Road of Functional Recruitment—The Evolution of a Gene Duplicate to Pyrrolizidine Alkaloid Biosynthesis in the Morning Glories (Convolvulaceae)." *Plant Direct* 6 (7). <https://doi.org/10.1002/pld3.420>.
- Purrington, Colin B. 2000. "Costs of Resistance." *Current Opinion in Plant Biology* 3 (4): 305–8. [https://doi.org/10.1016/S1369-5266\(00\)00085-6](https://doi.org/10.1016/S1369-5266(00)00085-6).
- Reimann, Andreas, Niknik Nurhayati, Anita Backenköhler, and Dietrich Ober. 2004. "Repeated Evolution of the Pyrrolizidine Alkaloid-Mediated Defense System in Separate Angiosperm Lineages." *The Plant Cell* 16 (10): 2772–84. <https://doi.org/10.1105/tpc.104.023176>.
- Rensing, Stefan A. 2014. "Gene Duplication as a Driver of Plant Morphogenetic Evolution." *Current Opinion in Plant Biology* 17 (February): 43–48. <https://doi.org/10.1016/j.pbi.2013.11.002>.
- Robins, D. J. 1982. "A Biogenetically Patterned Synthesis of the Pyrrolizidine Alkaloid Trachelanthamidine." *Journal of the Chemical Society, Chemical Communications*, no. 22: 1289. <https://doi.org/10.1039/c39820001289>.
- Robins, D. J. 1989. "Biosynthesis of Pyrrolizidine Alkaloids." *Chemical Society Reviews* 18: 375. <https://doi.org/10.1039/cs9891800375>.
- Robins, D.J. 1986. "Chemistry and Toxicology of Pyrrolizidine Alkaloids." *Phytochemistry* 25 (11): 2698–99. [https://doi.org/10.1016/S0031-9422\(00\)84554-9](https://doi.org/10.1016/S0031-9422(00)84554-9).
- Rosenthal, G. A. 1982. *Plant Non-Protein Amino and Imino Acids*. Academic press, New York, London.
- Ross, S. M., J. R. King, R. C. Izaurralde, and J. T. O'Donovan. 2009. "The Green Manure Value of Seven Clover Species Grown as Annual Crops on Low and High Fertility Temperate Soils." *Canadian Journal of Plant Science* 89 (3): 465–76. <https://doi.org/10.4141/CJPS08173>.
- Ryan-Salter, T.P., A.D. Black, M. Andrews, and D.J. Moot. 2014. "Identification and Effectiveness of Rhizobial Strains That Nodulate *Lupinus polyphyllus*." *Proceedings of the New Zealand Grassland Association* 76 (January): 61–66. <https://doi.org/10.33584/jnzg.2014.76.2961>.
- Sadowsky, Michael J., and B. Ben Bohlool. 1986. "Growth of Fast- and Slow-Growing Rhizobia on Ethanol." *Applied and Environmental Microbiology* 52 (4): 951–53. <https://doi.org/10.1128/aem.52.4.951-953.1986>.
- Saito, Kazuki, and Isamu Murakoshi. 1995. "Chemistry, Biochemistry and Chemotaxonomy of Lupine Alkaloids in the Leguminosae." In *Studies in Natural Products Chemistry*, 15:519–49. Elsevier. [https://doi.org/10.1016/S1572-5995\(06\)80142-0](https://doi.org/10.1016/S1572-5995(06)80142-0).
- Sajnaga, E., W. Małek, B. Łotocka, T. Stepkowski, and A. Legocki. 2001. "The Root-Nodule Symbiosis between *Sarothamnus scoparius* L. and Its Microsymbionts." *Antonie van Leeuwenhoek* 79 (3/4): 385–91. <https://doi.org/10.1023/A:1012010328061>.
- Salehi, Sharopov, Boyunegmez Tumer, Ozleyen, Rodríguez-Pérez, Ezzat, Azzini, et al. 2019. "Symphytum Species: A Comprehensive Review on Chemical Composition, Food Applications and Phytopharmacology." *Molecules* 24 (12): 2272. <https://doi.org/10.3390/molecules24122272>.
- Sander, Heiner, and Thomas Hartmann. 1989. "Site of Synthesis, Metabolism and Translocation of Senecionine N-Oxide in Cultured Roots of *Senecio erucifolius*."

- Plant Cell, Tissue and Organ Culture* 18 (1): 19–31. <https://doi.org/10.1007/BF00033462>.
- Sandmeier, Erika, Terence I. Hale, and Philipp Christen. 1994. "Multiple Evolutionary Origin of Pyridoxal-5'-Phosphate-Dependent Amino Acid Decarboxylases." *European Journal of Biochemistry* 221 (3): 997–1002. <https://doi.org/10.1111/j.1432-1033.1994.tb18816.x>.
- Schade, Fritz, and Harald Jockusch. 2018. "Goldregen." In *Betörend, berauschend, tödlich - Giftpflanzen in unserer Umgebung*. 83–86. Berlin, Heidelberg: Springer Berlin Heidelberg. https://doi.org/10.1007/978-3-662-56048-8_21.
- Schaller, Andreas, ed. 2008. *Induced Plant Resistance to Herbivory*. Berlin: Springer.
- Schillmiller, Anthony L., Dennis P. Miner, Matthew Larson, Eric McDowell, David R. Gang, Curtis Wilkerson, and Robert L. Last. 2010. "Studies of a Biochemical Factory: Tomato Trichome Deep Expressed Sequence Tag Sequencing and Proteomics." *Plant Physiology* 153 (3): 1212–23. <https://doi.org/10.1104/pp.110.157214>.
- Schimpl, Simon, Friedrich Fauser, and Holger Puchta. 2016. "CRISPR/Cas-Mediated Site-Specific Mutagenesis in *Arabidopsis thaliana* Using Cas9 Nucleases and Paired Nickases." In *Chromosome and Genomic Engineering in Plants: Methods and Protocols*, edited by Minoru Murata, 111–22. Methods in Molecular Biology. New York, NY: Springer. https://doi.org/10.1007/978-1-4939-4931-1_8.
- Schmeller, T., A. El-Shazly, and M. Wink. 1997. "Allelochemical Activities of Pyrrolizidine Alkaloids: Interactions with Neuroreceptors and Acetylcholine Related Enzymes." *Journal of Chemical Ecology* 23 (2): 399–416. <https://doi.org/10.1023/B:JOEC.0000006367.51215.88>.
- Schmittgen, Thomas D., and Kenneth J. Livak. 2008. "Analyzing Real-Time PCR Data by the Comparative C T Method." *Nature Protocols* 3 (6): 1101–8. <https://doi.org/10.1038/nprot.2008.73>.
- Schramm, Sebastian, Nikolai Köhler, and Wilfried Rozhon. 2019. "Pyrrolizidine Alkaloids: Biosynthesis, Biological Activities and Occurrence in Crop Plants." *Molecules* 24 (3): 498. <https://doi.org/10.3390/molecules24030498>.
- Schütte, H. R. 1969. "Chinolizidinealkaloide," Berlin: VEB Deutscher Verlag der Wissenschaften. In Mothes, K., Schütte, H. R., (Eds.): *Biosynthese der Alkaloide*: 324–43.
- Smith, T.A. 1977. "Homospermidine in Rhizobium and Legume Root Nodules." *Phytochemistry* 16: 278–79.
- Sprent, Janet I. 2007. "Evolving Ideas of Legume Evolution and Diversity: A Taxonomic Perspective on the Occurrence of Nodulation." *New Phytologist* 174 (1): 11–25. <https://doi.org/10.1111/j.1469-8137.2007.02015.x>.
- Sprent, Janet I., Julie Ardley, and Euan K. James. 2017. "Biogeography of Nodulated Legumes and Their Nitrogen-fixing Symbionts." *New Phytologist* 215 (1): 40–56. <https://doi.org/10.1111/nph.14474>.
- Stegemann, Thomas, Lars H. Kruse, and Dietrich Ober. 2018. "Radioactive Tracer Feeding Experiments and Product Analysis to Determine the Biosynthetic Capability of Comfrey (*Symphytum officinale*) Leaves for Pyrrolizidine Alkaloids." *Bio-Protocol* 8 (3).
- St-Pierre, Benoit, Felipe A. Vazquez-Flota, and Vincenzo De Luca. 1999. "Multicellular Compartmentation of *Catharanthus roseus* Alkaloid Biosynthesis Predicts

- Intercellular Translocation of a Pathway Intermediate." *The Plant Cell* 11 (5): 887–900. <https://doi.org/10.1105/tpc.11.5.887>.
- Swain, T. 1977. "Secondary Compounds as Protective Agents." *Annual Review of Plant Physiology* 28 (1): 479–501. <https://doi.org/10.1146/annurev.pp.28.060177.002403>.
- Sy, Abdoulaye, Eric Giraud, Philippe Jourand, Nelly Garcia, Anne Willems, Philippe de Lajudie, Yves Prin, et al. 2001. "Methylotrophic *Methylobacterium* Bacteria Nodulate and Fix Nitrogen in Symbiosis with Legumes." *Journal of Bacteriology* 183 (1): 214–20. <https://doi.org/10.1128/JB.183.1.214-220.2001>.
- Takatsuka, Y., Y. Yamaguchi, M. Ono, and Y. Kamio. 2000. "Gene Cloning and Molecular Characterization of Lysine Decarboxylase from *Selenomonas ruminantium* Delineate Its Evolutionary Relationship to Ornithine Decarboxylases from Eukaryotes." *Journal of Bacteriology* 182 (23): 6732–41. <https://doi.org/10.1128/jb.182.23.6732-6741.2000>.
- Tan, Qiao Wen, William Goh, and Marek Mutwil. 2020. "LSTrAP-Cloud: A User-Friendly Cloud Computing Pipeline to Infer Coexpression Networks." *Genes* 11 (4): 428. <https://doi.org/10.3390/genes11040428>.
- Tan, Zhiyuan, Thomas Hurek, Pablo Vinuesa, Peter Müller, Jagdish K. Ladha, and Barbara Reinhold-Hurek. 2001. "Specific Detection of *Bradyrhizobium* and *Rhizobium* Strains Colonizing Rice (*Oryza sativa*) Roots by 16S-23S Ribosomal DNA Intergenic Spacer-Targeted PCR." *Applied and Environmental Microbiology* 67 (8): 3655–64. <https://doi.org/10.1128/AEM.67.8.3655-3664.2001>.
- Tavladoraki, Paraskevi, Alessandra Cona, and Riccardo Angelini. 2016. "Copper-Containing Amine Oxidases and FAD-Dependent Polyamine Oxidases Are Key Players in Plant Tissue Differentiation and Organ Development." *Frontiers in Plant Science* 7. <https://www.frontiersin.org/article/10.3389/fpls.2016.00824>.
- Teuber, Michael, Mohammad E. Azemi, Foroogh Namjoyan, Anna-Carolin Meier, Anja Wodak, Wolfgang Brandt, and Birgit Dräger. 2007. "Putrescine *N*-Methyltransferases—a Structure–Function Analysis." *Plant Molecular Biology* 63 (6): 787–801. <https://doi.org/10.1007/s11103-006-9126-7>.
- Tholl, Dorothea, Dietrich Ober, William Martin, Josef Kellermann, and Thomas Hartmann. 1996. "Purification, Molecular Cloning and Expression in *Escherichia coli* of Homospermidine Synthase from *Rhodopseudomonas viridis*." *European Journal of Biochemistry* 240 (2): 373–79. <https://doi.org/10.1111/j.1432-1033.1996.0373h.x>.
- Tissier, Alain. 2012. "Glandular Trichomes: What Comes after Expressed Sequence Tags?" *The Plant Journal* 70 (1): 51–68. <https://doi.org/10.1111/j.1365-313X.2012.04913.x>.
- Triglia, T, M G Peterson, and D J Kemp. 1988. "A Procedure for in Vitro Amplification of DNA Segments That Lie Outside the Boundaries of Known Sequences." *Nucleic Acids Research* 16 (16): 8186. <https://www.ncbi.nlm.nih.gov/pmc/articles/PMC338531/>.
- Walker, Natalie, Colin Howe, Marewa Glover, Hayden McRobbie, Joanne Barnes, Vili Nosa, Varsha Parag, Bruce Bassett, and Christopher Bullen. 2014. "Cytisine versus Nicotine for Smoking Cessation." *New England Journal of Medicine* 371 (25): 2353–62. <https://doi.org/10.1056/NEJMoa1407764>.
- Walters, Dale R. 2003. "Polyamines and Plant Disease." *Phytochemistry* 64 (1): 97–107. [https://doi.org/10.1016/S0031-9422\(03\)00329-7](https://doi.org/10.1016/S0031-9422(03)00329-7).

- Wang, Linzhu, Till Beuerle, James Timbilla, and Dietrich Ober. 2012. "Independent Recruitment of a Flavin-Dependent Monooxygenase for Safe Accumulation of Sequestered Pyrrolizidine Alkaloids in Grasshoppers and Moths." Edited by Carlos Eduardo Winter. *PLoS ONE* 7 (2): e31796. <https://doi.org/10.1371/journal.pone.0031796>.
- Webb, Edwin C., ed. 1992. "Enzyme Nomenclature 1992: Recommendations of the Nomenclature Committee of the International Union of Biochemistry and Molecular Biology on the Nomenclature and Classification of Enzymes. San Diego: Published for the International Union of Biochemistry and Molecular Biology by Academic Press International Union of Biochemistry and Molecular Biology."
- Weisburg, W G, S M Barns, D A Pelletier, and D J Lane. 1991. "16S Ribosomal DNA Amplification for Phylogenetic Study." *Journal of Bacteriology* 173 (2): 697–703. <https://doi.org/10.1128/JB.173.2.697-703.1991>.
- White, James, Jurgen Prell, Euan K. James, and Philip Poole. 2007. "Nutrient Sharing between Symbionts." *Plant Physiology* 144 (2): 604–14. <https://doi.org/10.1104/pp.107.097741>.
- Wink, M. 2013. "Evolution of Secondary Metabolites in Legumes (Fabaceae)." *South African Journal of Botany* 89 (November): 164–75. <https://doi.org/10.1016/j.sajb.2013.06.006>.
- Wink, M., and T. Hartmann. 1982. "Diurnal Fluctuations of Quinolizidine Alkaloid Accumulation in Legumes and Cell Suspension Cultures.," no. Z. f. Naturforschung; Journal of Bioscience 37c: 369–75.
- Wink, M., and G.I.A. Mohamed. 2003. "Evolution of Chemical Defense Traits in the Leguminosae: Mapping of Distribution Patterns of Secondary Metabolites on a Molecular Phylogeny Inferred from Nucleotide Sequences of the Rbcl Gene." *Biochemical Systematics and Ecology* 31 (8): 897–917. [https://doi.org/10.1016/S0305-1978\(03\)00085-1](https://doi.org/10.1016/S0305-1978(03)00085-1).
- Wink, M., and L. Witte. 1985. "Quinolizidine Alkaloids as Nitrogen Source for Lupin Seedlings and Cell Cultures." *Z. Naturforsch.* 40c, 767–775 (1985).
- Wink, M. 1985. "Chemische Verteidigung der Lupinen: Zur biologischen Bedeutung der Chinolizidinalkaloide." *Plant Systematics and Evolution* 150 (1–2): 65–81. <https://doi.org/10.1007/BF00985568>.
- Wink, M. 1987. "Physiology of the Accumulation of Secondary Metabolites with Special Reference to Alkaloids." In *Cell Culture in Phytochemistry*, 17–42. Elsevier. <https://doi.org/10.1016/B978-0-12-715004-8.50008-9>.
- Wink, M. 1992. *Insect-Plant Interactions: Volume IV*. First edition. Boca Raton, FL: CRC Press.
- Wink, M. 2000. "Interference of Alkaloids with Neuroreceptors and Ion Channels." In *Studies in Natural Products Chemistry*, 21:3–122. Elsevier. [https://doi.org/10.1016/S1572-5995\(00\)80004-6](https://doi.org/10.1016/S1572-5995(00)80004-6).
- Wink, M. 2015. "Sekundärstoffe - die Geheimwaffen der Pflanzen: Vom Pfeilgift bis zum Rauschmittel." *Biologie in unserer Zeit* 45 (4): 225–35. <https://doi.org/10.1002/biuz.201510569>.
- Wink, M. 2019. "Quinolizidine and Pyrrolizidine Alkaloid Chemical Ecology – a Mini-Review on Their Similarities and Differences." *Journal of Chemical Ecology* 45 (2): 109–15. <https://doi.org/10.1007/s10886-018-1005-6>.

- Wink, M, and Hartmann, T. 1981. "Activation of Chloroplast-Localized Enzymes of Quinolizidine Alkaloid Biosynthesis by Reduced Thioredoxin." *Plant Cell Reports* 1 (1): 6–9. <https://doi.org/10.1007/BF00267646>.
- Wink, M., Meißner, C., and Witte, L. 1995. "Patterns of Quinolizidine Alkaloids in 56 Species of the Genus *Lupinus*." *Phytochemistry* 38 (1): 139–53. [https://doi.org/10.1016/0031-9422\(95\)91890-D](https://doi.org/10.1016/0031-9422(95)91890-D).
- Wink, M. and Witte, L. 1984. "Turnover and Transport of Quinolizidine Alkaloids. Diurnal Fluctuations of Lupanine in the Phloem Sap, Leaves and Fruits of *Lupinus albus* L." *Planta* 161 (6): 519–24. <https://doi.org/10.1007/BF00407083>.
- Witte, Ludger, Patrizia Rubiolo, Carlo Bicchi, and Thomas Hartmann. 1992. "Comparative Analysis of Pyrrolizidine Alkaloids from Natural Sources by Gas Chromatography-Mass Spectrometry." *Phytochemistry* 32 (1): 187–96. [https://doi.org/10.1016/0031-9422\(92\)80130-7](https://doi.org/10.1016/0031-9422(92)80130-7).
- Wittstock, Ute, and Jonathan Gershenzon. 2002. "Constitutive Plant Toxins and Their Role in Defense against Herbivores and Pathogens." *Current Opinion in Plant Biology* 5 (4): 300–307. [https://doi.org/10.1016/S1369-5266\(02\)00264-9](https://doi.org/10.1016/S1369-5266(02)00264-9).
- Woldemichael, Girma Moges, and Michael Wink. 2002. "Concomitant Occurrence of Pyrrolizidine and Quinolizidine Alkaloids in the Hemiparasite *Osyris alba* L. (Santalaceae)." *Biochemical Systematics and Ecology* 30 (2): 139–49. [https://doi.org/10.1016/S0305-1978\(01\)00065-5](https://doi.org/10.1016/S0305-1978(01)00065-5).
- Yang, Ting, Istvan Nagy, Davide Mancinotti, Sophie Lisa Otterbach, Trine Bundgaard Andersen, Mohammed Saddik Motawia, Torben Asp, and Fernando Geu-Flores. 2017. "Transcript Profiling of a Bitter Variety of Narrow-Leafed Lupin to Discover Alkaloid Biosynthetic Genes." *Journal of Experimental Botany* 68 (20): 5527–37. <https://doi.org/10.1093/jxb/erx362>.
- Zakaria, Mahmoud M., Brigitte Schemmerling, and Dietrich Ober. 2021. "CRISPR/Cas9-Mediated Genome Editing in Comfrey (*Symphytum officinale*) Hairy Roots Results in the Complete Eradication of Pyrrolizidine Alkaloids." *Molecules* 26 (6): 1498. <https://doi.org/10.3390/molecules26061498>.
- Zakaria, Mahmoud M, Thomas Stegemann, Christian Sievert, Lars H Kruse, Elisabeth Kaltenegger, Ulrich Girreser, Serhat S Çiçek, Manfred Nimtz, and Dietrich Ober. 2022. "Insights into Polyamine Metabolism: Homospermidine Is Double-Oxidized in Two Discrete Steps by a Single Copper-Containing Amine Oxidase in Pyrrolizidine Alkaloid Biosynthesis." *The Plant Cell*, February, koac068. <https://doi.org/10.1093/plcell/koac068>.

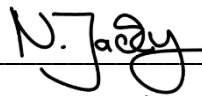
ERKLÄRUNG

Hiermit versichere ich, dass die vorliegende Doktorarbeit nach Inhalt und Form von mir selbstständig verfasst wurde, und keine anderen als die angegebenen Hilfsmittel und Quellen (wie auch die Beratung von meinem Betreuer Prof. Dr. Dietrich Ober und den genannten Beiträgen, vgl. Contributions) verwendet habe.

Die schriftliche Fassung entspricht der auf dem Speichermedium eingereichten Version. Weiterhin versichere ich, dass diese Doktorarbeit noch nicht an anderer Stelle vorgelegen hat und unter Einhaltung der Regeln guter wissenschaftlicher Praxis entstanden ist.

Einige Teilergebnisse wurden zuvor auf Tagungen der Wissenschaftsgemeinde zugänglich gemacht (Botaniker Tagung in Kiel, Deutschland (2017); Plant Biology Europe in Kopenhagen, Dänemark (2018); Workshop of the 'Natural Products' section German Society for Plant Sciences (DBG) in Warberg, Deutschland (2018).

Kiel, den 30.03.2023


Nadine Jacky